

https://dspace.org/

CORROSION TESTING TECHNIQUES AUTOMOTIVE EXHAUST SYSTEMS: EVALUATION, INTEGRATION AND DEVELOPMENT

Nkosi, Zakhele Wonderboy

2006-11-14T11:06:50Z
http://hdl.handle.net/10539/1682

Downloaded from a DSpace repository. https://dspace.org/

CORROSION TESTING TECHNIQUES FOR AUTOMOTIVE EXHAUST SYSTEMS: EVALUATION, INTERGRATION AND DEVELOPMENT

Zakhele Wonderboy Nkosi

A Dissertation submitted to the Faculty of Engineering and the Built Environment, University of the Witwatersrand, in fulfilment of the requirements of the degree of Master of Science.

Johannesburg 2006

Abstract

When specifying materials for use in exhaust systems, it is imperative that they exhibit sufficient corrosion resistance for the specific conditions to which exhaust components are exposed, since up to 80% of all failures is attributed to corrosion and oxidation. It is therefore necessary to establish the corrosion behaviour of the materials in conditions and environments to which the exhausts would typically come into contact with. Most car manufacturers, exhaust manufacturers and material providers have specific corrosion testing methods which they use to determine the corrosion resistance of candidate materials, but there appears to be no standard procedure. A summary comparing all the existing tests is given in section 2. 7. The corrosion testing methods utilise a wide range of conditions, testing temperatures and stages. However, careful investigation of the tests show some similarities, and it was possible to identify eleven key tests, that cover internal corrosion, external corrosion and oxidation for both diesel and petrol engines. Eight of these tests were used to rank the corrosion and oxidation resistance of selected stainless steels, namely AISI type 304, 321, 409, 434 and DIN 1.4509. It appears that the austenitic stainless steels perform better in the cold end conditions, while the ferritic types are more resistant in the hot end high temperature conditions.

Of all the eight tests performed, only the electrochemical tests for external corrosion of cold end components did not give reproducible results. The rest of the tests could be used to screen materials for exhaust system applications. In the internal condition of the cold end, the results of the electrochemical tests indicated that they can be used as a possible replacement for the long exposure tests.

The key tests also highlighted that the presence of NH_4^+ ions in an exhaust gas is beneficial to the corrosion resistance of the stainless steels in internal cold end application. Its inhibiting effect was more pronounced for the ferritic stainless steels. This project indicated that external corrosion due to salt environments is not the major cause of the failure of cold end components, but rather that internal corrosion due to the condensate is the most detrimental.

Dedication

I dedicate this work to my parents. I thank God for them and their everlasting support throughout my studies.

Declaration

I declare that this research dissertation is my own, unaided work. It is being submitted for the degree of Master of Science in Engineering at the University of the Witwatersrand, Johannesburg. It has not been submitted before for any degree or examination at any other university.

SIGNED: _____

DATE: _____

Acknowledgements

I would like to thank God for giving me strength and perseverance needed to complete this project. I must admit it sometimes felt like an emotional roller coaster making this project a success, but that is where the good inspiration comes from. Only my faith could have pulled me through the tough times, and I always kept in mind that God is in control of everything. I thank every single person, mostly my family and friends, who stood by my side throughout and kept on believing in me.

I would also like to express my sincere gratitude to the following people and organisations:

To Dr Michelle Sephton of the University of the Witwatersrand for her supervision of the project and her advice that made this work possible.

To Mr José Prozzi of the University of Johannesburg for his thoughtful discussions and advice for the execution of this work.

To Mrs Charmain De Wet of the University of the Witwatersrand and Mr Sean du Toit of Columbus Stainless for their support and supply of the necessities for this project.

To all the Workshop staff of the University of the Witwatersrand (School of Process and Material Engineering) for cutting the samples for this project.

To Columbus Stainless for financial support and providing the materials and use of their SEM.

To the NRF (DoL) for financial support.

Table of Contents

DEDICATION ..... **I**

DECLARATION ..... **II**

ACKNOWLEDGEMENTS ..... **III**

LIST OF FIGURES ..... **VIII**

LIST OF TABLES ..... **XIII**

1 INTRODUCTION **1**

2 LITERATURE SURVEY **5**

2.1 EXHAUST SYSTEMS 5

2.1.1 Hot end components *5*

Cylinder head gasket 5

Manifolds 6

Front pipe 7

Flexible pipe 7

Catalytic converters (catalyst carrier and shell) 8

2.1.2 Cold end components *9*

Silencer 9

Tail pipe 10

2.2 STAINLESS STEELS IN EXHAUST SYSTEMS 11

2.2.1 Ferritic stainless steels *11*

2.2.2 Austenitic stainless steels *12*

2.3 OPERATING CONDITIONS OF PETROL AND DIESEL VEHICLES 13

2.4 CORROSION OF EXHAUST SYSTEMS 15

2.4.1 Internal corrosion *15*

Condensate corrosion 16

2.4.2 External corrosion *17*

Localised corrosion 18

Intergranular corrosion 20

Poultice corrosion 20

2.4.3 External oxidation *21*

2.5 SIMULATION TESTS FOR EXHAUST SYSTEMS 22

2.5.1 Immersion tests *23*

2.5.2 Cabinet tests *24*

2.5.3 Electrochemical tests *25*

2.5.4 Oxidation tests *26*

2.6 TEST METHODS USED IN EXHAUST SYSTEMS 27

2.6.1 Internal corrosion *27*

Condensate tests 27

Cabinet tests 30
2.6.2 External corrosion *31*
Immersion tests 31
Cabinet tests 32
2.6.3 Electrochemical corrosion tests *35*
Localised corrosion (anodic and cyclic potentiodynamic polarisation) 35
2.6.4 Intergranular corrosion tests *39*
Procedure 39
2.6.5 Perforation and cosmetic tests *40*
Cabinet tests 41
2.6.6 External oxidation tests *42*
Continuous oxidation tests 43
Cyclic oxidation tests 43
2.7. SUMMARY OF THE TESTING METHODS 44
2.7.1 Cold end components *44*
Internal corrosion tests 45
External corrosion tests 48
2.7.2 Hot end components *49*
External corrosion tests 49
External oxidation tests 51

3 CORROSION TESTS FOR DIFFERENT SCENARIOS IN THE EXHAUST SYSTEM 53

3.1 INTERNAL CORROSION TESTS – FOR COLD END COMPONENTS 54
3.1.1 Condensate tests *54*
Test 1 54
Test 2 55
Test 3 55
3.1.2 Cabinet tests *56*
Test 4 57
3.2 EXTERNAL CORROSION – FOR COLD END AND HOT END COMPONENTS 57
3.2.1 Immersion tests *57*
Test 5 57
3.2.2 Cabinet tests *58*
Test 6 58
3.3 LOCALISED CORROSION 59
3.3.1 Potentiodynamic polarisation scan *59*
Test 7 59
Test 8 60
3.4 INTERGRANULAR CORROSION TESTS 60
Test 9 60
3.5 PERFORATION AND COSMETIC TESTS – FOR COLD END COMPONENTS 61
Test 10 61
3.6 EXTERNAL OXIDATION TESTS – FOR HOT END COMPONENTS 61
3.6.1 Cyclic oxidation tests *61*
Test 11 61

4 GENERAL EXPERIMENTAL PROCEDURE 63

4.1 TEST MATERIALS 63
4.2 TEST SOLUTIONS 65
4.2.1 Condensate solution (for internal corrosion) *65*
4.2.2 Salt solution (for external corrosion) *67*
4.3 ELECTROCHEMICAL TESTS 67
4.4 SURFACE ANALYSIS 68
4.5 SPECIMEN CLEANING AND EVALUATION 69

5 COLD END INTERNAL CORROSION TESTS 70

5.1 CONDENSATE TESTS – TEST 3 70
5.1.1 Petrol condensate results *71*
5.1.2 Diesel condensate results *75*
5.1.3 Comparison of corrosion in petrol and diesel condensates *80*
5.2 ELECTROCHEMICAL TESTS – TEST 7 81
5.2.1 Results *82*
5.2.2 The effect of ammonium ions (NH_4^+) in the condensate *88*
5.3 MODIFIED ELECTROCHEMICAL TEST – TEST 8 90
5.3.1 Results *90*
5.4 DISCUSSION AND CONCLUSIONS 94

6 COLD END EXTERNAL CORROSION TESTS 97

6.1 SALT DAMAGE TEST – TEST 5 97
6.1.1 Results *98*
6.2 MODIFIED SALT SPRAY TEST FOR TAIL PIPE – TEST 10 103
6.2.1 Results *103*
6.3 ELECTROCHEMICAL TESTS – TEST 7 108
6.3.1 Results *108*
6.3 DISCUSSION AND CONCLUSIONS 112

7 HOT END EXTERNAL CORROSION TEST 114

7.1 HOT SALT TEST – TEST 5 114
7.1.1 Results *115*
7.2 DISCUSSION AND CONCLUSIONS 121

8 HOT END OXIDATION TEST 123

8.1 CYCLIC OXIDATION TEST – TEST 11 123
8.1.1 Results *124*
8.2 DISCUSSION AND CONCLUSIONS 128

9 SUMMARY 131

REFERENCES 137

APPENDIX A 147

A.1 PHOTOGRAPHS OF THE STAINLESS STEELS AFTER EXPOSURE TO SALT STRAY CABINET. 147

APPENDIX B 149

B.1 ELECTROCHEMICAL POLARISATION RESULTS OF THE SYNTHETIC CONDENSATES 149
Petrol condensate *149*
Diesel condensate *152*
B.2 ELECTROCHEMICAL PARAMETERS FROM THE ELECTROCHEMICAL TEST 155
Petrol condensate *155*
Diesel condensate *156*

APPENDIX C 158

C.1 ELECTROCHEMICAL POLARISATION RESULTS OF THE EFFECT OF NH_4^+ ION IN THE CONDENSATE 158
C.2 ELECTROCHEMICAL PARAMETERS FROM THE EFFECT OF NH_4^+ IONS IN THE CONDENSATE 167

APPENDIX D 169

D.1 ELECTROCHEMICAL POLARISATION SCANS OF THE MODIFIED ELECTROCHEMICAL TEST 169
Petrol condensate *169*
Diesel condensate *171*
D.2 ELECTROCHEMICAL PARAMETERS FROM THE MODIFIED ELECTROCHEMICAL TEST 172
Petrol condensate *172*
Diesel condensate *173*

APPENDIX E 174

E.1 ELECTROCHEMICAL POLARISATION SCANS OF THE ELECTROCHEMICAL TEST IN 5% NACL SOLUTION 174
E.2 ELECTROCHEMICAL PARAMETERS FROM THE ELECTROCHEMICAL TEST IN 5% NACL SOLUTION 177

APPENDIX F 178

F.1 CALCULATIONS OF THE CORROSION RATES OF EXPOSURE IN IMMERSION TESTS 178

List of Figures

FIGURE 1.1: *COMPONENTS PARTS OF TYPICAL EXHAUST SYSTEM OF A VEHICLE* 1
FIGURE 2.1: *SCHEMATIC REPRESENTATION OF POLARIZATION DIAGRAM SHOWING CORROSION POTENTIAL (E_{CORR}) AT THE INTERSECTION OF THE TANGENTIAL OF CATHODIC CURRENT CURVE AND ACTIVE CURRENT CURVE* 37
FIGURE 2.2: *SCHEMATIC REPRESENTATION OF POLARIZATION DIAGRAM SHOWING PRIMARY PASSIVATION (E_{PP}) POTENTIAL AS THE POTENTIAL AT THE PEAK CURRENT WHERE ACTIVE-PASSIVE TRANSITION IS OCCURRED AND PITTING POTENTIAL (E_{PIT}) AT THE INTERSECTION OF THE TANGENTIAL OF PASSIVE CURRENT CURVE AND FORWARD TRANSPASSIVE CURRENT CURVE* 37
FIGURE 2.3: *SCHEMATIC REPRESENTATION OF POLARIZATION DIAGRAM SHOWING PRIMARY PASSIVATION POTENTIAL (E_{PP}) AT THE INTERSECTION OF THE TANGENTIAL OF ACTIVE CURRENT DENSITY CURVE AND PASSIVE CURRENT DENSITY CURVE* 38
FIGURE 2.4: *SCHEMATIC REPRESENTATION OF POLARIZATION DIAGRAM SHOWING PITTING POTENTIAL (E_{PIT}) AT THE INTERSECTION OF THE TANGENTIAL OF FORWARD SCAN TRANSPASSIVE CURRENT CURVE AND PASSIVE CURRENT CURVE AND PROTECTION POTENTIAL (E_{PROT}) AT THE INTERSECTION OF THE REVERSE SCAN TRANSPASSIVE CURRENT CURVE AND PASSIVE CURRENT CURVE* 38
FIGURE 4.1: *AS-RECEIVED SURFACE APPEARANCE FOR 321, APPEARANCE IS REPRESENTATIVE OF ALL THE OTHER STAINLESS STEELS.* 65
FIGURE 4.2: *SEM MICROGRAPH FOR THE 304 TAKEN BEFORE CORROSION, SHOWING A CLEAR SURFACE* 68
FIGURE 5.1: *(A) TEMPERATURE CYCLE AND (B) SCHEMATIC DIAGRAM OF THE INTERNAL CONDENSATE TEST SET-UP* 71
FIGURE 5.2: *CUMULATIVE WEIGHT LOSS IN PETROL CONDENSATE, SHOWING THE AVERAGE WEIGHT LOSS OF FOUR SAMPLES PER MATERIAL* 72
FIGURE 5.3: *PHOTOGRAPHS OF 304 AFTER TOTAL EXPOSURE TO THE PETROL CONDENSATE, SHOWING LITTLE CORROSIVE ATTACK* 72
FIGURE 5.4: *PHOTOGRAPHS OF 409 AFTER TOTAL EXPOSURE TO THE PETROL CONDENSATE, SHOWING LITTLE CORROSIVE ATTACK* 73
FIGURE 5.5: *PHOTOGRAPHS OF 434 AFTER TOTAL EXPOSURE TO THE PETROL CONDENSATE, SHOWING LITTLE CORROSIVE ATTACK* 73
FIGURE 5.6: *SEM MICROGRAPH OF 304 AFTER TOTAL EXPOSURE TO THE PETROL CONDENSATE, SHOWING PITS* 74
FIGURE 5.7: *SEM MICROGRAPH OF 409 AFTER TOTAL EXPOSURE TO THE PETROL CONDENSATE, SHOWING HIGH CONCENTRATION OF SMALL PITS* 74
FIGURE 5.8: *SEM MICROGRAPH OF 434 AFTER TOTAL EXPOSURE TO THE PETROL CONDENSATE, SHOWING PITS ON A RELATIVELY SMOOTH SURFACE* 75
FIGURE 5.9: *CUMULATIVE WEIGHT LOSS IN DIESEL CONDENSATE. THE AVERAGE WEIGHT LOSS OF FOUR SAMPLES PER MATERIAL IS SHOWN* 76
FIGURE 5.10: *PHOTOGRAPHS OF 304 AFTER TOTAL EXPOSURE TO THE DIESEL CONDENSATE, SHOWING CORROSIVE ATTACK, MOSTLY AT THE EDGES* 76
FIGURE 5.11: *PHOTOGRAPHS OF 409 AFTER TOTAL EXPOSURE TO THE DIESEL CONDENSATE, SHOWING PITS ON THE ENTIRE SURFACES* 77

FIGURE 5.12: *PHOTOGRAPHS OF 434 AFTER TOTAL EXPOSURE TO THE DIESEL CONDENSATE, SHOWING CORROSIVE ATTACK AND PITS AT THE EDGES* 77
FIGURE 5.13: *SEM MICROGRAPH OF 304 AFTER TOTAL EXPOSURE TO THE DIESEL CONDENSATE, SHOWING PITS ON A CORRODED SURFACE* 78
FIGURE 5.14: *SEM MICROGRAPH OF 409 AFTER TOTAL EXPOSURE TO THE DIESEL CONDENSATE, SHOWING CORROSIVE ATTACK AND PITS* 79
FIGURE 5.15: *SEM MICROGRAPH OF 434 AFTER TOTAL EXPOSURE TO THE DIESEL CONDENSATE, SHOWING MANY PITS ON A RELATIVELY SMOOTH SURFACE* 79
FIGURE 5.16: *COMPARISON OF CORROSION RATE IN BOTH PETROL AND DIESEL CONDENSATES (AFTER 16 CYCLES)* 80
FIGURE 5.17: *ANODIC POLARISATION SCANS OF 304 IN THE PETROL CONDENSATE, SHOWING GOOD REPRODUCIBILITY* 82
FIGURE 5.18: *CYCLIC POLARISATION SCANS OF 304 IN THE PETROL CONDENSATE; SCANS SHOWING GOOD REPRODUCIBILITY* 83
FIGURE 5.19: *COMPARISON OF CORROSION POTENTIALS IN THE PETROL AND DIESEL CONDENSATES, SHOWING HIGHLY ELECTRONEGATIVE POTENTIALS FOR THE DIESEL CONDENSATE* 84
FIGURE 5.20: *COMPARISON OF CORROSION RATES IN THE PETROL AND DIESEL CONDENSATES, SHOWING VERY LOW CORROSION RATE FOR THE PETROL CONDENSATE* 84
FIGURE 5.21: *COMPARISON OF PASSIVE CURRENT DENSITIES IN THE PETROL AND DIESEL CONDENSATES SHOWING THAT THE CURRENT DENSITIES OF THE 434 ARE ALMOST THE SAME IN THE TWO SOLUTIONS* 85
FIGURE 5.22: *COMPARISON OF PITTING POTENTIALS IN THE PETROL AND DIESEL CONDENSATES, SHOWING SIGNIFICANTLY HIGH PITTING POTENTIALS IN THE DIESEL CONDENSATE* 86
FIGURE 5.23: *COMPARISON OF* $[E_{PIT} - E_{PROT}]$ *IN THE PETROL AND DIESEL CONDENSATE SHOWING THAT THE* E_{PIT} *AND* E_{PROT} *WERE EQUAL FOR THE PETROL CONDENSATE* 87
FIGURE 5.24: *COMPARISON OF CORROSION RATES IN THE SYNTHETIC PETROL SOLUTION WITH VARYING AMMONIUM ION CONCENTRATIONS, SHOWING A SIGNIFICANT DECREASE IN CORROSION RATES WITH AN INCREASE IN THE ION CONCENTRATION* 89
FIGURE 5.25: *SCHEMATIC DIAGRAM OF THE HEAT TREATMENT CYCLE* 90
FIGURE 5.26: *COMPARISON OF CORROSION POTENTIALS IN THE CONDENSATES, SHOWING COMPARABLE POTENTIALS IN THE PETROL CONDENSATE* 91
FIGURE 5.27: *COMPARISON OF CORROSION RATES IN THE CONDENSATES, SHOWING VERY LOW CORROSION RATES IN THE PETROL CONDENSATE* 91
FIGURE 5.28: *COMPARISON OF PASSIVE CURRENT DENSITIES IN THE CONDENSATES, SHOWING COMPARABLE CURRENT DENSITIES IN THE PETROL CONDENSATE* 92
FIGURE 5.29: *COMPARISON OF PITTING POTENTIALS IN THE TWO CONDENSATES, SHOWING A LARGE DIFFERENCE IN 409 RESULTS* 93
FIGURE 6.1: *SCHEMATIC DIAGRAM OF THE SALT DAMAGE TEST EXPOSURE CYCLE: INITIAL 10 MINUTES IMMERSION FOLLOWED BY HEATING CYCLE* 98
FIGURE 6.2: *CUMULATIVE WEIGHT LOSS IN THE SALT DAMAGE TEST. THE AVERAGE WEIGHT LOSS OF FOUR SAMPLES PER MATERIAL IS SHOWN, ALONG WITH THE STANDARD DEVIATIONS. 434 APPEARED MORE RESISTANT* 98
FIGURE 6.3: *COMPARISON OF CORROSION RATES IN THE SALT DAMAGE TEST (AFTER 16 CYCLES), SHOWING VERY LOW CORROSION RATES FOR ALL THE MATERIALS* 99
FIGURE 6.4: *PHOTOGRAPHS OF 304 AFTER EXPOSURE TO THE SALT DAMAGE TEST, SHOWING ISLANDS OF CORROSIVE ATTACK* 100
FIGURE 6.5: *PHOTOGRAPHS OF 409 AFTER EXPOSURE TO THE SALT DAMAGE TEST, SHOWING ISLANDS OF CORROSIVE ATTACK* 100

FIGURE 6.6: *PHOTOGRAPHS OF 434 AFTER EXPOSURE TO THE SALT DAMAGE TEST, SHOWING ISLANDS OF CORROSIVE ATTACK* 100
FIGURE 6.7: *SEM MICROGRAPH OF 304 AFTER TOTAL EXPOSURE TO THE SALT DAMAGE TESTS, SHOWING GENERAL CORROSION AS WELL AS PITTING (ARROWS)* 101
FIGURE 6.8: *SEM MICROGRAPH OF 409 AFTER TOTAL EXPOSURE TO THE SALT DAMAGE TEST, SHOWING GENERAL CORROSION AND PITTING (INDICATED BY ARROWHEADS)* 102
FIGURE 6.9: *SEM MICROGRAPH OF 434 AFTER TOTAL EXPOSURE TO THE SALT DAMAGE TEST, SHOWING PITTING (INDICATED BY ARROWHEADS)* 102
FIGURE 6.10: *CORROSION RATE RESULTS IN THE MODIFIED SALT SPRAY TEST, SHOWING THE AVERAGE CORROSION RATE OF FOUR SAMPLES PER MATERIAL* 104
FIGURE 6.11: *PHOTOGRAPHS OF 304 AFTER EXPOSURE TO THE MODIFIED SALT SPRAY TEST (CORROSION PRODUCT REMOVED), SHOWING ISLANDS OF CORROSIVE ATTACK* 105
FIGURE 6.12: *PHOTOGRAPHS OF 409 AFTER EXPOSURE TO THE MODIFIED SALT SPRAY TEST (CORROSION PRODUCT REMOVED), SHOWING ISLANDS OF CORROSIVE ATTACK* 105
FIGURE 6.13: *PHOTOGRAPHS OF 434 AFTER EXPOSURE TO THE MODIFIED SALT SPRAY TEST (CORROSION PRODUCT REMOVED), SHOWING ISLANDS OF CORROSIVE ATTACK* 105
FIGURE 6.14: *SEM MICROGRAPH OF 304 AFTER TOTAL EXPOSURE TO THE MODIFIED SALT SPRAY TEST, SHOWING SMALL PITS* 106
FIGURE 6.15: *SEM MICROGRAPH OF 409 AFTER TOTAL EXPOSURE TO THE MODIFIED SALT SPRAY TEST, SHOWING MANY SMALL PITS* 107
FIGURE 6.16: *SEM MICROGRAPH OF 434 AFTER TOTAL EXPOSURE TO THE MODIFIED SALT SPRAY TEST, SHOWING A FEW PITS ON A LESS CORRODED SURFACE* 107
FIGURE 6.17: *COMPARISON OF CORROSION POTENTIALS IN THE 5% SALT SOLUTION, SHOWING A CLEAR VARIATION IN THE POTENTIALS* 109
FIGURE 6.18: *COMPARISON OF CORROSION RATES IN THE 5% SALT SOLUTION, SHOWING VERY LOW CORROSION RATES* 109
FIGURE 6.19: *COMPARISON OF PASSIVE CURRENT DENSITIES IN THE 5% SALT SOLUTION, SHOWING 409 WITH A VERY HIGH CURRENT DENSITY* 110
FIGURE 6.20: *COMPARISON OF PITTING POTENTIALS IN THE 5% SALT SOLUTION. THE VERY LOW PITTING POTENTIALS INDICATE LESS RESISTANCE TO THE SOLUTION* 111
FIGURE 7.1: *SCHEMATIC DIAGRAM OF THE HOT SALT TEST EXPOSURE CYCLE: INITIAL 5 MINUTES IMMERSION FOLLOWED BY HEATING CYCLE* 115
FIGURE 7.2: *CUMULATIVE WEIGHT LOSS IN THE HOT SALT TEST. THE AVERAGE WEIGHT LOSS OF FOUR SAMPLES PER MATERIAL IS SHOWN* 116
FIGURE 7.3: *COMPARISON OF CORROSION RATES IN THE HOT SALT TEST (AFTER 16 CYCLES), SHOWING THE FERRITIC STEELS EXHIBITING VARIATION IN BEHAVIOUR, WHILE THE AUSTENITICS BEHAVE SIMILARLY* 117
FIGURE 7.4: *PHOTOGRAPHS OF 304 AFTER EXPOSURE TO THE HOT SALT TEST, SHOWING SEVERELY CORRODED SURFACES* .. 117
FIGURE 7.5: *PHOTOGRAPHS OF 321 AFTER EXPOSURE TO THE HOT SALT TEST, SHOWING SEVERELY CORRODED AND PERFORATED SURFACES* 118
FIGURE 7.6: *PHOTOGRAPHS OF 434 AFTER EXPOSURE TO THE HOT SALT TEST, SHOWING SEVERELY CORRODED SURFACES* .. 118
FIGURE 7.7: *PHOTOGRAPHS OF 1.4509 AFTER EXPOSURE TO THE HOT SALT TEST, SHOWING SEVERELY CORRODED SURFACES* 118
FIGURE 7.8: *SEM MICROGRAPH OF 304 AFTER EXPOSURE TO THE HOT SALT TEST, SHOWING GENERAL CORROSIVE ATTACK* 119
FIGURE 7.9: *SEM MICROGRAPH OF 321 AFTER EXPOSURE TO THE HOT SALT TEST, SHOWING A GENERAL CORROSIVE ATTACK* 120

FIGURE 7.10: *SEM MICROGRAPH OF 434 AFTER EXPOSURE TO THE HOT SALT TEST, SHOWING A BROKEN SURFACE FILM* 120
FIGURE 7.11: *SEM MICROGRAPH OF 1.4509 AFTER TOTAL EXPOSURE TO THE HOT SALT TEST, SHOWING DISCRETE AREAS OF ADHERENT FILM* 121
FIGURE 8.1: *CUMULATIVE WEIGHT LOSS DURING CYCLIC OXIDATION TEST. THE AVERAGE WEIGHT LOSS OF FOUR SAMPLES PER MATERIAL IS SHOWN WITH STANDARD DEVIATION FROM THE MEAN VALUE* 124
FIGURE 8.2: *PHOTOGRAPHS OF 304 AFTER EXPOSURE TO THE CYCLIC OXIDATION TEST (AFTER 104 CYCLES), SHOWING DISCRETE AREAS OF BLISTERING AND SPALLING* 125
FIGURE 8.3: *PHOTOGRAPHS OF 321 AFTER EXPOSURE TO THE CYCLIC OXIDATION TEST (AFTER 104 CYCLES), SHOWING DISCRETE AREAS OF BLISTERING AND SPALLING, ALSO SURFACE WARPING* 125
FIGURE 8.4: *PHOTOGRAPHS OF 434 AFTER EXPOSURE TO THE CYCLIC OXIDATION TEST (AFTER 112 CYCLES), SHOWING DISCRETE AREAS OF BLISTERING* 125
FIGURE 8.5: *PHOTOGRAPHS OF 1.4509 AFTER EXPOSURE TO THE CYCLIC OXIDATION TEST (AFTER 112 CYCLES), SHOWING DISCRETE AREAS OF BLISTERING* 126
FIGURE 8.6: *SEM MICROGRAPH OF 304 AFTER TOTAL EXPOSURE TO THE CYCLIC OXIDATION TEST, SHOWING DEEP CONTINUOUS ATTACK* 126
FIGURE 8.7: *SEM MICROGRAPH OF 321 AFTER TOTAL EXPOSURE TO THE CYCLIC OXIDATION TEST, SHOWING RUPTURED FILM* 127
FIGURE 8.8: *SEM MICROGRAPH OF 434 AFTER TOTAL EXPOSURE TO THE CYCLIC OXIDATION TEST, SHOWING DISCRETE AREAS OF DEEPER CORROSIVE ATTACK* 127
FIGURE 8.9: *SEM MICROGRAPH OF 1.4509 AFTER TOTAL EXPOSURE TO THE CYCLIC OXIDATION TEST, SHOWING CONTINUOUS ATTACK* 128
FIGURE A.1: *PHOTOGRAPHS OF 304 AFTER EXPOSURE TO THE SALT SPRAY (BEFORE REMOVING THE CORROSION PRODUCTS), SHOWING RUSTED SURFACES* 147
FIGURE A.2: *PHOTOGRAPHS OF 409 AFTER EXPOSURE TO THE SALT SPRAY (BEFORE REMOVING THE CORROSION PRODUCTS), SHOWING RUSTED SURFACES* 147
FIGURE A.3: *PHOTOGRAPHS OF 434 AFTER EXPOSURE TO THE SALT SPRAY (BEFORE REMOVING THE CORROSION PRODUCTS), SHOWING RUSTED SURFACES* 148
FIGURE B1: *ANODIC POLARISATION SCANS OF 304 IN THE PETROL CONDENSATE* 149
FIGURE B2: *ANODIC POLARISATION SCANS OF 409 IN THE PETROL CONDENSATE* 150
FIGURE B3*: ANODIC POLARISATION SCANS OF 434 IN THE PETROL CONDENSATE* 150
FIGURE B4: *CYCLIC POLARISATION SCANS OF 304 IN THE PETROL CONDENSATE* 151
FIGURE B5: *CYCLIC POLARISATION SCANS 409 IN THE PETROL CONDENSATE* 151
FIGURE B6: *CYCLIC POLARISATION SCANS 434 IN THE PETROL CONDENSATE* 152
FIGURE B7: *ANODIC POLARISATION SCANS OF 304 IN THE DIESEL CONDENSATE* 152
FIGURE B8: *ANODIC POLARISATION SCANS OF 409 IN THE DIESEL CONDENSATE* 153
FIGURE B9: *ANODIC POLARISATION SCANS OF 434 IN THE DIESEL CONDENSATE* 153
FIGURE B10: *CYCLIC POLARISATION SCANS 304 IN THE DIESEL CONDENSATE* 154
FIGURE B11: *CYCLIC POLARISATION SCANS 409 IN THE DIESEL CONDENSATE* 154
FIGURE B12: *CYCLIC POLARISATION SCANS 434 IN THE DIESEL CONDENSATE* 155
FIGURE C1: *ANODIC POLARISATION SCANS OF 304 IN THE PETROL CONDENSATE WITH 3740 PPM OF* NH_4^+ 158
FIGURE C2: *ANODIC POLARISATION SCANS OF 409 IN THE PETROL CONDENSATE WITH 3740 PPM OF* NH_4^+ 158
FIGURE C3: *ANODIC POLARISATION SCANS OF 434 IN THE PETROL CONDENSATE WITH 3740 PPM OF* NH_4^+ 159
FIGURE C4: *ANODIC POLARISATION SCANS OF 304 IN THE PETROL CONDENSATE WITH 1800 PPM OF* NH_4^+ 159
FIGURE C5: *ANODIC POLARISATION SCANS OF 409 IN THE PETROL CONDENSATE WITH 1800 PPM OF* NH_4^+ 160

FIGURE C6: *ANODIC POLARISATION SCANS OF 434 IN THE PETROL CONDENSATE WITH 1800 PPM OF* NH_4^+ 160
FIGURE C7: *ANODIC POLARISATION SCANS OF 304 IN THE PETROL CONDENSATE WITH 1000 PPM OF* NH_4^+ 161
FIGURE C8: *ANODIC POLARISATION SCAN OF 409 IN THE PETROL CONDENSATE WITH 1000 PPM OF* NH_4^+ 161
FIGURE C9: *ANODIC POLARISATION SCAN OF 434 IN THE PETROL CONDENSATE WITH 1000 PPM OF* NH_4^+ 162
FIGURE C10: *ANODIC POLARISATION SCANS OF 304 IN THE PETROL CONDENSATE WITH 600 PPM OF* NH_4^+ 162
FIGURE C11: *ANODIC POLARISATION SCANS OF 409 IN THE PETROL CONDENSATE WITH 600 PPM OF* NH_4^+ 163
FIGURE C12: *ANODIC POLARISATION SCANS OF 434 IN THE PETROL CONDENSATE WITH 600 PPM OF* NH_4^+ 163
FIGURE C13: *ANODIC POLARISATION SCANS OF 304 IN THE PETROL CONDENSATE WITH 340 PPM OF* NH_4^+ 164
FIGURE C14: ANODIC POLARISATION SCANS OF 409 *IN THE PETROL CONDENSATE WITH 340 PPM OF* NH_4^+ 164
FIGURE C15: *ANODIC POLARISATION SCAN OF 434 IN THE PETROL CONDENSATE WITH 340 PPM OF* NH_4^+ 165
FIGURE C16: *COMPARISON OF CORROSION POTENTIALS (*E_{CORR}*) IN THE PETROL CONDENSATE WITH VARYING* NH_4^+ *CONCENTRATIONS FROM ANODIC POLARISATION SCANS* 165
FIGURE C17: *COMPARISON OF PASSIVE CURRENT DENSITIES IN THE PETROL CONDENSATE WITH VARYING* NH_4^+ *CONCENTRATIONS FROM ANODIC POLARISATION SCANS* 166
FIGURE C18: *COMPARISON OF PASSIVE RANGE (*$R_{PASS} = E_{PIT} - E_{CORR}$*) IN THE PETROL CONDENSATE WITH VARYING* NH_4^+ *CONCENTRATIONS FROM ANODIC POLARISATION SCANS* 166
FIGURE C19: *COMPARISON OF PITTING POTENTIALS IN THE PETROL CONDENSATE WITH VARYING* NH_4^+ *CONCENTRATIONS FROM ANODIC POLARISATION SCANS* 167
FIGURE D1: *ANODIC POLARISATION SCANS OF A HEAT TREATED 304 IN THE PETROL CONDENSATE* 169
FIGURE D2: *ANODIC POLARISATION SCANS OF A HEAT TREATED 409 IN THE PETROL CONDENSATE* 170
FIGURE D3: *ANODIC POLARISATION SCANS OF A HEAT TREATED 434 IN THE PETROL CONDENSATE* 170
FIGURE D4: *ANODIC POLARISATION SCANS OF A HEAT TREATED 304 IN THE DIESEL CONDENSATE* 171
FIGURE D5: *ANODIC POLARISATION SCANS OF A HEAT TREATED 409 IN THE DIESEL CONDENSATE (NOTE THE SCALE CHANGE OF THE POTENTIAL)* 171
FIGURE D6: *ANODIC POLARISATION SCANS OF A HEAT TREATED 434 IN THE DIESEL CONDENSATE* 172
FIGURE E1: *ANODIC POLARISATION SCAN OF 304 IN 5% NACL SOLUTION* 174
FIGURE E2: *ANODIC POLARISATION SCAN OF 409 IN 5% NACL SOLUTION* 174
FIGURE E3: *ANODIC POLARISATION SCAN OF 434 IN 5% NACL SOLUTION* 175
FIGURE E4: *CYCLIC POLARISATION SCAN 304 IN 5%NACL SOLUTION* 175
FIGURE E5: *CYCLIC POLARISATION SCAN 409 IN 5%NACL SOLUTION* 176
FIGURE E6: *CYCLIC POLARISATION SCAN 434 IN 5%NACL SOLUTION* 176

List of Tables

TABLE 1.1: *APPLICATION AND SERVICE TEMPERATURE OF STAINLESS STEELS IN THE EXHAUST COMPONENTS* 2
TABLE 2.1: *A COMPARISON OF THE STAINLESS STEELS USED FOR HOT END COMPONENTS AND THEIR OXIDATION/CORROSION RESISTANCE/PROPERTIES (DOUTHETT, 1995; WELTENS ET AL., 2001)* 13
TABLE 2.2: *PHYSICAL CHARACTERISTICS AND CHEMICAL COMPOSITION OF REPRESENTATIVE EXHAUST GAS CONDENSATES (WELTENS ET AL., 2001)* 14
TABLE 2.3: *EXPERIMENTAL PROCEDURES OF THE INTERNAL CONDENSATE TESTS* 28
TABLE 2.4: *EXPERIMENTAL PROCEDURES OF CABINET TESTS FOR INTERNAL CORROSION* 30
TABLE 2.5: *EXPERIMENTAL PROCEDURES OF IMMERSION TESTS FOR EXTERNAL CORROSION* 31
TABLE 2.6: *EXPERIMENTAL PROCEDURES OF THE EXTERNAL CORROSION OF CABINET TESTS* 32
TABLE 2.7: *EXPERIMENTAL PROCEDURES OF PERFORATION AND COSMETIC TESTS* 41
TABLE 2.8: *SUMMARY OF THE PUBLISHED COMPOSITIONS FOR SIMULATED CONDENSATE (TESTING ENVIRONMENT)* 44
TABLE 2.9: *SUMMARY FOR IMMERSION TESTS FOR INTERNAL CORROSION OF THE COLD END COMPONENTS AND THE VARIATIONS IN EACH STAGE* 46
TABLE 2.10: *SUMMARY OF THE SOLUTION AND STAGES IN THE CABINET TEST FOR INTERNAL CORROSION* 47
TABLE 2.11: *SUMMARY OF EXTERNAL CORROSION TESTS OF THE COLD END COMPONENTS* 48
TABLE 2.12: *SUMMARY FOR IMMERSION TESTS FOR EXTERNAL CORROSION OF THE HOT END COMPONENTS AND THE VARIATIONS IN EACH STAGE* 49
TABLE 2.13: *SUMMARY OF EXTERNAL CORROSION OF THE HOT END COMPONENTS: HUMIDITY CABINET TESTS* 50
TABLE 2.14: *SUMMARY OF EXTERNAL CORROSION OF THE HOT END COMPONENTS: SALT SPRAY TESTS* 51
TABLE 2.15: *SUMMARY FOR OXIDATION TESTS FOR EXTERNAL CORROSION OF THE HOT END COMPONENTS, AND THE VARIATIONS IN EACH STAGE* 52
TABLE 4.1: *AS-RECEIVED SURFACE FINISHES OF THE MATERIALS* 63
TABLE 4.2: *NOMINAL COMPOSITIONS OF THE STAINLESS STEELS* 64
TABLE 5.1: *PIT DENSITY AFTER EXPOSURE TO DIESEL CONDENSATE* 78
TABLE 5. 2: *COMPARISON OF PASSIVE POTENTIAL RANGES IN THE PETROL AND DIESEL CONDENSATES* 86
TABLE 5.3: *CHEMICAL COMPOSITION OF SIMULATED EXHAUST GAS CONDENSATES WITH VARYING* NH_4^+ *ION CONCENTRATIONS* 88
TABLE 5.4: *COMPARISON OF PASSIVE RANGES IN THE PETROL AND DIESEL CONDENSATES* 93
TABLE 6.1: *COMPARISON OF PASSIVE RANGES IN THE 5% SALT SOLUTION* 111
TABLE 9.1: *RANKING THE RELATIVE CORROSION RESISTANCE OF THE STAINLESS STEELS IN THE COLD END INTERNAL CORROSION TESTS* 133
TABLE 9.2: *RANKING THE RELATIVE CORROSION RESISTANCE OF THE STAINLESS STEELS IN THE COLD END EXTERNAL CORROSION TESTS* 134
TABLE 9.3: *RANKING THE RELATIVE CORROSION RESISTANCE OF THE STAINLESS STEELS IN THE HOT END CORROSION TESTS* 135
TABLE B.1: *ELECTROCHEMICAL PARAMETERS FROM ANODIC POLARISATION SCANS IN THE PETROL CONDENSATE* 155
TABLE B.2: *ELECTROCHEMICAL PARAMETERS FROM CYCLIC POLARISATION SCANS IN THE PETROL CONDENSATE* 156

TABLE B.3: *ELECTROCHEMICAL PARAMETERS FROM ANODIC POLARISATION SCANS IN THE DIESEL CONDENSATE* 156
TABLE B.4: *ELECTROCHEMICAL PARAMETERS FROM CYCLIC POLARISATION SCANS IN THE DIESEL CONDENSATE* 157
TABLE C.1: *ELECTROCHEMICAL PARAMETERS FROM ANODIC POLARISATION SCANS IN THE PETROL CONDENSATE WITH VARIOUS NH_4^+ IONS*..... 168
TABLE D.1: *ELECTROCHEMICAL PARAMETERS OF THE HEAT TREATED MATERIALS IN THE PETROL CONDENSATE*..... 172
TABLE D.2: *ELECTROCHEMICAL PARAMETERS OF THE HEAT TREATED MATERIALS IN THE DIESEL CONDENSATE*..... 173
TABLE E.1: *ELECTROCHEMICAL PARAMETERS FROM ANODIC POLARISATION SCANS IN THE 5% NACL SOLUTION* 177
TABLE E.2: *ELECTROCHEMICAL PARAMETERS FROM CYCLIC POLARISATION SCANS IN THE 5% NACL SOLUTION*..... 177
TABLE F.1: *CALCULATIONS OF THE CORROSION RATES OF INTERNAL CORROSION TESTS* 178
TABLE F.2: *CALCULATIONS OF THE CORROSION RATES OF EXTERNAL CORROSION TESTS*..... 178

Chapter 1

Introduction

The exhaust system is an often-ignored part of a vehicle, but in fact is a complex assembly which performs important tasks in harsh environments. At its simplest, the system conveys hot toxic gases, produced in the combustion chamber, from the engine exhaust ports and discharges them into the atmosphere through the tailpipe (Ashworth *et al*., 1996; Weltens *et al*., 2001). It reduces the noise produced by the engine inside and outside of the vehicle, reduces gas emissions and affects performance of the engine (Hooper, 1978; Weltens *et al.,* 2001).

The exhaust system is divided into two main parts: the hot (or front) end and the cold (or rear) end (Figure 1.1) on account of their different service temperatures (Sato and Tanoue, 1995). The hot end includes the exhaust manifold, front pipe and catalytic converter with a flexible coupling in some car models. The cold end includes the intermediate pipe, silencer and tail pipe. In past years, the cold end section has seen a dramatic increase in life expectancy and upgrade of materials (Douthett, 1995).

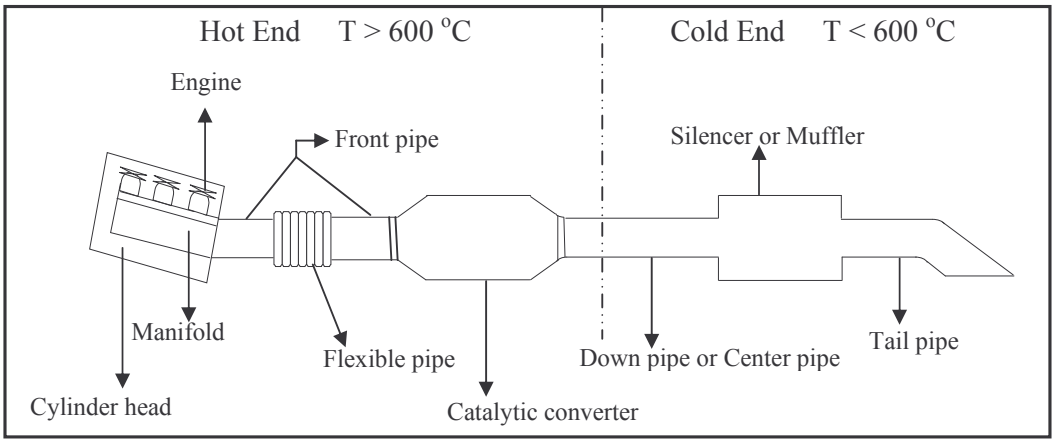


Figure 1.1: *Components parts of typical exhaust system of a vehicle*

There are a variety of material properties required in an exhaust system (Alves *et al*., 2002; Ashworth *et al*., 1993; Douthett, 1995; Sato and Tanoue, 1995). At the hot end of the system high temperature oxidation occurs, while at the cold end condensate corrosion is the prime factor

which has to be combated (Alves *et al*., 2002; Ashworth *et al*., 1993; Douthett, 1995). A breakdown of these requirements is given in Table 1.1. The table also shows the average operating temperatures of each component and the materials generally used for each component.

Table 1.1: *Application and service temperature of stainless steels in the exhaust components*

Exhaust system	**Hot End (T > 600 °C)**				**Cold End (T < 600 °C)**	
	Manifold	Front pipe	Flexible pipe	Catalytic converter	Center pipe	Silencer and tail pipe
Performance requirements	High temperature oxidation resistance Thermal fatigue strength	High temperature oxidation resistance High temperature corrosion resistance	High temperature oxidation resistance High temperature corrosion resistance	High temperature oxidation resistance	Corrosion resistance condensed liquid	Corrosion resistance condensed liquid
Service temperature (°C)	750 - 950	600 - 800	600 - 800	600 - 800	400 - 600	100 - 400
General materials used	**441, 409, 439, 18Cr-Cb, 321**	**409, 304, 321, 441, 410**	**321, 304, 302B**	**409, 441, 18Cr-Cb**	**409, 439, 304, 434, 436S, Al409, 18Cr-Cb, Al steel, 410, 444, 432**	

Carbon steel has been used extensively in the exhaust systems, but pressure to lower cost, increase fuel efficiency and lower hazardous emissions, weight savings and increased life expectancy have opened the door for other materials such as stainless steels (Douthett, 1995; Kwon *et al*., 2002; Inoue and Kikuchi, 2003) to be used. It has been shown that stainless steels considerably improve the service life of exhaust components (Alves *et al*., 2002).

It is expected that the use of stainless steels in exhaust systems of diesel-powered vehicles (mainly trucks) would increase to meet the growing social demand for stricter regulation of exhaust gas emissions, since these steels are able to withstand the higher temperatures needed to release cleaner gases (Sato and Tanoue, 1995). In addition, the demands for advanced properties of stainless steels in exhaust systems of both diesel and petrol-powered vehicles are increasing to

meet requirements for lighter weight and stricter regulations for exhaust gas (Miyazaki *et al*., 2000). These requirements for better properties have increased the consumption of stainless steels in the automotive industry where it has almost quadrupled in the past decade. Nowadays stainless steel is used in almost all the exhaust parts, from the gasket to the tail pipe as shown in Figure 1.1 (Sato and Tanoue, 1995).

The increasing need for better performance stainless steels includes ferritic stainless steels with high heat resistance for improved fuel economy in manifolds and with high condensate corrosion resistance for silencers. The need for austenitic stainless steels with good elevated-temperature salt corrosion resistance and better noise control for flexible pipes and silencers has also been increasing (Sato and Tanoue, 1995; Kawasaki *et al*. 1988; Kwon *et al*., 2002). The stainless steels listed in Table 1.1 are answers to some of these needs (Alves *et al*., 2002; Ashworth *et al*., 1993; Douthett, 1995; Kobayashi *et al*., 1988; Miyazaki *et al*., 1994; Sato and Tanoue, 1995).

In response to the growing consumption of stainless steel, it is essential to properly evaluate their mechanical and corrosion properties in order to ensure that they are suitable for use in exhaust systems. The mechanical properties are important since they control the ability to fabricate the steel into useful components and determine the ability of a component to withstand the service conditions of the exhaust system. Mechanical testing of stainless steels is the same as for any other material with regard both to fabrication and design stresses. Testing for corrosion is, however, a more specialised technology since it is not structured as in the case of mechanical testing, but is adapted to suit application specifications.

Therefore, this project aimed at evaluating the most common corrosion and oxidation tests that are used for materials for exhaust systems, to establish their similarities and differences and to integrate all the tests in order to develop standard test protocols for all areas and components of the exhaust system. This project aimed at providing the corrosion data and standardising the corrosion tests for exhaust systems. External corrosion, internal corrosion and oxidation tests were evaluated.

As shown in Table 1.1, the major degradation problems involving corrosion of the cold end are caused by condensation on the internal parts. In the hot end the problems are due to external high temperature corrosion (due to de-icing salt) and external high temperature oxidation. Therefore tests were developed to cover internal corrosion of the cold end and external corrosion of the hot end. In some exceptional cases external corrosion, due to de-icing salt, in the cold end has been reported (Baboian, 1996), therefore external corrosion tests of the cold end were also developed.

The developed tests focused on providing combinations of rapid, reliable and accurate results that can be obtained in an environment which closely simulates actual operating conditions. The most common materials which are used in manufacturing the components of exhaust systems were evaluated using the developed tests. This assisted in establishing whether the developed tests could be relied on. The reliability of the developed tests was established by comparing the material behaviour with expected trends from other researchers.

It is hoped that the technological advantage and knowledge gained from this project will be beneficial to the growing local industry of exhaust systems and components, since techniques to provide the reliable corrosion data and material performance monitoring required by exhaust design engineers and material suppliers are supplied. The techniques could also be used to assist in new material design through corrosion property and behaviour elucidation and characterisation. This project forms part of stainless steels producers' strategy to develop a comprehensive corrosion evaluation technique for automotive exhaust materials. This could assist in the sector's desire to establish itself as a globally competitive business, particularly in exhaust systems, since the findings provide them with a means to supply supporting documentation for their products, therefore rendering a more complete service to its clients.

The most common corrosion and oxidation tests are evaluated in the literature survey section, followed by a chapter on the developing of the corrosion and oxidation tests for all areas and components of the exhaust system (Chapter 3). The experimental work, results and discussion of the developed tests are covered separately in subsequent chapters: cold end internal corrosion (Chapter 5), cold end external corrosion (Chapter 6), hot end external corrosion (Chapter 7) and hot end external oxidation (Chapter 8). The discussion of the results are summarised together with overall conclusions and recommendations in the last chapter.

Chapter 2

Literature survey

2.1 Exhaust systems

As mentioned in Chapter 1, the exhaust system can be divided into two main sections, depending on their operating temperature range. In this section an in-depth look is taken at the various components of these sections, and their functions and operating conditions. The types of corrosion which exhaust systems experience are also discussed.

2.1.1 Hot end components

From the engine towards the catalytic converter, exhaust parts normally remain hot and dry when in operation. The properties required from the hot end components are high temperature strength and corrosion resistance, oxidation resistance, low coefficient of thermal expansion and scale spalling resistance, good thermal fatigue resistance, low thermal absorption, good weldability, and good impact properties in cold start conditions (Inoue and Kikuchi, 2003; Sato and Tanoue, 1995). The primary hot end components are:

Cylinder head gasket

Cylinder head gaskets were formerly made of asbestos, but its toxicity and increased government regulation, and the gas seal tightness problem following the increase of engine output, have facilitated the replacement of asbestos with other materials. In today's petrol-powered engines, the cylinder head gaskets are mostly made of graphite, while for diesel-powered engines they are mostly made of high strength stainless steel. In terms of heat resistance, thermal conductivity, sag resistance, maintainability and pollution control, metal gaskets are advantageous over asbestos gaskets (Sato and Tanoue, 1995).

Manifolds

The exhaust manifold collects the high temperature exhaust gas which is discharged from the engine cylinders and leads the gas to the front pipe (Inoue and Kikuchi, 2003; Miyazaki *et al*., 2000). It is attached with flanges to the engine and is exposed to very hot exhaust gases. The manifold has been traditionally made of cast iron (Miyazaki *et al*., 1994; Sato and Tanoue, 1995), however, global environment protection and essential vehicle requirements (e.g. lightweight) are forcing makers of passenger cars to deal with exhaust gas regulation, fuel consumption reduction, higher power to ease driving and lower maintenance. To offset some of these demands where a higher exhaust gas temperature is unavoidable, thermal reliability of the manifold becomes necessary (Sato and Tanoue, 1995). To address this, ferritic stainless steels, which allow thickness reduction and have excellent oxidation resistance, began to be used as manifold materials in the mid 1980s. These materials were also used with the aim of reducing weight and increasing output. The proportional use of cast iron started declining with the use of stainless cast steel; and the use of stainless steel in this application is expected to increase (Fujita *et al*., 1996; Miyazaki *et al.*, 1994; Sato and Tanoue, 1995). Heat resistant cast stainless and fabricated stainless steel pipe manifolds are being produced to meet the most demanding operating conditions (Miyazaki *et al*., 2000; Sato and Tanoue, 1995). Ideally, the exhaust manifold should be capable of withstanding continuous gas temperatures as high as 900 ºC, with occasional peaks of 950 ºC resulting from high-speed running. Thus austenitic or ferritic heat resistant steels which exhibit excellent corrosion and oxidation resistance at elevated temperature are being developed and used (Inoue and Kikuchi, 2003; Sato and Tanoue, 1995).

Other properties required in an exhaust manifold are oxidation resistance and thermal fatigue strength high enough to withstand hot exhaust gases, low thermal capacity to enhance the catalytic function, and good workability and weldability for manufacturing (Inoue and Kikuchi, 2003; Miyazaki *et al*., 2000).

The stainless steels which are used in exhaust manifold applications are ferritic type AISI 409 and type 439 used in the USA, while nickel-base alloys or austenitic stainless steels such as AISI type 321 are used in Europe (Sato and Tanoue, 1995).

Front pipe

The front pipe is located between the exhaust manifold and flexible pipe, and also between the flexible pipe and catalytic converter. In order to enhance the catalytic action or exhaust gas cleaning action of the catalytic converter the front pipe must minimize the heat loss due to radiation and must minimise the drop in the exhaust gas temperature. Oxidation resistance and thermal fatigue resistance are also required for this application (Inoue and Kikuchi, 2003; Sato and Tanoue, 1995). The front pipe is also essential to decrease the noise. In response to these reasons, manufacturers are increasingly using thin wall double pipe structures for the front pipe (Inoue and Kikuchi, 2003).

Like the exhaust manifold, the front pipe is fabricated from higher grade stainless steels with superior oxidation resistance and corrosion resistance. However, there is a strong need for cheaper stainless steels, possibly ferritic, with low coefficient of thermal expansion to prevent heat loss (Inoue and Kikuchi, 2003; Sato and Tanoue, 1995).

The stainless steels that are currently used in manufacturing the front pipe are ferritic AISI type 409, type 410 and DIN 1.4509 and austenitic type AISI 321 and 304.

Flexible pipe

The flexible pipe is located between the exhaust manifold and the catalytic converter and is used to prevent the transmission of engine vibration to the exhaust system. It consists of a bellow-shaped double pipe, usually 0.3 – 0.4 mm wall thickness material that covers a stainless wire mesh or braider (Inoue and Kikuchi, 2003; Sato and Tanoue, 1995).

The flexible pipe might also subjected to a severe external environment (in regions where de-icing salt is used on roadways to prevent freezing in winter) combining high temperature salt corrosion with high temperature fatigue. Austenitic stainless steels with silicon additions, increased nickel, molybdenum additions, and optimised chromium content are increasingly used (Inoue and Kikuchi, 2003; Sato and Tanoue, 1995).

Flexible pipes are usually made from austenitic stainless steels such as AISI type 304, type 321 and type 302B that have good workability and weldability properties (Sato and Tanoue, 1995).

Catalytic converters (catalyst carrier and shell)

In response to global stricter emission regulations, improved exhaust gas purification characteristics immediately after the engine starts (cold emissions) have become compulsory. Therefore, the presence of a catalytic converter is necessary. The catalytic converter is located below the exhaust manifold for cleaning the exhaust gas (Sato and Tanoue, 1995). It converts hydrocarbons (CH), carbon monoxide (CO) and oxides of nitrogen (NO_x) into carbon dioxide (CO_2), water (H_2O) and nitrogen gas (N_2) (Inoue and Kikuchi, 2003;Cayless, 1974; Kawasaki *et al*., 1988, Miyazaki *et al*., 2002). Since the catalyst is poisoned by lead, it can only be used in cars running on unleaded petrol (Kawasaki *et al*., 1988).

The shell temperature of the catalytic converter is low during cold starting and the exhaust gas purification reaction does not proceed to completion during cold starting. As a remedy to this problem, raising the exhaust gas temperature and adopting thinner wall thickness in the exhaust manifold have been successfully used. The thin willed materials improve fuel economy by reducing the weight. They also make it possible to flow the exhaust gas into the catalytic converter while still at high temperature and this accelerate the gas convection reaction (Miyazaki *et al*., 2000 and 2003).

The catalyst carrier is subjected to temperatures ranging from 1000 to 1200 ^{o}C (Inoue and Kikuchi, 2003). The cordierite monolith has been the traditionally used material as a catalyst carrier, however in recent years, ferritic stainless steel (Shimizu *et al*., 1994) foil with excellent thermal shock and low heat capacity has been increasingly used and has come to replace the cordierite monolith. The metal carrier is always exposed to rapid heating when the engine is started and accelerated as well as to localised thermal stress arising from radial temperature distribution. The stainless steel foil is assembled into a honeycomb structure with excellent thermal fatigue resistance (Ishii *et al*., 1999; Sato and Tanoue, 1995).

In order to satisfy stricter exhaust gas regulations, mounting a 3-way catalyst in catalytic converters have become common practice. As a consequence, highly corrosive condensates are now generated inside silencers. Thus, to meet the requirements of longer guaranteed life-time, materials which offer excellent corrosion resistance in the condensate corrosion environment inside silencers are now also required (Inoue and Kikuchi, 2003; Miyazaki *et al*., 2000).

The ferritic stainless steels used in manufacturing the catalytic converters are AISI type 409, DIN 1.4509 and 18Cr-Cb.

2.1.2 Cold end components

The required properties for cold end materials are good weldability, corrosion resistance to internal condensate and external salt solution, good formability, attractive cosmetic appearance, fatigue strength and NVH (noise, vibration, harshness) reduction (Sato and Tanoue, 1995). The primary cold end components are:

Silencer

This is also known as a muffler. In general, a silencer reduces the resultant sound waves to acceptable levels and ensures correct gas flow through the exhaust system. A silencer is a combination of tuning chambers, baffle partitions and solid and perforated tubes designed to dissipate noise pulses while conveying exhaust gas and vapour (Inoue and Kikuchi, 2003).

Although some small engines can satisfactorily be silenced with one silencer (main silencer), the most common arrangement is to use two silencers, with one situated right at the rear of the exhaust system (called main silencer) and the other one more forward towards the catalytic converter. There are three general types of silencer: a) absorption (straight through type), b) mechanical (baffle type), and c) combination of absorption and mechanical. The absorption type uses a principle of dumping while the mechanical type causes the gas to lose its energy by expansion and interference. The absorption type is considered the most effective in reducing high frequency noise, and the mechanical type is effective for low frequency noise (Cayless, 1974).

Because of the silencer's position (see Figure 1.1), the exhaust gas is much cooler in this part of the exhaust system (max. 400 ^{o}C) (Sato and Tanoue, 1995). As a result, the silencer is subjected to extreme corrosive conditions, because of exhaust gas condensation and lower rate of evaporation.

When automobiles are driven over a long distance for an extended period of time, the temperature of the exhaust gas at exit exceeds 100 ^{o}C and moisture in the silencer does not condensate. However, when an automobile is driven over a short distance for short period of time, the temperature of the exhaust gas does not rise so high, which results in the formation of exhaust gas condensate in the low-temperature section of the silencer. The condensate contains NH_4^+, CO_3^{2-}, SO_4^{2-}, SO_3^-, Cl^-, NO_3^-, NO_2^-, CH_3COO^-, $HCHO^-$, $HCOO^-$ and activated carbon and has a pH value

between 8 and 9. The pH can be reduced to as low as 2 and 1 during evaporation, however. Corrosion due to this condensate is a problem for stainless steel silencers (Lothongkum *et al*., 1999; Sato and Tanoue, 1995; Douthett, 1995).

The internal and external corrosion resistance required by the silencer, appears to be dependent on exhaust system design. The double-walled silencers (shell and wrap design) are more prone to early condensate failures than single-shell designs. Condensate formed between shell layers cannot escape and remains trapped for extended periods of time, resulting in crevice corrosion. However, it has been found that insulating blankets placed between the shell and wrap help to reduce crevice condition. The corrosion damage is also reduced by providing a means to remove the condensate via a drain hole or pitot tubes.

Silencers are manufactured from aluminised carbon steel and ferritic stainless steels such as AISI type 409, AL409, 410, 432, 434, 436S, 439, 444 and 18Cr – Cb. It was found that general corrosion proceeded with the formation of a thick rust layer for aluminised carbon steel silencers, while the corrosion was localised for stainless steels silencers, and that aluminised carbon steel silencers perforate in a fairly short time. Therefore, stainless steel silencers are much more common currently (Douthett, 1995; Sato and Tanoue, 1995).

The internal corrosion of stainless steels in silencers is mainly in the form of localised (pitting, crevice and intergranular) corrosion and is accelerated by wet exhaust gas environments (Sato *et al*., 1991). Pitting corrosion occurring in silencers is observed only in the condensate environment where chloride ions are present (Sato and Tanoue, 1995).

Tail pipe

The tail pipe is located behind the main silencer. It ensures that exhaust gas is emitted past the end of the body of the vehicle. This prevents exhaust gas entering the luggage compartment and, ultimately, the passenger space (Inoue and Kikuchi, 2003).

The materials used in manufacturing the tail pipe and the corrosion suffered by the tail pipe are similar to that of the silencer, since they are both subjected to similar conditions, characterised by relatively cooler temperatures (Sato and Tanoue, 1995). The cosmetic appearance of stainless steel in the exhaust system, particularly the tail pipe, is vital, since the tail pipe is the only section of the exhaust system visible. Therefore a stainless steel that will resist staining, by retaining its brightness, is often preferred for this application (AK Steel Exhaust Steel, 2002).

2.2 Stainless steels in exhaust systems

Exhaust system components have been manufactured traditionally from carbon steel. However due to the short life of the components relative to the warranty of the car and lifetime of the car, attempts have been made to improve the lifetime of the components by using stainless steel. Their excellent corrosion resistance to exhaust gas atmospheres, together with weldability, formability, relatively high strength-to-weight ration and good appearance make them very attractive to the automotive industry. Exhaust systems today are manufactured from both austenitic and ferritic stainless steels, although ferritic stainless steel is used more frequently (Hooper, 1978; Ishii *et al*., 1999; Kobayashi *et al*., 1988).

2.2.1 Ferritic stainless steels

Ferritic stainless steels are increasingly becoming the main materials for components of both the hot and the cold parts (Alves *et al*. 2002). It is known that with more chromium and molybdenum a super-ferritic stainless, which provides a higher level of corrosion and oxidation resistance, can be obtained (Jones, 1996, Mangonon, 1999).

The general corrosion resistance of the ferritic stainless steels is good and they are highly resistant to atmospheric corrosion in urban and rural atmospheres. However, they are readily corroded in environments containing chloride ions, and contaminants such as sulphur dioxide increase the corrosion rate. The corrosion resistance of 17% chromium ferritic stainless steels is less than that of austenitic stainless steels in a reducing media, however molybdenum additions improve their resistance under chloride containing and oxidising conditions (Pickering, 1979). Precipitates in the case of stabilised steels, particularly by titanium, may reduce their corrosion resistance in nitric acid. In chloride environments, precipitation of chromium carbides and nitrides can lower their corrosion resistance. Oxide and sulphide inclusions can also reduce the corrosion resistance (Pickering, 1979). Therefore, for optimum corrosion resistance, a high matrix chromium content is desirable, together with adequate stabilisation of the interstitial elements, carbon and nitrogen (Ashworth, 1993).

The development of higher alloyed ferritic stainless steels has been found to improve the service life of the exhaust components (Alves *et al*. 2002). These higher alloyed ferritic stainless steels have been developed to meet specific requirements for fabricability, corrosion resistance, hot

strength and oxidation resistance. However, type 409 remains attractive and widely used in exhaust systems because of its low cost (Ashworth, 1993). Ferritic stainless steels with improved thermal fatigue properties have been developed by making use of solid strengthening with niobium or molybdenum. The oxidation resistance and microstructural stability of stainless steels are also enhanced by the solid strengthening with either niobium or molybdenum (Sato and Tanoue, 1995).

2.2.2 Austenitic stainless steels

Austenitic stainless steels are chromium-nickel alloys that were developed for use in both mild and harsh corrosive environments. The addition of nickel stabilizes the austenitic crystal structure and interacts with chromium to maintain the passive film (Jones, 1996; Mangonon, 1999). These steels have good corrosion resistance in a wide range of corrosive environments. In particular, they have superb atmospheric corrosion resistance, but marine environments reduce their resistance. If the nickel content is increased it improves their resistance to many organic acids and also sulphuric acid, while passivation results in oxidising media. The addition of molybdenum is also advantageous in improving their general corrosion resistance and resistance in sulphuric acid media. The corrosion resistance of austenitic stainless steels is mostly impaired in chloride environments, where the chloride ions tend to penetrate the passive film and result in pitting corrosion, but the addition of molybdenum is also beneficial in these conditions (Pickering, 1979).

From the many austenitic stainless steel grades, 304 and 321 are the ones mostly used in exhaust systems (Alves *et al*., 2002; Ashworth *et al*., 1993; Douthett, 1995; Sato and Tanoue, 1995). They guarantee longer useful life of the exhaust system than ferritic types, but have disadvantages such as higher cost (Alves *et al*., 2002). New austenitic grades which could be candidates for exhaust applications have been developed for conditions where the ferritic stainless steels have proved to be inadequate. Their compositions are based on the standard austenitic grades but with significant additions of silicon, nitrogen and rare earth metals to improve their properties. The resulting improved properties are a high degree of oxidation resistance, good high temperature strength and creep strength exceeding most of the ferritic stainless steels (Ashworth *et al*., 1993).

A comparison of some stainless steels used in hot end applications is shown in Table 2.1, together with their oxidation and external corrosion resistance.

Table 2.1: *A comparison of the stainless steels used for hot end components and their oxidation/corrosion resistance/properties (Douthett, 1995; Weltens et al., 2001)*

Stainless Steel	Upper temperature oxidation limit	Hot salt resistance	Notes
F: AISI 409	816 °C	5	Improved corrosion resistance compared to surface coated carbon steel.
F: AISI 439	885 °C	3	ND
F: 18 Cr–Cb	899 °C	2	ND
F: 11 Cr–Cb	885 °C	3	ND
F: 18 SR	1093 °C	2	ND
F: 436S	885 °C	3	ND
F: Din 1.4509	950 °C	ND	Increased thermal stability, increased corrosion resistance (wet + hot) compared to 409 or 1.4512.
A: 304 and 304L	816 °C	2.5	Increased wet corrosion resistance.
F: 409 AL	871 °C	1	Aluminium coated, increased corrosion resistance compared to 409 or 1.4512.
A: 316 and 316Ti	850 °C	ND	Very high thermal stability and wet corrosion resistance better than 304 or 1.4301.
F: 434	816 °C	ND	Increased wet corrosion resistance bad deep drawing features, bad weldability.
A: 309 and 310S	1000 - 1150 °C	ND	Thermal stability and wet corrosion resistance (wet + hot)

*F = ferritic; A = austenitic; 1 = most desirable; 5 = least desirable, but not necessarily bad; ND = No Data.

2.3 Operating conditions of petrol and diesel vehicles

In terms of external corrosion, petrol and diesel-powered vehicles suffer the same type of corrosion namely, localised, poultice and intergranular corrosion. The characteristics and production of the condensate in the diesel and petrol engines differ, and this justifies the difference in the mechanism of internal corrosion. These fuels also differ in their chemical

composition as shown in Table 2.2 below (Weltens *et al*., 2001). These compositions were obtained by analysing exhaust components (usually the silencer) to determine the main cause of failure (Sato *et al.*, 1991).

Table 2.2: *Physical characteristics and chemical composition of representative exhaust gas condensates (Weltens et al., 2001)*

	Petrol engine with catalytic converter (unleaded)	Petrol engine without catalytic converter (unleaded)	Petrol engine with catalytic converter (leaded)	Diesel engine with catalytic converter	Diesel engine without catalytic converter
pH value	6.5	3.2	3.6	2.9	2.4
SO_4^{2-} (ppm)	15	320	-	41	175
Cl^- (ppm)	2.2	4.2	23.5	2.9	52
NH_4^+ (ppm)	60	1.1	-	<0.1	<0.1
NO_3^- (ppm)	10	<2	-	18	35
NO_2^- (ppm)	110	0.16	-	<0.01	<0.01
PO_4^{3-} (ppm)	<0.1	<0.5	-	0.19	1.3

As indicated in this table, the exhaust gas condensate of petrol engines with a three-way catalytic converter is neutral, while those in petrol engines without a catalytic converter, and in diesel engines, are highly acidic (pH < 3). The leaded fuel for petrol engines contains bromides and chlorides which are scavengers for harmful gases such as CO, the chlorides contribute considerably to the lower pH values. The aggressiveness of the exhaust gas condensate depends not only on the chemical composition and the pH values but also on the conducting capacity (Weltens *et al*., 2001).

The time spent by the exhaust gas in the exhaust system of a diesel engine is short and thus cooling is only slight. As a result, the gas temperature in the cold end of diesel engines exhaust is higher than that of petrol engines. The diesel is operating at high air excess, therefore the dew point (below which the exhaust gas condensates) is relatively low, between 10 ^oC (at low engine load) and 40 ^oC (at high engine load). This means that in diesel vehicles exhaust gas condensate is only produced in the silencer in winter. The dew point for the petrol engines is approximately at 50 ^oC, and exhaust gas condensate is produced both in winter and summer (Weltens *et al.*, 2001).

If the vehicle is continually driven over short distances or in 'stop and go' conditions, the rate of corrosion will accelerate, as the exhaust system is unable to reach condensation evaporation temperature. This is a key factor in premature corrosion-induced failure of exhaust systems.

The silencer of both the petrol and diesel engines is much cooler than the hot end components, with the maximum temperature of 400 ^{o}C (Inoue and Kikuchi, 2003). As a result, it is subjected to extremely high corrosion due to an increased rate of exhaust gas condensation coupled with lower rates of evaporation (Weltens *et al.*, 2001).

2.4 Corrosion of exhaust systems

Exhaust systems are degraded by both structural and cosmetic corrosion. Structural corrosion includes the deterioration of exhaust components, while cosmetic corrosion includes rust staining and corrosion of the exhaust components (Baboian, 1990). The corrosion behaviour of components is dependent upon a number of factors: alloy composition, surface condition, geometry and pre-treatment of the substrate alloy, corrosive environment, temperature (usually cyclic in exhaust systems) and time of exposure (Norton *et al.*, 1993), while the corrosion mechanisms are dependent on factors such as physical and chemical properties of the environment, materials in use and the specific application (e.g. condensation corrosion is the major cause of failure in silencer components) (Cayless, 1974). The exhaust systems of vehicles are exposed to two different environments; externally to the atmosphere and internally to exhaust gases with their products of combustion (Vigor *et al.*, 1977). It has also been found that in exhaust systems corrosion is involved in four out of five cases of failures while fatigue accounts for the remainder (Oliver and Sephton, 2003).

Each of the major degradation problems (internal corrosion, external corrosion and oxidation) are discussed in detail, in the following sections.

2.4.1 Internal corrosion

The relatively low exhaust gas temperatures in the cold end lead to condensate formation, particularly in the silencer components and tail pipes, and internal corrosion due to this condensate on the internal surfaces of the cold end is a major cause of degradation (Douthett, 1995). Cooler skin temperatures can also lead to external corrosion due to salts, in cold regions where the roads are treated with de-icing salts (Baboian, 1996).

Condensate corrosion is the principal concern of stainless steel exhaust system failure, particularly within the silencers or long tail pipes usually found in light trucks. Front wheel-drive vehicles are even more prone to condensate problems as silencers could be moved to even cooler locations close to the rear bumpers (Douthett, 1995; Fujita *et al*., 1996).

The condensate is formed by acid products of combustion (Cayless, 1974). There are two inorganic acids contained in the condensate:

a) Nitric Acid: This acid forms from certain nitrogen oxides that are converted from the nitrogen that is present in the atmosphere, and is taken into the engine (Cayless, 1974).

b) Sulphuric and sulphurous acids: Fuels and lubricating oils contain quantities of sulphur which is passed into the exhaust in the form of sulphur dioxide and sulphur trioxide. These oxides react with water vapour to form sulphurous and sulphuric acid (AK Steel Exhaust System Steel, 2002; Cayless, 1974).

The aggressiveness of internal corrosion results from the low pH of the condensate. The main cause of this low pH is sulphuric acid. In catalytic converters, the chloride compounds used in precious metal deposition have often been a source of exhaust gas chlorides. Some chlorides are from the fuel. The chloride compounds condense as hydrochloric acid and/or ammonium chloride. This can either increase or decrease the initial acidity, but either will result in chloride ions in the condensate (AK Steel Exhaust System Steel, 2002).

The temperature of the cold end is a vital factor governing internal corrosion; the dew point being in the region of 95 ^{o}C. Hence, if the ambient temperature or the use of the vehicle is such that the exhaust system never really becomes hot, the rate of corrosion will be much higher. On vehicles that are used for relatively long fast journeys the inside of the system is protected to some extent by a layer of hard carbonaceous deposit. When the vehicle is only used for short journeys, remaining in a virtually cold running condition, this deposit tends to be softer and thicker, thus retaining the acid condensation like a sponge. This also occurs in the filling material of absorption type silencers (Cayless, 1974).

Condensate corrosion

As mentioned, condensation corrosion is the major internal corrosion found in exhaust systems. It is caused by the corrosive acid products of combustion which attacks the internal surface of exhaust systems. Condensate corrosion is enhanced by low temperature and is severe where the

exhaust systems are operating at relatively low temperature especially in the cold end (Cayless, 1974).

Water, as one of the combustion products can be condensed in the silencer if the temperature is low enough, especially during the winter in non-tropical countries. This condensate consists of various ions such as Cl^-, NH_4^+, SO_3^- and SO_4^{2-} from the sulphur contained in the fuel, NO_3^- and NO_2^- from the atmospheric nitrogen present in the atmosphere which is taken into the engine and converted to nitrate ions (Lothongkum *et al*., 1999; Miyazaki *et al*., 2000). The concentration of these ions is low at the beginning of condensation and increase with time. This is because the condensate volume is changed as water evaporates during the stoppage or the combustion during running of the engine (Cayless, 1974; Lothongkum *et al*., 1999).

Sulphur dioxide (SO_2), nitrogen oxides (NO_x), hydrogen sulphide (H_2S), ammonia (NH_3) and particulate matters are known for their effect on corrosion of metals (Baboian, 1996). The nitrogen oxides are capable of forming nitric acid (HNO_3), while the conversion of sulphur dioxide to sulphuric acid (H_2SO_4) is enhanced in the presence of nitrogen dioxide (NO_2), according to the following reaction (Baboian, 1996):

$$SO_2 + NO_2 + H_2O \rightarrow H_2SO_4 + NO$$

The synergistic effect of these ions may have a greater contribution in the corrosion of automobiles than their individual effects. The severity of internal corrosion is determined by the strength or concentration of the corrosive solution (condensate), as well as the time and temperature of both heating time and wet time (AK Steel Exhaust System Steel, 2002).

2.4.2 External corrosion

This type of corrosion is experienced by both the hot and cold end. However, it is mainly the problem of the hot end due to the higher operating temperatures. External corrosion is caused by water condensing as the engine cools down, de-icing salt and dirt thrown up off the road by the wheels. Road de-icing salts, if kept in contact with hot components for long, remove the protective chromium oxide layer and result in intergranular and localised attack. The dirt (thrown up by wheels) can lie for some time on the upper surfaces of the components and accelerate the rate of corrosion. Poultice corrosion is especially accelerated in this way (Baboian, 1996). In colder countries during severe winter conditions, de-icing chemicals are used to maintain efficient road usage. Sodium chloride and calcium chloride are used for this purpose. The quantities (amount) of salts used have been found to be a major contributor in corrosion of exhaust systems (Baboian, 1996; Cayless, 1974). The combination of the chloride (a film

disrupter on metal) and acidic rain (which provide reducible hydrogen ions) can be much worse than their added separate effects. Thus, geographical areas which are subjected to both road salts and acid deposition are likely to be the most corrosive to automobiles (Lothongkum *et al*., 1999).

Localised corrosion

The corrosion of stainless steels by exhaust gas condensate is mainly in the form of localised corrosion such as pitting or crevice corrosion (Sato *et al*., 1991). The most corrosive salt is $FeCl_3$ (iron ions are from the corrosion product of the stainless steel) and its corrosivity is due to the high redox potential, a high concentration of chlorine ions and a low pH (Olsson and Hornstrom, 1994).

Pitting corrosion is a localised corrosion attaching the weak spots in an unusual corrosive resistant film which can result in small holes (pits) perforating the material (Malik *et al*., 1992; Jones, 1996). It is an insidious form of localised attack which has been attributed to the catalytically enhanced transfer of metal ions from the oxide matrix to the electrolyte, preventing oxide formation at the pit surface and enabling stable pit growth to occur (Ningshen *et al*., 2001). The most commonly encountered cause of pitting, chlorine ions, can penetrate and destroy the oxide film that is responsible for the corrosion resistance of stainless steels (Alhajji, 1997). The initiation phase of pitting corrosion is the result of breakdown of the passive film on the metal due to the presence of these chloride ions and subsequent establishment of an electrochemical cell in which the damaged site acts as an anode and the passive site acts as a cathode (Malik *et al*., 1992).

Non-metallic inclusions are favourable sites for initiation of localised corrosion (Newman, 2001). In basic stainless steel grades these inclusions tend to contain manganese and sulphur (Newman, 2001; Pistorius and Burstein, 1994), and in the presence of chloride ions, these manganese sulphide inclusions act as active anode sites, which corrode faster than the passive stainless steel surface, forming pits.

When localized areas of the surface passive layer are damaged (usually by grit impact), they are no longer able to protect the underlying metal against attack (Newman, 2001; Olsson and Hornstrom, 1994

Stainless steels have a pitting resistance equivalent (PRE) which is used to measure the relative susceptibility of a stainless steel to pitting corrosion. It is a measure of alloying elements which

reduce the tendency towards pitting i.e. chromium, molybdenum and nitrogen. The pitting resistance equivalent is given by (Alhajji, 1997; Lee *et al*., 2002):

$$PRE = \%Cr + 3.3\%Mo + 16\%N$$

The higher the PRE number, the better the resistance to pitting corrosion. Generally it is considered that a PRE greater than 34 is necessary for acceptable material performance in chloride containing environments (Lee *et al*., 2002).

The pitting behaviour of stainless steels in exhaust systems is greatly influenced by the variation in chloride ions, pH, dissolved oxygen, temperature and flow conditions. It has been found that low pH, high chloride ion concentration and stagnancy are the most favourable conditions for initiation and propagation of pits in austenitic stainless steels (Malik *et al*., 1992; Sato *et al*., 1991).

The pitting potential depends linearly on the logarithm of the chloride ion concentration (Yashiro and Tanno, 1990). This is of particular interests in exhaust system since the chloride ion concentration differs from petrol engine to diesel engine. This linear relationship between pitting susceptibility and logarithm of chloride ions concentration is up to 200 ^{o}C, the typical temperature encountered in the cold end. Pitting susceptibility becomes less pronounced above this temperature (i.e. in the hot end) because of the change in the nature of the passive film (Yashiro and Tanno, 1990).

The competitive adsorption of sulphate ions and chloride ions on the pit surface are the controlling factors on pit growth kinetics (Zhang *et al*., 1993). The sulphate ions catalyse the anodic dissolution. They enter into competition with hydroxyl groups which usually induce passivity and lead to a film structure containing defects. The absorbed sulphur induces an irreversible breakdown of passive film, leading to corrosion (El Hajjaji *et al*., 1995; Abd El Meguid *et al*., 1998).

The addition of sulphate ions in a neutral solution containing chloride ions has a dual effect on the characteristics of metastable and stable pits in that it affects both the initiation and propagation of pits. Pit initiation is partially inhibited by sulphate ions, in which case the number of available pit sites is lowered. At high potentials, this inhibitory effect is lost. Pit growth is also affected and the pits propagate at a lower current density in the presence of sulphates (Pistorius and Burstein, 1992).

Intergranular corrosion

Intergranular corrosion occurs near welds when the stainless steel has not been stabilised (Kain, 1993), when impurities are segregated or when passivating elements such as chromium in stainless steel are depleted at the grain boundaries, resulting in the grain boundary regions being less corrosion resistant. This may lead to preferential corrosion at the grain boundaries which can be severe enough for grains to drop out of the surface (Jones, 1996). Since some exhaust system components are welded, this type of corrosion is inevitable.

It is known that austenitic stainless steels through the temperature range of 475 to 850 ^{o}C become sensitised. Since the temperature range in the exhaust systems is between 300 to 950 ^{o}C (Sato and Tanoue, 1995), therefore these stainless steels are subjected to sensitisation.

Under certain conditions, the annealed stainless steels may result in intergranular corrosion without being first sensitised. The main reason for intergranular corrosion of nonsensitised stainless steels are: a) stainless steels containing active inclusions, in the form of stringers and these stainless steels results in intergranular corrosion in oxidising environments of nitric acid; and b) low temperature sensitisation – which becomes significant when operating temperatures are between 300 and 475 ^{o}C, as experienced by the cold end, however it may take years before this effect becomes significant (Kain, 1993).

Poultice corrosion

Poultice corrosion is the term used to describe the corrosion due to the collection of road salts and mud on ledges and pockets that are kept moist by rain and water pools on the road. During a routine driving of a car, water, mud, de-icing salts and dust controlling salts stick to the underside of the car, which then result in poultice corrosion which can be accelerated by grit impact. This corrosion (perforation) occurs at other entrapment areas where poultice can build up and also at failed coatings (Baboian, 1996).

Internal corrosion in the system leads to perforation corrosion, generally from inside to outside, which accelerate poultice corrosion (Baboian, 1996).

2.4.3 External oxidation

Oxidation is the major cause of failure in hot end components. However, in some instances, several hot end components fail due to exterior hot salt attack (i.e. due to external corrosion). Oxidation is a dynamic process which is mostly dependent on temperature, time, temperature fluctuation and environment (AK Steel Product data Bulletin, 2003).

The service environments in exhaust systems incorporate thermal cycling and contain combustion products such as water vapour, carbon oxides and sulphur from fuel. These combustion products have a detrimental effect on oxidation resistance (Jones, 1996), in that they aggravate external corrosion by weakening the inside layer of the components.

At the high operating temperatures of the hot end, a chromia film can form by selective oxidation of the chromium components of the stainless steel, and the corrosion is then controlled by the solid state diffusion of metal ions across the oxide layer (Corrosion Institute of South Africa, 1994). In general, at this high operating temperature, the material reacts with oxygen or other gases to form a film (chromia or other oxides) that may protect the underlying metal. This oxide film may be protective and persist for a finite time after which 'scale breakaway' occurs and thereafter a scaling rate develops. This oxide film can also be non-protective, allowing rapid oxygen penetration to the metal and resulting in rapid deterioration by internal oxidation, which may render the material brittle and unusable without much observable surface or weight change (Jones, 1996). The oxides formed are ductile at high temperature and are often brittle at lower temperatures. Oxides have coefficients of thermal expansion that differ from those of the metals from which they have formed. Therefore, stresses develop when the temperature changes, particularly during running and stopping of the vehicle, and may cause the oxides formed at high temperatures to loose their adherence to the substrate alloy when cooled to lower temperatures and become non-protective when reheated (Bradford, 2002; Jones, 1996). The chemical and physical properties of the oxide that forms are important when the rate of oxidation is determined and therefore allows determination of the probable life of the components exposed to oxidising environments.

In general, ferritic stainless steels can either oxidise non-selectively to form (Fe, Cr) spinel, or by the selective oxidation of the less noble constituent (chromium) to form chromia film (Robertson, 1991; Wouters *et al*., 2002). The chromium content of the stainless steel must exceed about 14%

for the formation of a chromia layer, whether the stainless steel is ferritic or austenitic. This is the same value needed to form a passive chromia film by selective dissolution (Robertson, 1991).

2.5 Simulation tests for exhaust systems

The corrosion tests discussed below are classified as accelerated laboratory tests. In general, these tests are more simplistic and usually differ from actual service conditions but can be conducted in such a way that they simulate actual operating conditions. Accelerated corrosion tests are designed to produce results in significantly shortened time periods and often deviate from actual service exposure. It is therefore advisable to take caution when attempting to correlate the results of most accelerated tests to actual in-service performance. However, by the very nature of accelerated corrosion tests, these procedures can rarely (if ever) be used to confidently predict service life. These tests are usually used to measure the relative field performance in terms of a particular corrosion mechanism or mode (Bradford, 2002).

There are many factors which make it difficult to correlate accelerated laboratory tests to in-service performance. Those factors are: a) the shortened time frame mentioned above; b) in general, laboratory tests are more simplistic and standardized, with fewer variables than actual service conditions; c) multiple failure mechanisms or modes and their interaction in the field are not easily reproduced in the laboratory. Artificially accelerating one corrosion mechanism may retard another; d) acceleration of corrosion by adjusting a few selected variables in laboratory tests usually does not represent the complex interaction of multiple variables under actual service conditions; and e) small coupon size, sample geometries and finite number of samples can affect laboratory studies compared to the actual service environment and laboratory specimens usually deviate from production parts or components used in actual service, especially when details pertaining to the surface condition are considered (Bradford, 2002; Jones, 1996).

It has been found that there is no simple accelerated corrosion test that will accurately correlate to in-service use. However, for specific applications (such as cosmetic automotive corrosion) some relatively sophisticated tests (such as cyclic corrosion tests) have been shown to correlate better to service performance than overly simplistic tests (such as conventional salt spray tests) (AK Steel Product data Bulletin, 409 SS).

There are different types of corrosion tests which are used to evaluate materials for exhaust systems. These tests are thoroughly detailed below.

2.5.1 Immersion tests

Immersion tests are considered as relatively uncomplicated tests involving constant or cyclic immersion. Since immersion of specimens in a gaseous or liquid corrosion environment provides relatively simple conditions, there are a number of factors that must be controlled to obtain adequate reproducibility of the results. These factors are: a) state of the surface of the specimen; b) size, shape and method of suspension of the specimen; c) depth of immersion; d) size and shape of the vessel and particularly its cross section; d) volume of the corroding liquid; e) stability of the apparatus e.g. whether truly stagnant condition are obtained; and f) temperature and its variations (Champion, 1964).

As mentioned, immersion tests can be divided into two categories: direct (simple) immersion tests and alternate (or cyclic) immersion tests. Simple immersion tests are tests where small sections or samples of candidate materials are exposed to the test medium for a period of time and the weight loss or pit depth of the material measured. In alternate immersion tests a specimen is immersed for a period of time in an environment, then removed and dried before re-immersion to continue the cycle. The conditions are of practical importance since they simulate, for example, the running and stopping of an engine. In addition, they often provide relatively rapid results. Normally hundreds of these cycles are completed during the course of a test program (Champion, 1964).

Immersion tests (either simple or alternate tests) can further be divided in to two types: Total immersion and partial immersion. In partial immersion, it is recommended that the depth of immersion must be more than 20 mm of the sample height. The volume of solution is required to be at least 100 L/m^2 of surface exposed. This is done in order to minimise contamination of the solution by corrosion products. Coupons of different materials are required to be tested separately if the corrosion products could affect the results of another (Bradford, 2002). In partial immersion, when the attack is largely at the 'water-line' the effects of corrosion may be accelerated by accurate maintenance of the liquid level (Champion, 1964).

In immersion testing, acceleration is achieved by: a) lengthening the exposure to the critical conditions that are suspected to cause corrosion damage; b) applying cyclic temperature ranges; c) acidifying the corrosive medium; d) increasing the corrosivity of the medium by other chemical changes (e.g. salt concentration, degree of aeration, addition of oxidizing species, temperature, pressure etc.); and e) alternate wetting and drying (can lead to a surface

concentration effect of corrosive species). However, the danger that conditions may be shifted away from actual service conditions, with the risk of poor correlations between test and actual service performance must be kept in mind. The degree of damage during testing will in most cases be greater than in actual operation (Champion, 1964; ASTM G48, 2002).

The most serious disadvantage of this method of corrosion study is the assumed average-time weight loss. The corrosion rate could be high initially and then decrease with time (it could fall to zero). In other cases the rate of corrosion might increase very gradually with time or it could cycle or be some combination of these conditions (Siebert, 1983). Another potential disadvantage in immersion tests is that corrosion may be locally accelerated by contact with the sample-support. The contact may be minimized by using an insulated support or using point contacts and minimum number of contacts (Champion, 1964).

2.5.2 Cabinet tests

Cabinet testing refers to tests conducted in closed cabinets where the conditions of exposure are controlled and mostly designed to accelerate specific situations while trying to simulate as closely as possible the corrosion mechanisms at play.

There are three main types of cabinet tests (Bradford, 2002; Jones, 1996; Mangonon, 1999):

a) Controlled humidity tests. There are many different variations of creating and controlling fog and humidity in cabinets for corrosion testing of a broad spectrum of products. The basic humidity test is most commonly used to evaluate the corrosion resistance of materials or the effects of residual contaminants. Cyclic humidity tests are conducted to simulate exposure to high humidity and heat typical of tropical environments.

b) Corrosive gas tests. In these tests, controlled amounts of corrosive gases are added to the humidity to replicate more severe environments. Some of these tests are designed to reveal and amplify certain characteristics of a material. This test is particularly adapted to the needs of the electronics industry.

c) Salt spray testing. This is the oldest and most wildly used cabinet test. See for example ASTM B117 (Test Method of Salt Spray [Fog] Testing), a test that introduces a spray in a closed chamber where some specimens are exposed at specific locations and angles. The concentration of the NaCl solution is usually varied from 3.5 to 20%, and humidity from low to 100%. This test is only appropriate to simulate marine atmospheres, particularly coastal environments. It is

used extensively for specification purposes and determining coating resistances, but results from salt spray testing seldom correlate well with service performance. Increasingly, modern accelerated atmospheric corrosion tests are based on cyclic exposure conditions rather than the continually wet (constant exposure) conditions of the more simplistic, traditional salt fog tests.

It is sometimes possible to correlate cabinet test results with service performance by establishing the acceleration factor and also by verifying that the corrosion mechanisms are indeed following the same path. As a result a representative and exact forecast for the outside corrosion stability of silencers and connecting pipes is possible. In cabinet test it is possible to test the wet corrosion stability of sheet metal for exhaust systems under conditions which match those found in the rear silencer (Weltens *et al.*, 2001). These tests are always preferred when testing a large number of specimens.

Cabinet tests are often criticised, for unrealistic test conditions leading to poor correlation with in-service or real environment performance and the question of how meaningful the test data is, as well for sample-to-sample and cabinet-to-cabinet variations. However, it has also been found that simplistic salt fog testing is value in its ability to highlight shortcomings and advantages of certain corrosion protection schemes, its widespread use and its track record as a quality control tool (Bradford, 2002).

2.5.3 Electrochemical tests

While all laboratory corrosion tests require accelerating corrosion processes, only electrochemical tests can directly amplify the impact of corrosion processes. The main reason why this is possible is the fact that all the electrochemical tests use some fundamental model of the electrode kinetics associated with corrosion processes to quantify corrosion rates. The amplification of the electrical signals generated during these tests permit very precise and sensitive measurements to be carried out (Pardo *et al.*, 2002).

Electrochemical tests are mainly used to obtain instantaneous corrosion rates, and to evaluate the susceptibility of materials to localized corrosion or passivation in specific environments. These polarization curves show how the solution potential affects the corrosion rate (Bradford, 2002; Pardo *et al.*, 2002). Electrochemical tests produce results more quickly than any other laboratory testing method. There are four main types of electrochemical (which apply an external current) tests: a) linear polarisation resistance b) potentiodynamic polarization; c) electrochemical impedance spectroscopy; and d) electrochemical noise.

Potentiodynamic polarization is a technique where the potential of the electrode is varied at a selected rate by application of a current through the electrolyte. It is probably the most commonly used polarization testing method for measuring corrosion resistance and is used for a wide variety of functions. It uses a test cell consisting of working electrode (sample), reference electrode, and counter electrode (Bradford, 2002). These tests determine instantaneous corrosion rates, indicate the susceptibility of materials to passivate and/or to pit, as well as the condition (active or passive) of the material in an environment.

Electrochemical impedance spectroscopy permits the determination of corrosion rates, and provides information about corrosion kinetics and mechanism of the corrosion. The advantage of this technique compared to polarization tests is that only a small perturbation is necessary to obtain the response of the system under investigation. It is a non-destructive method which allows corrosion monitoring at increasing times (Bradford, 2002).

Cyclic polarization scans – these tests provide one more complication to the polarization curve but gives valuable information about susceptibility to pitting and crevice corrosion of active passive metals, particularly stainless steels (Laitinen, 2000).

Electrochemical techniques are frequently the quickest and most satisfactory method of making a preliminary selection of the best candidate materials. The usefulness of electrochemical corrosion tests for short term, accelerated testing is based on a) the application of external current that allows corrosion damage, such as pitting corrosion, to be induced and studied in very short time frames (typically within minutes) and b) electrochemical corrosion rate measurements can be made almost instantly, long before a conventional weight change would be measurable (Siebert, 1983).

2.5.4 Oxidation tests

Laboratory oxidation tests provide useful information for preliminary screening or ranking of candidate alloys for various elevated temperature applications (Allegheny Ludlum, 2003). The test temperature and exposure times depend greatly on the purpose of the test and often simulate a specific application. There are two types of oxidation tests: isothermal (continuous) and cyclic oxidation. The cyclic oxidation test is most frequently used for exhaust system conditions (Nicholls and Bennett, 2000).

The prediction of cyclic oxidation lifetimes requires: a) an understanding of the causes of cyclic oxidation failure; b) the determination of reliable, possibly reproducible, cyclic oxidation data;

and c) the development of predictive models for cyclic oxidation that can take into account the stoichastic nature of all failure modes, such that material performance under both normal and extreme operating conditions can be deduced (Nicholls and Bennett, 2000).

2.6 Test methods used in exhaust systems

In this section all the tests that could be discovered from literature are listed in detail. The various tests that deal with this same aspect are grouped together so that their similarities and differences can be compared.

2.6.1 Internal corrosion

The internal corrosion referred to in this section occurs only in the cold end components since their lower temperatures allow for the condensation of corrosive exhaust gases. The tests to evaluate material performance under these types of conditions are given here, exactly as found in literature. At this stage no distinction between petrol and diesel engines are made.

Condensate tests

As far as could be established, only cyclic immersion tests are conducted of which the primary tests are condensate tests. All the tests listed below are stopped after stable weight loss rates are reached and significant differences are detectable.

Table 2.3: *Experimental procedures of the internal condensate tests*

Test name and source	Condensate	Testing Procedure
Exhaust system condensate corrosion test (Allegheny Ludlum Technical Data Blue Sheet, 2003; Stainless Steel AL 409 HP™ Ferritic Stainless Steel, 2003)	1000 ppm Cl^- 2000 ppm CO_3^{2-} 3740 ppm NH_4^+ 5000 ppm SO_4^{2-} 100 ppm NO_3^- pH 8.7 – 8.9	• Sample is fully immersed in a beaker containing about 100 ml a condensate solution and then exposed to controlled temperature cycles consisting of: a) heating from ambient temperature to 250 ^oC in one hour b) holding at 250 ^oC for two hours c) cooling to ambient temperature in three hours. • After the six hour cycle, only solid residue remains from the original test solution, and another 100 ml solution is added to the beaker with the sample. The cycle is then repeated. • Samples are cleaned to bare metal and weighted after every ten cycles.
Condensate corrosion test (Lothongkum *et al*., 1999; Miyazaki *et al*., 2000)	250 ppm Cl- 1250 ppm SO_3^- 1250 ppm SO_4^{2-} 2000 ppm CO_3^{2-} 100 ppm NO_2^- 20 ppm NO_3^- 400 ppm CH_3COO^- 250 ppm HCHO 100 ppm $COOH^-$ 2500 ppm NH_4^+ 50 g/l Activated carbon	• The samples (50 mm by 100 mm) are first heat treated at 400 ^oC for five hours in air. This is done only at the start of the test • Cycle – samples are fully immersed in a beaker containing the condensate solution. • The beaker with the sample is then placed in a water bath at 80 ^oC and kept for 24 hours, which completely evaporates the condensate solution. • This is followed by softly brushing the samples and washing the beaker to complete a cycle. • Evaluation of pit depth and measurement of weight loss is done after every 10 cycles.
Continuous condensate corrosion test (AK Steel Product data Bulletin 439 SS, 2003)	Synthetic condensate solution	• The samples are oxidised at 350 ^oC for five hours before exposure to the condensate solution. • Half the lengths of the 90 mm by 40 mm coupons are immersed in a 500 ml beaker of condensate solution. • The solution level is kept constant in the beaker by

		means of water chilled glass condenser tops. • The temperature of the condensate solution is kept at 80 ^{o}C by using a constant temperature bath. • Pit depths are measured periodically.
Nippon steel condensate (NSC) test (Sato and Tanoue, 1995)	50 ppm Cl^- 500 ppm CO_3^{2-} 220 ppm NH_4^+ 100 ppm SO_4^{2-} pH 8.5 pH is adjusted with NH_4OH	• The samples (50 mm by 100 mm) are preheated by heating in air at 300 ^{o}C for one hour before the test. • The samples are partially immersed in a 200 ml beaker containing the condensate solution. • The beaker is heated to 130 ^{o}C for 30 minutes and held at this temperature for four hours, followed by cooling in the furnace for 30 minutes. • Samples are cleaned to bare metal and weighed after every cycle.
Half immersion test (Kobayashi *et al*., 1988; Hooper, 1978)	0.1 wt % HCl 1.0 wt % H_2SO_4 1.0 wt % CH_3COOH 1.0 wt % HCOOH pH 8.0 is adjusted by adding NH_4OH	• Samples are half immersed in the beaker containing the condensate solution. • Temperature is maintained at 80 ^{o}C • This test is run for four weeks. • Samples are cleaned to bare metal and weighed after the test and visual evaluation is done.
Diesel cyclic immersion test (Nkosi and Sephton, 2003)	52 ppm Cl- 175 ppm SO_4^{2-} 0.1 ppm NH_4^+ 35 ppm NO_3^- 0.01 ppm NO_2^- 1.3 ppm PO_4^{3-} pH 1.3	• The samples are fully immersed in the beaker and charged in to a furnace. • They are heated at a rate of 13 ^{o}C/min up to 400 ^{o}C and held for 4 hours at 400 ^{o}C, followed by cooling in the furnace for 30 minutes and then removed from the furnace and left in the open for overnight. • Corrosion products are either removed or not before commencing a consecutive cycle while replacing new solution to the beaker. • Weight loss is measured after each cycle.

Cabinet tests

These tests listed below simulate the condition of the cold end where, when the condensate forms, it does not evaporate immediately. They are all stopped after significant differences on the pit depth measurements are detectable.

Table 2.4: *Experimental procedures of cabinet tests for internal corrosion*

Test name and source	Solution	Testing Procedure
Silencer condensate corrosion test (AK Steel Product data Bulletin, 2003; Aluminised Steel Type 1 STAINLESS 409 and 439, 2003)	100 ppm Ammonium chloride salts 100 ppm NO_3^- 3000 ppm CO_3^{2-} 5000 ppm SO_4^{2-} pH 8.5	• The samples are partially immersed in the condensate solution. • The solution is slowly but completely evaporated at 90 ^oC (about 12 – 16 hours). • When the samples are dry, they are heated to 250 ^oC for one hour and then charged in to a humidity cabinet at 50 ^oC 85% RH for six hours. • Pit depth is measured after each such cycle.
Cold end synthetic condensate corrosion test (AK Steel Product data Bulletin 409 SS, 2003)	5000 ppm SO_4^{2-} 50 ppm Cl^- pH 2.5	• The samples are dipped daily for 15 minutes in the solution and air dried for 1.25 hours (75 minutes). • Then they are charged in a humidity cabinet at 85% RH for 22.5 hours and the temperature is cycled from 35 ^oC to 60 ^oC (and back) eight times in the 22.5 hours. • Once a week the samples are heated at 315 ^oC for 1 hour in air. (1 test cycle = 1 week). • Pit depths are measured periodically.
Boiling beaker internal condensate corrosion comparisons test (AK Steel Product data Bulletin 409 SS, 2003)	5000 ppm SO_4^{2-} 100 ppm Cl^- 100 ppm NO_3^- 100 ppm HCOOH initial pH 5.3 – 5.5 final pH 3.3 – 3.5	• The condensate with samples is boiled for 16 hours and then the samples are removed and heated at 260 ^oC for one hour, this is followed by exposure of the samples to 85% RH at 50 ^oC for six hours. • Pit depths are measured after every cycle.

2.6.2 External corrosion

The external corrosion taking place on the petrol and diesel exhausts is and is primarily due to de-icing salts (Weltens *et al.*, 2001). The simulation below consists of similar heating cycles and test solutions. Generally, for the cold end the test temperature is below 400 ^{o}C and for the hot end, it is above 400 ^{o}C. Material resistance to this type of corrosion is also evaluated by immersion and cabinet tests, and their procedures are explained below.

Immersion tests

These tests simulate cyclic conditions experienced in the hot end of an exhaust system. They are stopped after appreciable weight loss rates are reached.

Table 2.5: *Experimental procedures of immersion tests for external corrosion*

Test name and source	Solution	Testing Procedure
Hot salt damage (Hot end) (Fujita *et al*., 1996)	Saturated NaCl solution	• The cycle of the test comprises of holding the samples at 600 ^{o}C to 750 ^{o}C for two hours. • Then cooled in air and finally immersed in a saturated NaCl solution for five minutes. • The test is run for a maximum of 40 cycles and weights are measured before and after the test.
Hot salt resistance (front pipe simulation) (The Catalyst, 2002)	5 wt % NaCl	• The cycle consists of immersing the samples in the salt solution for 5 minutes. • Followed by heating at 700 ^{o}C and 760 ^{o}C for 90 minutes. • 15 cycles are conducted where weight loss is only determined after the entire test.

Cabinet tests

All the tests listed below are stopped after significant weight loss rates or/and pit depths are reached. They simulate cyclic conditions experienced in the hot and cold ends of an exhaust system.

Table 2.6: *Experimental procedures of the external corrosion of cabinet tests*

Test name and source	Solution	Testing Procedure
Cyclic corrosion test (CCT) (Lothongkum *et al*., 1999)	5 wt % NaCl	• Samples are salt sprayed for four hours at 35 ^{o}C and 98% RH. • The samples are then dried for two hours at 60 ^{o}C and 30% RH. • Finally the samples are humidified for two hours at 50 ^{o}C and 98% RH. • Pit depth is measured at the end of the test.
Cold end synthetic salt corrosion test (AK Steel Product data Bulletin 409 SS, 2003)	5 wt % NaCl	• Samples are dipped for 15 minutes daily in the NaCl solution and air dried for 75 minutes. • Then placed in a humidity cabinet at 85% RH for 22.5 hours and the temperature is cycled between 35 ^{o}C and 60 ^{o}C eight times in the 22.5 hours. • Once a week the samples are heated at 315 ^{o}C for 1 hour in air (1 test cycle = 1 week), starting before the test begins. • Pit depths are measured periodically.
External exhaust salt-humidity pitting corrosion test (AK Steel Product data Bulletin Aluminised Steel Type 1 STAINLESS 409 and 439, 409 SS, 2003)	5 wt % NaCl	• Samples are heated for one hour per week as follows: ▪ Silencer simulation: 316 ^{o}C ▪ Center pipe simulation: 427 ^{o}C ▪ Converter simulation: 538 ^{o}C ▪ Front pipe simulation: 760 ^{o}C • The samples are dipped daily in the solution for 15 minutes.

		• Followed by air drying for 75 minutes. • The samples are placed in the humidity cabinet at 85% RH and 60 ^{o}C for the remainder of the day. • Pit depths are measured after each weekly cycle.
High temperature salt corrosion test (Hot end) (AK Steel Product data Bulletin 409 SS, 2003)	5 wt % NaCl	• The sheet samples with a 90^{o} bend in and 5 mm Olson cup are dipped in the salt solution for 5 minutes. • Then the samples are exposed at 650 ^{o}C for 90 minutes in a furnace. • Followed by water quenching for one minute. • All these are repeated four times a day and then the samples are to a humidity cabinet at 85% RH and 60 ^{o}C for 18 hours. • Pit depths and weight loss are measured after every cycle.
Cyclical corrosion test (Cold end) (AK Steel Product data Bulletin, 439 SS, 2003)	Salt solution	• 100 mm by 50 mm in size samples are exposed to 260 ^{o}C in a furnace for one hour. • Then subjected to six hour cycle consisting of: ▪ Immersing the samples for 15 minutes in a salt solution followed by drying for 20 minutes at 4 ^{o}C and 35% RH. ▪ Followed by five hours and 25 minutes at 24 ^{o}C and 85% RH • The six hour cycle is repeated for the remainder of the week. • Pit depths are measured after every cycle.

Cyclical test (Option A) (AK Steel Product data Bulletin 439 SS, 2003)	5 wt % NaCl	• This test is run from Monday to Friday and consist of four cycles per day. • Firstly the samples are heated at 538 ^{o}C for one hour and water quenched before beginning the cycle exposure. • Cycle 1, 2, 3, and 4: the samples are exposed to 538 ^{o}C for one hour, cooled for one hour, immersed in NaCl solution for five minutes. • Evening and weekends: the samples are cycled between 35% RH at 4 ^{o}C for two hours and 85% RH at 24 ^{o}C for two hours. • Pit depths are measured after every weekly cycle.
Cyclical test (Option B) (AK Steel Product data Bulletin 439 SS, 2003)	5 wt % NaCl	• This test is run from Monday to Friday and consist of four cycles per day. • The samples are heated at 538 ^{o}C for one hour and water quenched before beginning the cycle exposure. • Cycle 1, 2, 3, and 4: samples are immersed in the NaCl solution for 15 minutes and dried for 20 minutes at 35% RH and 40 ^{o}C, and then the temperature is raised to 60 ^{o}C and RH to 85% and held for five hours and 25 minutes. • Evening and weekends: samples are held at 85% RH and 24 ^{o}C. • Pit depths are measured after every weekly cycle.
Hot end component test (Oliver and Sephton, 2003)	5 wt % salt solution which consists of: 95 wt % NaCl and 5 wt % $CaCl_2$	• Samples are exposed in the salt spray chamber and the temperature is slowly increased from 20 ^{o}C to 50 ^{o}C in 1.5 hours. • The salt spray is switched off while leaving the samples in the chamber for 1.5 hours. • The samples are then exposed to the furnace at 900 ^{o}C for three hours. • Followed by re-loading into salt spray chamber where the temperature is slowly decreased from 50 ^{o}C to ambient in 1.5 hours. • The salt spray is then switched off and samples

		remain in the salty humid environments overnight. • Weight loss is determined after the last cycle.
Hot salt corrosion tests (AK Steel Product data Bulletin 439 Ultra Form SS, 2003)	5 wt % NaCl solution	• Specimens are dipped in the solution for 5 minutes and then exposed for 90 minutes at 650 ^{o}C in a furnace. • Then water quenched for 1 minute. • This is repeated 4 times per day. • Followed by placing the samples in the humidity cabinet (85 percent RH at 60 ^{o}C) for 18 hours, to complete a cycle • The duration of a cycle is one week. • Weight loss is determined weekly.
Exhaust system cyclic corrosion tests (Allegheny Ludlum, 2003)	5 wt % NaCl solution	• Samples are heated in air at 650 ^{o}C for one hour. • Followed by natural cooling in air to ambient temperature. • The oxidised samples are then exposed as per ASTM B117 to salt spraying at 35 ^{o}C for 24 hours, to complete the cycle. • Weight loss is determined after every five cycles.

2.6.3 Electrochemical corrosion tests

Localised corrosion (anodic and cyclic potentiodynamic polarisation)

Testing for localized corrosion resistance usually aims at meeting one (or more) of four general goals: alloy ranking for selection or development; failure analysis; determination of the effects of changes in process parameters; and prediction of penetration rates. Of the four, the last is by far the most difficult to accomplish, but also the most important in many cases (Bradford, 2002).

Potentiodynamic anodic polarisation and cyclic or pitting polarisation measurements are used to evaluate the susceptibility of materials to localised corrosion (pitting and crevice corrosion). Potentiodynamic polarisation scans involve applying a potential between the counter and working electrodes (sample), using the reference electrode for measurement. Corrosion occurs due to the anodic oxidation of a metal e.g. iron ($Fe \rightarrow Fe^{2+} + 2e^{-}$). At the open circuit potential, E_{corr}, the

current generated by this reaction is balanced by current generated by the cathodic reduction reaction of hydrogen evolution ($2H^+ + 2e^- \rightarrow H_2$ or $O_2 + 4H^+ + 4e^- \rightarrow 2H_2O$) (Jones, 1996).

The corrosion potential (E_{corr}), primary passivation potential (E_{pp}), pitting potential (E_{pit}) and protection potential (E_{prot}) can be evaluated from polarization curves. The E_{corr} is a potential (voltage) that encourages the electrochemical reactions on the surface of the metal that corrode the metal. The corrosion potential (E_{corr}) is a potential at the intersection of the tangential line of cathodic current curve and active current curve as shown in Figure 2.1 (Vongbandit *et al*., 2002). The corrosion current density (i_{corr}) is the current density that relates to the open circuit potential and is proportional to the general corrosion rate. The general corrosion rates are obtained by using the following equation (Jones, 1996):

$$CR = 0.129\left(\frac{a}{nD}i\right)$$

Where CR is the corrosion rate in mils per year (mpy), a/n is the equivalent weight of the alloy, D is the density in g/cm^3, and i is the current density in A/cm^2.

The passive current density is shown by the region where the current density is independent of the potential. Primary passivation potential (E_{pp}) can be obtained by two methods; (1) E_{pp} is the potential at the peak current where the active-passive transition is occurred as shown in Figure 2.2 (Vongbandit *et al*., 2002) or (2) E_{pp} is the potential at the intersection of the tangential of passive current curve and active current curve as shown in Figure 2.3 (Vongbandit *et al*., 2002). Pitting potential (E_{pit}) can also be obtained by two methods; (1) E_{pit} is the potential at the intersection of the tangential line of passive current curve and forward scan transpassive current curve as shown in Figure 2.2 or (2) E_{pit} is the potential at the sudden change of transpassive current density curve due to initiation of localised (mostly pitting) attack (Allegheny Ludlum, 2003) as shown in Figure 2.4 (Vongbandit *et al*., 2002). Pitting resistance is defined by R_{pass}, which is the difference between E_{pit} and E_{corr}.

The protection potential (E_{prot}) is obtained from the intersection of passive current density curve and reverse scan transpassive current density curve as shown in Figure 2.4 (Vongbandit *et al*., 2002).

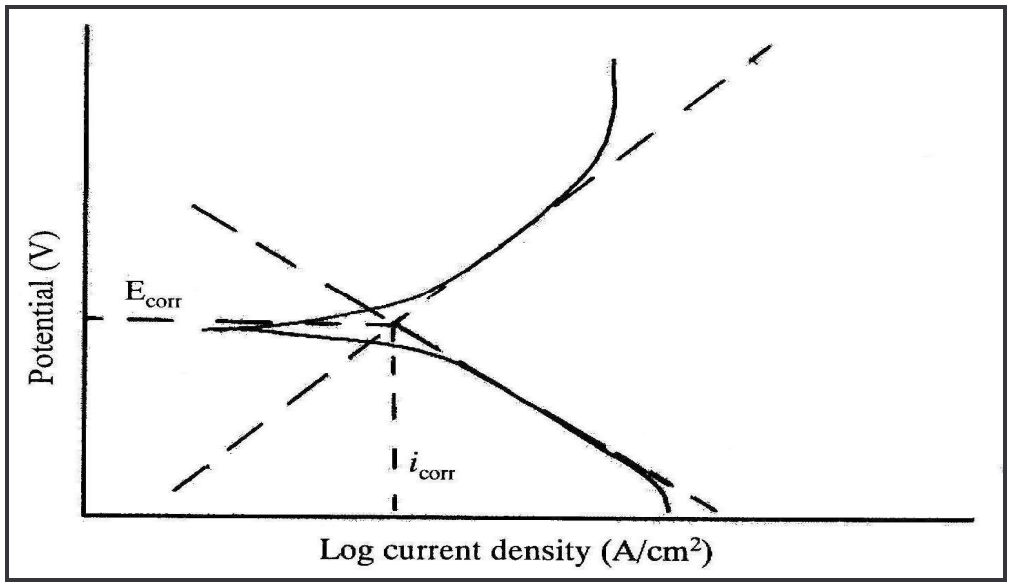


Figure 2.1: *Schematic representation of polarization diagram showing corrosion potential (E_{corr}) at the intersection of the tangential of cathodic current curve and active current curve*

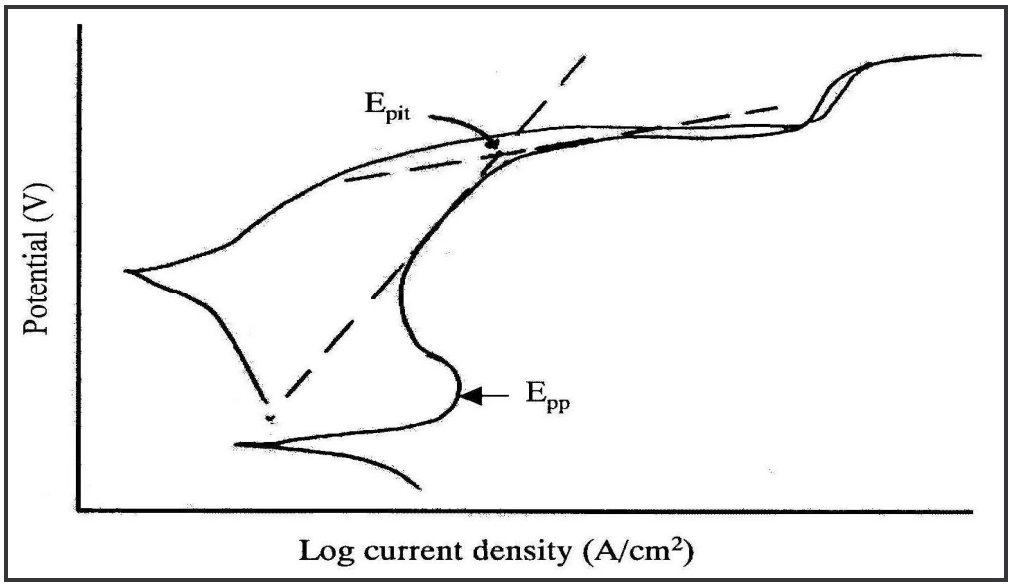


Figure 2.2: *Schematic representation of polarization diagram showing primary passivation (E_{pp}) potential as the potential at the peak current where active-passive transition is occurred and pitting potential (E_{pit}) at the intersection of the tangential of passive current curve and forward transpassive current curve*

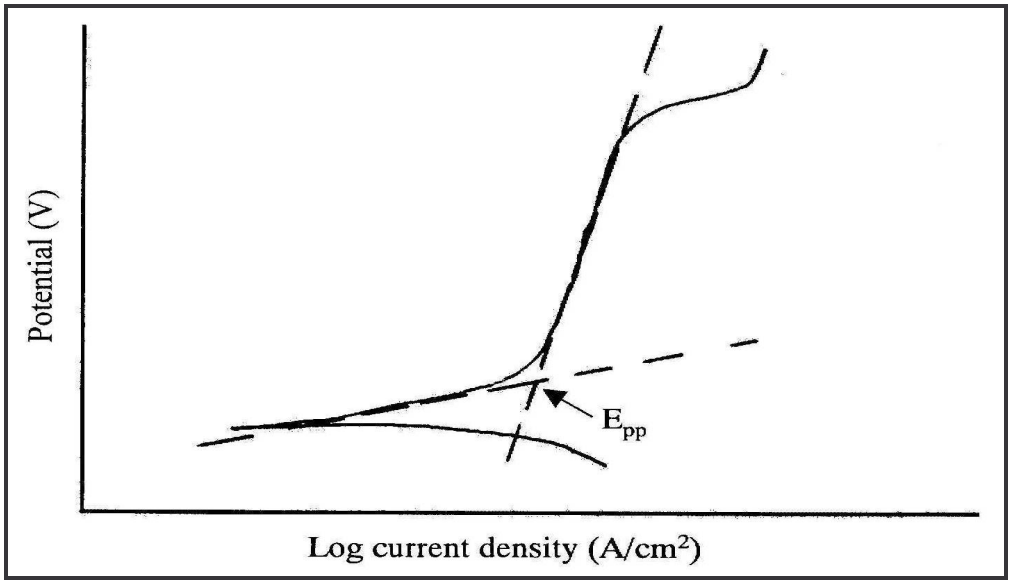


Figure 2.3: *Schematic representation of polarization diagram showing primary passivation potential (E_{pp}) at the intersection of the tangential of active current density curve and passive current density curve*

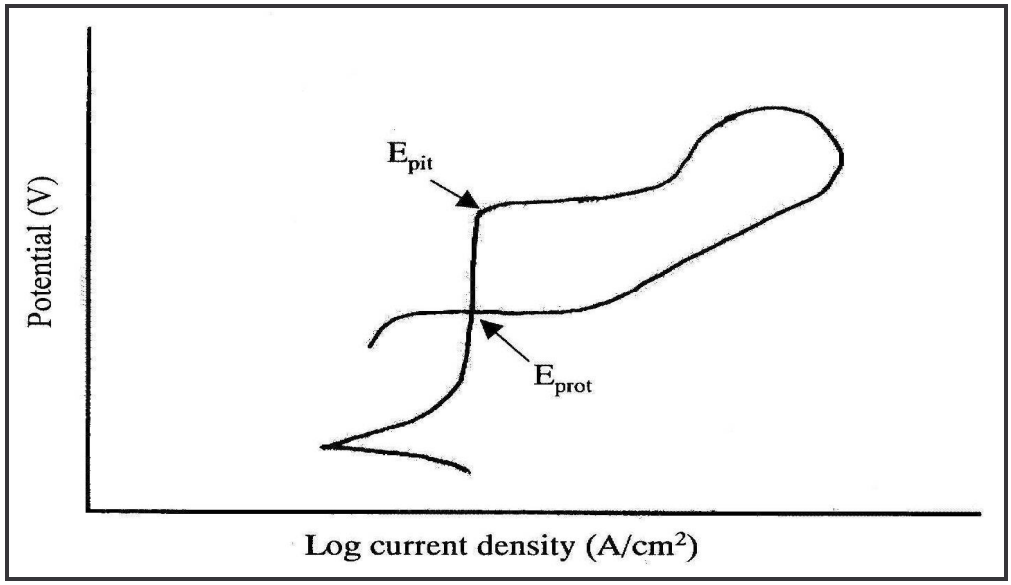


Figure 2.4: *Schematic representation of polarization diagram showing pitting potential (E_{pit}) at the intersection of the tangential of forward scan transpassive current curve and passive current curve and protection potential (E_{prot}) at the intersection of the reverse scan transpassive current curve and passive current curve*

In the cyclic polarisation diagrams, after some degree of anodic polarisation above pitting potential, the direction of polarisation is reversed and a hysteresis is observed in which the return polarisation curve follows an active path compared to the initial anodic one, as shown in Figure

2.4. Protection potential is defined by the crossover at the passive current density below which established pits presumably cannot continue to grow. By contrast, new pits initiate only above pitting potential. Between pitting potential and protection potential, new pits cannot initiate, but old ones can still grow. An alloy that is resistant to pitting shows no hysteresis, whereas susceptible alloys show increasing hysteresis (Vongbandit *et al*., 2002; Jones, 1996).

Potentiodynamic tests measure pitting corrosion by using a plain surface in its as-received condition or polished with a SiC paper to the desirable finish (between 240 to 1500 grit finish), rinsed in acetone and decreased in acetone under ultrasonic vibration for 5 minutes. Finally a cyclic potentiodaynamic or potentiodynamic sweep scan is performed (Sato *et al.*, 1991; Nkosi and Sephton, 2003)

In these tests, for internal corrosion, exhaust gas condensate solutions for either diesel or petrol engines are used. For external corrosion a salt solution, similar for both petrol and diesel engines is used. The experimental procedures and conditions are similar for the petrol and diesel engines because these tests are mostly conducted at room temperature (i.e. the potentiodynamic sweeps are conducted at room temperature for all the materials) (AK Steel Product data Bulletin, 2003).

Potentiodynamic tests can also be used to measure crevice corrosion, but requires a special sample configuration. A 6mm diameter hole is drilled at the center of the specimen, polished with a 400 emery paper, rinsed in acetone and decreased in acetone under ultrasonic vibration for 5 minutes. The specimens are then heated to 300 ^{o}C for 24 hours in the atmosphere, followed by fitting a polycarbonate bolt and nut to the 6 mm diameter hole to make an artificial crevice. Around the test area the specimens are sealed with silicone resin. After this procedure is complete a cyclic potentiodynamic scan is performed (Sato *et al.*, 1991).

2.6.4 Intergranular corrosion tests

There are various procedures which can be followed to evaluate the resistance of materials to intergranular corrosion. These tests are often conducted to investigate the corrosion behaviour of the welded baffle plates of a silencer (Lothongkum *et al.*, 1999).

Procedure

The different procedures which can be performed to sensitise specimens are:

a) The specimens are solution annealed at 1200 ^{o}C for one hour, water quenched, and subsequently sensitised between 500 and 650 ^{o}C for 15 minutes to 50 hours (Kwon *et al.*, 2002).
b) The specimens are solution annealed at 1100 ^{o}C for two hours then water quenched and sensitised by heating at 600 ^{o}C for one hour. All heat treatments are carried out in air (Putatunda, 1987).
c) The materials are welded (Lothongkum *et al.*, 1999).

The different procedures used to evaluate intergranular corrosion are as follows:
a) The sensitised specimens are ground with emery papers and polished with 1 μm diamond paste prior to corrosion tests. They are then immersed in boiling solution of 120 g/l of $CuSO_4.5H_2O$ and 60 vol % H_2SO_4 for 5 minutes, followed by washing with warm water. The surface is optically examined to determine the degree of grain boundary attack. Precipitates and grain boundaries are examined using Scanning Electron Microscope (SEM), Transmission Electron Microscope (TEM) and X-ray Spectroscopy (Kwon *et al.*, 2002).
b) The sensitised specimens are subjected to a modified Strauss test. The test solution consists of 10% $CuSO_4.5H_2O$ and 5% of H_2SO_4. This test is run for 24 hours after which the results are evaluated by visually rating copper plating to indicate the extent of sensitisation on the surface of specimens (Lothongkum *et al.*, 1999).

2.6.5 Perforation and cosmetic tests

Perforation and cosmetic tests are the most important tests in evaluating the duration of cosmetic appearances of exhaust systems, particularly the tail pipe. The slightest evidence of surface corrosion on exhaust systems can leave owners with a perception that the exhaust systems are of poor quality, despite the use of improved materials. As a result automotive corrosion engineers have worked hard to design tests which will ensure the material used appeal to car owners. These materials must also meet a variety of rigorous performance requirements for the exhaust system (AK Steel The Catalyst, 2002). These two tests were especially designed for such requirements.

Cabinet tests

Table 2.7: *Experimental procedures of Perforation and cosmetic tests*

Test name and source	Solution	Testing Procedure
Cosmetic corrosion (Neutral salt spray resistance) test (AK Steel Product data Bulletin, Black Coat SS)	Neutral salt solution	a) GM Standard 9984299. • Specimens are heated at 450 ^{o}C for 30 minutes. • Then quenched in water. • This thermal cycle is repeated five times, followed by exposure to the neutral salt spray for one week to complete the test.
		b) Ford Specification WSA-M2P170-A2. • Painted specimens are heated at 450 ^{o}C for 15 minutes, and water quenched. • This thermal cycle is repeated five times • They are then exposed to the neutral salt spray for 240 hours to complete the test. Results are visually analysed to rank the degree of rust and pit depth is measured.
Perforation corrosion resistance test (AK Steel Product data Bulletin, Black Coat SS)	Salt solution	a) Test A: • Samples are heated at 260 ^{o}C for one hour, once at the beginning of every week. • This is followed by a daily six hour corrosion cycle: ▪ Specimens are immersed in the salt solution for 15 minutes ▪ Then dried for 20 minutes at 40 ^{o}C and 35% RH ▪ Followed by a 5.4 hr humidity exposure at 60 ^{o}C and 85% RH. Pit depths are measured after a week.

		b) Test B: • Samples are heated at 260 °C for one hour, five times per week. • This is followed by six hour corrosion cycle: ▪ Specimens are immersed in the salt solution for 15 minutes ▪ Then dried for 20 minutes at 40 °C and 35% RH ▪ Followed by 5.4 hr humidity exposure at 60 °C and 85% RH. Pit depths are measured after a week.

2.6.6 External oxidation tests

Oxidation is the most important high temperature degradation form and the presence of a liquid electrolyte is not required. Sometimes the type of corrosion is called 'dry corrosion' or 'scaling' (Bullard *et al.*, 1992). The outside surface of an automotive exhaust system in use is hot and exposed to air, and therefore can undergo oxidation. Road de-icing salts may also come in to contact with the exhaust components, enhancing corrosion. External corrosion is of main concern in both the cold and hot end, but oxidation tests often simulate hot end conditions only because of its high temperature operation.

Various types of cyclic oxidation tests have been designed for stainless steels or other alloys to provide comparative data. In oxidation, there is a weight gain limit which is generally set: It is assumed that if any material gains or looses a weight of 1.55 mg/cm^2 or more within 100 hours (in continuous oxidation) or 135 hours (in cyclic oxidation), that material has failed, and such material can not be used under the simulated environment (AK Steel Product Data bulletin, 2003; Allegheny Ludlum, 2003). During the cyclic oxidation tests it is impossible to collect all the oxide scales, but in continuous oxidation the oxide scales can be collected in a covered crucible (e.g. of Al_2O_3) which to prevent the scattering of scales while cooling. However, measuring the weight-gain is often possible.

Since the automobile exhaust is usually heated cyclically, cyclic oxidation tests are the most widely used tests (Moroishi *et al.*, 1979).

Continuous oxidation tests

The different procedures of continuous oxidation tests are as follows:

a) Continuous oxidation test (Bullard *et al.*, 1992)

Continuous oxidation testing is conducted in a furnace for 24, 48 or 100 hours at temperature intervals between 750 – 1050 ^{o}C. The weight change of the samples is evaluated after the exposure.

b) Isothermal Oxidation test (Chassagne *et al.*, 2002)

The isothermal oxidation tests are carried out at 850 ^{o}C or 950 ^{o}C in air for up to 400 hours. Weight change measurements are done after the full exposure.

c) Oxidation resistance test (Miyazaki *et al.*, 1994)

The specimens are polished to a 320 grit finish and heated at 800, 900 or 1000 ^{o}C for 200 hours. Weight change is determined after the full exposure.

Cyclic oxidation tests

The different procedures of cyclic oxidation tests are as follows:

a) Cyclic oxidation (Chassagne *et al.*, 2002)

The resistance to thermal cycling of alloys is characterised at 850 ^{o}C or 950 ^{o}C up to 1200 cycles (or 400 hours total dwell time) using a severe thermal cycle (15 minutes heating, 20 minutes dwell time, 5 minutes air forced cooling). The weight change is evaluated daily.

b) Cyclic service scaling tests (AK Steel Product data Bulletin; Kwon *et al.*, 2002)

The materials are heated at 760 ^{o}C, 816 ^{o}C, 871 ^{o}C, 927 ^{o}C or 1093 ^{o}C up to 1000 cycles (or 500 hours total dwell time) using a severe thermal cycle (25 minutes heating and 5 minutes cooling). The weight change of the samples is evaluated daily.

c) Cyclic oxidation resistance tests (The Catalyst, 2002)

The samples are heated at 816 ^{o}C or 899 ^{o}C up to 1050 cycles (or 525 hours total dwell time) using a severe thermal cycle (25 minutes heating and 5 minutes cooling). The weight change of the samples is evaluated daily.

2.7. Summary of the testing methods

As a conclusion to this chapter, the testing procedures and solutions are summarised in this section since they are fundamental in developing the generic test protocol. The tests are classified according to the components and conditions of the exhaust system.

2.7.1 Cold end components

As mentioned, internal corrosion is mainly due to the exhaust gas condensing, causing very aggressive conditions in the cold end. In order to effectively reproduce the conditions, a solution closely simulating the condensate should be used as testing environment. In Table 2.8, below, the variations in the published composition of this simulated condensate solutions are summarised:

Table 2.8: *Summary of the published compositions for simulated condensate (testing environment)*

Ions	Concentrations (ppm)
Cl^-	50 (Sato and Tanoue, 1995) , 52 (Nkosi and Sephton, 2003), 100 (AK Steel Product data Bulletin, 2003), 250 (Lothongkum et al., 1999; Miyazaki *et al*., 2000) and 1000 (Allegheny Ludlum Technical Data Blue Sheet, 2003)
CO_3^{2-}	500 (Sato and Tanoue, 1995), 2000 (Allegheny Ludlum Technical Data Blue Sheet, 2003; Lothongkum *et al*., 1999; Miyazaki *et al*., 2000) and 3000 (AK Steel Product data Bulletin, 2003)
SO_4^{2-}	100 (Sato and Tanoue, 1995), 175 (Nkosi and Sephton, 2003), 1250 (Lothongkum *et al*., 1999; Miyazaki *et al*., 2000) and 5000 (Allegheny Ludlum Technical Data Blue Sheet, 2003; AK Steel Product data Bulletin, 2003)
SO_3^-	1250 (Lothongkum *et al*., 1999; Miyazaki *et al*., 2000)
NO_3^-	20 (Lothongkum *et al*., 1999; Miyazaki *et al*., 2000) , 35 (Nkosi and Sephton, 2003) and 100 (Allegheny Ludlum Technical Data Blue Sheet, 2003; AK Steel Product data Bulletin, 2003)

NO_2^-	0.01 (Nkosi and Sephton, 2003) and 100 (Lothongkum *et al*., 1999; Miyazaki *et al*., 2000)
PO_4^{3-}	1.3 (Nkosi and Sephton, 2003)
NH_4^+	0.1 (Nkosi and Sephton, 2003), 220 (Sato and Tanoue, 1995), 2500 (Lothongkum *et al*., 1999; Miyazaki *et al*., 2000) and 3740 (Allegheny Ludlum Technical Data Blue Sheet, 2003)
HCHO	250 (Lothongkum *et al*., 1999; Miyazaki *et al*., 2000)
$COOH^-$	100 (Lothongkum *et al*., 1999; Miyazaki *et al*., 2000)
$CH3COO^-$	400 (Lothongkum *et al*., 1999; Miyazaki *et al*., 2000)
HCl	0.1 (Hooper, 1978; Kobayashi *et al*., 1988) (wt%)
H_2SO_4	1.0 (Hooper, 1978; Kobayashi *et al*., 1988) (wt%)
CH3COOH	1.0 (Hooper, 1978; Kobayashi *et al*., 1988) (wt%)
HCOOH	1.0 (Hooper, 1978; Kobayashi *et al*., 1988) (wt%) and 100 ppm (AK Steel Product data Bulletin, 2003)
Activated carbon	50 (Lothongkum *et al*., 1999; Miyazaki *et al*., 2000) (g/l)
pH (adjusted with NH_4OH)	1.29 (Nkosi and Sephton, 2003), 8.0 (Hooper, 1978; Kobayashi *et al*., 1988). 8.5 (Sato and Tanoue, 1995) and 8.7 – 8.9 (Allegheny Ludlum Technical Data Blue Sheet, 2003)

From the ions and concentrations listed here, it is clear that a wide range of compositions and pH's are specified by the various authors. The implications of these values are discussed in more detail in Chapter 3.

Internal corrosion tests

The first summary of tests for testing internal corrosion of the cold end components is that of immersion tests and the second is that of cabinet tests. The stages and variations that the published tests show in each case are listed in Tables 2.9 and 2.10, respectively.

Table 2.9: *Summary for immersion tests for internal corrosion of the cold end components and the variations in each stage*

Stage	Variations
Prior heat treatment	No heat treatment (Allegheny Ludlum Technical Data Blue Sheet, 2003; Nkosi and Sephton, 2003; Hooper, 1978; Kobayashi *et al*., 1988)
	Heat at 300 ^{o}C for one hour (Sato and Tanoue, 1995)
	Heat at 350 (AK Steel Product data Bulletin, 2003) or 400 (Lothongkum *et al*., 1999; Miyazaki *et al*., 2000) ^{o}C for five hours
Immersion	Immerse fully (Allegheny Ludlum Technical Data Blue Sheet, 2003; Lothongkum *et al*., 1999; Miyazaki *et al*., 2000; Nkosi and Sephton, 2003)
	Immerse partially/halfway (Sato and Tanoue, 1995; Hooper, 1978; Kobayashi *et al*., 1988; AK Steel Product data Bulletin, 2003)
Heating cycle	Keep the samples in an 80 ^{o}C thermal bath, for 24 hours ((Lothongkum *et al*., 1999) to complete evaporation (Lothongkum *et al*., 1999; Miyazaki *et al*., 2000; Hooper, 1978; Kobayashi *et al*., 1988; AK Steel Product data Bulletin, 2003)
	Heat to 250 ^{o}C in one hour, keep for 2 hours and follow by cooling to ambient temperature in 3 hours to complete a 6 hour cycle (Allegheny Ludlum Technical Data Blue Sheet, 2003)
	Heat to 130 (Sato and Tanoue, 1995) or 400 (Nkosi and Sephton, 2003) ^{o}C for 30 minutes and hold for 4 hours, follow by cooling in the furnace for 30 minutes (Sato and Tanoue, 1995; Nkosi and Sephton, 2003)
Corrosion product	Removed by washing with running water after each cycle or 10 cycles (Allegheny Ludlum Technical Data Blue Sheet, 2003; Lothongkum *et al*., 1999; Miyazaki *et al*., 2000; Sato and Tanoue, 1995; Nkosi and Sephton, 2003; Hooper, 1978; Kobayashi *et al*., 1988; AK Steel Product data Bulletin, 2003)
Evaluation of results	Weight loss measurement (Allegheny Ludlum Technical Data Blue Sheet, 2003; Lothongkum *et al*., 1999; Miyazaki *et al*., 2000; Sato and Tanoue, 1995; Nkosi and Sephton, 2003; Hooper, 1978; Kobayashi *et al*., 1988) after every each cycle or 10 cycles
	Pit depth measurement (Lothongkum et al., 1999; Miyazaki *et al*., 2000; AK Steel Product data Bulletin, 2003)

In terms of cabinet test procedures for internal corrosion, only AK Steel (AK Steel Product data Bulletin, 2003) seems to have published any reports. Even though the tests are from the same facility, variations do exist in some of the stages, as listed in Table 2.10:

Table 2.10: *Summary of the solution and stages in the cabinet test for internal corrosion*

Stage	Variations	
Solution (all ppm)	Cl^-	50 (AK Steel Product data Bulletin, 2003b) (ammonium salt) or100 (AK Steel Product data Bulletin, 2003a; AK Steel Product data Bulletin, 2003c)
	CO_3^{2-}	3000 (AK Steel Product data Bulletin, 2003a)
	SO_4^{2-}	5000 (AK Steel Product data Bulletin, 2003a; AK Steel Product data Bulletin, 2003b; AK Steel Product data Bulletin, 2003c]
	NO_3^-	100 (AK Steel Product data Bulletin, 2003a; AK Steel Product data Bulletin, 2003c)
	HCOOH	100 (AK Steel Product data Bulletin, 2003c)
Heating cycle	Samples are heated at 250 (AK Steel Product data Bulletin, 2003a), 260 (AK Steel Product data Bulletin, 2003c) or 315 ^oC (AK Steel Product data Bulletin, 2003b) for one hour in every cycle (AK Steel Product data Bulletin, 2003a; AK Steel Product data Bulletin, 2003c) or once a week (AK Steel Product data Bulletin, 2003b)	
Immersion cycle	Samples are partially immersed and the solution is slowly evaporated in a thermal bath at 90 ^oC (12 to 16 hours) (AK Steel Product data Bulletin, 2003a)	
	Samples are dipped daily for 15 minutes in the solution and dried for 75 minutes (AK Steel Product data Bulletin, 2003b)	
	Samples are completely immersed and the solution is boiled for 16 hours (AK Steel Product data Bulletin, 2003c)	
Cabinet exposure	Samples are charged in the humidity cabinet at 50 ^oC (85% RH) for six hours (AK Steel Product data Bulletin, 2003a; AK Steel Product data Bulletin, 2003c)	

	Samples are charged at 85% RH for 22.5 hours and the temperature is cycled from 35 to 60 ^{o}C (and back) eight times in the 22.5 hours (AK Steel Product data Bulletin, 2003b)
Evaluation of results	Pit depths are measured after every cycle (AK Steel Product data Bulletin, 2003a; AK Steel Product data Bulletin, 2003b; AK Steel Product data Bulletin, 2003c)

External corrosion tests

The test procedures for determining material resistance to external salt damage are varied, as summarised in Table 2.11. The only commonality is that they all specify 5 wt% NaCl solution.

Table 2.11: *Summary of external corrosion tests of the cold end components*

Stage	Variations
Dipping in salt solution/ Salt spray	Spray: 4 hrs, 98% RH (Lothongkum *et al*., 1999), Dipped: daily for 15 min (AK Steel Product data Bulletin, 2003a), dipped: 15 min (AK Steel Product data Bulletin, 2003b), and dipped: daily for 15 min (AK Steel Product data Bulletin, 2003d)
Drying	2 hrs at 60°C, 30% RH (Lothongkum *et al*., 1999), in air for 75 min (AK Steel Product data Bulletin, 2003a and d), and 20 min at 4°C, 35% RH (AK Steel Product data Bulletin, 2003b)
Humidifying	2 hrs at 50°C, 98% RH (Lothongkum *et al*., 1999), cyclic: 35 to 60°C, 85% RH (8 times in 22.5 hrs) (AK Steel Product data Bulletin, 2003a), 25 min 24°C, 85% RH 25 min 24°C, 85% RH (AK Steel Product data Bulletin, 2003b), and rest of day 60°C, 85% RH (AK Steel Product data Bulletin, 2003d)
Heating	No heating (Lothongkum *et al*., 1999), once a week: 1 hr at 315°C (AK Steel Product data Bulletin, 2003a), once a week, 1 hr at 260°C (AK Steel Product data Bulletin, 2003b), and 1 hr per week, silencer simulation: 316 ^{o}C and center pipe simulation: 427 ^{o}C (AK Steel Product data Bulletin, 2003d)
One cycle	8 hrs (Lothongkum *et al*., 1999), 24 hrs: repeated for 1 week (AK Steel Product data Bulletin, 2003a), 24 hrs, 6 hrs, repeated for 1 week (AK Steel Product data Bulletin, 2003b), and repeated for 1 week (AK Steel Product data Bulletin, 2003d)

Evaluation: pit depths	At end of cycle (Lothongkum *et al*., 1999), periodically (AK Steel Product data Bulletin, 2003a), and weekly (AK Steel Product data Bulletin, 2003b and 2003d)

2.7.2 Hot end components

As mentioned before, the hot end components fail mainly due to external corrosion and oxidation. There is a variety of test published for comparing the corrosion resistance of materials in hot end external exhaust conditions. Tables 2.12 to 2.15 summarise all the tests together with the variations in each stage.

External corrosion tests

The heating and immersion tests as summarised in Table 2.12 are basically cyclic oxidation tests combined with immersion in a salt solution.

Table 2.12: *Summary for immersion tests for external corrosion of the hot end components and the variations in each stage*

Stage	Variations
Solution	Saturated NaCl solution (Fujita *et al*., 1996)
	5 wt % NaCl (The Catalyst, 2002).
Immersion	Samples are immersed for 5 minutes, either before heating (Fujita *et al*., 1996) or after (The Catalyst, 2002). This, with the heating cycle, is repeated 15 (The Catalyst, 2002) or 40 times (Fujita *et al*., 1996).
Heating cycle	Samples are heated at 600 to 750 ^{o}C for 2 hours (Fujita *et al*., 1996), followed by cooling
	Samples are heated at 700 to 760 ^{o}C for 90 minutes (The Catalyst, 2002).
Evaluation of results	Weight loss measurement after 15 cycles (The Catalyst, 2002) or after 40 cycles (Fujita *et al*., 1996).

Cabinet tests, as summarised in Tables 2.13 and 2.14, include salt spray and humidity cabinets in their methods. The procedures of these tests are also varied, as can be seen in the following tables:

Table 2.13: *Summary of external corrosion of the hot end components: humidity cabinet tests*

Stage	Variations
Dipping in salt solution	5 minutes (AK Steel Product data Bulletin, 2003a), 4 times per day: 5 min (AK Steel Product data Bulletin, 2003b), 4 times per day: 15 min (AK Steel Product data Bulletin, 2003c), and daily for 15 min (AK Steel Product data Bulletin, 2003d)
Drying	4 times per day: 20 min at 40 ^{o}C, 35% RH (AK Steel Product data Bulletin, 2003c) and In air for 75 min (AK Steel Product data Bulletin, 2003d)
Humidifying	18 hrs at 60°C, 85% RH (AK Steel Product data Bulletin, 2003a), Evenings and weekends cyclic: 2 hrs at 4 ^{o}C, 35% RH and 2hrs at 24 ^{o}C, 85% RH (AK Steel Product data Bulletin, 2003b), 4 times per day: 5h25min at 60 ^{o}C, 85% RH, eevenings and weekends: 24 ^{o}C, 85% RH (AK Steel Product data Bulletin, 2003c), and Rest of day 60°C, 85% RH (AK Steel Product data Bulletin, 2003d)
Heating	90 min at 650°C (water quench for 1 min) (AK Steel Product data Bulletin, 2003a), 1 hr per week 538°C (water quench) AND 4 times per day: 1 hr at 538°C (1 hr cooling) (AK Steel Product data Bulletin, 2003b), 1 hr per week 538°C (water quench) (AK Steel Product data Bulletin, 2003c), and 1 hr per week, converter simulation: 538 ^{o}C and front pipe simulation: 760 ^{o}C (AK Steel Product data Bulletin, 2003d)
One cycle	24 hrs with dipping and heating 4 times before humidified (AK Steel Product data Bulletin, 2003a), 2h5min four times per day total cycle 1 week (AK Steel Product data Bulletin, 2003b), 6 hrs four times per day total cycle 1 week (AK Steel Product data Bulletin, 2003c), and 24 hrs, repeated for 1 week (AK Steel Product data Bulletin, 2003d)
Evaluation: pit depths	After every cycle, also weight loss (AK Steel Product data Bulletin, 2003a), weekly (AK Steel Product data Bulletin, 2003b; c; and d)

Table 2.14: *Summary of external corrosion of the hot end components: salt spray tests*

Stage	Variations
Dipping in salt solution/ Salt spray	Dipping: 4 times per day: 5 min (AK Steel Product data Bulletin, 2003) and Salt spraying: 24 hrs at 35°C (ASTM B117) (Allegheny Ludlum Technical Data Blue Sheet, 2003)
Humidifying	18 hrs at 60°C, 85% RH (AK Steel Product data Bulletin, 2003)
Heating	4 times per day: 90 min at 650°C (1 min water quench) (AK Steel Product data Bulletin, 2003), and 1 hr at 650°C (air cooling) (Allegheny Ludlum Technical Data Blue Sheet, 2003)
One cycle	24 hrs with dipping and heating 4 times before humidifying (AK Steel Product data Bulletin, 2003), and ± 25 hrs (Allegheny Ludlum Technical Data Blue Sheet, 2003)
Evaluation: pit depths	Weekly (AK Steel Product data Bulletin, 2003), and at 5 cycle intervals (Allegheny Ludlum Technical Data Blue Sheet, 2003)

External oxidation tests

As mentioned before, oxidation is a high temperature process and occurs when the metal reacts with the air to form oxides. Therefore no special atmospheres are created for the furnace-based tests summarised below. Oxidation is only a problem for hot end components as their operating temperatures range between 750° and 1050°C.

Table 2.15: *Summary for oxidation tests for external corrosion of the hot end components, and the variations in each stage*

Stage		Variations
Sample preparation		Samples are tested in their as-received condition (Bullard *et al*., 1992; Chassagne *et al*., 2002) or first ground to a 320 grit finish (Miyazaki *et al*., 1994).
Exposure	Continuous	Conducted for 24, 48, 100 hr (Bullard *et al*., 1992), 200 (Chassagne *et al*., 2002) or 400 (Miyazaki *et al*., 1994) hours at temperatures ranging between 750 to 1150 ^{o}C (Bullard *et al*., 1992). 850 to 950 ^{o}C (Chassagne *et al*., 2002).
	Cyclic	Samples are subjected to a severe thermal cycle of 15 minutes heating, 20 minutes hold time and 5 minutes air forced cooling for 1200 cycles (400 hours) (Chassagne *et al*., 2002).
		Samples are subjected to 25 minutes heating and 5 minutes cooling for 1000 cycles (525/500 hours) (AK Steel Product data Bulletin, 2003; The Catalyst, 2002).
		Temperatures range between 850 –950 ^{o}C (Chassagne *et al*., 2002), 760, 871, 927, 1093 ^{o}C (AK Steel Product data Bulletin, 2003; 14), and 816 ^{o}C (AK Steel Product data Bulletin, 2003; The Catalyst, 2002; 14) depending on which component of the exhaust is tested.
Evaluation of results		Weight gain measurements: At the end of the test of continuous tests (Bullard *et al*., 1992; Miyazaki *et al*., 1994). Daily for cyclic tests (AK Steel Product data Bulletin, 2003; The Catalyst, 2002; Chassagne *et al*., 2002)

Of these, the cyclic tests are the most aggressive, since they include thermal cycling which could lead to scale flaking off.

This section has summarised all the most common corrosion and oxidation tests that are used for materials for exhaust systems, to establish their similarities and differences. These tests were evaluated and integrated to develop standard test protocols for all areas and components of the exhaust system, as discussed in the next chapter.

Chapter 3

Corrosion tests for different scenarios in the exhaust system

After a thorough assessment of the tests that are used to evaluate materials for exhaust applications (outlined in the previous chapter), the tests listed in this chapter were developed by identifying commonalities and differences, integrating them where possible, and as far as possible simulating actual environments and operating conditions. For the development, three main factors were considered: aggressiveness of the tests to obtain rapid results; reproducibility of the results from the tests; and reliability of the test. Therefore, in the developed tests, the heating and exposure cycles are based on existing tests, but have been modified to some extent to meet the objectives of this research. This includes the development of tests for both petrol and diesel engines.

The developed tests listed below are proposed because of their many advantages. They are relatively simple laboratory tests which are easy to perform and require inexpensive laboratory equipment. They consist of simple cycles which closely simulate actual environments. All the proposed generic tests, except electrochemical tests, are stopped after an appreciable weight loss has been achieved. These tests are useful for ranking and comparing materials performance for exhausts system because they give useful and reliable results and, although more aggressive, the tests can be adjusted in terms of temperature and concentrations. Some of these tests are performed (see Chapter 4) to verify whether the results obtained from them are reliable. The credibility of these tests were determined by comparing the behaviour of materials subjected to these tests to the available data in literature, and also to the expected behaviour of the materials (see Chapters 5, 6,7 and 8).

The developed tests evaluate corrosion and oxidation for both the cold and hot ends of the exhaust system, and for both petrol and diesel engine components.

3.1 Internal corrosion tests – for cold end components

This type of corrosion is a major problem in cold end components since their temperature is much lower than the hot end, which means the exhaust gas condenses in the cold end creating aggressive corrosion conditions. Internal corrosion is evaluated by performing various tests such as immersion (often called condensate tests) and cabinet tests. These general tests simulate the cold end conditions were the heating cycle for both diesel and petrol engines are similar, and only the condensate solutions differ.

3.1.1 Condensate tests

During vehicle operation, as condensate forms in the cold end, one of three scenarios can occur: a) once the condensate comes in contact with the surface of the components, it evaporates immediately, without reducing the temperature of the components; b) the condensate evaporates but reduces the temperature of the components; or c) when the condensate forms, it does not evaporate (Inoue and Kikuchi, 2003). References do not say, but on analysis it seems that some of the general tests are for scenario 1 or 2 or 3. The various condensate solutions for both the petrol and diesel engines are mentioned in section 4.2.

Test 1

This test is designed for the situation where, in the cold end the condensate evaporates immediately once it comes in contact with the surface of the components and does not reduce the component temperature. Diesel-power automobiles mostly experience this condition during summer (Weltens *et al.,* 2001). The cycle is designed to simulate trips of average distances of no longer than three hours, because vehicles that are used for relatively long, fast journeys the inside of the system is protected to some extent by a layer of hard carbonaceous deposit. When the vehicle is only used for short journeys, and the exhaust remains in a virtually cold running condition this deposit tends to be softer and thicker, thus retaining the acid condensation like a sponge (Cayless, 1974), resulting in severe condensate corrosion. A typical test cycle would simulate the temperature of the cold end components as the car heats from ambient to about 250 ^{o}C to 300 (or 400 ^{o}C occasionally) (Alves *et al.*, 2002; Inoue and Kikuchi, 2003), remains at this

temperature for the duration of the journey and cools down as the car stops. In this test the heating temperature is taken to the maximum temperature of 300 ^{o}C to increase aggressiveness.

The procedure of the test is as follows:

- Samples are fully immersed in a beaker containing approximately 250 ml condensate solution.
- Then exposed to controlled temperature cycles consisting of:
    - Heating from ambient temperature to 300 ^{o}C in 1 hour
    - Holding at 300 ^{o}C for 2 hours
    - Cooling to ambient temperature in 3 hours.
- After the 6 hour cycle, only solid residue will remain from the original test solution.
- Therefore, fresh 250 ml solution will be added to the beaker with the sample, repeating the cycle.
- All corrosion products are cleaned off and the samples are weighed after every cycle or every ten cycles.

Test 2

This test is designed for situations where, in the cold end when the car starts the formed condensate evaporates fast and the components remain dry, but experience a slight reduction in temperature (Sato and Tanoue, 1995). This temperature is assumed to be 130 ^{o}C. In this test the samples are pre-heated at 400 ^{o}C to enhance the severity of the test and to obtain rapid results.

The procedure is as follows:

- Samples are preheated in air at 400 ^{o}C for 1 hour before the test.
- The samples are then fully immersed in a 250 ml beaker containing the condensate solution.
- The beaker is heated to 130 ^{o}C for 30 minutes and held at this temperature for four hours.
- Followed by cooling in the furnace for 30 minutes.
- Samples are cleaned to bare metal and weighed after every cycle or ten cycles.

Test 3

This test is designed to simulate the condition where the condensate forms inside the cold end components and does not evaporate. This normally takes place at temperatures of up to 95 ^{o}C (Cayless, 1974). However, the thermal bath for these tests is kept at 80 ^{o}C (Lothongkum *et al*., 1999) so that samples are in contact with the condensate for longer at increased condensate

severity. This temperature also decreases the rate at which the water evaporates from the thermal bath.

The procedure is as follows:

- The samples are pre-heated at 400 ^{o}C for 5 hours in air (this is done only at the beginning of the test)
- The cycle is as follows:
    - The samples are fully immersed in a beaker containing the condensate solution
    - The beaker with the sample is then placed in a water bath at 80 ^{o}C and kept for 24 hours for complete evaporation.
    - This is followed by softly brushing the samples and then washing the beaker to complete a cycle.
- The samples are then cleaned to bare metal before pit depth and weight loss are measured after every cycle, or every ten cycles.

In all the abovementioned condensate tests, the samples are fully immersed. This is proposed because when samples are fully immersed, they experience the same conditions as partially immersed samples particularly when the solution evaporates. The samples are exposed to the condition experienced by partially immersed samples until the solution completely evaporates. Therefore, fully immersing the samples is advantageous; also because the samples are exposed to the condensate for longer times which increases the aggressiveness of the tests, enabling the rapid obtaining of results.

3.1.2 Cabinet tests

The following test is developed because of the ability of cabinet tests to highlight shortcomings and advantages of certain corrosion protection schemes, its widespread used, and its extensive track record as a quality control tool. The test simulates the condition of the cold end where, when the condensate forms, it does not evaporate immediately. This test is similar to Test 3 (above) in a sense that it uses the water thermal bath to evaporate the condensate solution, however this one incorporates the use of a cabinet cycle and higher thermal bath temperature so as to increase the aggressiveness. This gives rapid results and allows the ranking of samples according to their resistance to the condensate solution. This test could be used as an alternative to Test 3.

Test 4

- The samples are fully immersed in the synthetic condensate solution.
- The solution is slowly but completely evaporated at 90 ^{o}C by using a thermal bath (about 12 – 16 hours).
- When the samples are dry, they are heated to 300 ^{o}C for 1 hour and then charged in to a humidity cabinet at 50 ^{o}C and 98% RH for six hours.
- Pit depth and weight loss are measured after each such cycle.

3.2 External Corrosion – for cold end and hot end components

The external corrosion experienced in petrol and diesel automobiles is similar and therefore tests for each end would consist of similar heating cycles, temperatures and test solutions.

The most aggressive external corrosion conditions occur in countries where severe winter conditions prevail because de-icing chemicals are used to maintain efficient road usage. The most commonly used salt solution consists of sodium chloride and (occasionally) calcium chloride (Baboian, 1996; Cayless, 1974). Usually 5% salt solution is used in laboratory tests (Ak Steel). It could be only sodium chloride salt or a mixture of 95% sodium salt and 5% calcium chloride salt that make up a 5% salt solution (Oliver and Sephton, 2003).

This type of corrosion is also evaluated by performing immersion and cabinet tests, as explained in section 2.6.2. After thorough assessment of the tests outlined in the literature, the following experimental tests were developed:

3.2.1 Immersion tests

Test 5

This test is designed to simulate conditions of both the hot end and cold end. The salt concentration of 5% NaCl salt is more than the normal encountered - this is done deliberately to increase the aggressiveness of the test and to produce rapid results. This test is also designed to simulate the cyclic conditions experienced by the components. The temperatures higher than normally encountered are chosen to increase the aggressiveness.

The procedure is as follows:

- The cycle of the test comprises holding the samples for 2 hrs at:
    - 350 ^{o}C for silencer and tail pipe simulation,
    - 450 ^{o}C for center pipe simulation,
    - 600 ^{o}C for catalytic converter simulation,
    - 800 ^{o}C for front pipe simulation, or
    - 1000 ^{o}C for exhaust manifolds simulation.
- This is followed by cooling in air (to room temperature)
- Then finally, immersion in a salt solution for 5 minutes.
- The test is run for a minimum of 10 such cycles and weights are measured before and after each cycle.

3.2.2 Cabinet tests

Test 6

This test is based on the external exhaust salt-humidity pitting corrosion test and was modified to simulate both the hot end and cold end. Again, higher temperatures are chosen to increase the aggressiveness, of the test.

The procedure is as follows:

- Samples are heated for 1 hour per week as follows:
    - 350 ^{o}C for silencer and tail pipe simulation,
    - 450 ^{o}C for center pipe simulation,
    - 600 ^{o}C for catalytic converter simulation,
    - 800 ^{o}C for front pipe simulation, or
    - 1000 ^{o}C for exhaust manifolds simulation.
- The samples are dipped daily in the salt solution for 15 minutes
- Followed by forced air drying for 75 minutes
- The samples are then placed in the salt spray cabinet at 50 ^{o}C for the remainder of the day.
- Pit depths and weight loss are measured after each weekly cycle.

3.3 Localised corrosion

The most commonly encountered cause of pitting, namely chlorine ions, are encountered in both the exhaust gas (internal corrosion) and road salts (external corrosion). Therefore these tests are designed to use both the condensate solution and external corrosion solution to investigate the pitting resistance of candidate materials.

3.3.1 Potentiodynamic polarisation scan

Test 7

Potentiodynamic polarisation (both anodic polarisation and pitting/cyclic polarisation) scans in condensate and salt solutions can be used to rank materials according to their resistance to pitting corrosion under the external and internal corrosion conditions. This test utilises a standard three-electrode corrosion cell consisting of a working electrode (WE), a counter electrode (CE) and a saturated calomel reference electrode (SCE). A luggin probe and salt bridge is also used to minimise solution resistance. The probe is positioned approximately 1 mm from the working electrode (approximately two times the diameter of the probe). The WE is ground to a 600 grit surface finish, in accordance with ASTM-G59 – 97, followed by degreasing the WE ultrasonically in acetone for 5 minutes and rinsing with distilled water.

The procedure is as follows (ASTM G5 – 99; ASTM G61 – 98):
For anodic potentiodynamic polarisation scans, the WE is polarised at -0.7 V for 10 minutes (van Bennekom *et al*., 1999) to clean off any oxide layer on the surface, followed by scanning the potential from -250 mV vs. E_{corr} to 1600 mV vs SCE

For cyclic scans, the WE is held for one hour in the electrolyte, which is always enough to stabilise the open circuit potential, before performing the cyclic scan. The scan is started at -50 mV vs E_{corr} and reversed when the current density exceeded 5 mA/cm^2 to end at 0 mV vs E_{corr}.

Test 8

This test is developed to simulate the condition of the cold end components as the car heats from ambient to about 250 ^{o}C (or 400 ^{o}C occasionally) (Inoue and Kikuchi, 2003), remains at this temperature for the duration of the journey and cools down as the car stops. In this test the samples are oxidised in air at the maximum temperature of 400 ^{o}C for 5 hours.

After oxidising the samples, a standard three-electrode corrosion cell, consisting of working electrode (WE), a counter electrode (CE) and a saturated calomel reference electrode (SCE), is used. Since this test is for the cold end components, for internal corrosion synthetic petrol and diesel condensates are used, while for external corrosion a 5% NaCl solution is used as an electrolyte. A luggin probe and salt bridge are used to minimise any effect of solution resistance as per ASTM G5 - 99.

The procedure is as explained in Test 7 above.

3.4 Intergranular corrosion tests

These tests are conducted to investigate the corrosion behaviour of the welded or coupled baffle plates of a silencer. After considering the published procedures (see section 2.6.4) the following test was designed. It was noted that, in an attempt to sensitise samples, some researchers weld them. However, more frequently in exhaust systems the components are not welded but coupled. Therefore the developed test rather employs the route of heat treating the materials to sensitise them. This route closely simulates actual manufacturing conditions.

Test 9

The specimens are prepared by solution annealing at 1100 ^{o}C for 2 hours, followed by water quenching and sensitising at 600 ^{o}C for one hour. All heat treatments are carried out in air (Putatunda, 1987).

The sensitised specimens are then subjected to a modified Strauss test. The test solution consists of 10% $CuSO_4.5H_2O$ and 5% of H_2SO_4. This test is run for 24 hours, after which the results are

evaluated by visually rating amount and/or thickness of copper plating to indicate the extent of sensitisation on the surface of specimens (Lothongkum *et al*., 1999).

3.5 Perforation and Cosmetic tests – for cold end components

The test developed below was adopted and modified to take in to account the actual surface condition of tail pipe components. Some researchers paint the samples, but where stainless steels (in themselves aesthetically appealing) are used, this is not done. This test can therefore be seen as more of an external corrosion test, where 5% sodium chloride (NaCl) salt solution is used.

Test 10

- Specimens are heated at 400 ^{o}C for 30 minutes,
- Then quenched in water,
- This thermal cycle is repeated five times, followed by exposure to the 5% NaCl salt spray for one week to complete the test,
- Results are visually analysed to rank the degree of corrosion and pit depth is measured.

3.6 External oxidation tests – for hot end components

After considering all the possibilities outlined in the literature the following test was developed to investigate the resistance of the materials intended for different components of the hot end. Both continuous and cyclic tests are mentioned in the literature section. However, only the cyclic tests are considered here since they best simulate the actual conditions experienced by exhaust systems.

3.6.1 Cyclic oxidation tests

Test 11

The cyclic oxidation tests are carried out at different temperatures and these temperatures are (again) higher than normally encountered to increase the aggressiveness, of the test.

The procedure is as follows:

- Samples are heated in air to the maximum of 1000 cycles (or 500 hours total dwell time) using a severe thermal cycle (25 minutes heating and 5 minutes cooling).
- The exposure temperatures are as follows:
    - 750 ^{o}C for catalytic converter simulation,
    - 850 ^{o}C for flexible pipe simulation,
    - 950 ^{o}C for front pipe simulation, or
    - 1050 ^{o}C for exhaust manifolds simulation.
- The weight change of the samples is evaluated at a fixed time interval (e.g. four cycles).

Chapter 4

General experimental procedure

In Chapter 2, tests which are employed in evaluating the corrosion resistance of exhaust system components were outlined. After a thorough assessment of these tests, the procedures listed in Chapter 3 were designed. In this chapter, the materials that were used to evaluate and verify the reproducibility of the tests and the solutions that were used in the tests are discussed, and the general specimen preparation and evaluation methods are explained. The arrangements for the electrochemical testing, and surface analyses are also briefly given.

4.1 Test materials

Five different types of stainless steels were supplied by Columbus Stainless: AISI type 304, 321, 409, 434 and DIN type 1.4509. These stainless steels were commercially produced by Columbus Stainless (details of the process can be obtained on request), and supplied in sheet form. The surface finishes and sheet thickness of the materials are summarised in Table 4.1, and their general chemical composition are given in Table 4.2 below:

Table 4.1: *As-received surface finishes of the materials*

Stainless steel	Standard finish	Thickness (mm)
AISI 304	Standard cold rolled	1.3
AISI 321	Cold rolled bright annealed	0.3
AISI 409	Cold rolled with dull finish	1.0
AISI 434	Cold rolled bright annealed	0.8
DIN1.4509	Cold rolled with dull finish	1.3

Table 4.2: *Nominal compositions of the stainless steels*

Elements	AISI 304	AISI 321	AISI 409	AISI 434	DIN 1.4509
Carbon	0.08 max	0.08 max	0.08 max	0.08 max	0.03 max
Manganese	2.0 max	2.0 max	1.0 max	1.0 max	1.0 max
Phosphorous	0.045 max	0.045 max	0.045 max	0.040 max	0.040 max
Sulphur	0.030 max	0.030 max	0.015 max	0.015 max	0.015 max
Silicon	0.75 max	0.75 max	1.0 max	1.0 max	1.0 max
Chromium	18.0–20.0	17.0–19.0	10.5–11.75	16.0–18.0	17.5–18.5
Nickel	8.0–10.5	9.0–12.0	0.5 max	-	0.75 max
Molybdenum	-	-	-	0.9-1.4	-
Titanium	-	6x(C+N)–0.7	6xC–0.75	-	0.1–0.6
Nitrogen	0.10 max	-	-	-	0.045 max
Niobium	-	-	-	-	3xC+0.3–1.0
Iron	Balance	Balance	Balance	Balance	Balance

The materials were tested in their as-received condition, except for the electrochemical tests (details are given in section 4.3). They were degreased ultrasonically in acetone for 5 minutes and rinsed with distilled water before exposure. For the exposure-type tests, the samples were 50 mm by 80 mm in size and they were tested in quadruple. For the electrochemical tests at least two samples were tested per condition.

In this report the stainless steels are abbreviated as follows:

- AISI type 304 ≡ 304
- AISI type 321 ≡ 321
- AISI type 409 ≡ 409
- AISI type 434 ≡ 434
- DIN type 1.4509 ≡ 1.4509

The surface of a 321 sample before exposure to corrosion and oxidation testing is shown in Figure 4.1. The photograph is a representative of all the other stainless steels.



Figure 4.1: *As-received surface appearance for 321, appearance is representative of all the other stainless steels.*

4.2 Test solutions

4.2.1 Condensate solution (for internal corrosion)

For the tests developed in this research it was important to synthesise a condensate solution that closely simulates actual working environments. In evaluating the existing tests and the synthetic condensate solutions used in each, it became apparent that there is wide variation in the concentrations of the condensate solutions (see Chapter 2). In all the solutions mentioned, the concentration of the ions is higher than that found when physically analysing failed components. The primary reason for this is probably to make the tests more aggressive, to obtain results in an acceptably short testing period.

The synthetic condensate solution for this project was made up from ions found by Weltens *et al.* (2001) and Sato *et al.* (1991) when they analysed exhaust components to determine the main cause of failure. The advantage of this was that these ions are present in the actual exhaust gas, thus leading to better simulation of exhaust conditions. The results of these researchers show that the most common ions present are Cl^-, SO_4^{2-}, CO_3^{2-}, NO_3^- and NH_4^+ (listed in Table 2.2, Chapter 2).

An important objective of this research is that conditions in both petrol and diesel engines should be simulated. From the literature it was found that the difference in solutions lies not in the ions present, but only in their concentrations (see Table 2.2 in Chapter 2). For example, looking at the most aggressive ion (i.e. Cl^-) in this table, the concentration ranges between 2.2 and 23.5 ppm for

petrol engines, and between 2.9 and 52 ppm for diesel engines (Weltens *et al*, 2001). The most aggressive conditions seem to occur in diesel engines, and in both the petrol and diesel engines, the most aggressive conditions seem to occur in engines without catalytic converters. It can be safely assumed that, if the most aggressive testing conditions are used, any material able to withstand those conditions would automatically be resistant to less aggressive situations.

Most researchers do not specify whether the synthetic condensate is for diesel or petrol engines. In this research it was assumed that the concentration level of the ions which most researchers use is for petrol engines because the condensate solutions they list are less aggressive than those of diesel engines. Therefore, the condensate solution from Sato *et al.* (1991) was adopted and assumed to be for petrol engines as seen Table 4.3 below. Table 2.2 (Chapter 2) was used to obtain the diesel synthetic condensate, by using the ratio of the concentrations of the ions between petrol and diesel engines (without catalytic converters). For example, 320 ppm of SO_4^{2-} ion in petrol engine without a catalytic converter corresponds to 175 ppm of SO_4^{2-} ion in a diesel engine without a catalytic converter. Therefore, 1000 ppm of SO_4^{2-} ion in a synthetic petrol solution (Sato *et al*., 1991) will correspond with x of synthetic diesel solution, and x is calculated as follows:

$$x = \frac{(175)(5000)}{320} = 2734 \approx 2750\,\text{ppm}$$

By using the ratio of the concentrations of the other ions, except Cl^- and CO_3^{2-}, the concentration of diesel solution was calculated, see Table 4.3 below. The Cl^- and CO_3^{2-} were adopted from the synthetic concentration by Sato *et al*. (1991).

Table 4.3: *Chemical composition of simulated exhaust gas condensates for both petrol and diesel engines*

Ions (ppm)	Petrol engine	Diesel engine
Cl^-	1000	1250
SO_4^{2-}	5000	2750
CO_3^{2-}	3000	3000
NO_3^-	100	1750
NH_4^+	3740	340

4.2.2 Salt solution (for external corrosion)

The most commonly used salt solution in external corrosion is sodium chloride and (occasionally) calcium chloride. Therefore, for the external corrosion, a 5% NaCl solution was used (Baboian, 1996; Cayless, 1974; The Catalyst, 2002) for all tests.

4.3 Electrochemical tests

A standard three-electrode cell (as per ASTM G5 – 99) consisting of a mounted working electrode (WE), a platinum counter electrode (CE) and a saturated calomel reference electrode (SCE) was used. The electrolytes were synthetic petrol condensate, synthetic diesel condensate and 5% NaCl solution. These solutions have a high conductivity, which translates into little or no ohmic resistance between the reference electrode and the working electrode. Therefore, no IR compensation was used (van Bennekom *et al.*, 1999). However, a luggin probe and salt bridge were used to minimise any effect of solution resistance that might still be there. The probe was positioned approximately 1 mm from the working electrode (i.e. approximately two times the diameter of the probe) (Ashassi-Sorkhabi e*t al.*, 2004; ASTM G61 – 98; ASTM G5 - 99). The cell was placed in a Faraday cage to eliminate external interference of the surrounding conditions. The test temperature was maintained at 30 ± 1^{o}C throughout the tests, according to the procedure followed by Ashassi-Sorkhabi *et al*. (2004). The experiments were carried out using a Princeton Instruments Potentiostat/Galvanostat Model 273. At least two tests per material per test condition were done.

20 mm by 20 mm specimens for these tests were cut from the sheets of the candidate materials and a hole drilled at one of each corner for electrochemical connection. The hole was then fitted with a self-taping screw to tighten the connection and a plastic coated copper wire was connected to this assembly. The samples were then cold mounted with a 1935 batch resin. After cold mounting the screw was masked off such that it would not come in contact with the electrolyte during testing.

Each sample was ground to a 600 grit surface finish, in accordance with ASTM-G59 – 97. The metal surfaces to be exposed were degreased ultrasonically in acetone for 5 minutes and rinsed with distilled water. The edges of each specimen were masked off with a commercial glue to prevent crevice corrosion and to expose approximately 1 cm^2 of the surface to the test solution.

The samples were masked off in such a way that the remaining area was approximately square or rectangular, which allowed the exposed area to be measured as accurately as possible prior to testing.

4.4 Surface analysis

Surface analysis of the samples was done by using a Scanning Electron Microscope (SEM). The acceleration voltage was kept at 20 kV and the working distance was varied. The analysis was performed on all the materials before and after exposure testing.

The specimens (20 mm by 20 mm) for surface analyses were cut from randomly picked sheets of the candidate exposed materials, and analysed in their as-exposed condition. The as-received samples were carbon coated for this analysis, but the corroded samples were not carbon coated, as the corrosive attack on the surface was of interest.

Figure 4.2 shows a SEM micrograph of 304 sample before exposure, this SEM micrograph is a representative of all the other stainless steels.

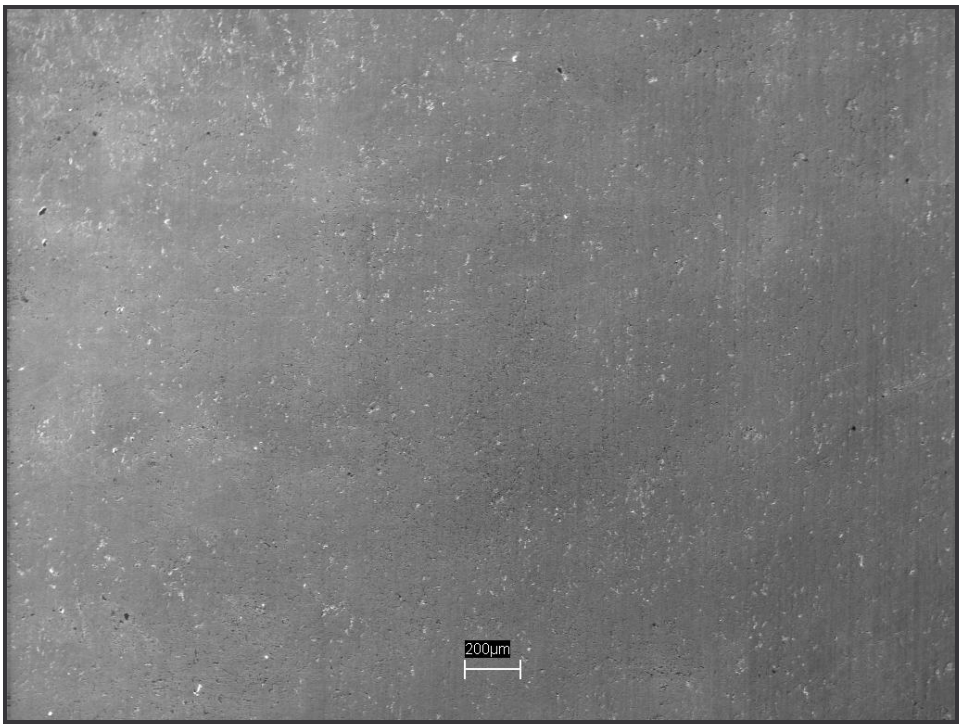


Figure 4.2: *SEM micrograph for the 304 taken before corrosion, showing a clear surface*

4.5 Specimen cleaning and evaluation

Cleaning of specimens after exposure testing involved scrubbing of the specimens with a nylon brush under running tap water. To verify the reliability of this cleaning procedure, blank specimens for all the materials were weighed before and after exposure to this cleaning process. This was done in all tests involving weight loss measurements. It was found that this method does not remove the base metal, since there was no change in the weight of the control (blank) specimens before and after the cleaning exposure.

The specimens were evaluated by immediately photographing them after removal of the corrosion products and drying. They were then re-weighed to calculate weight loss. After evaluation, the samples were kept in the desiccator for surface analysis (see section 4.4).

For the electrochemical tests, data such as corrosion rate, corrosion potential (E_{corr}) and linear polarisation resistance (R_p) were determined by extrapolation of the cathodic and anodic Tafel regions (Ashassi-Sorkhabi e*t al*, 2004). The standard electrochemical commercial software (Model 342C), was also used in calculating these electrochemical parameters via the linear polarisation method (van Bennekom *et al*, 1999).

Chapter 5

Cold end internal corrosion tests

This chapter presents the experimental procedure and results of the cold end internal corrosion tests as discussed in Chapter 3: Immersion tests in synthetic petrol and diesel condensates and electrochemical testing in both solutions.

5.1 Condensate tests – Test 3

As explained in Chapter 3, during vehicle operation, as condensate forms in the cold end, one of three scenarios can occur: a) once the condensate comes in contact with the surface of the components, it evaporates immediately, without reducing the temperature of the components; b) the condensate evaporates but reduces the temperature of the components; or c) when the condensate forms, it does not evaporate. The experimental procedures which simulate these scenarios were given in Chapter 3. Of these, the third scenario would be the most aggressive, because the materials are immersed and kept in the boiling solution for longer hours. Only this scenario was investigated, since it is expected that the other two would give similar results.

Ferritic 409 and 434 and austenitic 304 stainless steels were tested in both petrol and diesel condensates. The experimental procedure consisted of:

- Pre-heating the samples at 400 ^{o}C for 5 hours in air (this was done only at the beginning of the test).
- The cycle was then as follows (see also Figure 5.1):
    - The samples were fully immersed in a beaker containing the condensate solution
    - The beaker with the sample was immersed in a water bath at 80 ^{o}C and kept for 24 hours for complete evaporation.
    - This was followed by softly brushing off the corrosion product from the samples and then washing the beaker to complete a cycle.
- Weight loss was measured after every cycle (1 cycle = 24 hours).

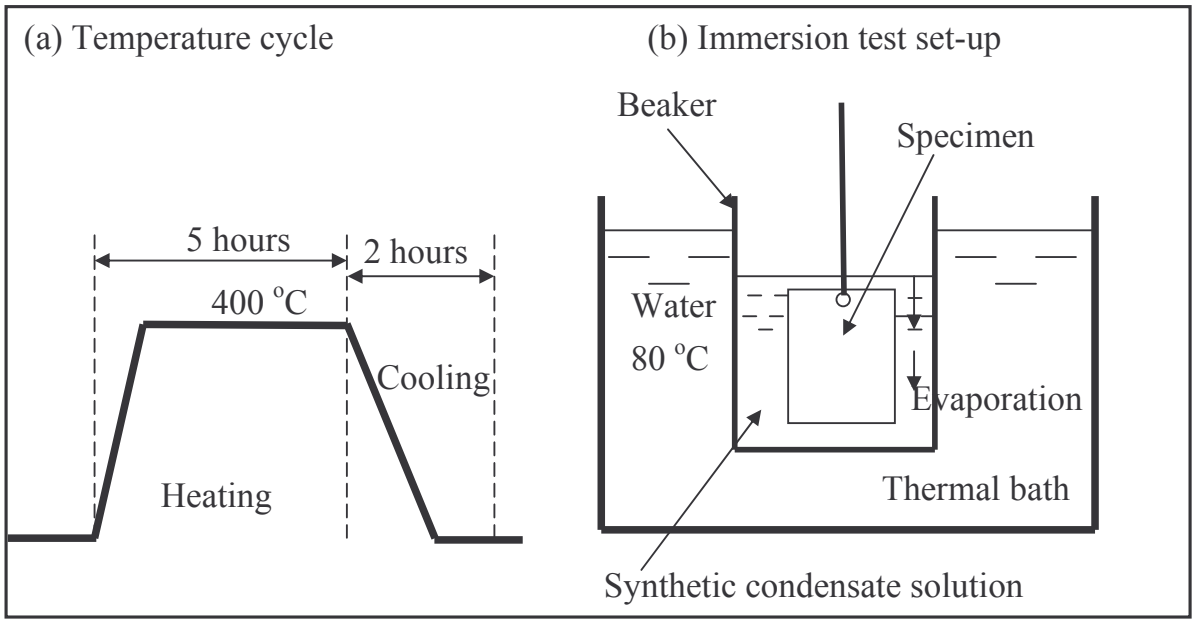


Figure 5.1: *(a) Temperature cycle and (b) schematic diagram of the internal condensate test set-up*

The specimen evaluation and cleaning were carried out as explained in section 4.5.

5.1.1 Petrol condensate results

Figure 5.2 shows the results of exposure in the petrol condensate. These results were average values from four candidate samples. The error bars indicate the minimum and maximum values from the mean value per point on the graph.

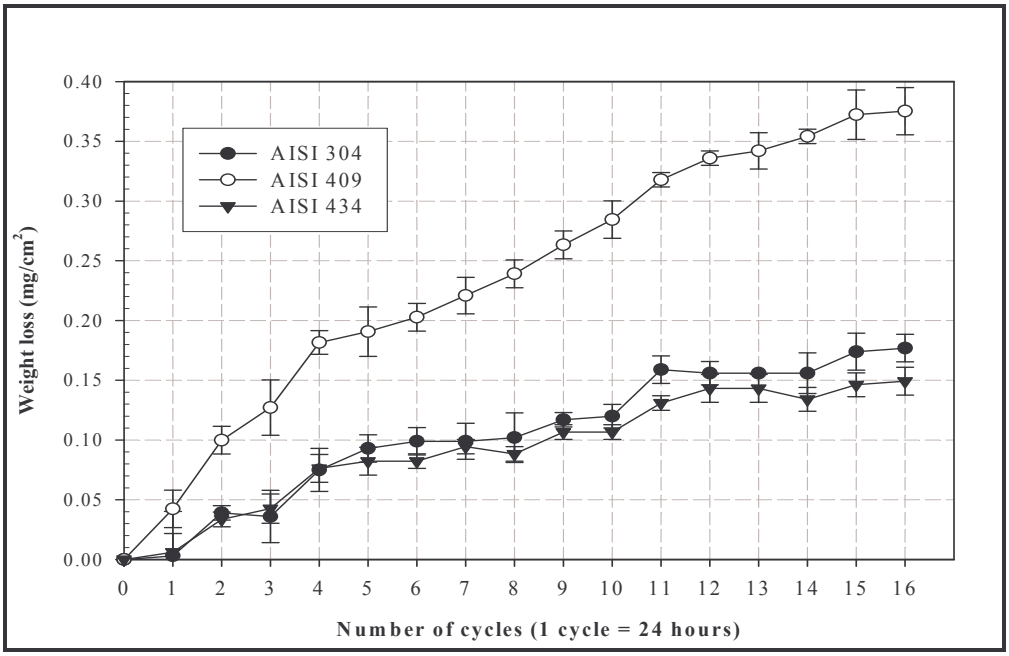


Figure 5.2: *Cumulative weight loss in petrol condensate, showing the average weight loss of four samples per material*

In the petrol condensate 409 was the least resistant of all the stainless steels. 434 performed the best, but the difference to 304 was very small. It appeared that there was a slight decrease in weight loss rate of both 304 and 434 after the fourth cycle. 409 also had a slight change in slope after the fourth cycle, but not so pronounced.

Figures 5.3 to 5.5 show the photographs of the samples after total exposure to the petrol condensate.

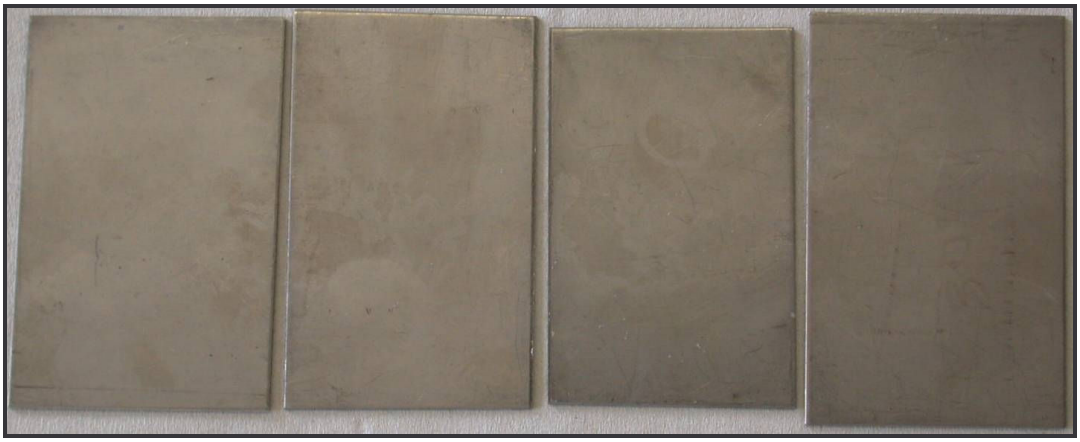


Figure 5.3: *Photographs of 304 after total exposure to the petrol condensate, showing little corrosive attack*



Figure 5.4: *Photographs of 409 after total exposure to the petrol condensate, showing little corrosive attack*

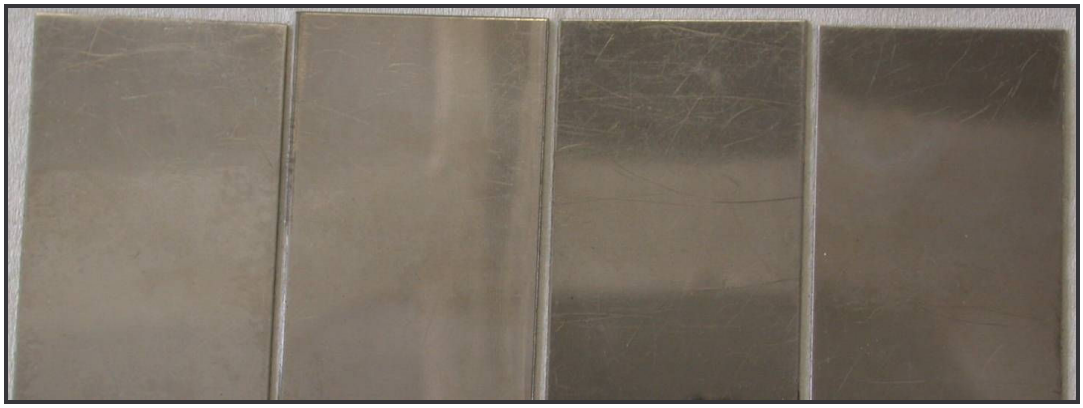


Figure 5.5: *Photographs of 434 after total exposure to the petrol condensate, showing little corrosive attack*

All the samples showed very little weight loss and there was little evidence of corrosive attack. In fact, the samples retained the lustre they had at the beginning of the exposure period. However, with the SEM investigation, some corrosive attack was visible, as shown in Figures 5.6 to 5.8.

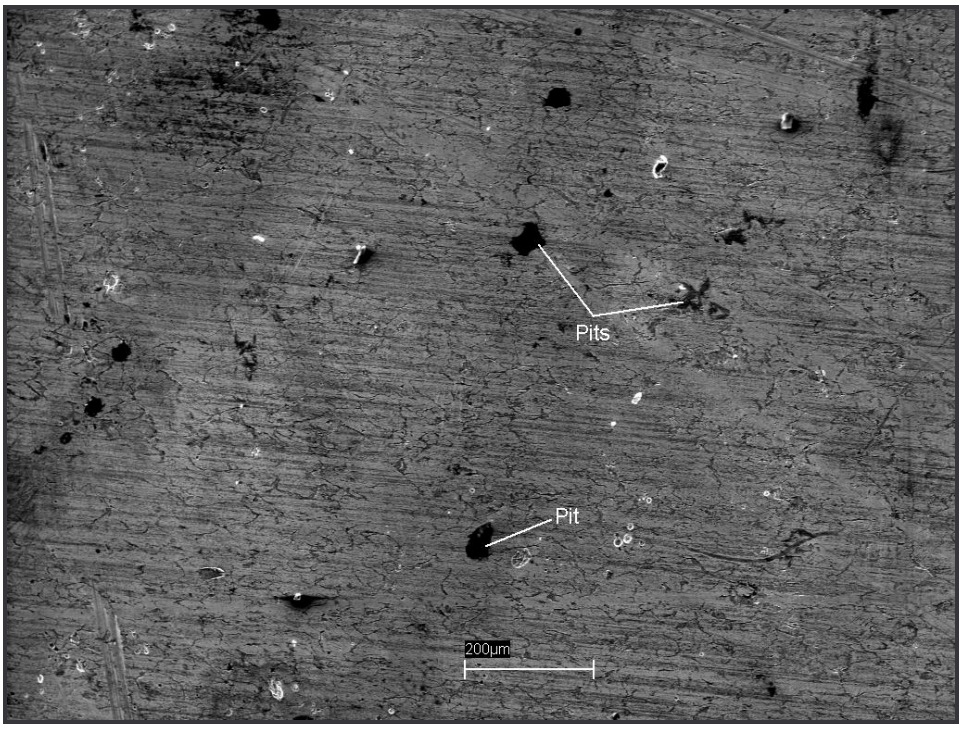


Figure 5.6: *SEM micrograph of 304 after total exposure to the petrol condensate, showing pits*



Figure 5.7: *SEM micrograph of 409 after total exposure to the petrol condensate, showing high concentration of small pits*

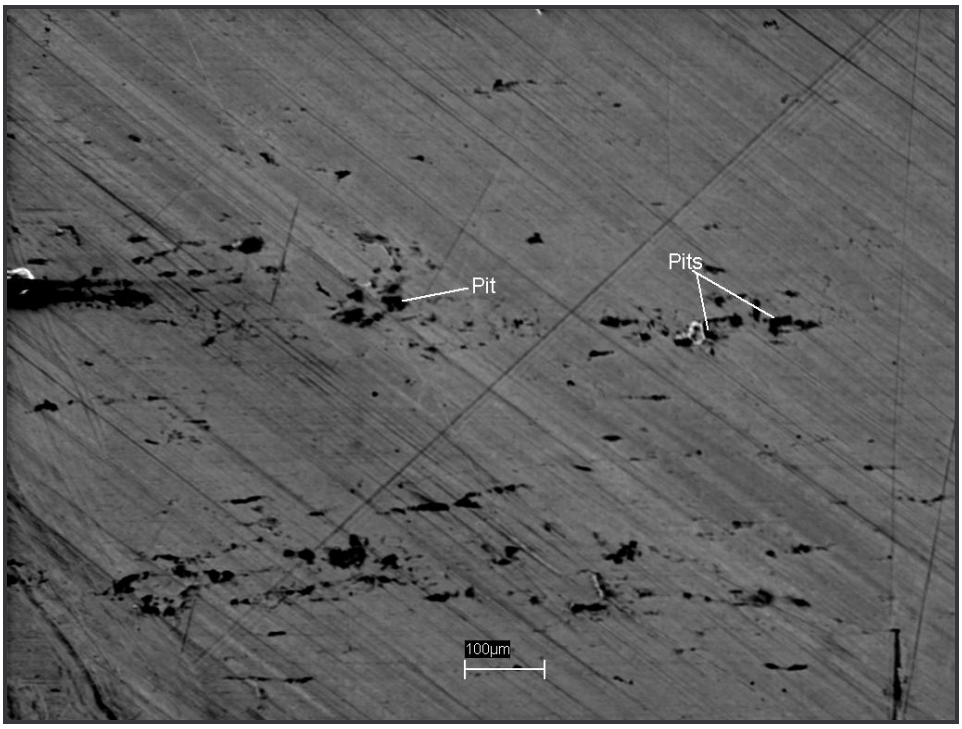


Figure 5.8: *SEM micrograph of 434 after total exposure to the petrol condensate, showing pits on a relatively smooth surface*

The SEM investigation revealed corrosion attack in the form of pits which were not there before exposure (compare with Figure 4.2). 409 had a few large and many small pits. The large pits apparently grew from the agglomeration of small pits, resulting in concentrated areas of attack. The 304 sample had a few larger pits on the surface, while the 434 sample also had many small pits and a few large pits in discrete areas.

The pit density and morphology agree with the weight loss results, where 409, with the highest weight loss, had the most (and deepest) pits.

5.1.2 Diesel condensate results

Figure 5.9 shows the results of exposure in the diesel condensate.

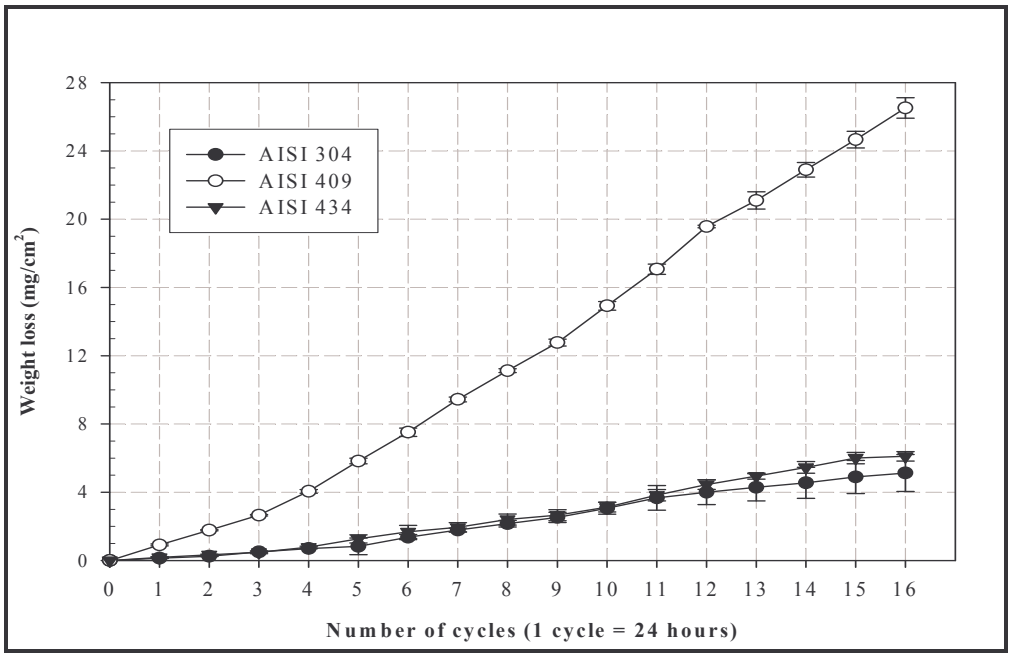


Figure 5.9: *Cumulative weight loss in diesel condensate. The average weight loss of four samples per material is shown*

In this condensate, the 304 performed the best, which was expected because of its known resistance to severe corrosive environments (AK Steel data bulletin, 2003). The 434 compared very well to the 304, but the 409 did not seem to be resistant at all, as its weight loss increased constantly.

Figures 5.10 to 5.12 show the photographs of the stainless steels after total exposure to the diesel condensate.

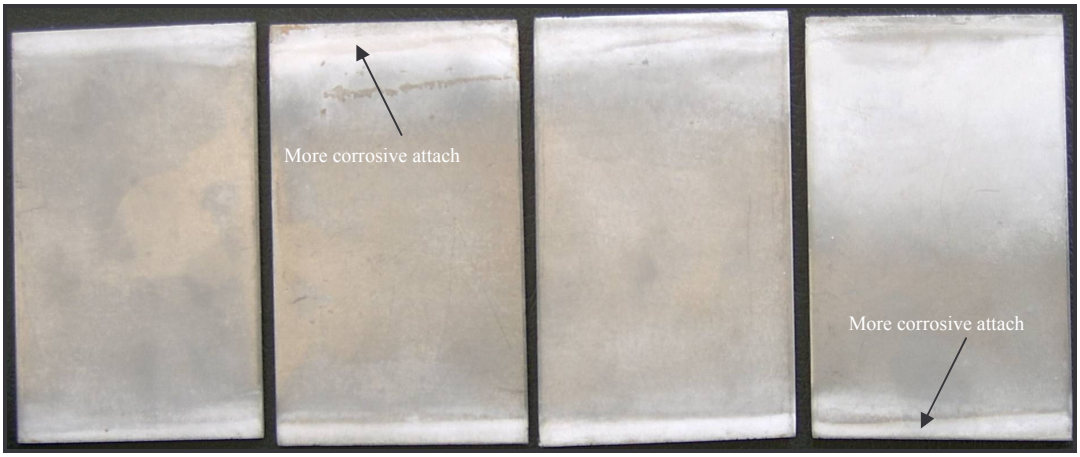


Figure 5.10: *Photographs of 304 after total exposure to the diesel condensate, showing corrosive attack, mostly at the edges*



Figure 5.11: *Photographs of 409 after total exposure to the diesel condensate, showing pits on the entire surfaces*

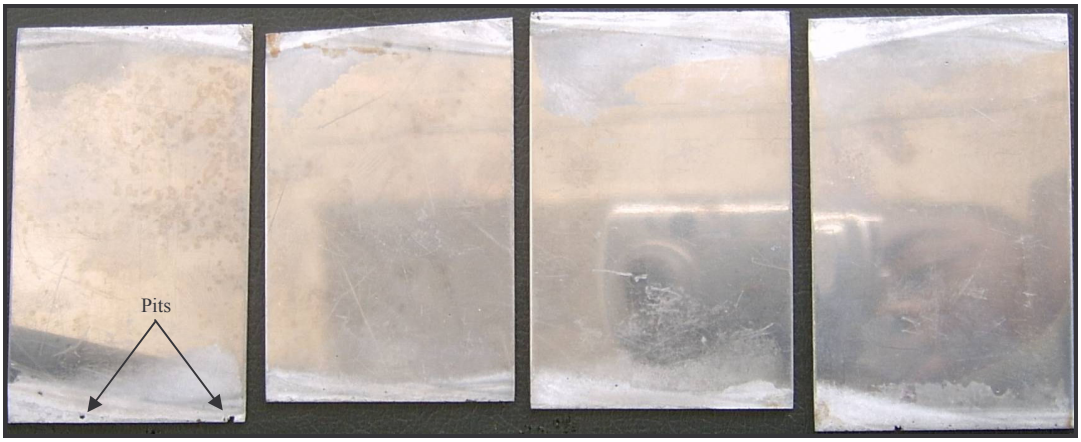


Figure 5.12: *Photographs of 434 after total exposure to the diesel condensate, showing corrosive attack and pits at the edges*

Visual examination of the exposed samples after cleaning and drying revealed evidence of corrosive attack. Pits were observed on all the materials. As early as the third cycle, pits formed on the surface of the 409, and, on 434, after the fourth cycle. The 304 started to show pits after the sixth cycle. The pit density for all the steels was calculated and is shown in Table 5.1. As expected, overall 409 had the most pits and 304 had the least. On both 304 and 434 the pits were concentrated at the bottom and top surfaces, as can be seen in Figures 5.10 and 5.12. This is probably an indication that the solution gets more aggressive as it evaporates.

Table 5.1: *Pit density after exposure to diesel condensate*

Stainless Steels	Pit density (pits/cm^2)
AISI 304	0.12
AISI 409	3.00
AISI 434	0.67

A SEM was used to view the surface of the corroded samples, and the results are shown in Figures 5.13 to 5.15 below.

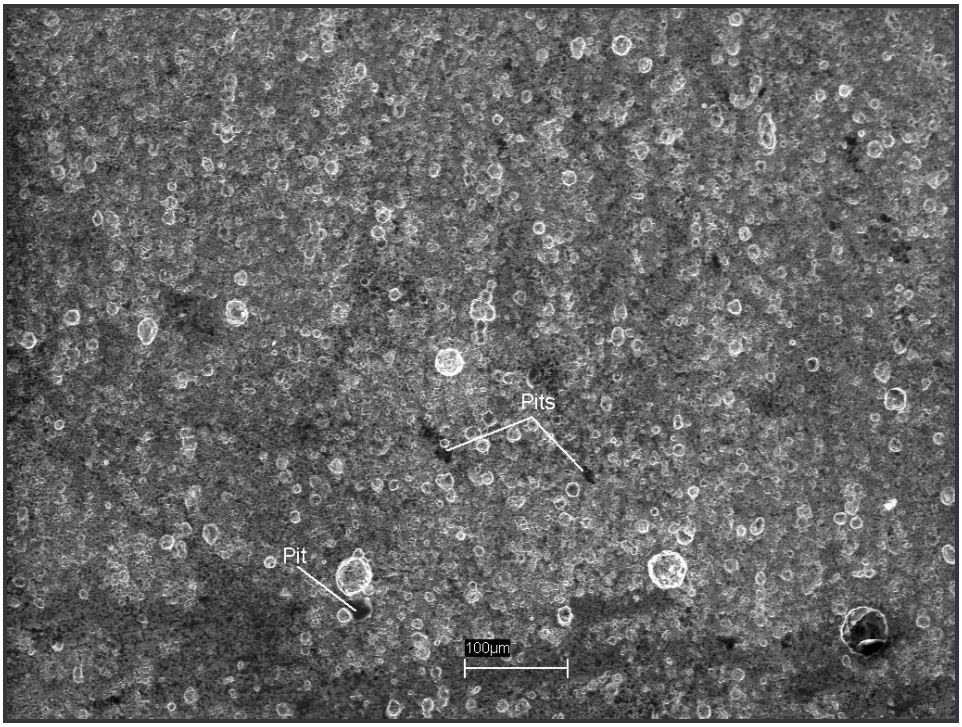


Figure 5.13: *SEM micrograph of 304 after total exposure to the diesel condensate, showing pits on a corroded surface*

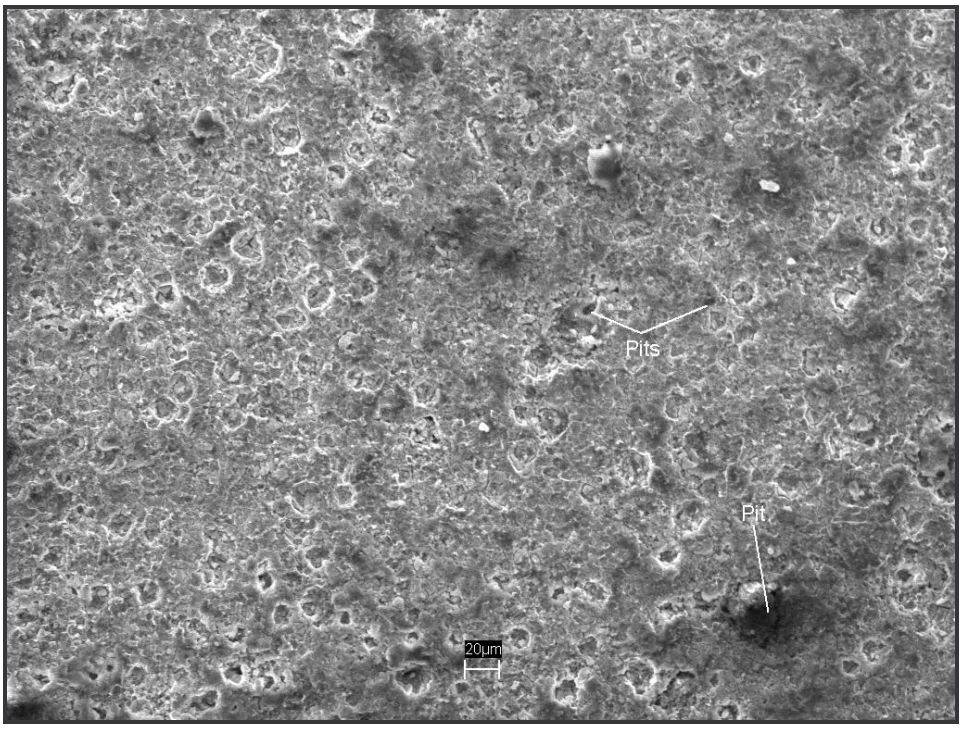


Figure 5.14: *SEM micrograph of 409 after total exposure to the diesel condensate, showing corrosive attack and pits*

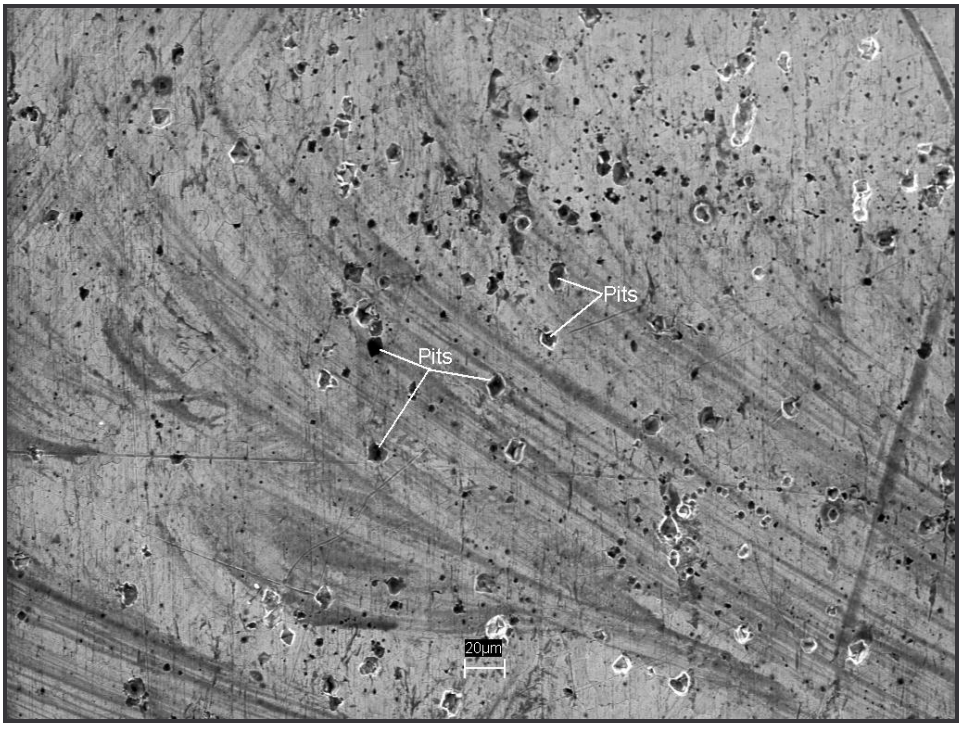


Figure 5.15: *SEM micrograph of 434 after total exposure to the diesel condensate, showing many pits on a relatively smooth surface*

Also from these SEM micrographs, it could be seen that 409 had corroded the most. The surfaces of 304 and 409 showed blistering. The 434 sample had a smooth surface with many small pits and a few larger pits.

These results agree with those of the weight loss tests, since 409 had lost more weight than the other stainless steels and had the most severe surface attack.

5.1.3 Comparison of corrosion in petrol and diesel condensates

A comparison of the corrosion rate results of exposure in both the petrol and diesel condensates is shown in Figure 5.16. The corrosion rates were calculated from:

$$mm/y = 87.6\frac{W}{DAT}$$

Where W is the weight loss in mg, D is the density in g/cm^3, A is area in cm^2, and T is time in hrs.

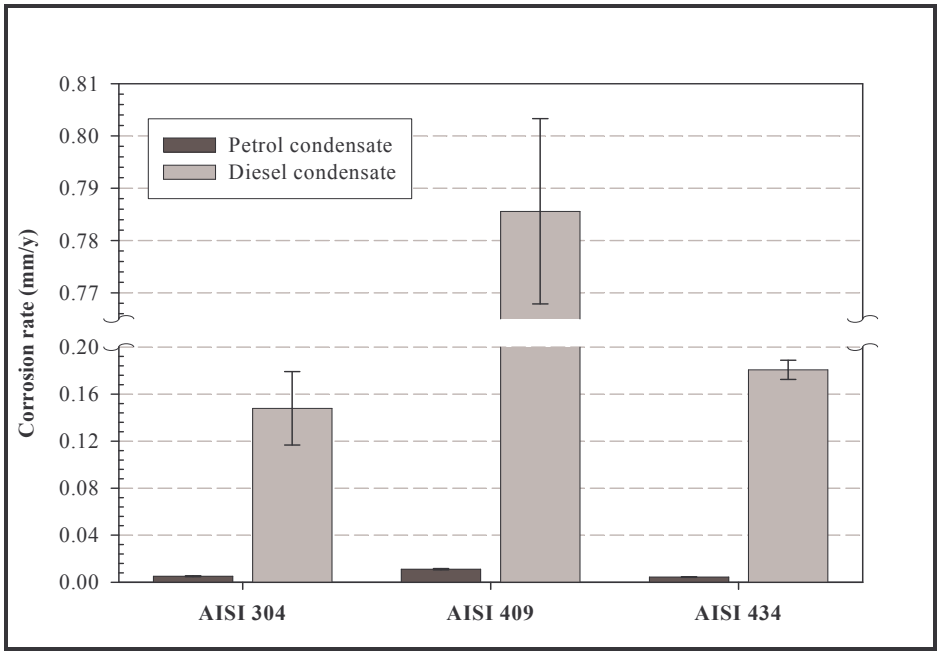


Figure 5.16: *Comparison of corrosion rate in both petrol and diesel condensates (after 16 cycles)*

The corrosion rates of all the materials in the diesel condensate were significantly higher than in the petrol condensate. In both condensates 409 corroded the most. In the petrol condensate, the

uniform corrosion rates of all the materials were below 0.02 mm/y, which are considered to be outstanding levels of relative uniform corrosion resistance, according to Jones (1996).

The surface analysis showed the same trends as the corrosion rates, namely less corrosive attack on the materials exposed to the petrol condensate.

An interesting feature of these experiments was that the corrosion product which formed in the petrol condensate was more than those formed in the diesel condensate. The petrol corrosion product was white in colour which probably resulted from crystallisation of the condensate while the diesel corrosion product was brownish. The brownish colour of the corrosion products was probably an indication of the high rate of metal loss.

From the corrosion rates it was clear that both 304 and 434 had very good corrosion resistance to petrol and diesel condensates. However, 434 could be chosen for application in the cold end due to the possible saving in cost (Alves, *et al.*, 2002).

5.2 Electrochemical tests – Test 7

As mentioned in Chapter 3, the most commonly encountered cause of pitting, namely the presence of chlorine ions, is encountered in the composition of both the exhaust gas (internal corrosion) and road salt (external corrosion); and therefore electrochemical tests in petrol and diesel condensates were performed.

Anodic potentiodynamic polarisation scans were performed to determine the effect of the condensates on the corrosion potential, corrosion current density and passive current density. In these tests the samples were polarised at -0.7 V for 10 minutes (van Bennekom *et al*., 1999) to clean off any oxide layer on the surface, followed by scanning the potential from -250 mV vs. E_{corr} to 1600 mV vs SCE.

To determine the ability of these steels to repassivate and protect the pitted sites, cyclic (also known as pitting) scans were performed. By running these scans, the protection potential (E_{prot}) which determines the ability of the stainless steels to repassivate was established, along with the pitting potential (E_{pit}). In these tests, the samples were held for one hour in the electrolyte, which was enough to stabilise the open circuit potential, before performing the cyclic scans. The scans were started at -50 mV vs E_{corr} and, when the current density exceeded 5 mA/cm^2, the scans were reversed to end at 0 mV vs E_{corr} (ASTM G61 – 98).

The specimens were prepared as explained in section 4.3.

In all these tests, at least two runs per condition were performed to check reproducibility. A scanning rate of 0.5 mV/sec was used.

5.2.1 Results

Typical anodic polarisation scans and cyclic scans for 304 in the petrol condensate are shown in Figures 5.17 and 5.18, respectively. The other polarisation scans of these and subsequent electrochemical tests are presented in Appendix B.

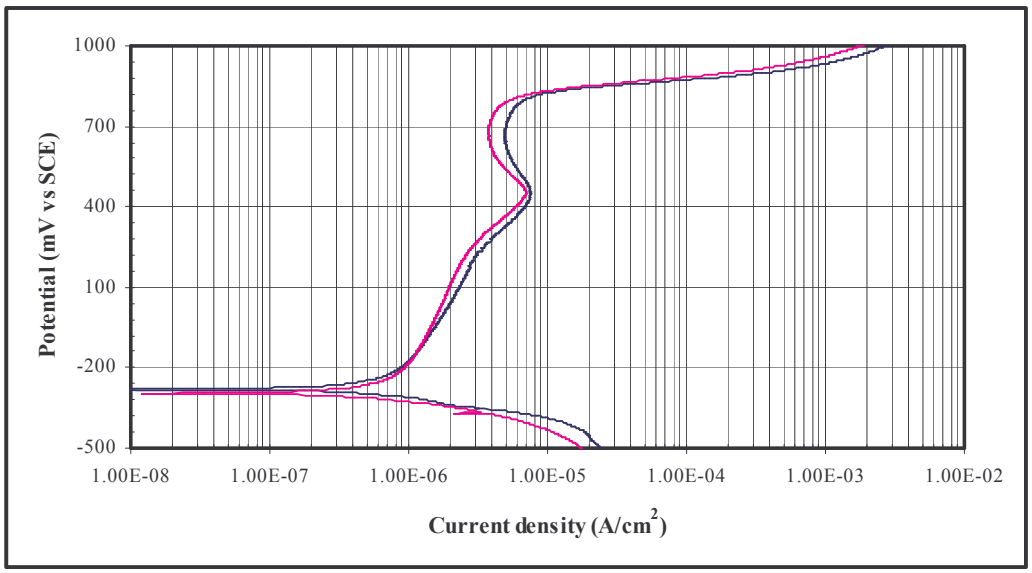


Figure 5.17: *Anodic polarisation scans of 304 in the petrol condensate, showing good reproducibility*

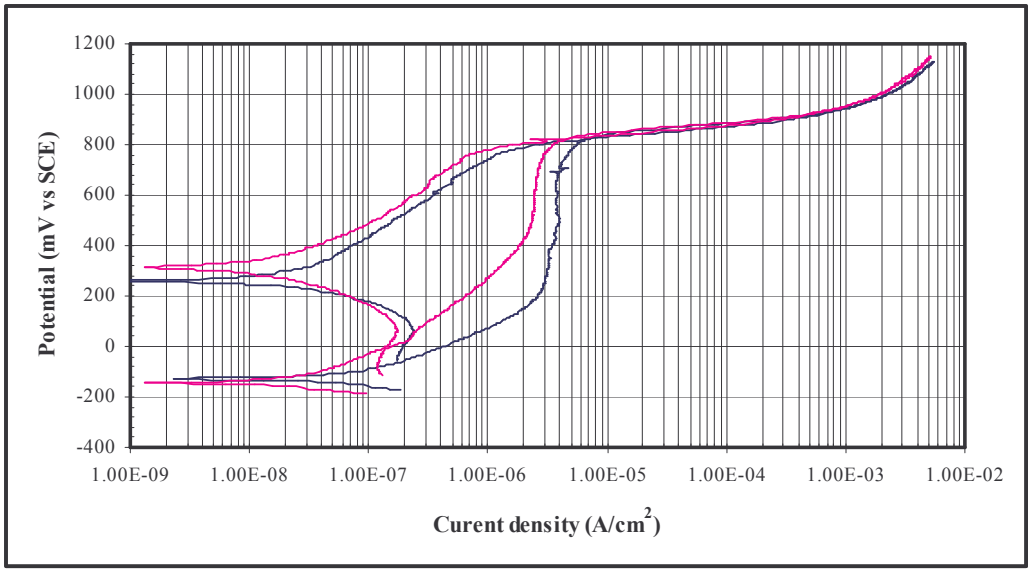


Figure 5.18: *Cyclic polarisation scans of 304 in the petrol condensate; scans showing good reproducibility*

The electrochemical parameters obtained from these polarisation scans are presented in the graphs below with a list of the actual values in table form in Appendix B. These parameters were determined as explained in section 2.6.3.

The corrosion potentials are given in Figure 5.19 and the corrosion rates in Figure 5.20. The corrosion rates were calculated as explained in section 4.5.

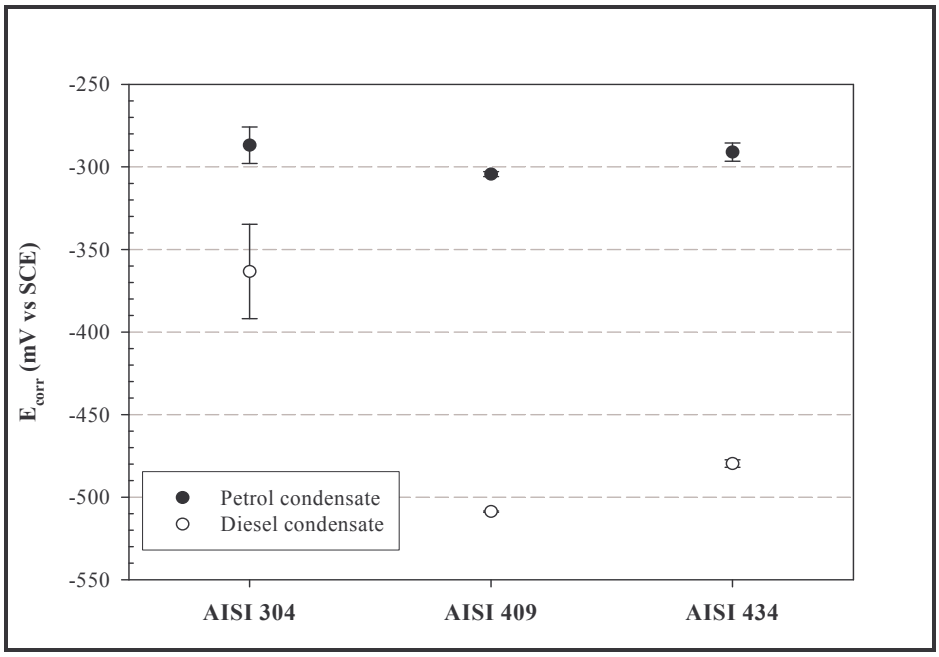


Figure 5.19: *Comparison of corrosion potentials in the petrol and diesel condensates, showing highly electronegative potentials for the diesel condensate*

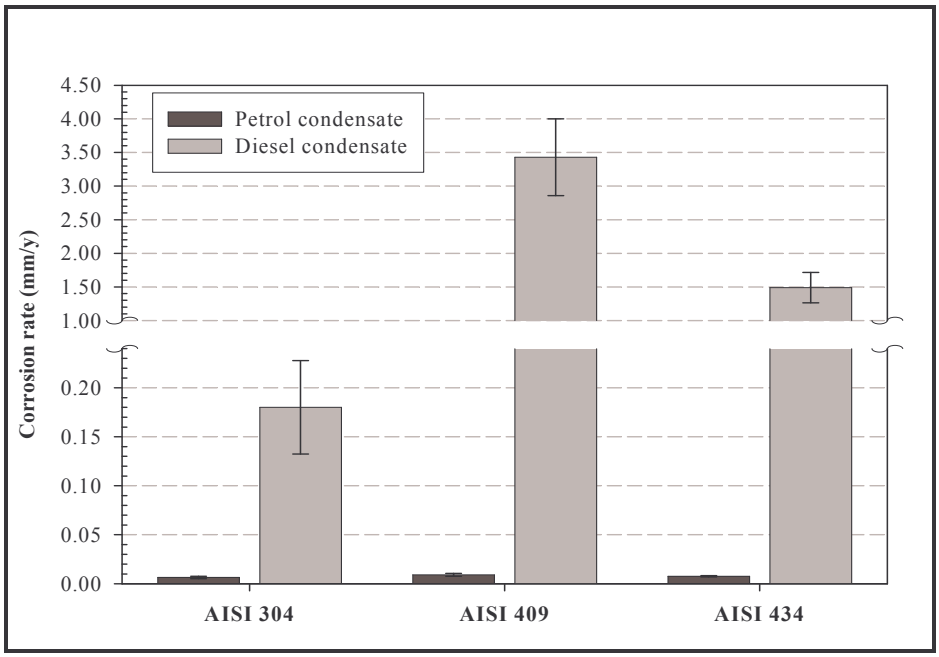


Figure 5.20: *Comparison of corrosion rates in the petrol and diesel condensates, showing very low corrosion rate for the petrol condensate*

The 304 was the most resistant in both condensates, followed by 434 and then 409. The corrosion potentials in the petrol condensate were within the same scatter band, while in the

diesel condensate the 304 had a less electronegative potential. The corrosion rates of all the steels were almost the same in the petrol condensate, but in the diesel 304 corroded much slower.

The corrosion potentials were less electronegative and the corrosion rates higher in the diesel condensate, indicating its greater aggressiveness. The results agree with the immersion test results and, considering the very low corrosion rates of these stainless steels, indicate that all three can be used successfully in petrol engines. These results further suggest that electrochemical tests can be used to predict the corrosion behaviour of stainless steels in exhaust systems. This could be an advantage considering that they are easier to perform and less time consuming than the immersion tests, provided that the equipment is available.

The passive current densities for the stainless steels in the condensates are shown in Figure 5.21.

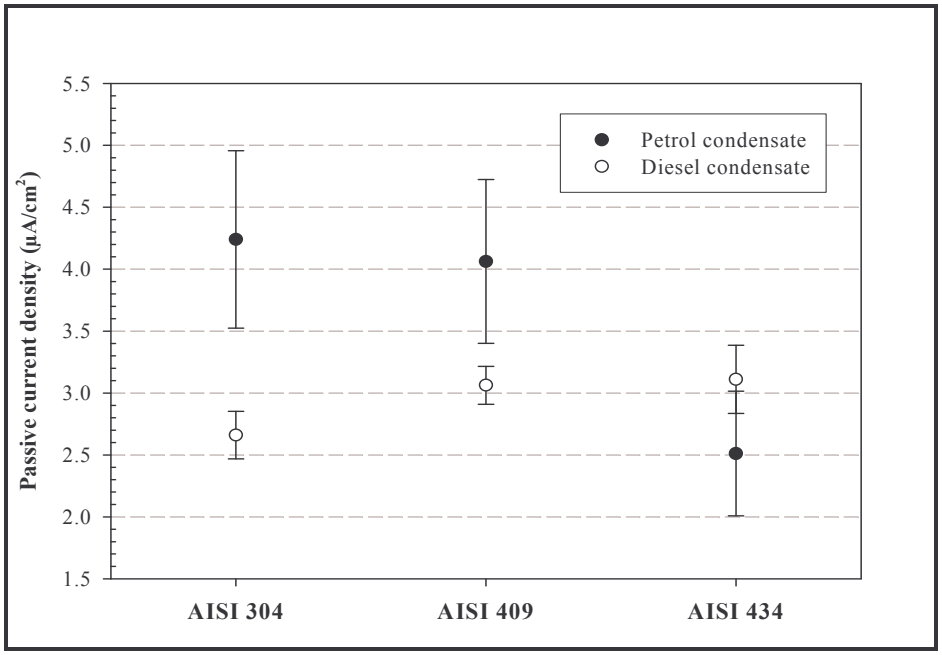


Figure 5.21: *Comparison of passive current densities in the petrol and diesel condensates showing that the current densities of the 434 are almost the same in the two solutions*

In the diesel condensate the passive current densities varied only slightly, indicating that, once passivated, the materials will corrode at more or less the same rate. In the petrol condensate, 304 and 409 had comparable passive current densities, slightly higher than in the diesel condensate, while 434 had the lowest passive current density. The higher the passive current density the lower the corrosion resistance, therefore, this lower passive current density of 434 could explain its good performance during the immersion testing in the petrol condensate.

The pitting potentials and passive potential ranges are given in Figure 5.22 and Table 5.2.

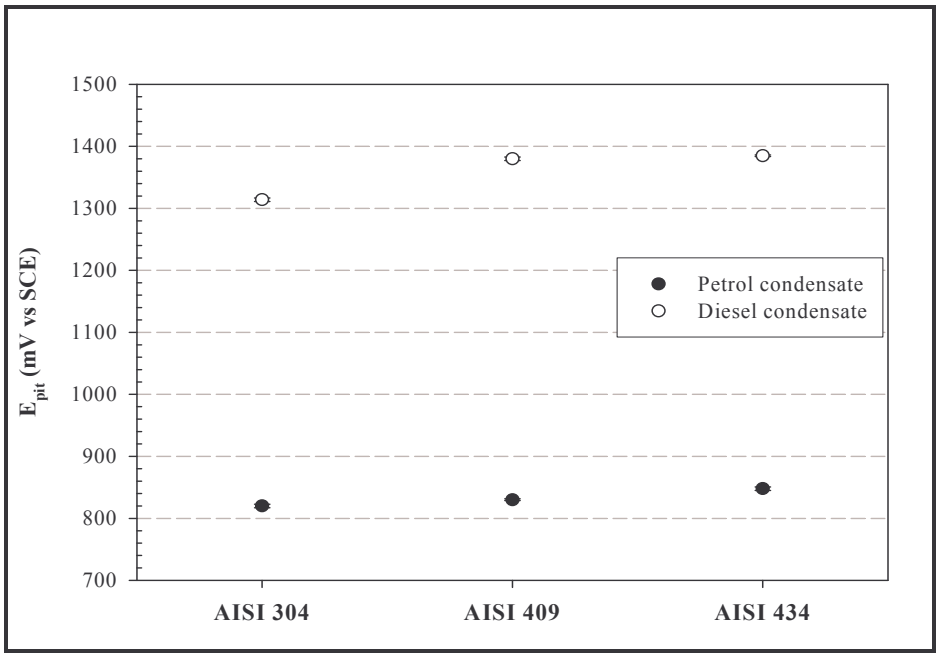


Figure 5.22: *Comparison of pitting potentials in the petrol and diesel condensates, showing significantly high pitting potentials in the diesel condensate*

Table 5. 2: *Comparison of passive potential ranges in the petrol and diesel condensates*

	Petrol condensate			Diesel condensate		
	AISI 304	**AISI 409**	**AISI 434**	**AISI 304**	**AISI 409**	**AISI 434**
E_{corr} (mV vs SCE)	-135	-182	-199	-196	-514	-401
E_{pit} (mV vs SCE)	820	830	848	1314	1380	1385
R_{pass} (mV)	**955**	**1012**	**1047**	**1510**	**1894**	**1786**

A higher pitting potential (E_{pit}) value means the material is more resistant to pitting corrosion. The passive potential range (R_{pass}), defined as $E_{pit} - E_{corr}$, indicates pitting resistance of the materials. The fact that 304 had a fairly low pitting potential and a narrow passive range, implied that it is less resistant to pitting corrosion.

An exclusive feature of the pitting scans is the ability to determine whether or not materials repassivate to protect the pitted sites. The repassivation abilities (as explained in section 2.6.3) for the stainless steels in the condensates are shown in Figure 5.23.

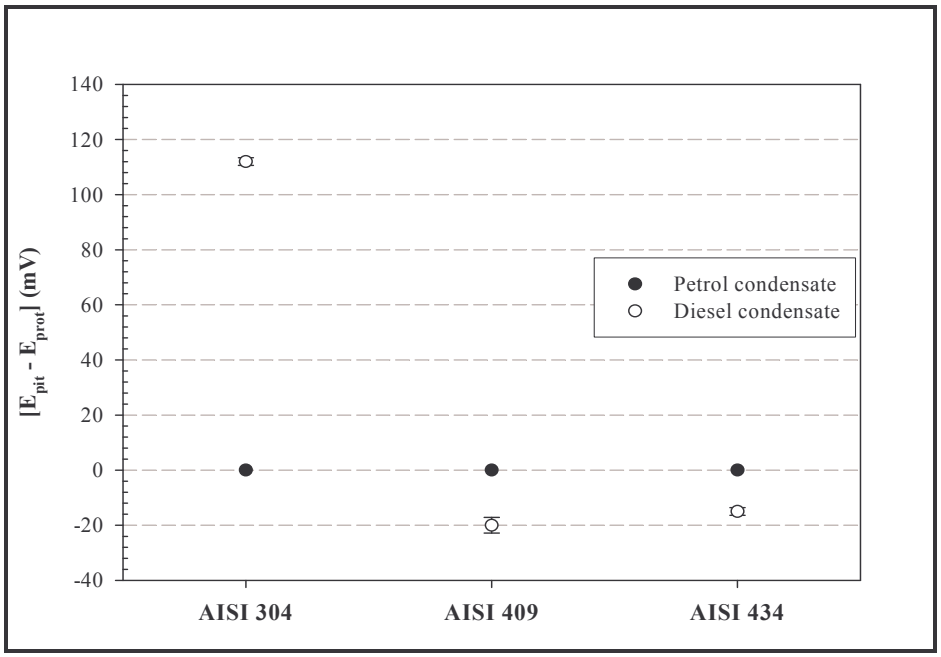


Figure 5.23: *Comparison of [$E_{pit} - E_{prot}$] in the petrol and diesel condensate showing that the E_{pit} and E_{prot} were equal for the petrol condensate*

All the materials passivated spontaneously (see Figure 5.18 and the rest in Appendix B). In the diesel condensate, the forward scans of 304 reversed to the right indicating that the pitting potential was higher than the protection potential, and creating a hysterisis which means that 304 was less resistant to localised corrosion than ferritic stainless steels whose loops returned to the left in the diesel condensate. In the petrol condensate, all the stainless steels showed excellent resistance to localised corrosion, since the pitting potential was equal to the protection potential.

In comparing the results obtained in the two test condensates, consideration has to be paid to the fact that different concentration ranges of the ions were used. The difference in concentration of the most detrimental ions (SO_4^{2-} and Cl^-) was not much, however. The concentration of the SO_4^{2-} ions was reduced from 5000 ppm in petrol condensate to 2750 ppm in the diesel condensate. The Cl^- ions of the diesel condensate were 1250 ppm compared to 1000 ppm in the petrol condensate. However, corrosion rate results (see Figures 5.16 and 5.20) indicate that the difference in material behaviour in these two test solutions is significant. This suggests that the variations in concentrations of the so-called less detrimental ions, particularly NO_3^- and NH_4^+ influence the corrosion rates to a great extent. The presence of NO_3^- is known to reduce stainless steel corrosion. It reacts with the metal surface and becomes incorporated in the passive film to strengthen, complete, and repair it (Bradford, 2002). Therefore, it was expected that the corrosion rates would be less in diesel condensate since it has a higher concentration of NO_3^- (1750 ppm compared to the 100 ppm in the petrol). However, the results of this investigation

show the opposite. It therefore appears that the NH_4^+ is responsible for the low corrosion rates of the materials in the petrol condensate. The concentration of NH_4^+ in petrol was 3740 ppm, while only 340 ppm in the diesel solution, and hence it seems that at high concentrations, NH_4^+ acts as an inhibitor.

The behaviour of stainless steels in Cl^-, SO_4^{2-}, and NO_3^- has been investigated in detail (Hakkarainen, 1999; Abd El Meguid, *et al.,* 1997; Isaacs and Kaneko, 1999). It was found that an increase in the Cl^- and SO_4^{2-} reduces the corrosion resistance of stainless steels, while as mentioned, an increase in NO_3^- acts as an oxidiser (direct passivator) and increases corrosion resistance (Bradford, 2002). However, the effect of the NH_4^+ ion on the behaviour of stainless steels is not known. Therefore, the effect of increasing NH_4^+ concentration on the corrosion resistance of the stainless steels was investigated.

5.2.2 The effect of ammonium ions (NH_4^+) in the condensate

In order to establish the effect of NH_4^+ on the corrosion behaviour of stainless steel, electrochemical tests were performed in the petrol condensate (as a base solution) with varying NH_4^+ ion concentrations. These tests were also performed to try and understand why 434 performed slightly better than type 304 in the petrol condensate and slightly worse in the diesel condensate. The solutions for investigation were as follows:

Table 5.3: *Chemical composition of simulated exhaust gas condensates with varying NH_4^+ ion concentrations*

Ions (ppm)	Solution 1	Solution 2	Solution 3	Solution 4	Solution 5
Cl^-	1000	1000	1000	1000	1000
SO_4^{2-}	5000	5000	5000	5000	5000
CO_3^{2-}	3000	3000	3000	3000	3000
NO_3^-	100	100	100	100	100
NH_4^+	**3740**	**1800**	**1000**	**600**	**340**

Solution 1 is equivalent to the petrol condensate and solution 5 to the diesel condensate.

The electrochemical scans are shown in Figures C1 to C15 in Appendix C. The average electrochemical parameters obtained from these figures namely corrosion potential, corrosion rate, pitting potential and passive current density are summarised in Table C.1 in Appendix C.

A comparison of the corrosion rate results from the condensates with varying NH_4^+ ion are shown in Figure 5.24:

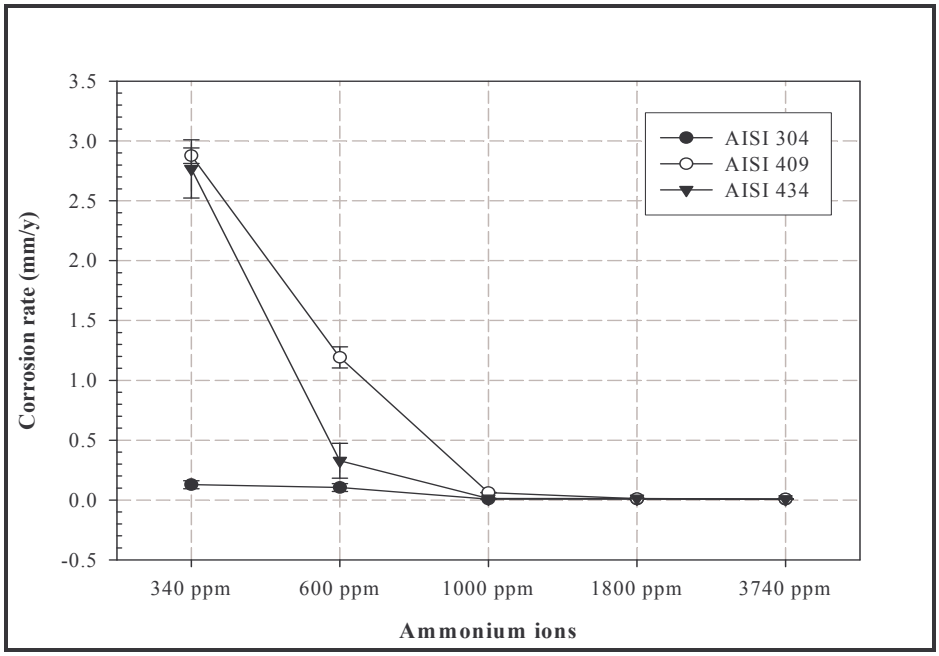


Figure 5.24: *Comparison of corrosion rates in the synthetic petrol solution with varying ammonium ion concentrations, showing a significant decrease in corrosion rates with an increase in the ion concentration*

The corrosion rates clearly illustrate the beneficial effects of NH_4^+. Especially the ferritic stainless steels benefit by these additions as can be seen by the marked reduction in their corrosion rates. These results explain the significant drop in corrosion rate of the ferritic stainless steels in the petrol condensate in both the electrochemical and immersion tests. The optimum concentration seems to be 1000 ppm where the rates of both ferritics were reduced to that of the 304.

5.3 Modified electrochemical test – Test 8

As mentioned in Chapter 3, this test was developed to simulate the condition of the cold end components as the car heats from ambient to 400 ^{o}C, remains at this temperature for the duration of the journey and cools down as the car stops (Inoue and Kikuchi, 2003).

The procedure was as follows (see also Figure 5.25):

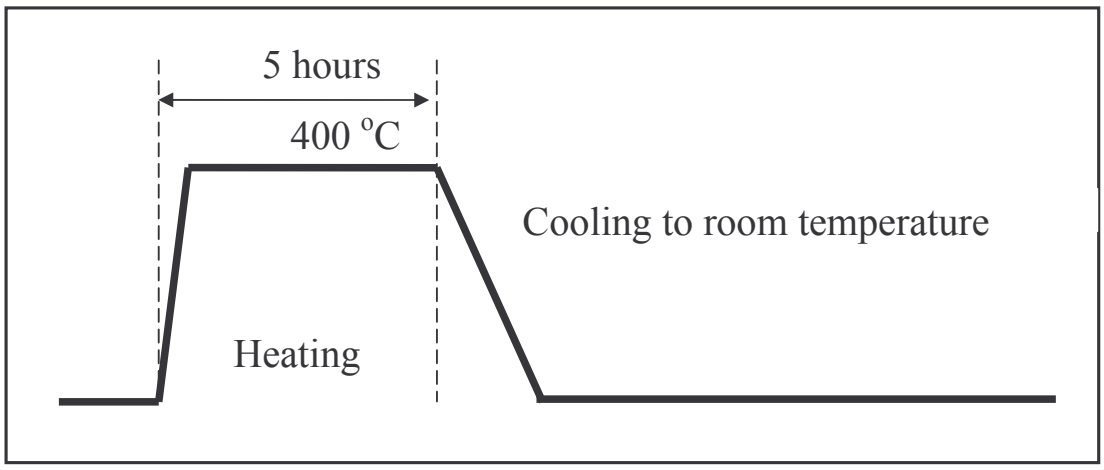


Figure 5.25: *Schematic diagram of the heat treatment cycle*

The specimens were cut from the sheets of the candidate materials and heated in air at 400 ^{o}C for 5 hours. They were then allowed to cool down completely in air. The samples were tested in their as-heat treated condition. Anodic polarisation scans in the condensate solutions were performed.

The mounting procedure, experimental arrangement and scan parameters were as described in the electrochemical tests of sections 5.2 above.

5.3.1 Results

To some extend this test is similar to the electrochemical tests above, except that the materials were tested in the oxidised state and that only anodic potentiodynamic polarisation scans were performed. The scans and parameters are presented in Appendix D.

The corrosion potentials and corrosion rates are given in Figures 5.26 and 5.27, respectively.

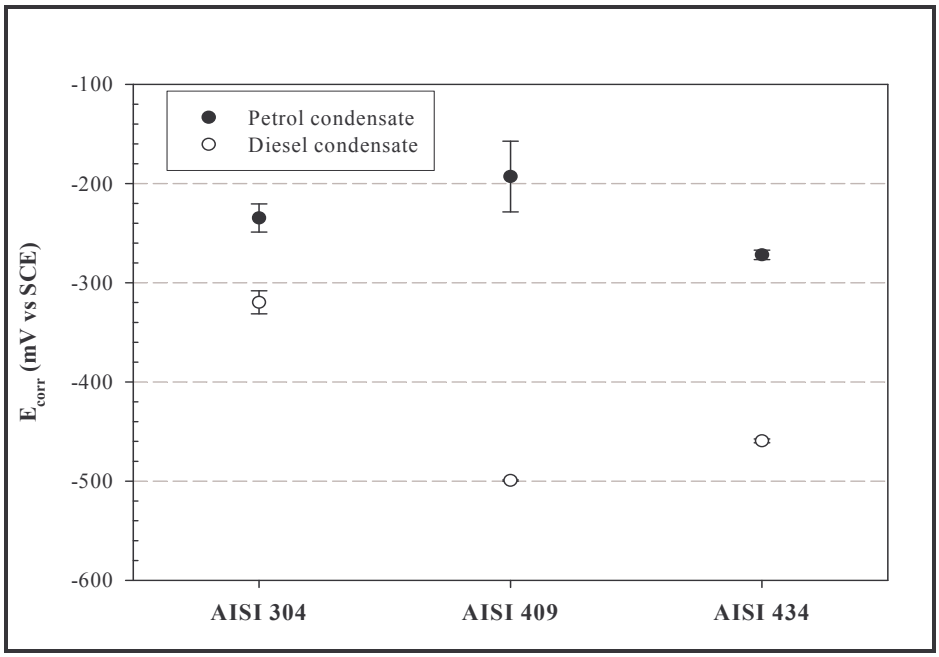


Figure 5.26: *Comparison of corrosion potentials in the condensates, showing comparable potentials in the petrol condensate*

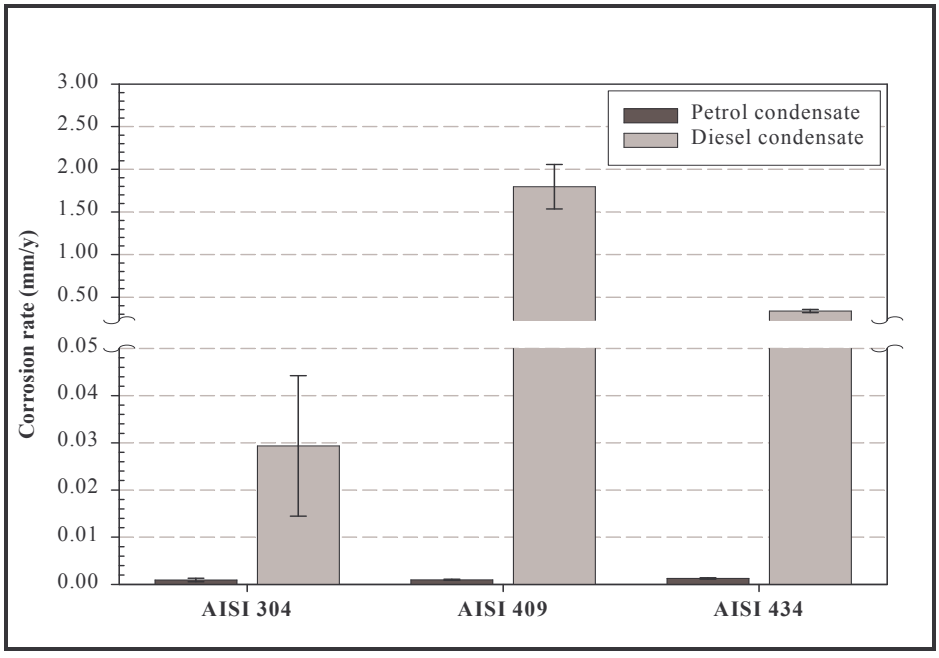


Figure 5.27: *Comparison of corrosion rates in the condensates, showing very low corrosion rates in the petrol condensate*

The corrosion potentials in the petrol condensate were within the same scatter band, while in the diesel condensate the 304 had a less electronegative potential. The corrosion rates were the same in the petrol condensate, the very low values indicating very good corrosion resistance. In the diesel condensate, the 304 was the most resistant, followed by 434 and then 409. The difference in resistance between the austenitic stainless steel and the ferritics was pronounced.

Again, in the heat treated (oxidised) conditions, the materials had more electronegative corrosion potentials and higher corrosion rates in the diesel condensate, indicating its greater aggressiveness. These results also agree with the immersion (condensate) test (section 5.1.3) and electrochemical test of unoxisided condition (section 5.2.1) results. Again, the very low corrosion rates of these stainless steels indicate that all three can be used successfully in petrol engines.

The passive current densities for the stainless steels in the condensates are shown in Figure 5.28.

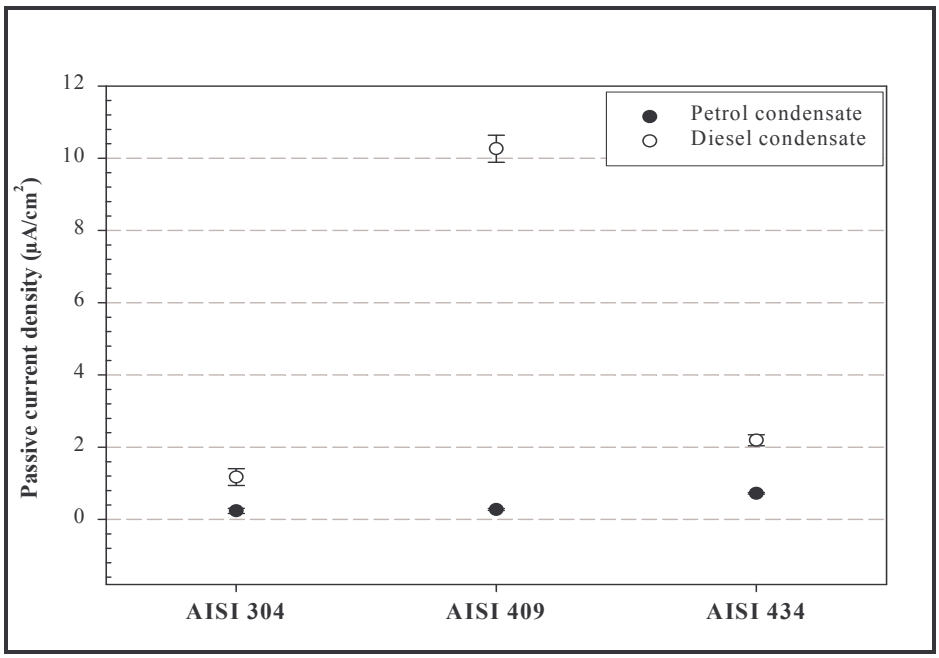


Figure 5.28: *Comparison of passive current densities in the condensates, showing comparable current densities in the petrol condensate*

The passive current densities do not vary much, except for 409 in the diesel condensate. The fact that 409 showed a high corrosion rate in the diesel condensate (Figure 5.28) is probably explained by its inability to passivate to low current densities. This seems to indicate that oxidising the 409 had weakened its passive film because in the unoxidised condition it performed comparable to the other steels.

The pitting potentials and passive ranges are given in Figure 5.29 and Table 5.4.

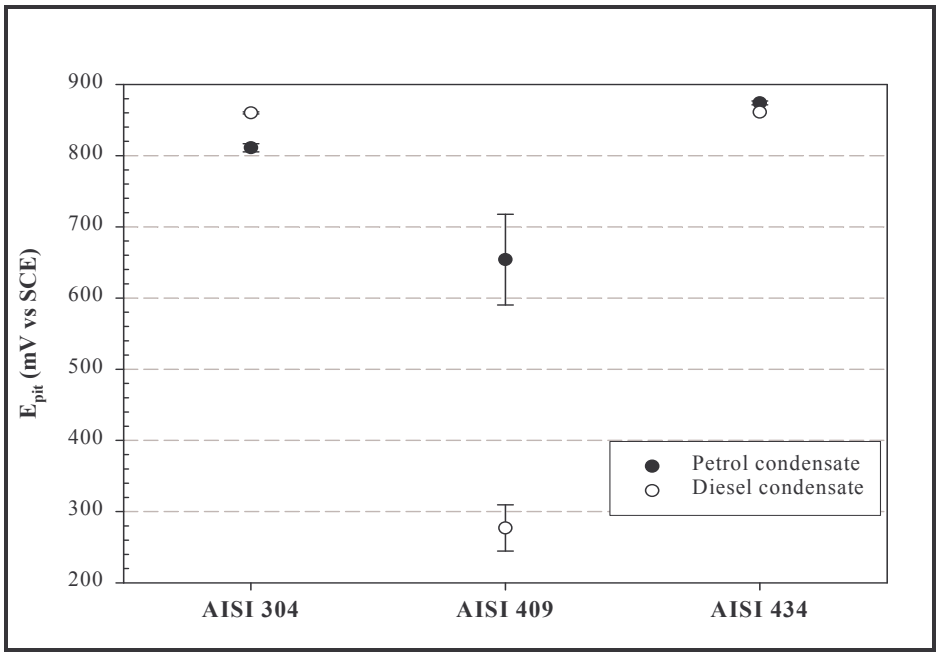


Figure 5.29: *Comparison of pitting potentials in the two condensates, showing a large difference in 409 results*

Table 5.4: *Comparison of passive ranges in the petrol and diesel condensates*

	Petrol condensate			**Diesel condensate**		
	AISI 304	**AISI 409**	**AISI 434**	**AISI 304**	**AISI 409**	**AISI 434**
E_{corr} (mV vs SCE)	-235	-193	-272	-320	-499	-459
E_{pit} (mV vs SCE)	811	654	847	860	277	847
R_{pass} (mV)	**1046**	**847**	**1119**	**1180**	**776**	**1306**

As said before, a lower pitting potential (E_{pit}) and narrow passive range (R_{pass}) mean the material is less resistant to pitting corrosion; as shown by the 409 sample. 304 and 434 had approximately the same values for both parameters in both condensates. These results are contrary to the unoxidised electrochemical test where all the materials were more resistant to pitting corrosion in the diesel condensate. This could be due to the fact that 409 seemed to be less resistant in the oxidised condition. 409 also recorded a very high passive current density, which indicates that it is less resistant than 304 and 434.

Comparing these results with the unoxidised results indicate that 409 is less resistant in the oxidised condition, while 304 and 434 performed basically the same in both conditions.

5.4 Discussion and conclusions

The previous sections of this chapter explained in detail all the results obtained from internal corrosion tests of the cold end components. In this section the results are discussed by comparing the developed tests with each other, their credibility, and finally comparing the behaviour of the stainless steels in all the tests performed.

The results obtained from both the immersion and electrochemical were consistent: The expected trend that 304 was the most resistant, followed by 434 and then 409 was obtained. All these tests were aggressive, particularly with the diesel condensate, with the electrochemical test the most aggressive since it recorded the highest corrosion rates. The small error bars (showing the minimum and maximum values from the mean) in the results indicate very little scatter and showing that results are reproducible and therefore can be relied on. Because electrochemical testing give the same results as obtained by immersion tests but much more rapidly it a desirable test to use – if equipment is available.

One of the aims of this research was to develop tests that could possibly be used as standard tests in the future, and the results obtained in this chapter prove that all the tests performed here are reliable and reproducible, and therefore can be recommended for use as standard tests.

In the electrochemical tests, the oxidised and unoxidised materials gave similar corrosion rate results. The other parameters showed that 409 had a reduced resistance in the oxidised condition. 409 is known to be resistant to oxidation conditions up to 816 ^{o}C (less than that of 304 and 434), however 400 ^{o}C seemed to weaken its passive film, hence the recorded high passive current density, low pitting potential and narrow passive range. The trends in corrosion rates were similar in both conditions (oxidised and unoxidised), probably because in anodic polarisation scans, the materials were polarised for 10 minutes at -0.7 V to clean off any oxide build-up, which would also have removed any lightly adhering oxide film. This probably happened with this test because on the oxidised materials after the scan was completed the oxidised film was cleaned off. It could be recommended that materials are tested in their unoxidised condition with the surface prepared according to standards. There was no standard specifying that materials had to be tested in their as-oxidised condition.

In comparing the behaviour of the materials with each other, it was found that in most cases 304 was the most resistant in both the petrol and diesel condensates followed by 434 and then 409. However, the resistance of 434 compared very well to that of 304. It was only on immersion testing in the petrol condensate where 434 performed slightly better than 304. It was expected that the ferritic 434 will be inferior to the austenitic 304 (AK Steel data bulletin, 2003) and therefore it is suspected that its superior performance in the petrol condensate may be due to the high NH_4^+ concentration in this condensate. Electrochemical tests were performed to determine the effect of the NH_4^+ ions on the condensate, and it was found that NH_4^+ has a much greater inhibiting effect on the ferritic stainless steels than the austenitic one. The presence of NH_4^+ ions in a chloride solution is known to reduce the acid formation, i.e. it increases the pH (Baba et al, 2002; Jargelius-Pettersson; 1999). The results of this investigation show that this is beneficial to the corrosion resistance of the stainless steels. These results illustrated that ferritic stainless steel life can be significantly improved by introducing these ions in to exhaust systems, especially in the diesel engines. The inhibiting effect for the austenitic stainless steel was relatively small.

The 304 is known to be superior to condensate conditions containing chloride and sulphate ions and the results of this investigation agree with this. In the diesel condensate, 304 performed better than the ferritics, as expected because of its resistance to severe corrosive environments. This trend was also found by other researchers (AK Steel data bulletin, 2003; Allegheny Ludlum data bulletin, 2003). This validates the credibility of the developed tests for internal corrosion of the cold end components. In these condensate conditions, 409 was the least resistant of all the stainless steels. These results were expected, as other researchers (Alves *et al.*, 2002; Maximovitch *et al.*, 1994) have also found that in the chloride containing environments 409 stainless steel is inferior to stainless steels with high chromium contents. The reason why 434 performed comparable to 304 in the diesel condensate with low NH_4^+ concentrations is probably because of its Mo content. Mo is known to improve the corrosion resistance of stainless steels (Kaneko and Isaacs, 2002). These results show that its resistance to chloride containing environments is comparable to that of 304, thereby confirming findings of other researchers (AK Steel data bulletin, 2003). In the petrol condensate, the corrosion rates of all the materials were very low and comparable, indicating that all three can be used successfully in petrol engines.

All steels pitted in these condensates, but in many tests the pits were only visible with the SEM. The presence of these pits was expected since both condensates contain the detrimental Cl^- ions. When Mo and Ni are added as alloying elements (as in 304 and 434), they reduce the rate of this reaction and result in improved corrosion resistance (Maximovitch *et al.*, 1994, Kaneko and Isaacs, 2002).

When comparing the condensates, the diesel condensate was more corrosive than the petrol one in all the tests. The lower aggressiveness of the petrol condensate was due to the high level of NH_4^+ which seems to act as an inhibitor. The surface analysis also confirmed the trend observed from the corrosion rates. The photographs and SEM micrographs also show less corrosive attack on the materials exposed to the petrol condensate than diesel.

The other parameters from the electrochemical tests show interesting results. The corrosion potentials in the petrol condensate were less electronegative than in the diesel condensate. The less electronegative potentials indicate that passivity conditions were promoted. The austenitic 304 showed less electronegative corrosion potentials and this was expected due to its resistance to chloride environments. 409 seemed to show more electronegative values, while those of 434 were intermediate. Therefore, from the free corrosion potentials values only, it can be concluded that type 304 is the most resistant material to the synthetic condensate solutions.

The cyclic scans from the electrochemical test showed that all the materials passivated spontaneously. In the diesel condensate, the forward scans of 304 reversed to the right, while the scans of both 409 and 434 returned to the left. This means the pitting potential was higher than the protection potential in the 304, creating a hysterisis which indicate that, in the diesel condensate, the 304 is less resistant to localised corrosion than the ferritic stainless steels. This was further illustrated by the lower pitting potential and narrow passive range of 304. In the petrol condensate, all the stainless steels showed excellent resistance to localised corrosion since the pitting potential was equal to the protection potential.

The internal corrosion of the cold end results show that 304 and 434 are comparable to some extent and both superior to type 409. 434 could be chosen for application in the cold end rather than 304, since 434 is cheaper than 304 (Alves, *et al.*, 2002), and performs comparable to it.

Chapter 6

Cold end external corrosion tests

The experimental procedure, results and discussion of the cold end external corrosion tests are presented in this chapter. The tests employed here are the salt damage test, the modified salt spray test and electrochemical testing in a 5% salt solution, as discussed in Chapter 3.

6.1 Salt damage test – Test 5

This test was designed to simulate conditions of the cold end. The salt concentration of 5% sodium chloride and temperature of 400 ^{o}C were chosen to be a little higher than normally encountered, in order to increase the aggressiveness of the test and to produce rapid results. This test was also designed to simulate the cyclic conditions experienced by exhaust components. Ferritic 409 and 434 and austenitic 304 stainless steels were tested.

One exposure cycle consisted of (see also Figure 6.1):

- Initially immersing the samples in a 5% NaCl solution for 10 minutes
- Holding the samples for 2 hours at 400 ^{o}C.
- Natural cooling in air for 1 hour.

The corrosion product was softly brushed-off before the samples were weighed, followed by repeating of the immersion and heating cycle. Fresh solution was used for every sample in every cycle.

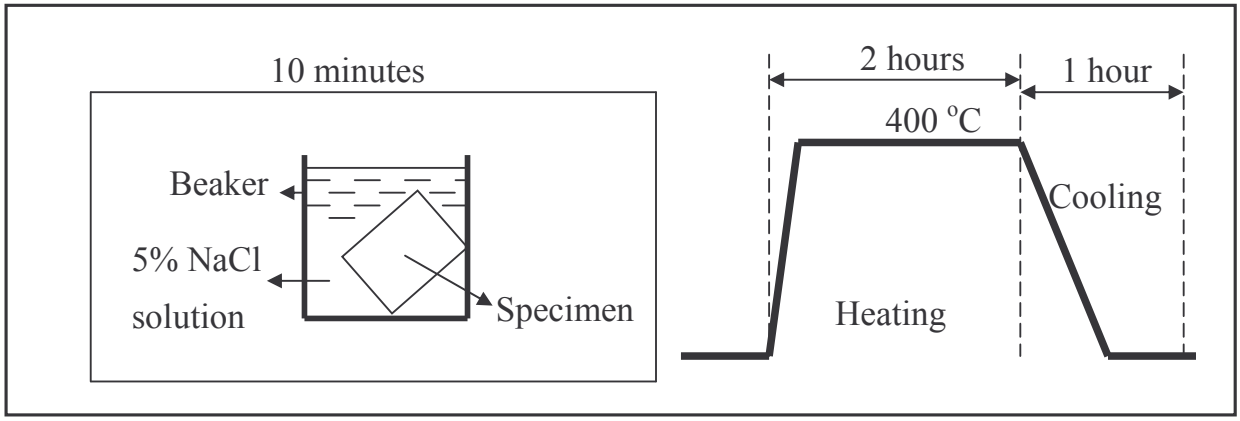


Figure 6.1: *Schematic diagram of the salt damage test exposure cycle: initial 10 minutes immersion followed by heating cycle*

After an exposure period of 16 cycles, the specimens were cleaned and evaluated as described in section 4.4.

6.1.1 Results

The results of exposure in the salt damage test for a period of 16 cycles are shown in Figure 6.2. The error bars indicate minimum and maximum values from the mean, since four samples were tested per condition.

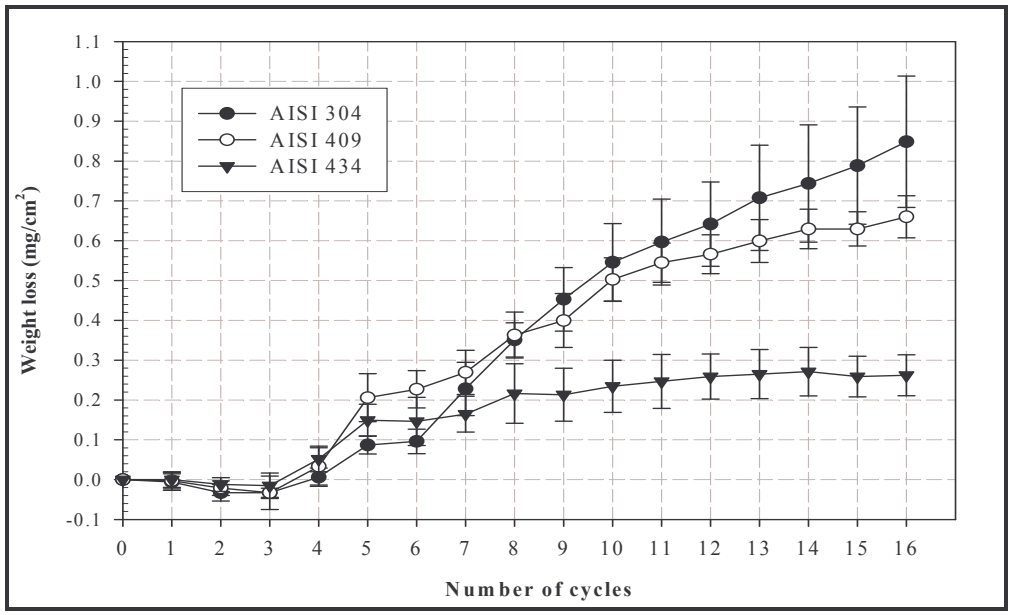


Figure 6.2: *Cumulative weight loss in the salt damage test. The average weight loss of four samples per material is shown, along with the standard deviations. 434 appeared more resistant*

In this chloride environment, 304 was the least resistant, though comparable to 409. However it showed more scatter than the 409. 434 was the most resistant of all the materials. Upon comparison it appeared that it was only after the 8th cycle that clear differences in weight loss arise.

Corrosion rates of the materials were calculated as mentioned in section 5.3.1 and a comparison is shown in Figure 6.3.

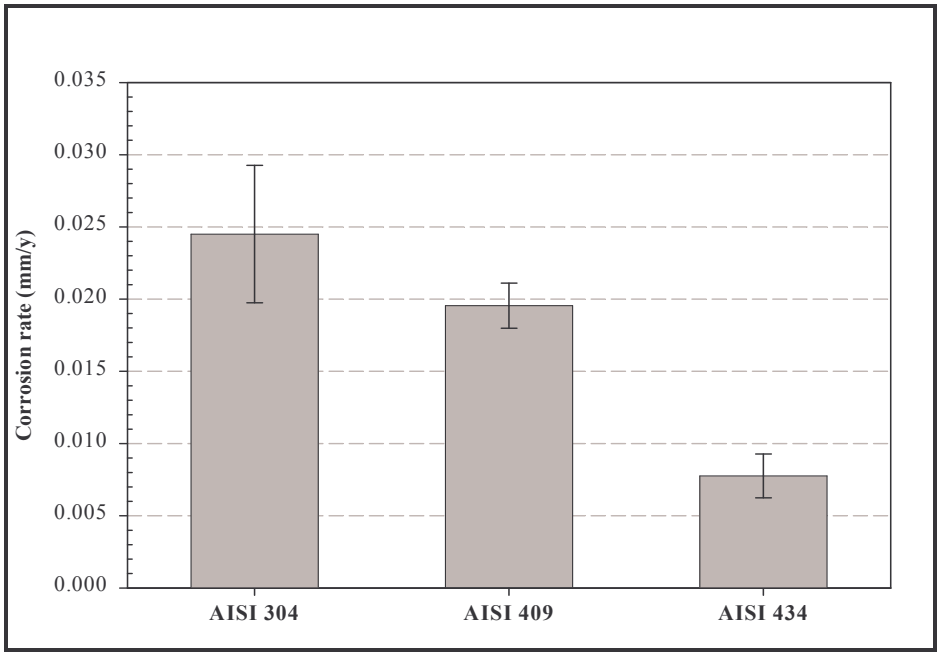


Figure 6.3: *Comparison of corrosion rates in the salt damage test (after 16 cycles), showing very low corrosion rates for all the materials*

In these salt conditions, 434 was the most resistant, followed by 409 and then 304, but since all the corrosion rates are low, all the materials are resistant to these conditions, and it seems that in the cold end, salt damage is not a problem - at least not for these materials.

Figures 6.4 to 6.6 show the photographs of the stainless steels after total exposure to the salt damage test.



Figure 6.4: *Photographs of 304 after exposure to the salt damage test, showing islands of corrosive attack*

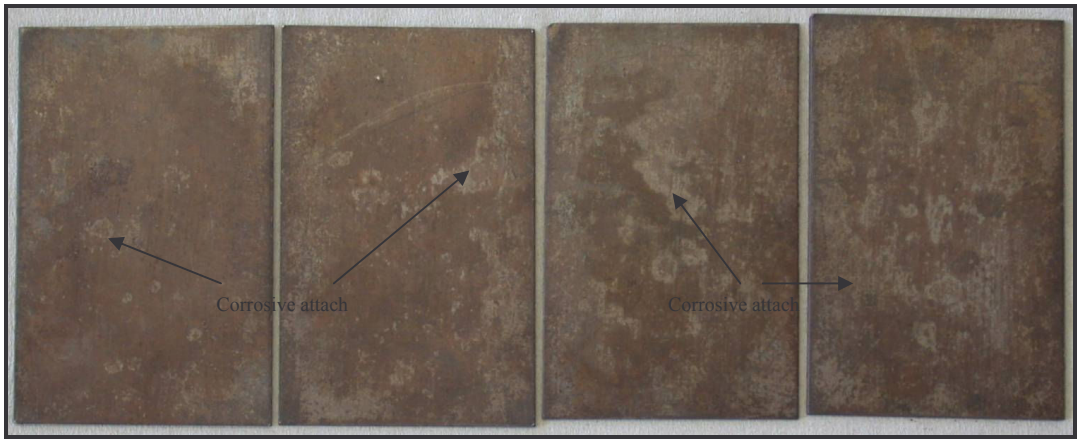


Figure 6.5: *Photographs of 409 after exposure to the salt damage test, showing islands of corrosive attack*



Figure 6.6: *Photographs of 434 after exposure to the salt damage test, showing islands of corrosive attack*

Visual examination of the exposed samples after cleaning and drying showed islands of general corrosive attack, and no pits could be observed. However, as shown by the SEM results in Figures 6.7 to 6.9, small pits did form on all the surfaces.

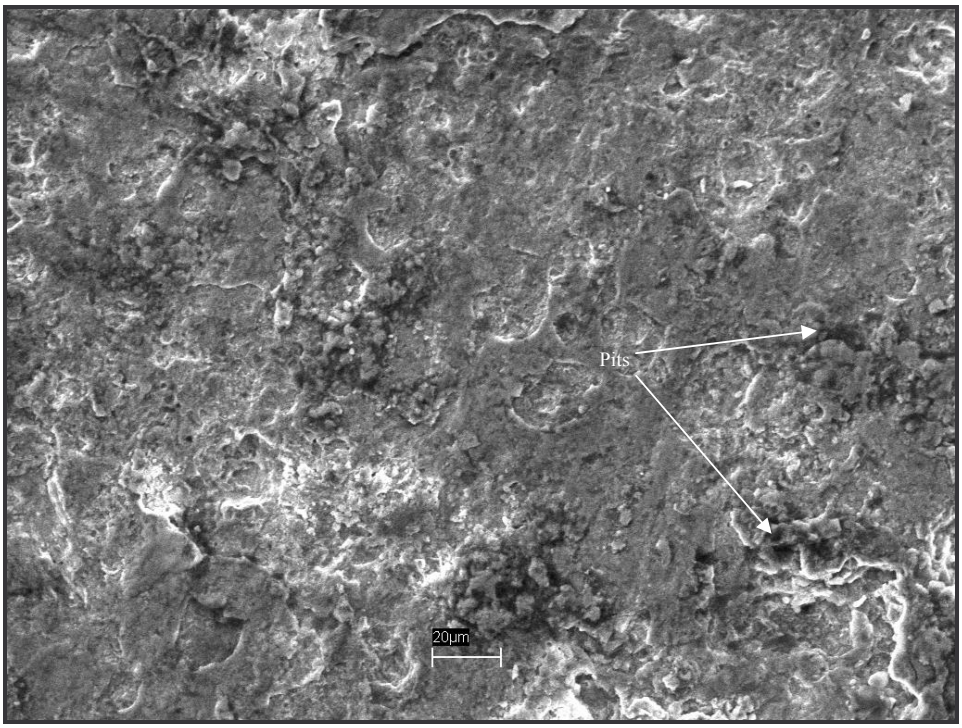


Figure 6.7: *SEM micrograph of 304 after total exposure to the salt damage tests, showing general corrosion as well as pitting (arrows)*

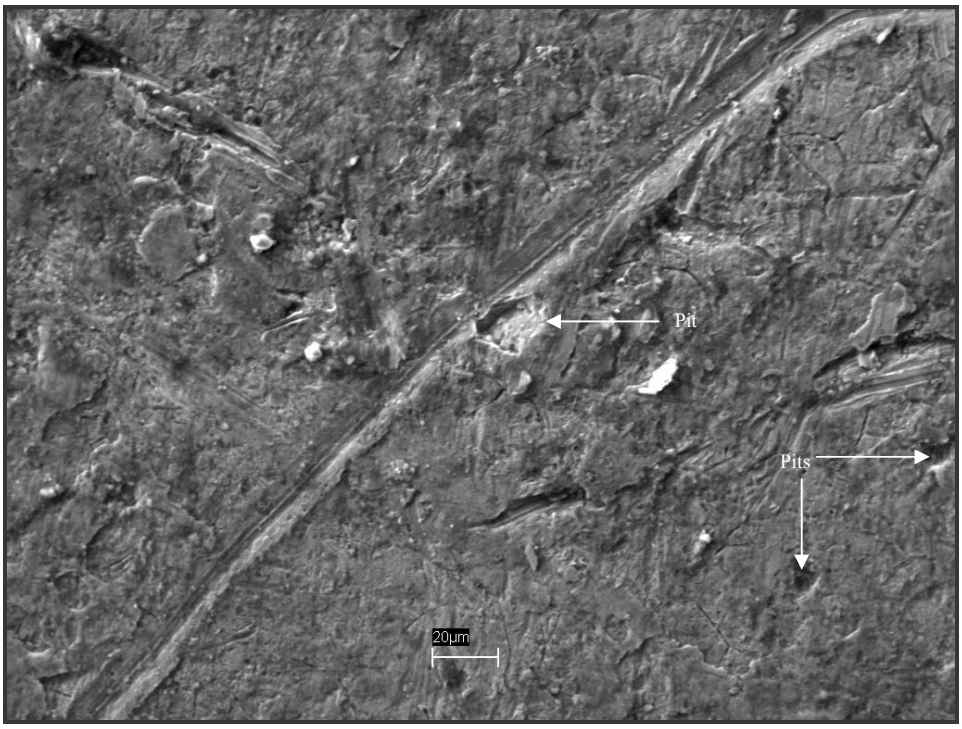


Figure 6.8: *SEM micrograph of 409 after total exposure to the salt damage test, showing general corrosion and pitting (indicated by arrowheads)*

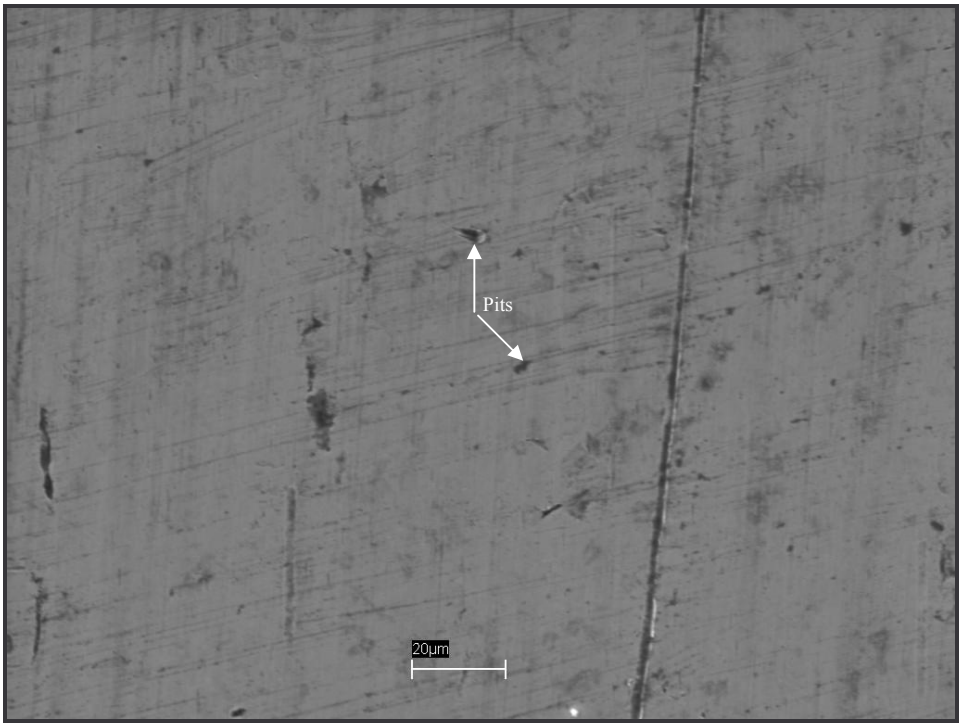


Figure 6.9: *SEM micrograph of 434 after total exposure to the salt damage test, showing pitting (indicated by arrowheads)*

409 had a few large pits, which apparently grew from the agglomeration of small pits, resulting in concentrated areas of attack. 304 had concentrated corrosive attack which appeared to be pits, while the 434 sample had only a very few pits.

The corroded surfaces agree with the weight loss results, where 304 had the highest weight loss and showed the most severe corrosive attack.

6.2 Modified salt spray test for tail pipe – Test 10

The test below was designed to take into account the actual surface condition of the tail pipe components. Some researchers paint the samples before they are heat treated to simulate the tail pipe temperatures (AK Steel Exhaust System Steels, 2002). However, where stainless steels (in themselves aesthetically appealing) are used, painting is not done. This test focuses on the appearance of tail pipe components.

Ferritic 409 and 434 and austenitic 304 stainless steels were tested. The procedure was as follows:

- Specimens were heated at 260 ^{o}C for 1 hour, and water quenched. This was repeated five times.
- This thermal cycle was followed by exposure to the 5% NaCl salt spray as per ASTM B117 - 1997 for one week to complete the test.

After an exposure period of seven days in the salt spray cabinet, the samples were removed from the cabinet and photographed immediately. They were then cleaned and evaluated as described in section 4.4. Samples were visually analysed to rank the degree of corrosion and weight loss was also measured.

6.2.1 Results

Figure 6.10 shows the results of exposure (168 hours) to the modified salt spray test. The corrosion rates were calculated as explained in section 5.3.1.

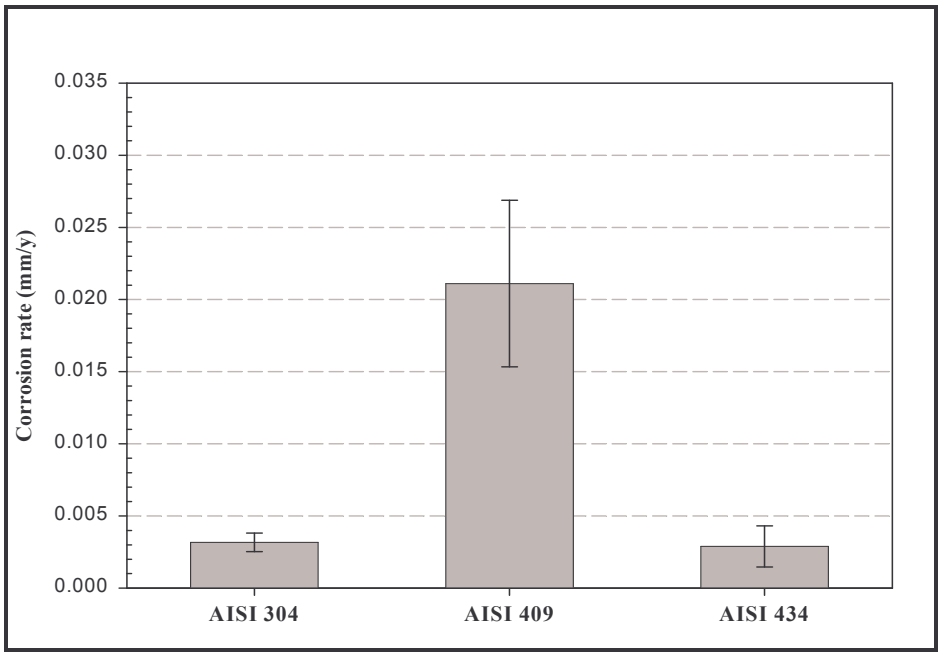


Figure 6.10: *Corrosion rate results in the modified salt spray test, showing the average corrosion rate of four samples per material*

In these chloride conditions, both 304 and 434 performed very well. This was expected because both of them are known to be resistant to chloride containing environments (AK Steel data bulletin, 2003). The 409 did not seem to be resistant at all and its corrosion rate was the highest.

The low corrosion rate results obtained here were expected since the dominant form of corrosion in salt spray exposure would be pitting corrosion not general corrosion.

Figures 6.11 to 6.13 show the photographs of the stainless steels after total exposure to the modified salt spray test.

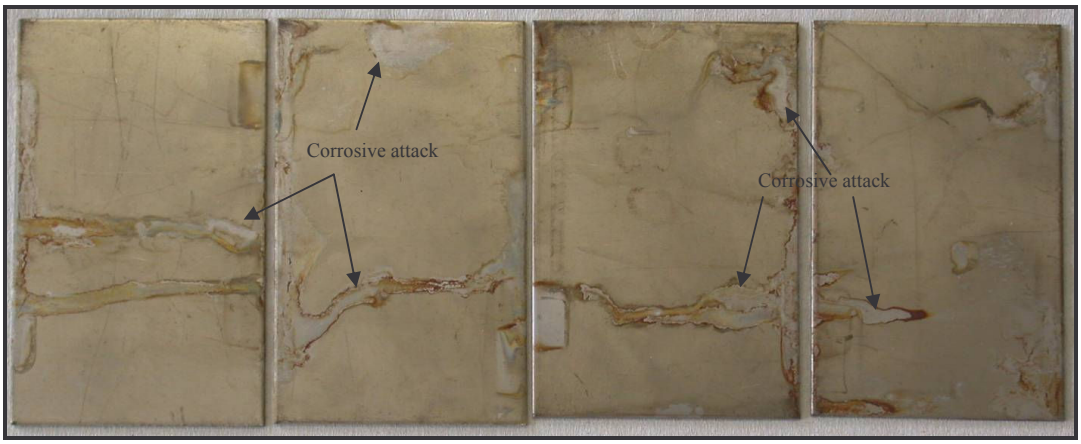


Figure 6.11: *Photographs of 304 after exposure to the modified salt spray test (corrosion product removed), showing islands of corrosive attack*

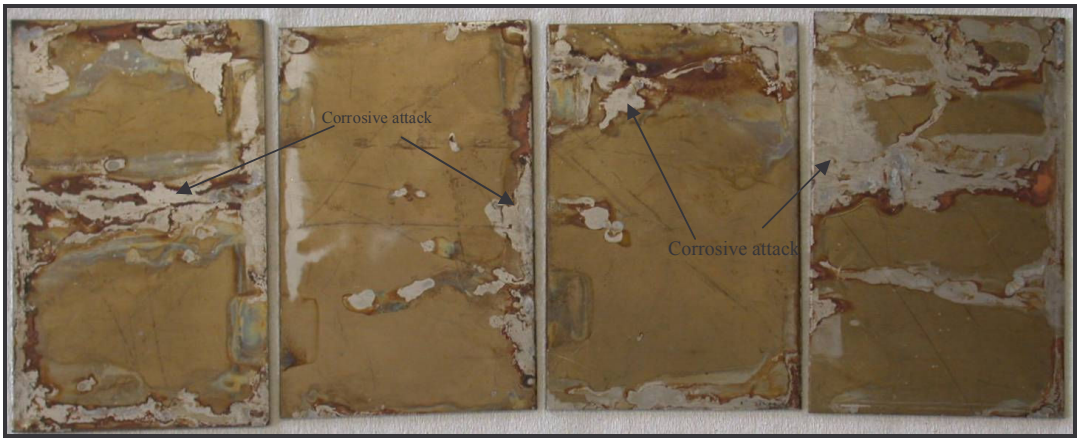


Figure 6.12: *Photographs of 409 after exposure to the modified salt spray test (corrosion product removed), showing islands of corrosive attack*

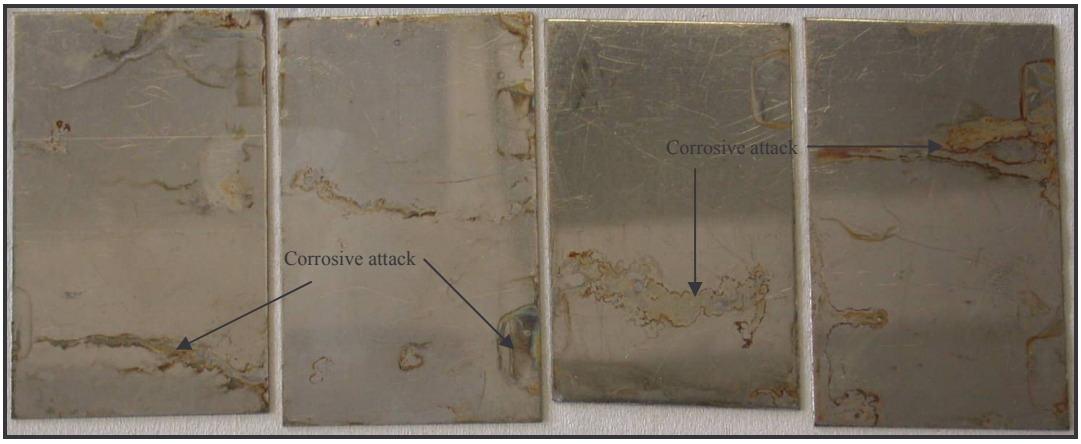


Figure 6.13: *Photographs of 434 after exposure to the modified salt spray test (corrosion product removed), showing islands of corrosive attack*

Visual examination of the samples after exposure to this test showed that, in these salt conditions, the 409 was the least resistant, while 304 and 434 were more resistant and showed comparable results. The rust covered about 60% of the whole surface of 409. 434 and 304 rusted slightly and about 25% of the whole surface rusted. Photographs taken immediately after total exposure before the corrosion product was washed off are presented in Figures A1 to A3 in Appendix A.

This visual examination, showed pits only on the 409. However, as shown by the SEM results in Figures 6.14 to 6.16, pits did form on all the surfaces.

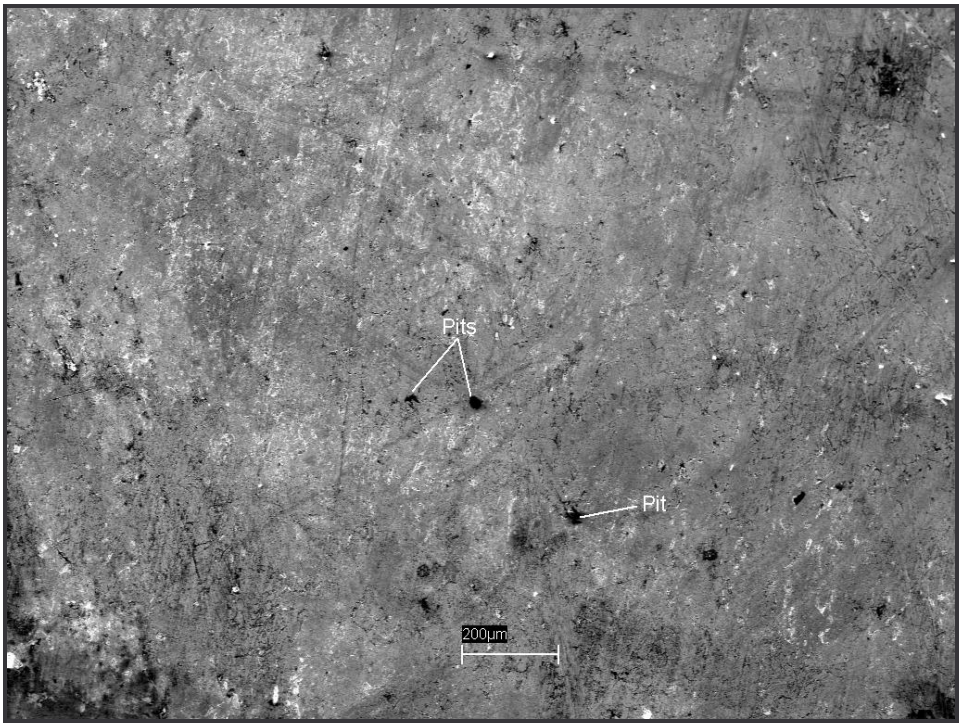


Figure 6.14: *SEM micrograph of 304 after total exposure to the modified salt spray test, showing small pits*

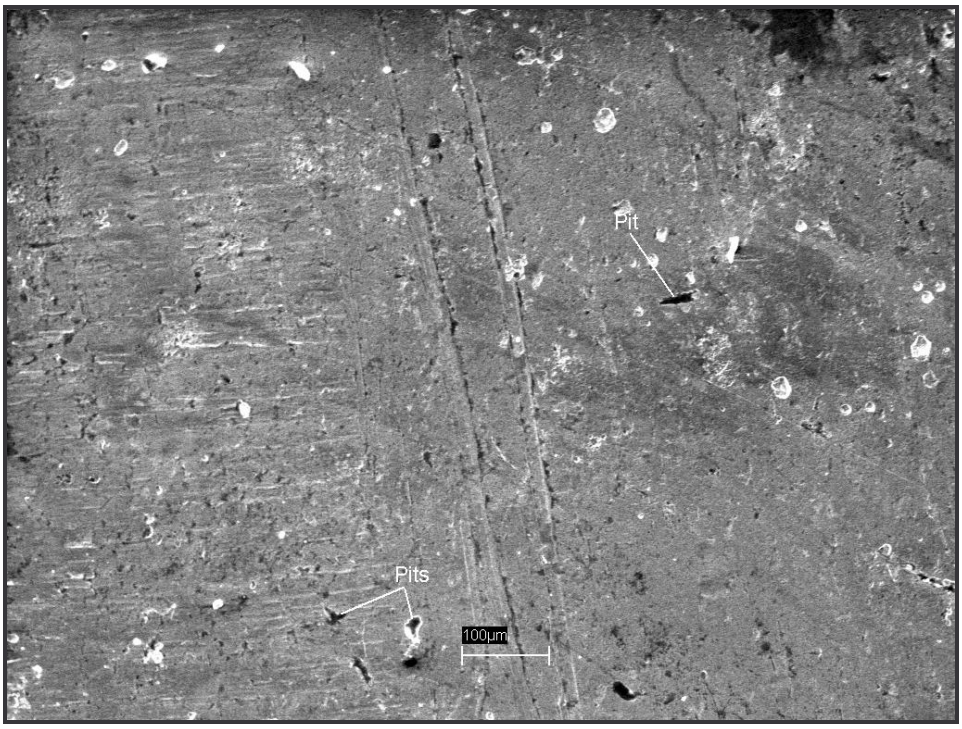


Figure 6.15: *SEM micrograph of 409 after total exposure to the modified salt spray test, showing many small pits*

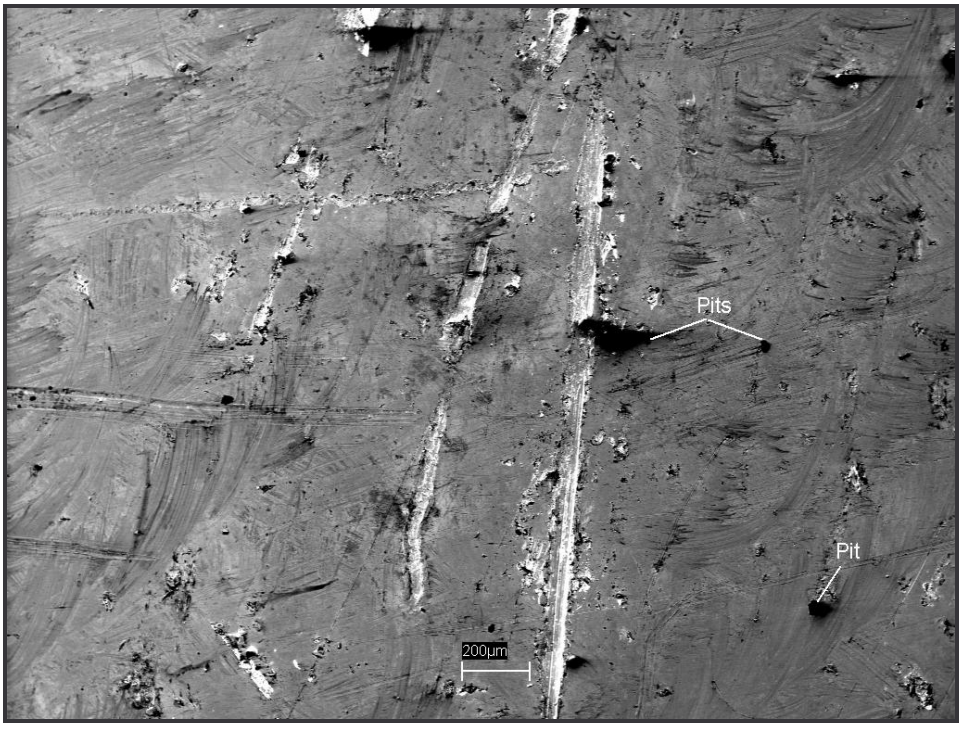


Figure 6.16: *SEM micrograph of 434 after total exposure to the modified salt spray test, showing a few pits on a less corroded surface*

From these SEM micrographs many small pits could be seen on the 304 and 409. The 434 sample had only a few. 409 seem to have been affected more by the corrosive attack, indicating its lower resistance to these conditions compared to the rest. These results agree with those of the weight loss, because 409 had the most weight loss and had corroded the most.

6.3 Electrochemical tests – Test 7

The most common cause of pitting, namely the presence of chlorine ions, is encountered in large amounts in road salts used for de-icing in colder countries. This test was developed to determine whether an electrochemical test can be used as a substitute to weight loss tests. This test was conducted using 5 % NaCl solution to investigate the pitting resistance of candidate materials under external corrosion conditions.

Again for anodic polarisation scans, samples were polarised at -0.7 V for 10 minutes (van Bennekom *et al*., 1999) to clean off any oxide layer on the surface, followed by scanning from -250 mV vs. E_{corr} to 1600 mV vs SCE.

For cyclic scans, samples were held for one hour in the electrolyte, which was enough to stabilise the open circuit potential, before performing the cyclic scans. The scan was begun at -50 mV vs E_{corr} and, when the current density exceeded 5 mA/cm^2, the scan was reversed to end at 0 mV vs E_{corr} (ASTM G61 – 98).

A scanning rate of 0.5 mV/sec was used in all the tests. At least two samples were tested per condition.

6.3.1 Results

Typical anodic polarisation and cyclic scans were shown in Chapter 5 in Figures 5.17 and 5.18, respectively. The polarisation scans generated by this test (Test 7) are presented in Appendix E1 (Figures E1 to E6). The electrochemical parameters obtained from these polarisation scans are presented in graphs and the actual values are presented in table form in Appendix E2.

The corrosion potentials and corrosion rates are given in Figures 6.17 and 6.18:

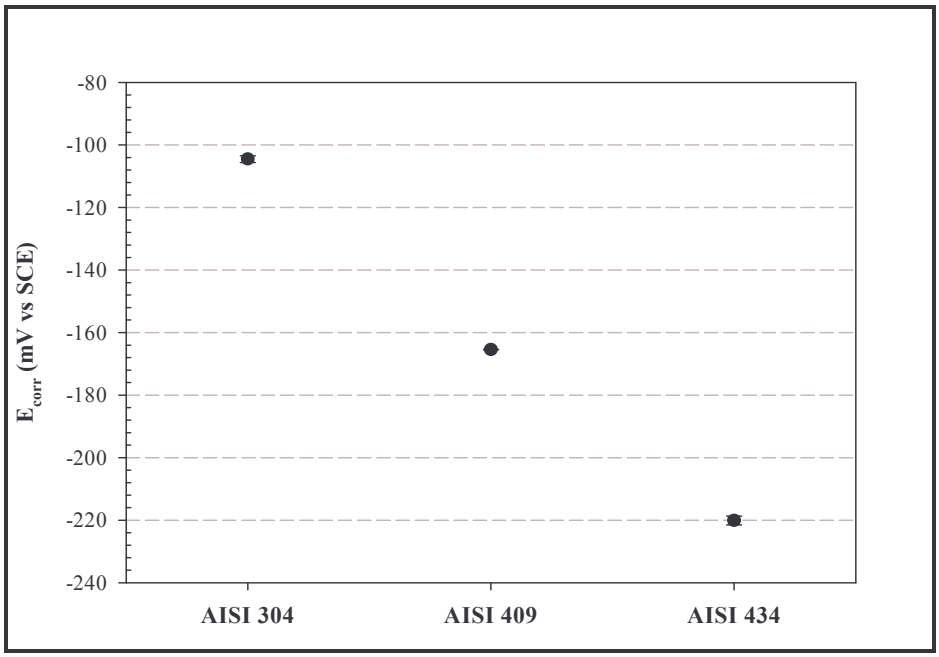


Figure 6.17: *Comparison of corrosion potentials in the 5% salt solution, showing a clear variation in the potentials*

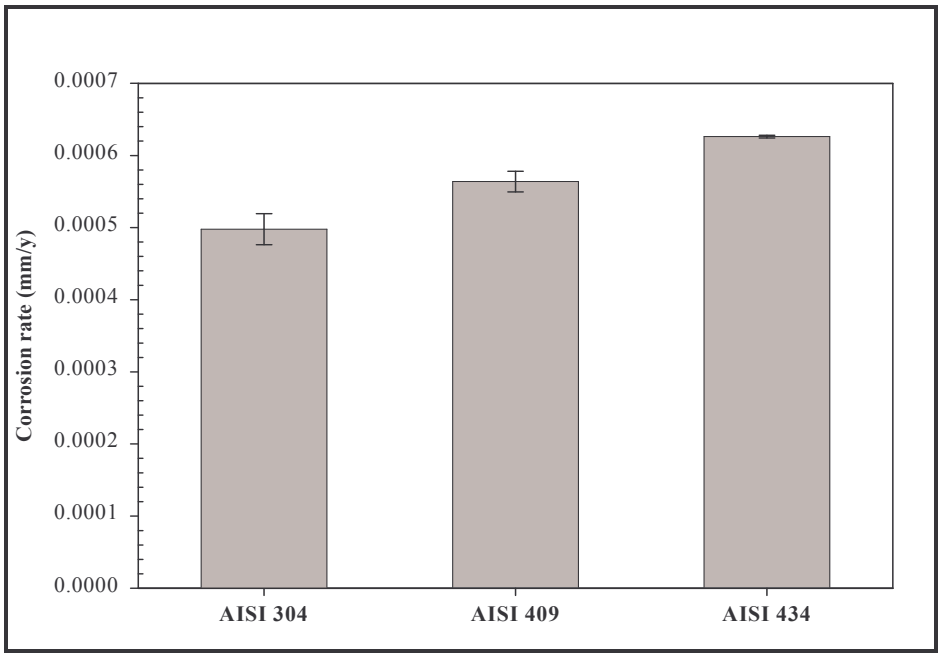


Figure 6.18: *Comparison of corrosion rates in the 5% salt solution, showing very low corrosion rates*

The corrosion potentials and corrosion rates show that the 304 was the most resistant, followed by 409 and then 434, however all the corrosion rates were very low, indicating that all the

materials were resistant to the salt condition. These results were expected since the dominant form of corrosion under these conditions would be pitting corrosion, not general corrosion. Therefore, this corrosion rates only proved that all the stainless steels are resistant to general corrosion. Again, these results indicate that external corrosion in the cold end due to salt is not a major problem.

The passive current densities for the stainless steels in the salt solution are shown in Figure 6.19.

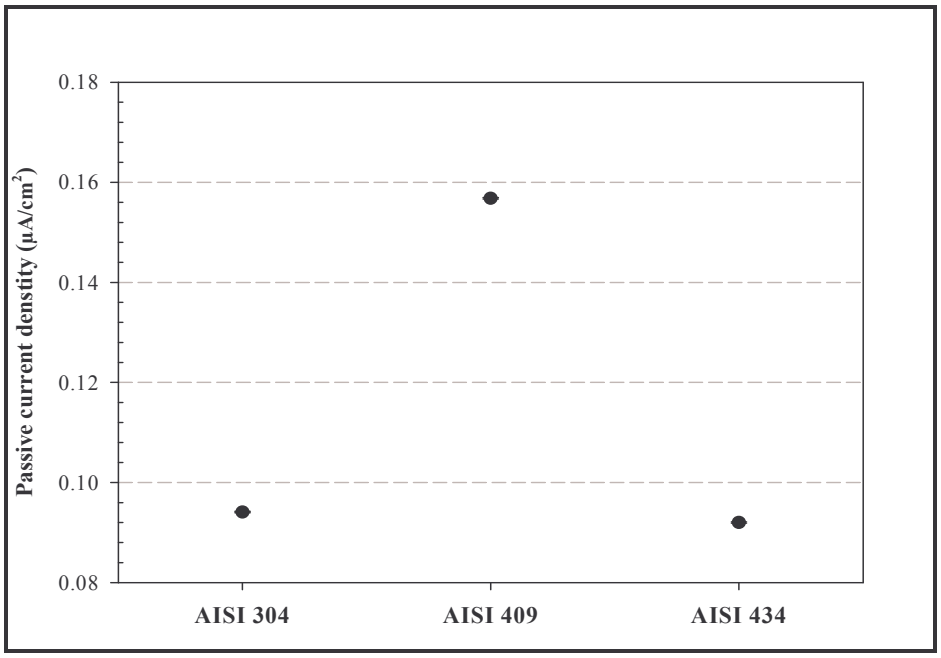


Figure 6.19: *Comparison of passive current densities in the 5% salt solution, showing 409 with a very high current density*

In this salt solution, 304 and 434 had almost the same passive current densities, which were lower than that of 409. This higher passive current density of 409 could be the reason it being the least resistant in the salt solution, in the exposure tests. However the very low passive current density values of all the stainless steels seem to indicate that they could passivate with ease in this salt solution.

The pitting potentials and passive ranges are given in Figure 6.20 and Table 6.1, respectively.

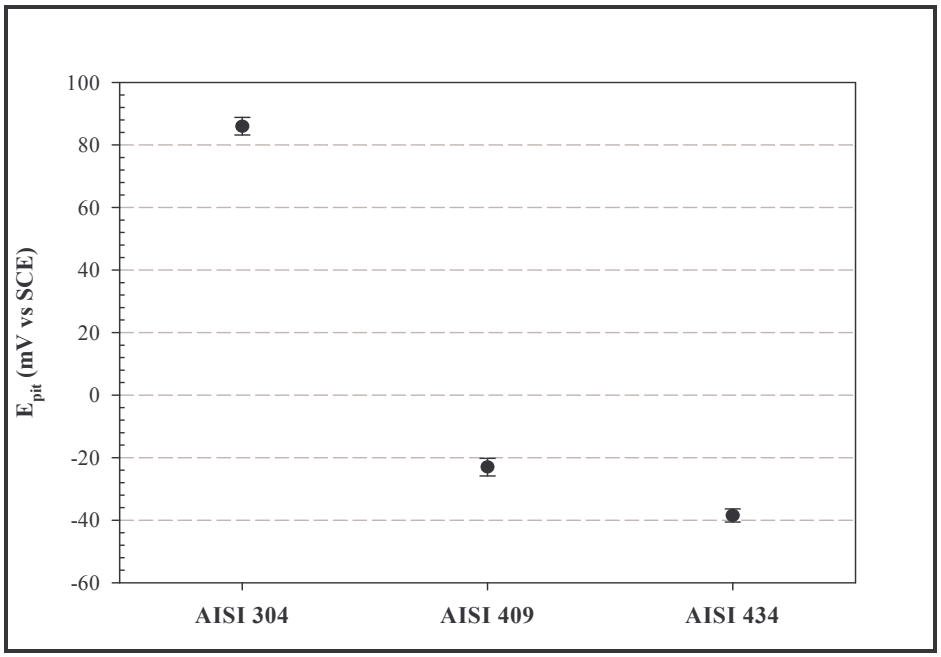


Figure 6.20: *Comparison of pitting potentials in the 5% salt solution. The very low pitting potentials indicate less resistance to the solution*

Table 6.1: *Comparison of passive ranges in the 5% salt solution*

	AISI 304	**AISI 409**	**AISI 434**
E_{corr} (mV vs SCE)	-91	-168	-107
E_{pit} (mV vs SCE)	86	-22	-39
R_{pass} (mV)	**177**	**146**	**68**

A higher pitting potential (E_{pit}) value means the material is more resistant to pitting corrosion. The fact that 434 had a lower pitting potential and a narrow passive range, seemed to indicate that it was less resistant to pitting corrosion in this salt solution (see Table 6.1).

The visual examination results after testing showed that all the samples were badly damaged with pits all over the surface. There were no trends in the pit density or pit depths of the repeat samples (tested under the same condition).

An examination of the cyclic polarisation scans (Figures E4 to E6) indicates that none of the materials repassivated. The forward scan reversed on the right, creating a hysterisis loop. The formation of such large loops indicated that none of the stainless steels were very resistant to localised corrosion in this salt solution.

6.3 Discussion and conclusions

A comparison of these tests indicates that the exposure tests (salt damage and modified salt spray tests) give comparable results. The results agreed with expected trends from other researches (as discussed below). The exposure tests were developed to closely simulate cyclic conditions experienced by the cold end components in costal areas and colder countries (where salt is used to de-ice the roads), and their reproducible results indicate that they can be used successfully as standard tests for screening materials under these conditions. In the modified salt spray test, which was designed to take into account the actual surface condition of the tail pipe components, the materials appearance after exposure was as expected: the austenitic 304 and the high chromium and Mo alloyed ferritic 434 retained their lustre after exposure. This test can be very useful in ranking materials for tail pipe components since this is the only part of an exhaust system that is clearly visible on a vehicle, and a credible test such as the modified salt spray for tail pipe is therefore important.

None of the immersion tests were aggressive under these conditions (i.e. the recorded low corrosion rates), but they were able to indicate expected and important results after exposure.

The electrochemical test was not reproducible. The reason for this poor reproducibility in the salt conditions is unclear, because for the condensates (see Chapter 5), the results were reproducible. It does not seem that electrochemical testing could be used to rank materials or predict the corrosion performance of materials in these conditions.

A comparison of the behaviour of the materials indicate that all the tests recorded very low general corrosion rates, confirming that pitting corrosion is the major form of corrosion in these conditions. The exposure tests were slightly more aggressive than the electrochemical test.

In the following discussion of material behaviour, only the results of the exposure tests were taken into account, since the electrochemical tests showed poor reproducibility with no clear trends in the electrochemical parameters.

In the exposure tests, the 434 was the most resistant, followed by 304 and then 409. The resistance of 304 was comparable to 434, especially in the modified salt spray for tail pipe components. 304 is known for its resistance to chloride environments, but 434 probably performed better because it is alloyed with Mo, which would improve its corrosion resistance to

chloride containing environments (Kaneko and Isaacs, 2002) and therefore to de-icing salts (Maximovitch *et al.*, 1994; AK Steel data bulletin, 2003). The resistance of 434 to the salt solution was further supported by the SEM micrographs which showed that the 434 was attacked less than the other stainless steels.

In the modified salt spray (cosmetic and perforation test), 409 was clearly less resistant than the other materials. This was attributed to the fact that 409 is not so resistant to chloride salt conditions because of its lower chromium content (Allegheny Ludlum data bulletin, 2003).

Even though there are apparently large differences between the corrosion rates of 409, and 434 and 304, the actual values were very low. This seems to imply that external corrosion due to salt environments will not be a major cause of cold end exhaust failure.

The electrochemical tests indicated that the corrosion and pitting resistance of 304 are superior. In all the materials pits formed. There was also no repassivation potential after pits were formed, as could be shown by the hysterisis loops that formed in the cyclic polarisation scans.

All the results indicated that pitting corrosion is the dominate form of external corrosion in these salt conditions. The exposure tests gave reproducible results and therefore could be used as standard tests for external corrosion of the cold end. However, it should be noted that the external tests of the cold end conditions were not as aggressive as the internal corrosion tests for cold end, therefore, immersion tests for external corrosion will need to be performed before a material could be considered for cold end applications.

Chapter 7

Hot end external corrosion test

This chapter presents the experimental procedure, results and discussion of the hot end external corrosion test, the hot salt test, in a 5% NaCl solution.

7.1 Hot salt test – Test 5

As explained in Chapter 3, this test was designed to simulate conditions of the hot end. The salt concentration of 5% sodium chloride and temperature of 800 ^{o}C are higher than normally encountered, to increase the aggressiveness of the test and produce rapid results. This test was also designed to simulate the cyclic conditions experienced by the exhaust components.

Ferritic 434 and 1.4509, and austenitic 304 and 321 stainless steels were tested, since these stainless steels are commonly used for hot end components (see Table 1.1), and the experimental procedure consisted of (see also Figure 7.1):

- Initially immersing the samples in a 5% NaCl solution for 5 minutes
- Holding the samples for 2 hours at 800 ^{o}C in the furnace
- Natural cooling in air for 1 hour
- Followed by gentle brushing-off of the corrosion product and weighing of the samples.

The immersion and heating cycles were repeated a number of times and fresh solution was used for every sample in every cycle.

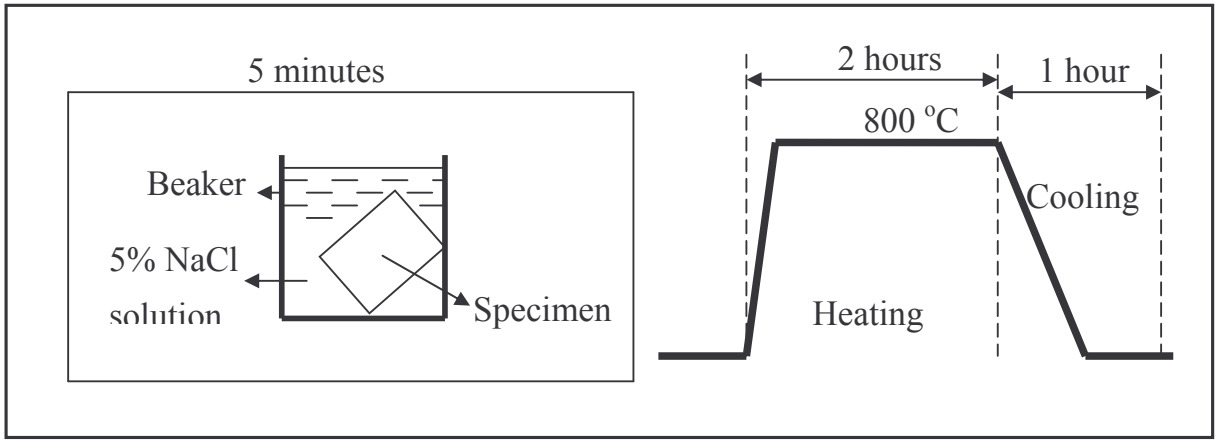


Figure 7.1: *Schematic diagram of the hot salt test exposure cycle: initial 5 minutes immersion followed by heating cycle*

The test was run for 16 cycles, except for the 321 (because it was thinner than the other sheets, only 6 cycles were performed). After the total exposure period, the samples were cleaned and evaluated as described in section 4.4.

7.1.1 Results

The results of exposure in the hot salt test for 16 cycles are shown in Figure 7.2. Again, the error bars indicate the minimum and maximum values from the mean.

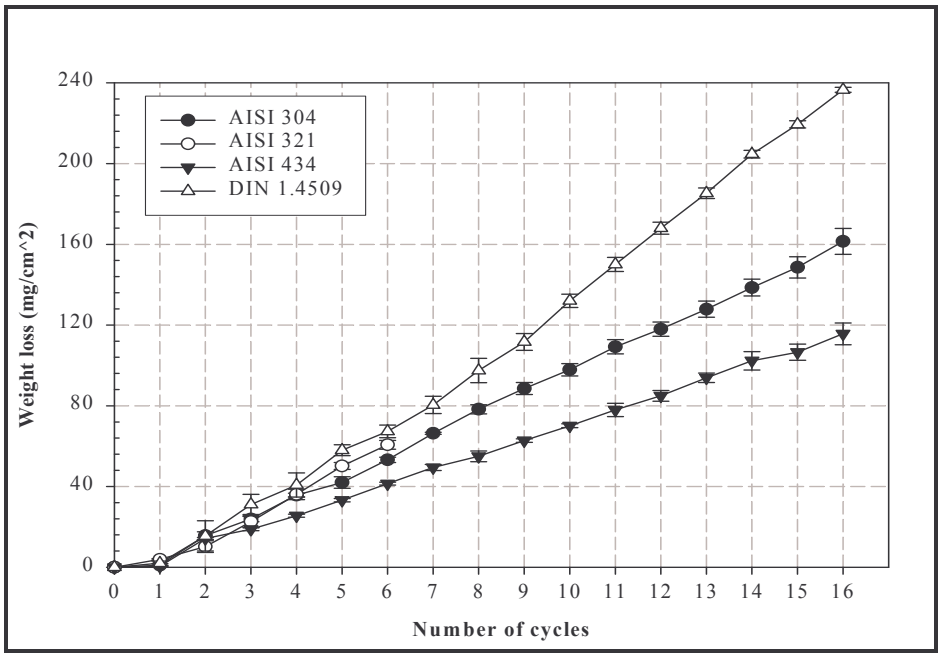


Figure 7.2: *Cumulative weight loss in the hot salt test. The average weight loss of four samples per material is shown*

The test on 321 was discontinued after six cycles because it was perforating. The results from this test showed a large amount of weight loss. In these high temperature, chloride environments, 1.4509 was the least resistant, followed by the austenitic 304 and 321 stainless steels, which showed more or less comparable results, while 434 was the most resistant. The rate, at which the materials lost weight, appeared to be increasing linearly for all the stainless steels.

Another interesting feature of the materials was that the corrosion product on the 1.4509 was peeling away very easily while it had to be brushed off from the others to be removed.

A comparison of the corrosion rates (calculated as explained in section 5.3.1) is shown in Figure 7.3.

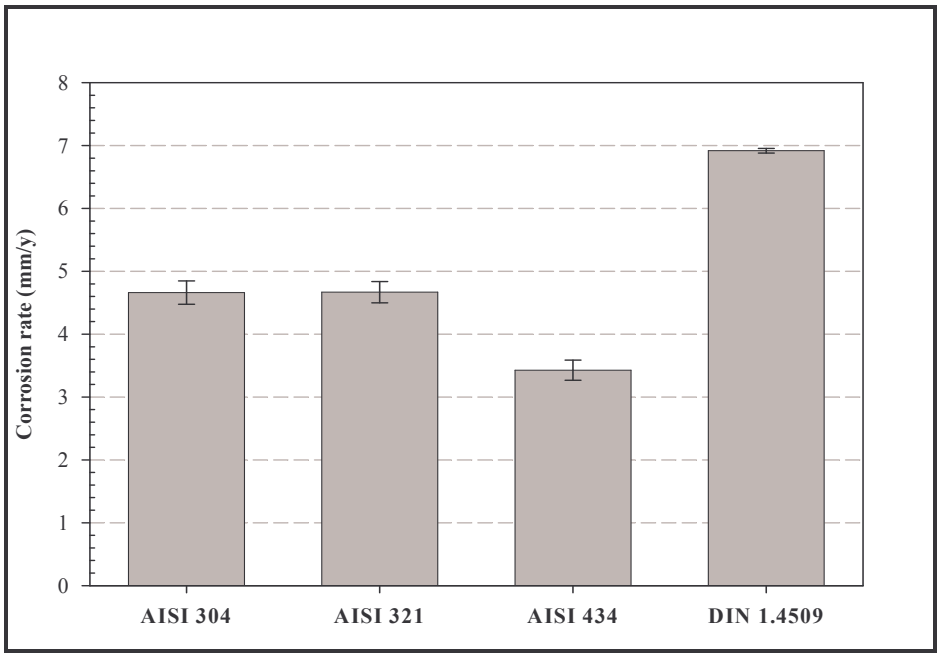


Figure 7.3: *Comparison of corrosion rates in the hot salt test (after 16 cycles), showing the ferritic steels exhibiting variation in behaviour, while the austenitics behave similarly*

The corrosion rates of all the materials were high, indicating that they were not very resistant to these conditions, and that salt damage could be problem in the hot end. 434 was only marginally better than the other stainless steels.

Figures 7.4 to 7.7 show the photographs of the stainless steels after total exposure to the hot salt test.



Figure 7.4: *Photographs of 304 after exposure to the hot salt test, showing severely corroded surfaces*



Figure 7.5: *Photographs of 321 after exposure to the hot salt test, showing severely corroded and perforated surfaces*



Figure 7.6: *Photographs of 434 after exposure to the hot salt test, showing severely corroded surfaces*



Figure 7.7: *Photographs of 1.4509 after exposure to the hot salt test, showing severely corroded surfaces*

Visual examination of the exposed samples after cleaning and drying showed islands of corrosive attack. Pits were observed on the 1.4509 surfaces, and could clearly be seen on the SEM micrographs.

The results of the SEM examination of these corroded surfaces are shown in Figures 7.8 to 7.11 below.

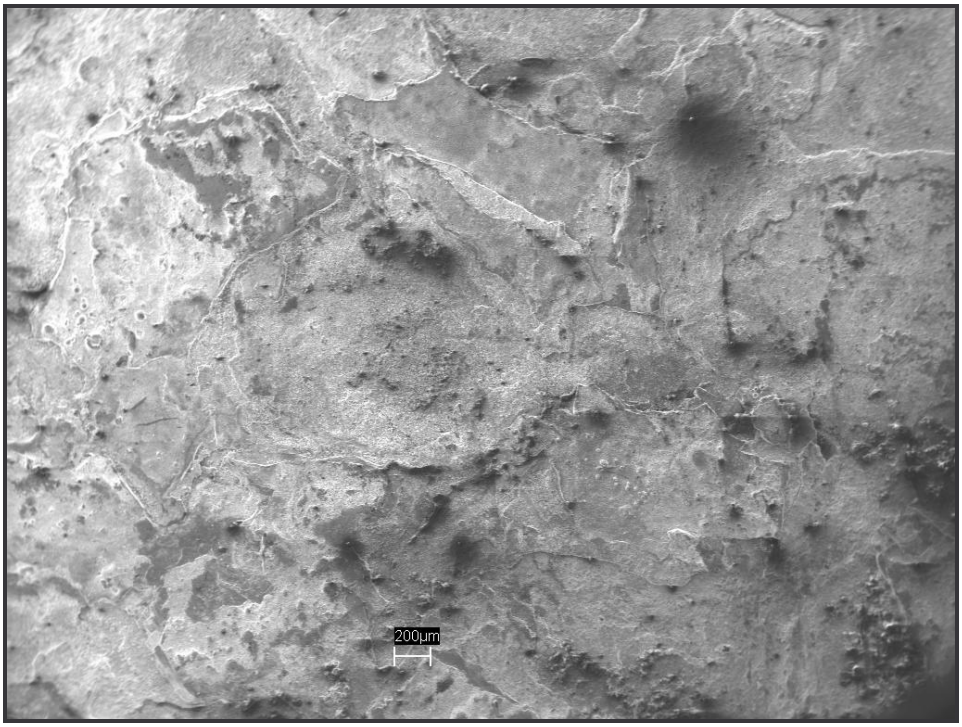


Figure 7.8: *SEM micrograph of 304 after exposure to the hot salt test, showing general corrosive attack*

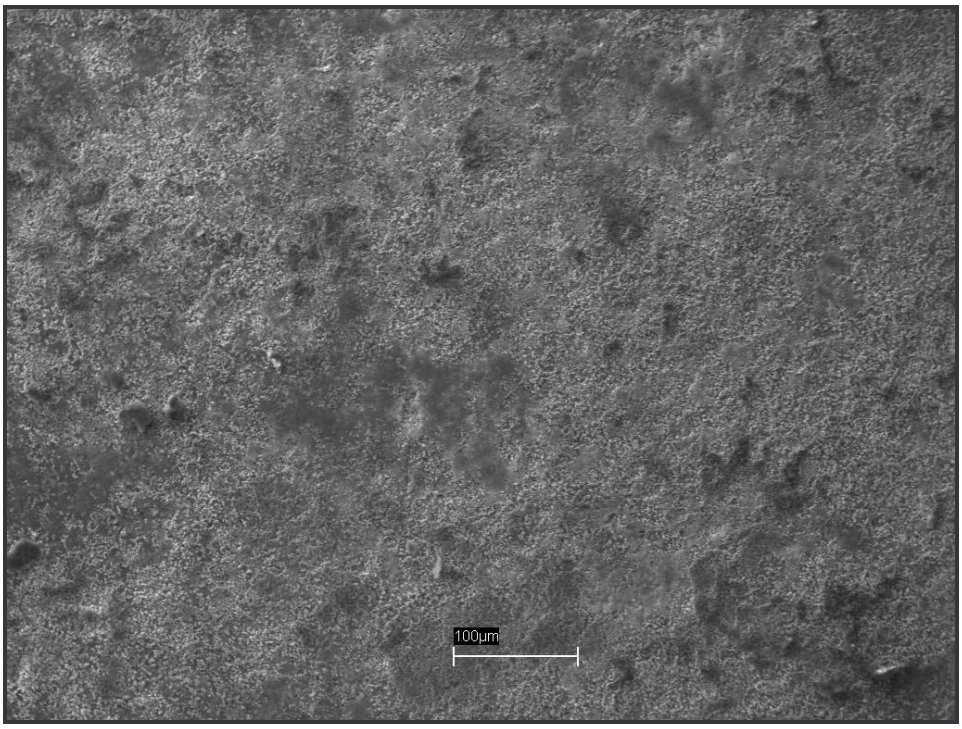


Figure 7.9: *SEM micrograph of 321 after exposure to the hot salt test, showing a general corrosive attack*

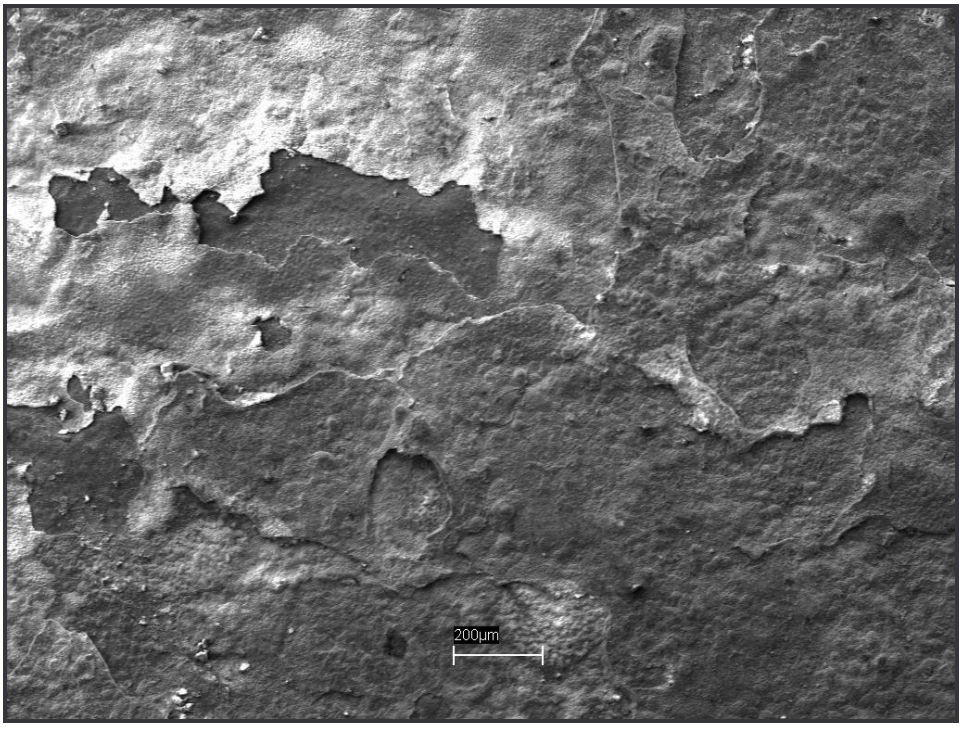


Figure 7.10: *SEM micrograph of 434 after exposure to the hot salt test, showing a broken surface film*

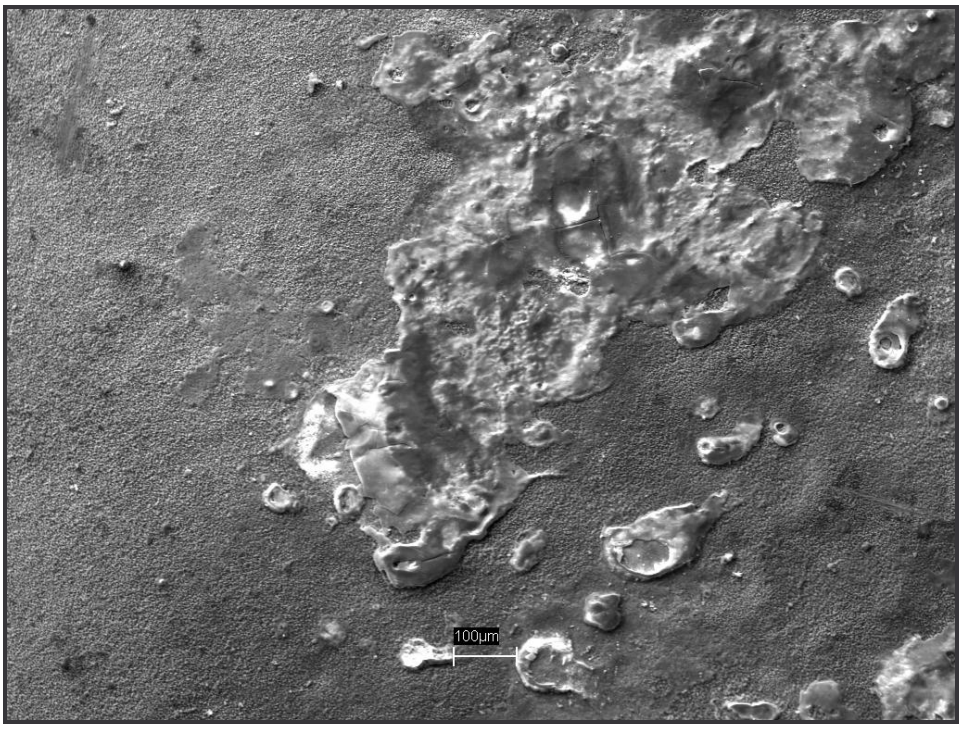


Figure 7.11: *SEM micrograph of 1.4509 after total exposure to the hot salt test, showing discrete areas of adherent film*

From these SEM micrographs it could be seen that 1.4509 had adherent film surrounded by corroded areas. The 304 and 321 showed corrosive attack on the entire surfaces, while the surface film of 434 was rupturing in discrete areas throughout the surface.

7.2 Discussion and conclusions

The results obtained from this test, showed material behaviour similar to what other researchers obtained (AK Steel data bulletin, 2003), namely that austenitic stainless steels have good resistance to salt (NaCl) environment but are less resistant to the oxidation environment. This test gave rapid results, was aggressive, and characterised by high corrosion rates – most probably due to the high testing temperature.

The high testing temperature and salt solution makes this test unique for evaluating external corrosion of the hot end components, and is ideal to evaluate all the properties required for hot end applications. From literature it was noted that more emphasis has been placed on high temperature strength and oxidation resistance (AK Steel data bulletin, 2003), and this test would be a good companion test to ensure all properties for hot end application are evaluated.

A comparison of the materials indicated that in the salt (5% NaCl) environment, 304 and 321 performed better than 1.4509, although it was expected that at higher temperatures the austenitic grades would be inferior to the ferritic grades due to the relatively high coefficient of thermal expansion of the austenitic stainless steels. The reason that the austenitic stainless steels performed better than the 1.4509 ferritic could possibly be attributed to the fact that austenitic stainless steels are more resistant to chloride environments. It is known that ferritic stainless steels are inferior to austenitics in high temperature strength (Inoue and Kikuchi, 2003) and this could also play a role in this behaviour.

434 was the most resistant stainless steel in these conditions. This could be because of the synergistic effect of good high temperature performance (oxidation environments) and the Mo increasing its resistance to chloride environments (Miyazaki *et al.*, 2003; Kaneko and Isaacs, 2002). As a ferritic stainless steel, it is expected that 434 would have better thermal fatigue properties and oxidation resistance at this relatively high temperature. It is also known to be more resistant than other 18% Cr ferritic stainless steels in de-icing chemicals (e.g. chloride salts), and its general resistance to chloride induced corrosion is close to that of 304 (Maximovitch *et al.*, 1994; AK Steel data bulletin, 2003). These characteristics could be the main reason it performed better than the austenitic 304 and 321. This test highlighted that not all ferritic stainless steels perform better than austenitics, ferritics need to have a relatively high resistance to salt conditions.

Chapter 8

Hot end oxidation test

In this chapter, the experimental procedure, results and discussion of the hot end cyclic oxidation test are presented.

8.1 Cyclic oxidation test – Test 11

Oxidation is reaction of a metal with oxygen (or other gases) at high temperature. It initiates by absorbing oxygen to form the surface oxide, and grows laterally into a continuous film.

Since oxidation is a high temperature process, it is only experienced by the hot end components. The test conducted here is cyclic, since it best simulates the actual conditions experienced by the hot end parts of exhaust systems.

In this test ferritic 434 and 1.4509, and austenitic 304 and 321 stainless steels were tested. The test was conducted in still air.

The experimental procedure was as follows:

- Samples were heated in air for at least 104 cycles (or 52 hours total dwell time) using a severe thermal cycle (25 minutes holding at 900 ^{o}C and 5 minutes natural cooling).
- The weight change of the samples was measured after every 4 cycles.

After an exposure period of 104 cycles, the samples were cleaned and evaluated as described in section 4.5.

8.1.1 Results

Figure 8.1 below shows the results of exposure for a period of at least 104 cycles (52 hours) in the cyclic oxidation test.

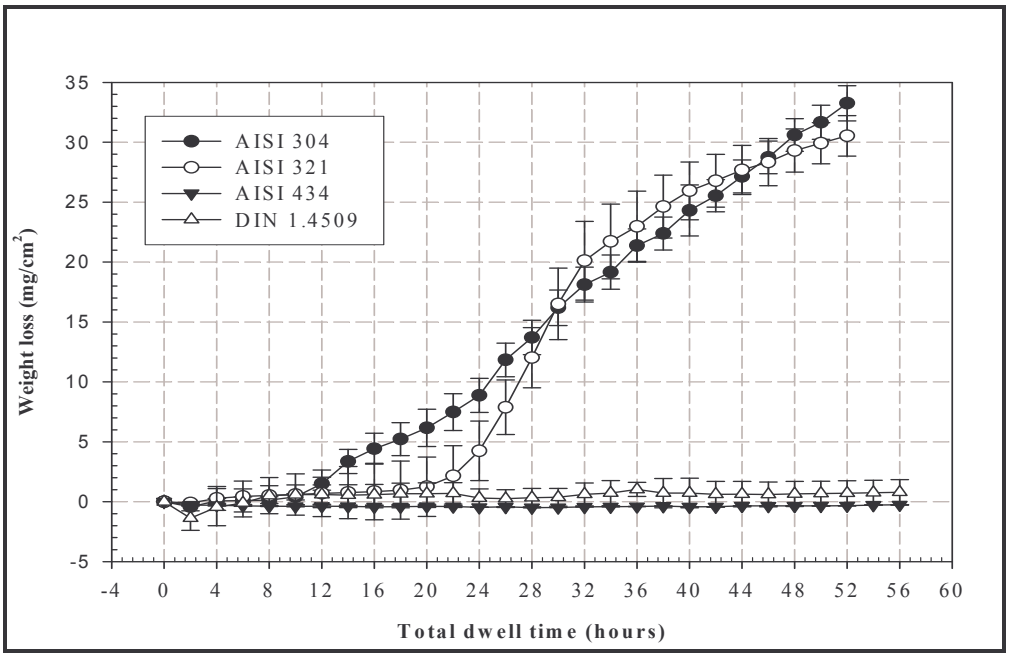


Figure 8.1: *Cumulative weight loss during cyclic oxidation test. The average weight loss of four samples per material is shown with standard deviation from the mean value*

From Figure 8.1, it can be seen that the ferritic stainless steels performed significantly better than the austenitic stainless steels. There was very little difference between the weight loss results of the two types of ferritic, or between the weight loss of the two types of austenitic stainless steels.

Considering oxidation resistance, a rule of thumb is that if a material gains or loses a weight of 1.55 mg/cm^2 in less than 135 hours in cyclic oxidation, that material is considered to have prematurely failed, and can only be used with care under the simulated environments (AK Steel data bulletin, 2003). Using this rule 304 failed after 12 hours of residence time and 321 after 20 hours.

Figures 8.2 to 8.5 show photographs of the samples after total exposure to the cyclic oxidation test.

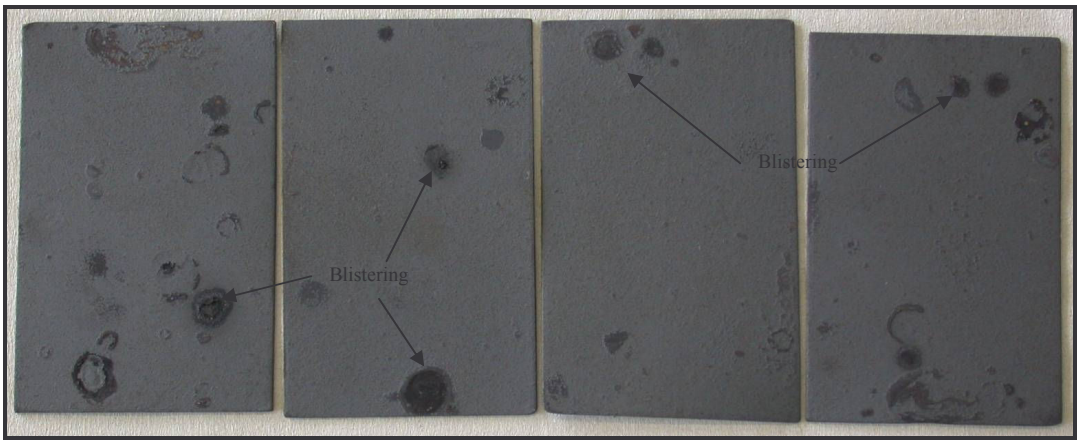


Figure 8.2: *Photographs of 304 after exposure to the cyclic oxidation test (after 104 cycles), showing discrete areas of blistering and spalling*

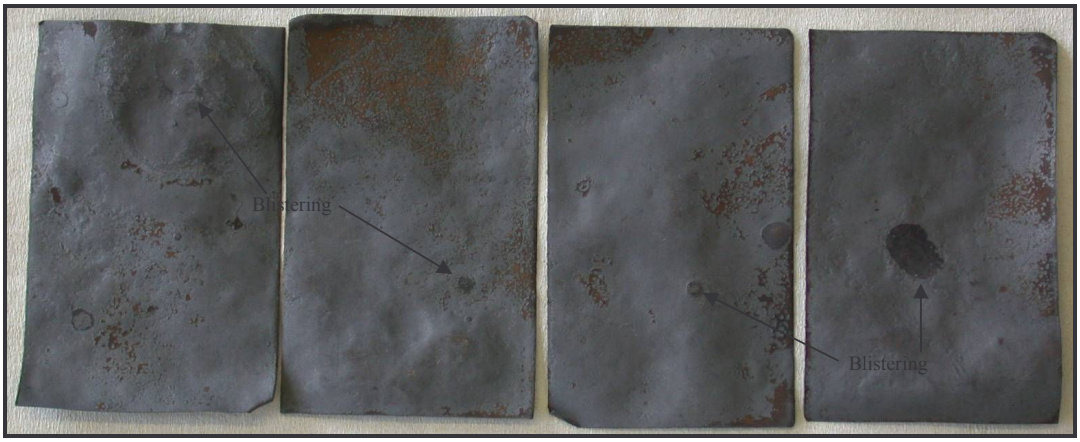


Figure 8.3: *Photographs of 321 after exposure to the cyclic oxidation test (after 104 cycles), showing discrete areas of blistering and spalling, also surface warping*

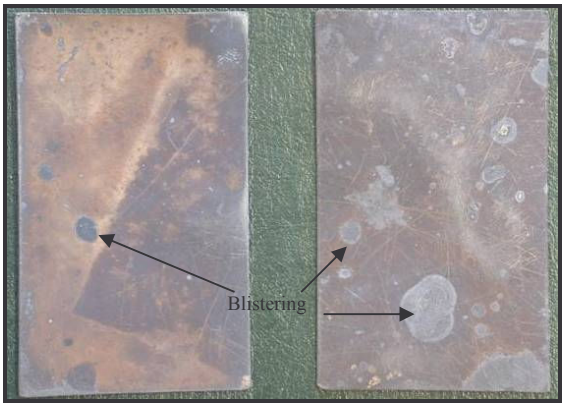


Figure 8.4: *Photographs of 434 after exposure to the cyclic oxidation test (after 112 cycles), showing discrete areas of blistering*

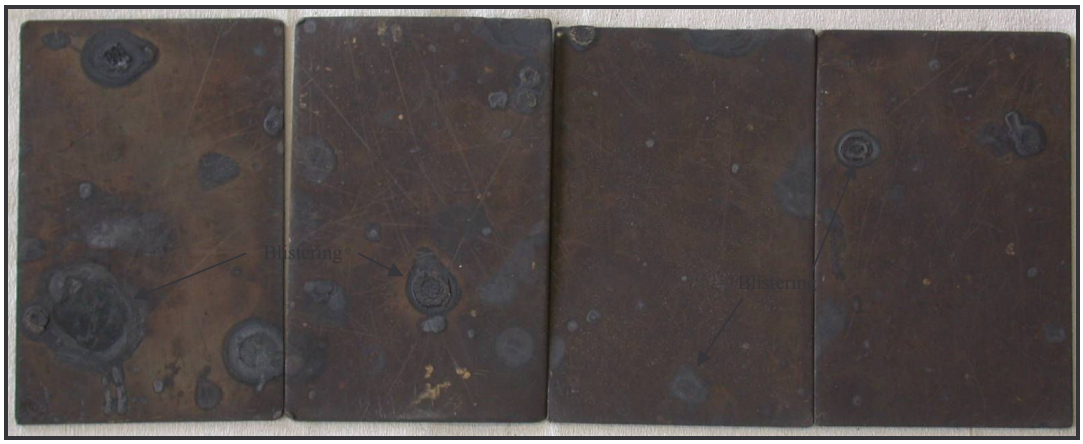


Figure 8.5: *Photographs of 1.4509 after exposure to the cyclic oxidation test (after 112 cycles), showing discrete areas of blistering*

The photographs show discrete areas of blistering and spalling on the surfaces. 321 warped due to thinner thickness compared to the rest. The austenitic stainless steels lost their surface layer while the ferritics seemed to still have their surface layer with little weight change. These results support the measured weight loss of the austenitic stainless steels.

Figures 8.6 to 8.9 show the SEM micrographs after total exposure to the cyclic oxidation test.

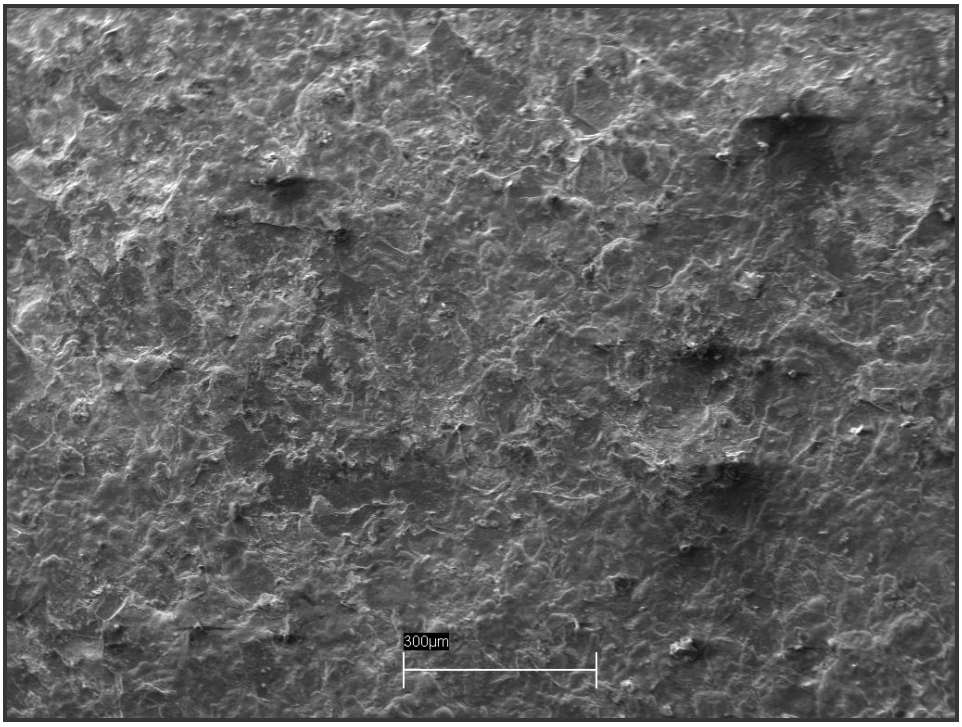


Figure 8.6: *SEM micrograph of 304 after total exposure to the cyclic oxidation test, showing deep continuous attack*

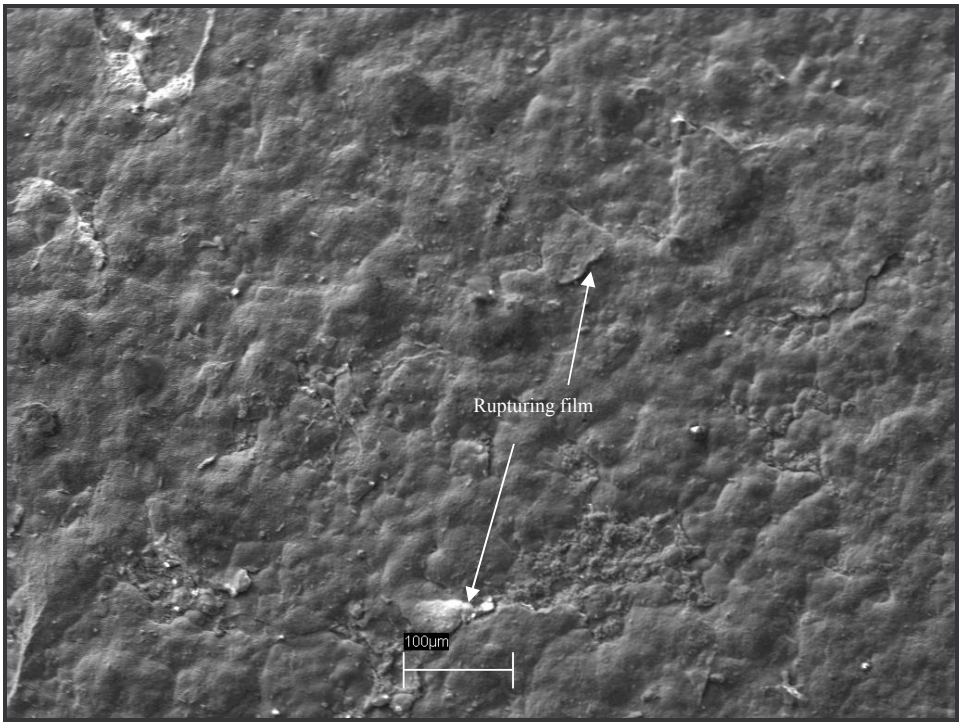


Figure 8.7: *SEM micrograph of 321 after total exposure to the cyclic oxidation test, showing ruptured film*

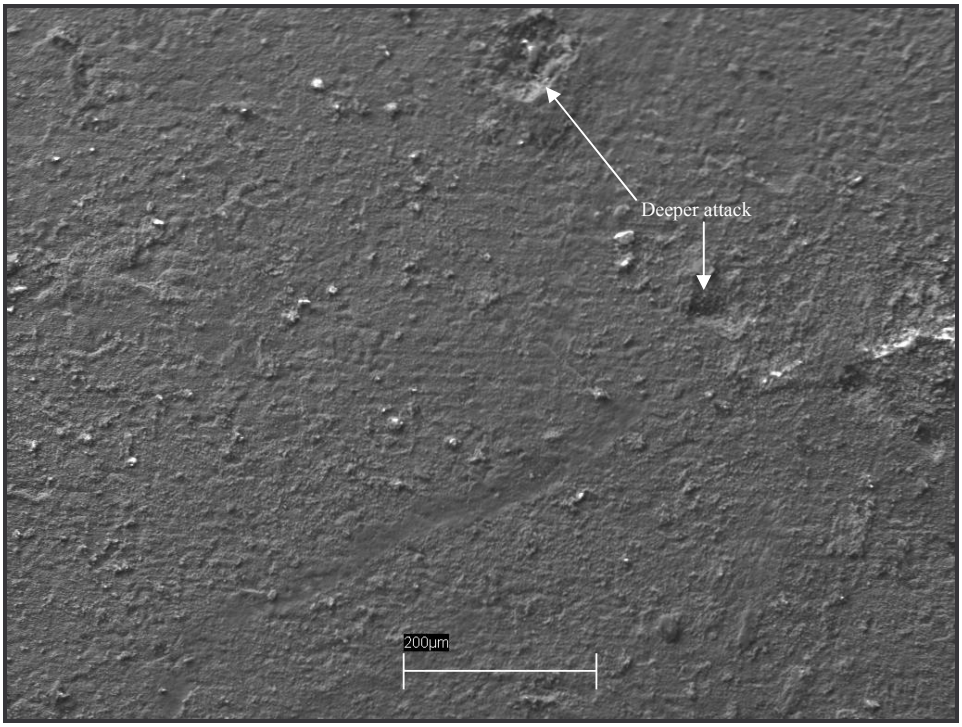


Figure 8.8: *SEM micrograph of 434 after total exposure to the cyclic oxidation test, showing discrete areas of deeper corrosive attack*

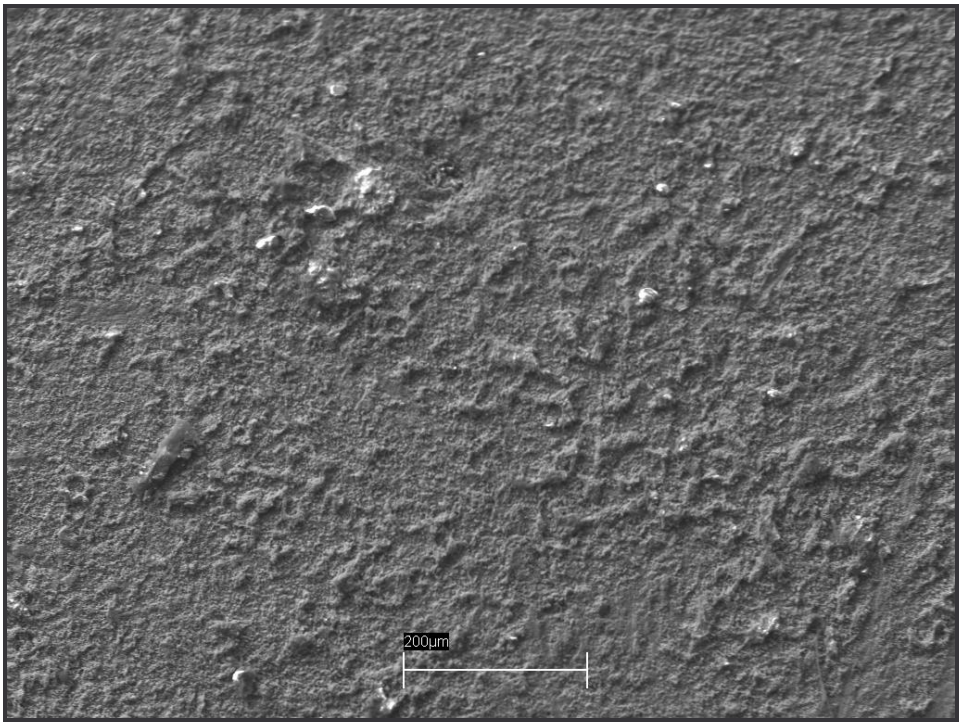


Figure 8.9: *SEM micrograph of 1.4509 after total exposure to the cyclic oxidation test, showing continuous attack*

These SEM micrographs show oxidation attack on all the surfaces. The oxidation attack seemed to be deeper on the austenitic stainless steels than the ferritic stainless steels. The attack on 304 seemed to be continuous deep attack, whereas on the 321 the surface film was rupturing. The ferritic stainless steels were characterised by the relatively small discrete attack on the surfaces. This surface analysis seemed to agree with the recorded weight loss results.

8.2 Discussion and conclusions

When these oxidation test results are considered, it can be seen that the test is reliable since the behaviour of the materials was similar to what other researchers found (AK Steel data bulletin, 2003; Allegheny Ludlum Technical data blue sheet, 2003), namely that austenitics are inferior to the ferritic stainless steels under these oxidation conditions . This test gave rapid results and was aggressive, especially on the austenitic stainless steels. This was indicated by the high weight loss. This test seems to be reliable and therefore could be performed to screen materials for hot end application.

The external oxidation was specifically developed to simulate severe cyclic conditions at temperatures that are typical to exhaust systems for both petrol and diesel engines. It tests the resistance of materials to oxidation and spalling. The expected trend indicates that a material that would be resistant to this developed test could be successfully used to manufacture the hot end components.

A comparison of the hot end tests indicates that the external oxidation test gave results that are not similar to the hot end salt test (described in Chapter 7) indicating that both tests need to be performed. The oxidation tests took in to account only the effect of temperature which is useful to countries where salt is not used or encountered. However, in colder countries where salt is used, the hot end salt test will give a more reliable data to screen materials for hot end application.

This work strove to highlight the importance of these developed tests for hot end application, but the owners will be on the researcher to decide the best tests for a specific application. The recommendation covered in this work is that if salt conditions are present, the hot end salt test can be used, but in salt-free countries the external oxidation test can be used.

A comparison of the materials in this cyclic oxidation test indicated that the ferritic stainless steels performed significantly better than the austenitic stainless steels. This was because thermal cycles induce differential thermal expansion and contraction in the developing oxide film and metal substrate, causing the scale to flake or spall (Allegheny Ludlum Technical data blue sheet, 2003; AK Steel data bulletin, 2003). Since ferritic stainless steels have a relatively low coefficient of thermal expansion, they are more resistant to progressive scaling at higher temperatures (e.g. 900 ^{o}C) under cyclic conditions. The ferritic stainless steels exhibited excellent oxidation resistance under these conditions, and are expected to have better thermal fatigue properties than austenitic stainless steels, but their lower high temperature strength might be a problem (Inoue and Kikuchi, 2003).

Of the ferritic stainless steels, 1.4509 in particular, is known for its good resistance in progressive scaling or oxidation in both cyclic and continuous oxidising laboratory tests (AK Steel data bulletin, 2003; Chassagne *et al.*, 2002). 434 is also known to be resistant to oxidation (AK Steel data bulletin, 2003) because of its Mo and Si contents (Miyazaki *et al.*, 2003). Mo additions in stainless steel increase oxidation resistance and high temperature strength and Si additions also significantly increase the oxidation resistance but have a little effect on high temperature strength (Miyazaki *et al.*, 2003). The ferritic stainless steels have higher silicon contents than the austenitic stainless steels. Therefore, this chemistry difference could be the reason why the ferritic stainless steels performed better. The Mo addition to 434 could be the reason why the 434

performed better than 1.4509. These results seem to confirm the observations by other researchers (AK Steel data bulletin, 2003; Allegheny Ludlum Technical data blue sheet, 2003). The surface analysis which showed that oxidation attack was deeper on the austenitics than the ferritic stainless steels also highlighted that the ferritic performed better than the austenitic stainless steels.

Chapter 9

Summary

The objective of this research was to evaluate the most common existing tests which are used in exhaust systems, to determine their similarities and differences and then to integrate them into standard test protocols for all areas and components of the exhaust system. The different tests used to evaluate materials for exhaust systems were thoroughly assessed and common practices on their heating temperatures, procedures and solutions used were identified. They were then integrated into eleven key tests which closely simulate the actual working conditions of automotive exhaust systems. The project looked at external corrosion, internal corrosion and oxidation for both the petrol and diesel engines.

Eight of these key tests were performed to determine whether the results obtained from them can be relied on. This was established by comparing the behaviour the materials with the expected results obtained by other researchers. The cold end internal corrosion followed the expected trend where 304 was the most resistant, followed by 434 and then 409. All these tests were aggressive, particularly with use of the diesel condensate. The electrochemical test was more aggressive (recorded high corrosion rates) than the immersion tests and the oxidised and unoxidised materials gave comparable corrosion rates results. The electrochemical test also gave results more rapidly than can be obtained through immersion tests and this characteristic makes it a desirable test because it is easy to perform. In all the tests the results were reproducible and therefore can be relied on.

The cold end external corrosion tests indicated that the exposure tests (salt damage and modified salt spray tests) give comparable results. The results agreed with expected trends from other researchers. The electrochemical test was not reproducible under the same conditions, and indicates that, until further investigation, electrochemical testing should not be used to rank the materials or predict the performance of materials in the salt environments.

The hot end tests also gave results similar to what others found (AK Steel data bulletin, 2003; Allegheny Ludlum Technical data blue sheet, 2003), namely the austenitics were inferior to the ferritic stainless steels under thee oxidation conditions.

As a summary to the materials behaviour, their relative performance in all the tests performed was determined by ranking them according to three criteria: Weight loss (WL), general corrosion rate (CR) and pitting resistance (PR). The stainless steel showing the lowest weight loss, the lowest corrosion rate and lowest pit density (or highest pitting potentials in electrochemical tests) was given a value of one. The worst performer was given a value of three. The pit density was determined from the SEM micrographs, and any material on which the pits could be seen by naked eye was considered the worst performer. This procedure was followed for all the materials in all the test procedures. The ratings for the materials per test were added together and the alloy with the lowest total was judged the best performer. It must be stressed, however, that this is a fairly subjective approach and intended to serve as a very rough guide.

The relative performance of the materials in the internal cold end tests are shown in Table 9.1:

Table 9.1: *Ranking the relative corrosion resistance of the stainless steels in the cold end internal corrosion tests*

Cold end internal corrosion tests		SS	WL	CR	PR	Total
Condensate test	Petrol solution	**AISI 304**	2	2	1	**5**
		AISI 409	3	3	3	**9**
		AISI 434	1	1	2	**4**
	Diesel solution	**AISI 304**	1	1	1	**3**
		AISI 409	3	3	3	**9**
		AISI 434	2	2	2	**6**
Electrochemical test	Petrol solution	**AISI 304**	-	1	3	**4**
		AISI 409	-	3	2	**5**
		AISI 434	-	2	1	**3**
	Diesel solution	**AISI 304**	-	1	3	**4**
		AISI 409	-	3	2	**5**
		AISI 434	-	2	1	**3**
Modified electrochemical test	Petrol solution	**AISI 304**	-	1	2	**3**
		AISI 409	-	2	3	**5**
		AISI 434	-	3	1	**4**
	Diesel solution	**AISI 304**	-	1	1	**2**
		AISI 409	-	3	3	**6**
		AISI 434	-	2	2	**4**
	Overall performance		**AISI 304**	**AISI 409**	**AISI 434**	
	Total		**21**	**39**	**24**	

The relative ranking showed that, in the internal conditions of the cold end, 409 was the least resistant, and 304 was the best. However, 434 seemed to be just as resistant as 304, since its value only differed by three points. Both are known to be resistant to chloride ion environments (Kaneko and Isaacs, 2002), while 409, with its lower chromium content, was expected to be less resistant (Maximovitch *et al.*, 1994).

The relative performance of the materials in the external cold end tests are shown in Table 9.2:

Table 9.2: *Ranking the relative corrosion resistance of the stainless steels in the cold end external corrosion tests*

Cold end external corrosion tests	SS	WL	CR	PR	Total
Salt damage test	**AISI 304**	3	3	2	**8**
	AISI 409	2	2	3	**7**
	AISI 434	1	1	1	**3**
Modified salt spray test	**AISI 304**	1	1	2	**4**
	AISI 409	3	3	3	**9**
	AISI 434	2	2	1	**5**
Electrochemical test	**AISI 304**	-	1	1	**2**
	AISI 409	-	2	3	**5**
	AISI 434	-	3	2	**5**

Overall performance	AISI 304	AISI 409	AISI 434
Total	**14**	**21**	**13**

According to this rating, 434 was the most resistant, followed by 304 and then 409. However, their relative performances differ very little, and since the actual corrosion rates were very low, it seems that salt damage is not a major problem for the cold end. The pitting resistances of these materials were also good. Comparing these results with the internal corrosion results, it was confirmed that the major degradation problem of the cold end is corrosion due to internal condensation of the exhaust gas, and not external corrosion by salt.

The relative performance of the materials in the external hot end tests are shown in Table 9.3:

Table 9.3: *Ranking the relative corrosion resistance of the stainless steels in the hot end corrosion tests*

Hot End corrosion tests	SS	WL	CR	PR	Total
Hot salt test	**AISI 304**	2	3	4	**9**
	AISI 321	3	2	3	**8**
	AISI 434	1	1	1	**3**
	DIN 1.4509	4	4	2	**10**
Cyclic oxidation test	**AISI 304**	4	-	4	**8**
	AISI 321	3	-	3	**6**
	AISI 434	1	-	2	**3**
	DIN 1.4509	2	-	1	**3**

Overall performance	**AISI 304**	**AISI 321**	**AISI 434**	**DIN 1.4509**
Total	**17**	**14**	**6**	**13**

These results indicate that 434 was by far the most resistant, followed by 1.4509 and 321, and then 304. It can be seen that in the oxidation test, generally ferritic stainless steels were more resistant than the austenitic stainless steels. In the salt condition 1.4509 was the least resistant.

When comparing both condensate solutions, the diesel solution was more corrosive than the petrol solution in all the tests. The lesser aggressiveness of the petrol synthetic condensate was due to the high level of NH_4^+ ion which seems to act as an inhibitor. It increases the pH of the solution and renders the solution less aggressive. It was illustrated that ferritic stainless steel life can be significantly improved by introducing NH_4^+ ions in the exhaust systems, especially in the diesel engine.

For all the conditions in the exhaust system 434 seemed to be the most resistant material (comparable to 304 in the most aggressive cold end conditions) and, because of its lower cost compared to austenitic stainless steels, it is a strong candidate material for replacing austenitic stainless steels.

The results from the cold end internal corrosion tests suggest that electrochemical tests can be used to some extend to predict the corrosion behaviour of stainless steels in exhaust systems in

place of immersion tests. This could be an advantage considering that they are easy to perform (given the availability of laboratory equipment) and produce results faster than immersion tests.

Since only eight of the eleven key tests were performed, it is recommended that the remaining three tests be done, to complete the whole set of tests. The results of this investigation highlighted that petrol engines are less corrosive than diesel engines, and that it was due to the high concentration level of NH_4^+ in the petrol solution. This inhibiting effect can be studied further and the mechanisms involved elucidated. This investigation also highlighted that ferritic stainless steel service life can be significantly improved by introducing NH_4^+ ions in the exhaust condensate, especially in the diesel engine. Further studies would be necessary to investigate feasible ways of introducing this ion into the exhaust system. The optimal economical levels would also need to be determined.

References

References

Abd El Meguid, E. A., Mahmoud, N. A. and Gouda, V. K. **Pitting Corrosion Behaviour of AISI 316L Steel in Chloride Containing Solutions**. British Corrosion Journal, Vol. 33, No. 1 (1998). Pp. 42 – 48.

Abdulsalam, M. I. and Shinohara, T. **Crevice Corrosion of Stainless Steel in Hot Salt Water**. Corrosion, Vo. 59, No. 4 (2003). Pp. 291 – 294.

AK Steel Exhaust System Steels. **The Catalyst**. Issue No. 1 (2002).

Alhajji, J. **Pitting Corrosion of Stainless Steels in Acidic Environment**. British Corrosion Journal, Vol. 32, No. 4 (1997). Pp.291 – 296.

Alves, H. J. B., Carvalho, J. N., Aquino, M. V. and Mantel, M. J. **Development of Ferritic Stainless Steels for Automotive Exhaust Systems**. 4th Stainless Steel Science and Market Congress, 10 – 13 June 2002, Paris, France[1].

American Society for Testing and Materials (ASTM), **Annual Book of ASTM Standards 2000**, Volume 03.02 – ASTM G48

Ashworth, R., Dulieu, D and King, K. J. **Materials Requirements for Modern Exhaust Systems**. STFFI Times International (1993). Pp. 36 – 38.

Ashassi-Sorkhabi, H., Majidi, M.R. and Seyyedi K. **Investigation of inhibition effect of some amino acids against steel corrosion in HCl solution**. Applied Surface Science, 225 (2004). Pp 176 – 185.

Baba, H., Kodama, T., and Katada, Y. **Role of Nitrogen on the Corrosion Behavior of Austenitic Stainless Steels**. Corrosion Science, Vol. 44 (2002). Pp 2393 – 2407.

Baboian, R. **Advances in Automotive Corrosion Resistance**. Proceedings of the 13th International Corrosion Congress, November 25th – 29th, 1996, Melbourne, Australia (1996): paper 076. Pp. 1 – 8.

[1] No page numbers provided

Baboian, R. **Mechanisms of Automobile Corrosion and Prevention**. Proceedings of the 11th International Corrosion Congress, (Vol. 2), 2 – 6 April 1990, Florence, Italy (1990). Pp. 489 – 498.

Banu, A. and Radovici, O. **The Effect of Alloying and of the Structure on Active-Passive Transition Potential Range of 17% Chromium Ferritic Stainless Steels**. Proceedings of the 15th International Corrosion Congress, September 22nd – 27th, 2002, Granada, Spain[i].

Bondonno, A. **Microbial Corrosion of Aluminium Alloys in Mine water**. Masters Degree Thesis, University of the Witwatersrand, Johannesburg (1990). Pp. 107 – 127.

Bradford, S. A**. Corrosion Control**, 2nd edition. By Casti publishing Inc. (2002). Pp. 9 – 64, 122 – 139, 189 – 229, 271 – 281, 345 – 365 and 431 – 445.

Bullard, S. J., Larson, D. E. and Dunning, J. S. **Oxidation and Corrosion Resistance of Two Fe-8Cr-16Ni-Si-Cu Alloys**. Corrosion, Vol. 48, No. 11 (1992). Pp. 891 – 897.

Burstein, G. T., Pistorius, P. C. and Matin, S. P. **The Nucleation and Growth of Corrosion Pits on Stainless Steel**. Corrosion Science, Vol. 35, No. 1 – 4 (1993). Pp. 57 – 62.

Cayless, G. E. **Corrosion of the Exhaust Systems**. The Institute of Mechanical Engineers, Corrosion of Motor Vehicles. Published by Mechanical Engineering Publications, London, 13-14 November (1974). Pp. 60 – 65.

Champion, F. A. **Corrosion Testing Procedures**, 2nd edition. Published by Chapman and Hall (London) (1964). Pp. 66 – 105.

Chassagne, F., Antoni, L., Cleizergues, O., Lovato, G., Gardon, M. and Moiron, J. L. **Development of a Nb Stabilised 15%Cr Ferritic Stainless Steel for Hot Part of Automotive Exhaust Systems**. 4th Stainless Steel Science and Market Congress, 10 – 13 June 2002, Paris, France[i].

Corrosion Institute of South Africa. **Corrosion Control in Southern Africa**. Published by the Corrosion Institute of South Africa (1994). Pp. 1, 33.

Douthett, J. A. **Designing Stainless Exhaust Systems**. Automotive Engineering, November (1995). Pp. 45 – 49.

Edwards, A. M., Hooper, R. A. E. and Marriott, J. B. **Stainless Steel Exhaust Systems. The Institute of Mechanical Engineers, Corrosion of Motor Vehicles**. Published by Mechanical Engineering Publications, London, 13 – 14 November (1974). Pp. 87 – 94.

El Hajjaji, S., Aries, J., Audouard, J. P. and Dabosi F. **The Influence of Alloying Elements on the Corrosion Resistance of Stainless Steels in Phosphoric Acid Medium Polluted By Sulphide Ions**. Corrosion Science, Vol. 37, No. 6 (1995). Pp.927 – 939.

El Hajjaji, S., Roy, J., Aries, L. and Dabosi F. **Influence of Sulphide Ions on Corrosion Resistance of Special Austenitic Stainless Steels in Phosphoric Acid**. British Corrosion Journal, Vol. 28, No. 3 (1993). Pp.201 – 208.

Ergun, M. and Balbasi, M. **Mathematical Model for Pitting Potential of Fe-16% Chromium Steel**. Corrosion Science, Vol. 36, No. 9 (1994). Pp. 1569 – 1574.

Fujita, N., Ohmura, K., Sato, E. and Yamamoto, A. **Development of Ferritic Stainless Steel YUS 450 with High Heat Resistance for Automotive Exhaust System Components**. Nippon Steel Technical Report No. 71 October (1996). Pp. 25 – 30.

Gonzalez-Rodriguez, J. G., Dehesa, M. and Porcayo-Caderon, J. **Corrosion Performance of Heat Resistant Alloy in Molten Salts**. Proceedings of the 15th International Corrosion Congress, September 22nd – 27th, 2002, Granada, Spain[i].

Hong, T. and Nagumo, M. **Effect of Surface Roughness on Early Stages of Pitting Corrosion of Type 301 Stainless Steel**. Corrosion Science, Vol. 39, No. 9 (1997). Pp. 1665 – 1672.

Hooper, R. A. E**. Manufacture and Testing of Exhaust Systems in Stainless Steel**. Sheet Metal Industries, January (1978). Pp. 15 – 22.

Ike, H. and Okabe, H. **The Oxidation Behaviour of Fe-14Cr Alloys with Small Additions of Al at High Temperatures**. Trans. JIM Vol. 20 (1979): p 186 – 196.

Inoue, Y. and Kikuchi, M. **Present and Future Trends of Stainless Steel for Automotive Exhaust System**. Nippon Steel Technical Report No. 88 July (2003). Pp. 62 – 69.

Ishii, K., Kohno, M. and Satoh, S. **Effect of La and Zr Addition on High-Temperature Oxidation Resistance of 20%Cr-5%Al Steel Foil**. Kawasaki Steel Technical Report No. 40 May (1999). Pp. 30 – 35.

Ishii, K., Miyazaki, A. and Satoh, S. **Stainless Steels for Automotive Exhaust System**. Kawasaki Steel Technical Report No. 40 May (1999). Pp. 39 – 41.

Jargelius-Pettersson, R. F. A. **Electrochemical Investigation of the Influence of Nitrogen Alloying on Pitting Corrosion of Austenitic Stainless Steels**. Corrosion Science, Vol. 41 (1999). Pp 1639 -1664.

Jiangnan, Y., Lichang, W. and Wenhao, S. **The Effect of Copper on the Anodic Dissolution Behaviour of Austenitic Stainless Steel in Acidic Chloride Solution**. Corrosion Science, Vol. 33, No. 6 (1992). Pp. 851 – 859.

Jones, D. A. **Principles and Prevention of Corrosion**, 2nd edition. Published by Prentice-Hall (1996). Pp.24 – 34, 144 – 162, 199 – 221, 291 – 327, 357 – 395, 399 – 435, and 515 – 518.

Kain, V. **Intergranular Corrosion of Stainless Steels**. Metallurgy Division, Bhabha Atomic Research Centre, Trombay 400 085 (1993). Pp. 107 – 127.

Kaneko, M. and Isaacs H. S. **Effects of Molybdenum on the Pitting of Ferritic- and Austenitic-Stainless Steels in Bromide and Chloride Solutions**. Corrosion Science, Vol. 44 (2002). Pp. 1825 -1834.

Kawasaki, H., Karasawa, J., Nishida, Y., Kawasaki, T., Toyoka, T. and Shibagaki, M. **High Formability Stainless Steel Pipe for Automotive Exhaust Systems**. Kawasaki Steel Technical Report No. 19 November (1988). Pp. 30 – 32.

Kobayashi, M., Kawasaki, T., Mihara, Y., Sato, H., Takada, M. and Yanagishima, F. **Characteristics of Stainless Steel for Automotive Exhaust Systems and Its Production by Tandem Cold Rolling**. Kawasaki Steel Technical Report No. 19, November (1988). Pp. 63 – 71.

Kwon, J., Ahn, S., Kim, H. and Lee, Y. **Effect of Minor Alloying Elements on the Properties of Stainless Steels for Hot Ends of Automotive Exhaust Systems**. 4th Stainless Steel Science and Market Congress, 10 – 13 June 2002, Paris, France[i].

Laitinen, T. **Localised Corrosion of Stainless Steel in Chloride, Sulphate and Thiosulfate Containing Environments**. Corrosion Science, Vol. 42, No. 3 (2000). Pp 421 – 441.

Lancaster, J. F. **Metallurgy of Welding**, 6th edition. Published by Abington Publishing (1999). Pp. 169 – 350.

Lee, Y. H., Kim, H. and Lee, I. G. **Corrosion Resistance of Stainless Steels in Various Corrosive Environments**. Proceedings of the 15th International Corrosion Congress, September 22nd – 27th, 2002, Granada, Spain[i].

Lemaitre, C., Abdel Monel, A., Djoudjou, R., Baroux, B. and Beranger, G. **A Statistical Study of the Role of Molybdenum in the Pitting Resistance of Stainless Steels**. Corrosion Science, Vol. 34, No. 11 (1993). Pp. 1913 – 1822.

Lin, H., Tsai, W., Lee J. and Huang, C. **The Electrochemical and Corrosion Behaviour of Austenitic Stainless Steel Containing Copper**. Corrosion Science, Vol. 33, No. 5 (1992). Pp. 691 – 697.

Lothongkum, G., Hirasawa, H., Ishii, K., Ujiro, T. and Satoh, S. **Corrosion Behaviour of Spot Welds of Ti Stabilised 11% Cr Stainless Steel in the Modified Strauss Test,**

Synthetic Exhaust Gas Condensate Corrosion Test and Cyclic Corrosion Test. Proceedings of the 14th International Corrosion Congress, September 26th – October 1st, 1999, Cape Town, South Africa. Paper No. 82.

Lu, Y. C., Ives, M. B. and Clayton, C. R. **Synergism of Alloying Elements and Pitting Corrosion Resistance of Stainless Steels**. Corrosion Science, Vol. 35, No. 1 – 4 (1993). Pp. 89 – 96.

Malik, A. U., Mayal-Kutty, P. C., Siddiqi, N. A., Andijani, I. N. and Ahmed, S. **The Influence of pH and Chloride Concentration on the Corrosion Behaviour of AISI 316L Steel in Aqueous Solutions**. Corrosion Science, Vol. 33, No. 11 (1992). Pp. 1809 – 1827.

Mangonon, P. L. **The Principles of Materials Selection for Engineering Design**. Published by Prentice hall (1999). Pp. 390 – 424 and 502 – 512.

Maximovitch, S., Barral, G., Le Cras, F. and Claudet, F. **The Electrochemical Incorporation of Molybdenum in the Passive Layer of a 17% Cr Ferritic Stainless Steel. Its Influence on Film Stability in Sulphuric Acid and on Pitting Corrosion in Chloride media**. Corrosion Science, Vol. 37, No. 2 (1995). Pp. 221 – 291.

Miyazaki, A., Gunji, M. and Baba, Y. **Ferritic Stainless Steels and Pipes for Automotive Exhaust Systems to Meet Weight Reduction and Stricter Emission Requirements**. Kawasaki Steel Technical Report No. 46, June (2002). Pp. 19 – 24.

Miyazaki, A., Gunzi, M. and Yoshioka, K. **High formability R429X and Heat-Resistant R44EX Stainless Steels for Automotive Exhaust Manifold**. Kawasaki Steel Technical Report No. 31, November (1994). Pp. 21 – 28.

Miyazaki, A., Hirasawa, J. and Furukimi, O. **Development of High Heat-Resistant Ferritic Stainless Steels with High Formability, "RMH-1", for Automotive Exhaust Manifolds by Optimizing Mo Composition design**. Kawasaki Steel Technical Report No. 48, March (2003). Pp. 28– 32.

Miyazaki, A., Hirasawa, J. and Satoh, S. **Advanced Stainless Steels for Stricter Regulations of Automotive Exhaust Gas**. Kawasaki Steel Technical Report No. 43, October (2000). Pp. 21– 28.

Moroishi, T., Fujikawo, H. and Mukiuro, H. **The effect of Carbon, Zirconium, Niobium, and Titanium on the Oxidation Resistance of Chromium Stainless Steel**. Journal of the Electrochemical Society, Vol. 126, No. 12, December (1979). Pp. 2173 – 2182.

Newman, R. C. **Understanding the Corrosion of Stainless Steel**. Corrosion, Vol. 57, No. 12 (2001). Pp. 1031 – 1041.

Nicholls, J. R. and Bennett, M. J. **Cyclic Oxidation – Guidelines for Test Standardisation, Aimed at the Assessment of Service Behaviour**. Materials at High Temperatures, Volume 17, No. 3 (2000). Pp. 413 – 428.

Ningshen, S., Kamachi-Mudali, U. and Dayal, R. K. **Electrolyte and Temperature Effects on Pitting Corrosion of Type 316LN Stainless Steels**. British Corrosion Journal, Vol. 36, No. 1 (2001). Pp. 36 – 40.

Nkosi, Z. and Sephton, M. **Evaluation of Corrosion Properties of Type 434 Stainless Steel in Exhaust Systems**. Corrosion, Paint & Coatings Industries S.A. Volume 5 No. 3 (2003). Pp. 12 – 13.

Norton, J. F., Baxter, D. J., Santorelli, R. and Bregani, F. **The Corrosion of AISI 310 Stainless Steel Exposed to Sulphurising or Oxidising or Carburizing Atmospheres at 600 ^{o}C**. Corrosion Science, Vol. 35, No. 5-8 (1993). Pp. 1085 – 1090.

Oliver, D. C. and Sephton, M. **External Corrosion Resistance of Steel and Ferritic Stainless Steel Exhaust Systems**. The Journal of The South African Institute of Mining and Metallurgy, Vol. 103, N0. 2 (2003). Pp. 93 – 100.

Olsson, C. A. and Hornstrom, S. E. **An AES and XPS Study of the High Alloy Austenitic Stainless Steel 254 SMO® Tested in a Ferritic Chloride Solution**. Corrosion Science, Vol. 36, No. 1 (1994). Pp. 141 – 151.

Pardo, A., Merino, M. C., Botella, J., Lopez, M. D., Matres, V., Carboneras, M. and Huertas, T. **Influence of Cu Addition on the Corrosion Resistance of AISI 304 Stainless Steel in Acid Mediums**. Proceedings of the 15th International Corrosion Congress, September 22nd – 27th, 2002, Granada, Spain[i].

Pickering, F. B. **Introduction: The Metallurgical Evolution of Stainless Steel**. Published by American Society for Metals and The Metal Society (1979). Pp. 1 – 42.

Pistorius, P. C. and Burstein, G. T. **Aspects of the Effects of Electrolyte Composition on the Occurrence of Metastable Pitting on Stainless Steel**. Corrosion Science, Vol. 36, No. 3 (1994). Pp. 525 – 538.

Pistorius, P. C. and Burstein, G. T. **Growth of Corrosion Pits on Stainless Steel in Chloride Solution Containing Dilute Sulphate**. Corrosion Science, Vol. 33, No. 12 (1992). Pp. 1885 – 1897.

Putatunda, S. K. **Corrosion Behaviour of Sensitised Austenitic (AISI 304) Stainless Steel in a CO_2 Atmosphere**. Materials Science and Engineering, Vol. 91 (1987). Pp. 89 – 95.

Riley, A. M., Wells, D. B. and Williams, D. E. **Initiation Events for Pitting Corrosion of Stainless Steel**. Corrosion Science, Vol. 32, No. 12 (1991). Pp. 1307 – 1313.

Robertson, J. **The Mechanism of High Temperature Aqueous Corrosion of Stainless Steels**. Corrosion Science, Vol. 32, No. 4 (1991). Pp. 443 – 465.

Rowe, L. C. and Chance, R. L. **Fundamentals of Corrosion Testing. Automotive Corrosion By Deicing Salts**. Edited by R. Baboian. Published by National Association of Corrosion Engineers (1981). Pp. 133 – 163.

Russell, J. H., Covino, B. S., Bullard S. J. **Application of Electrochemical Methods for Investigations of Localised Corrosion of Nitrogen-Molybdenum Stainless Steels**. Corrosion, Vol. 57, No. 4 (2001). Pp. 360 – 368.

Sato, E. and Tanoue, T. **Present and Future Trends of Materials for Automotive Exhaust Systems**. Nippon Steel Technical Report No. 64 January (1995). Pp. 13 – 19.

Sato, E., Ito, S., Matsuhashi, R. and Abo, H. **Method of Evaluation of Localised Corrosion of Stainless Steels by Exhaust Gas Condensate**. JSAE Review Vol. 12 No. 2 (1991). Pp. 58 – 63.

Semchyshen, M., Bond, A. P. and Dundas, H. J. **Effect of Composition on Ductility and Toughness of Ferritic Stainless Steels**. The Metallurgical Evolution of Stainless Steel, published by American Society for Metals and The Metal Society (1979). Pp. 260 – 273.

Shaikh, H., Rao B. P. C., Gupta S., George R. P., Venugopal S., Sasi B., Jayakumar T. and Khatak H. S. **Assessment of Intergranular Corrosion in AISI Type 316L Stainless Steel Weldments**. British Corrosion Journal, Vol. 37 No. 2 (2002). Pp. 129 – 140.

Shimizu, H., Kohno, M. and Yoshioka, K. **R20-5USR, 20%Cr-5%Al-La-Zr Steel with Improved Oxidation Resistance at High Temperatures**. Kawasaki Steel Technical Report No. 31 November (1994). Pp. 29 – 34.

Siebert, O. W. **Laboratory Electrochemical Test Methods**. Laboratory Corrosion Tests and Standards. A symposium by ASTM Committee G-1 on Corrosion of Metals, Bal Harbour, FL, 14 – 16 November (1983). Pp. 65 – 90.

Streicher, M. A. **Stainless Steel: Past, Present and Future**. The Metallurgical Evolution of Stainless Steel, published by American Society for Metals and The Metal Society (1979). Pp. 442 – 475.

Szummer, A. and Janik-Czachor, M. **Corrosion Behaviour of Low-Manganese Stainless Steels**. Corrosion Science, Vol. 35, No. 1 – 4 (1993). Pp. 317 – 327.

Tan, W., Akiyama, E., Kawashima, A., Asami, K. and Hashimoto, K. **The Influence of Pre-Immersion on the Potentiostatic Polarisation Behaviour of Amorphous Fe-Cr-Mo-P-C Alloys in De-Aerated 1 M HCl**. Corrosion Science, Vol. 38, No. 9 (1996). Pp. 1495 – 1511.

van Bennekom, A. **The Corrosion and Mechanical Properties of Modified 3Cr12 Type Alloys.** Masters Degree Thesis, University of the Witwatersrand, Johannesburg (1990). Pp. 25 – 55.

van Bennekom, A., Hung, P. M. and Potgieter, J. H. **An Investigation into Corrosion Behaviour of a Commercial Type Superferritic Stainless Steel Containing Small Amount of Ruthenium and Silver**. Proceedings of the 14th International Corrosion Congress, September 26th – October 1st, 1999, Cape Town, South Africa. Paper 300.

Vera Cruz, R. P., Nishikata, A. and Tsuru, T. **Pitting Corrosion Mechanism of Stainless Steels Under Wet-Dry Exposure in Chloride-Containing Environments**. Corrosion Science, Vol. 40, No. 1 (1998). Pp. 125 – 139.

Vigor, C. W., Johnson, J. N. and Hunter, J. E. **Stainless Steel in Transportation systems**. Handbook of Stainless Steel. (Editors: Peckner, D. and Bornstein, I. M.). Published by McGraw-Hill Book Company (New York) (1977). Pp. 39-1 – 39-15.

Vongbandit, P., Lothongkum, G. and Nongluck, P. **Investigation of Pourbaix Diagrams of 316L Stainless Steel in Air-Saturated Aqueous Solutions Containing Chloride by Cyclic Polarization Technique.** Proceedings of the 15th International Corrosion Congress, September 22nd – 27th, 2002, Granada, Spain[i]

Weltens, P., Garcia, P. and Walther, H. **Internal and External Corrosion of Exhaust Systems for Passenger Vehicles – Test Procedures, Laboratory and Field Results. Tenneco Automotive Internal Report**. Available on request (contact Columbus Stainless library) (2001). Pp. 1- 22.

Williams, D. E., Stewart, J. and Balkwill, P. H. **The Nucleation, Growth and Stability of Micropits in Stainless Steel**. Corrosion Science, Vol. 36, No. 7 (1994). Pp. 1213 – 1235.

Wouters, Y., Henry, S., Galerie, A., Chemarin, C., Mermoux, M. and Petit, J. P. **Influence of Silicon Content on the High Temperature Breakaway Corrosion of Ferritic Stainless Steels in Water Vapour**. Proceedings of the 15th International Corrosion Congress, September 22nd – 27th, 2002, Granada, Spain[i].

www.aksteel.com. **Product Data Bulletin. Aluminised Steel Type 1 STAINLESS 409 and 439; Black Coat; 18 SR; 11 Cr-Cb; 18 Cr-Cb; 409 SS; 409 ULTRA FORM; 439 SS; 439 ULTRA FORM, SS**. Accessed date July 2003.

www.alleghenyludlum.com. **Technical Data Blue Sheet. Martensitic SS Type 410, 420, 425 Mod, and 440A; Stainless Steel AL 409HP™ Ferritic SS; Stainless Steels Type 439/AL, 439HP™; Stainless Steel Type 441, AL 441HP™ Alloys**. Accessed date July 2003.

Yashiro, H. and Tanno, K. **The Effect of Electrolyte Corrosion on the Pitting and Repassivation Behaviour of AISI 304 Stainless Steel at High Temperature**. Corrosion Science, Vol. 31 (1990). Pp. 485 – 490.

Yazawa, Y., Yoshioka, K. and Togashi, F. **Effects of Cr, Mo and Cu on the Atmospheric Corrosion Resistance of Ferritic Stainless Steels in a Costal Environment**. Kawasaki Steel Technical Report No. 31, November (1994). Pp. 35 – 43.

Zhang, P. Q., Wu, J. X., Zhang, W. Q., Lu, X. Y. and Wang, K. **A Pitting Mechanism for Passive 304 Stainless Steel in Sulphuric Acid in Sulphuric Acid Media Containing Chloride Ions**. Corrosion Science, Vol. 34, No. 8 (1993). Pp. 1343 – 1354.

Appendices

Appendix A

A.1 Photographs of the stainless steels after exposure to salt stray cabinet.

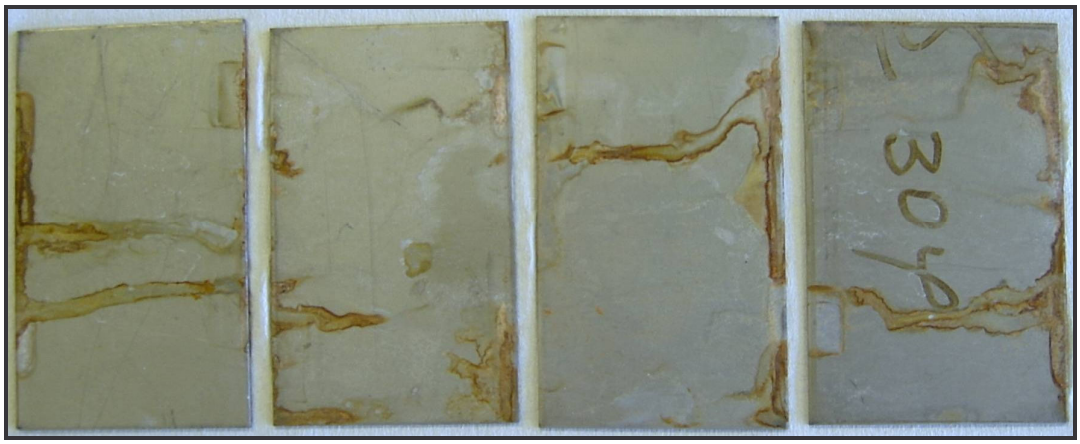


Figure A.1: *Photographs of 304 after exposure to the salt spray (before removing the corrosion products), showing rusted surfaces*

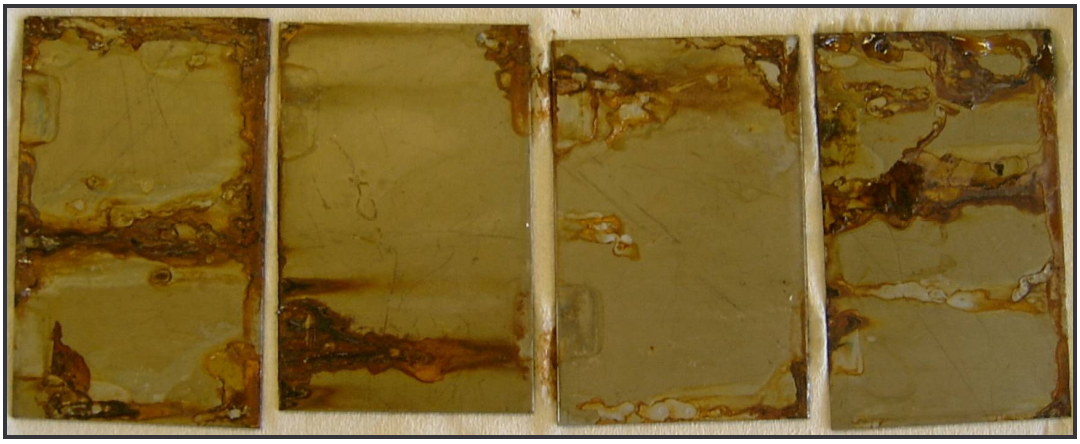


Figure A.2: *Photographs of 409 after exposure to the salt spray (before removing the corrosion products), showing rusted surfaces*

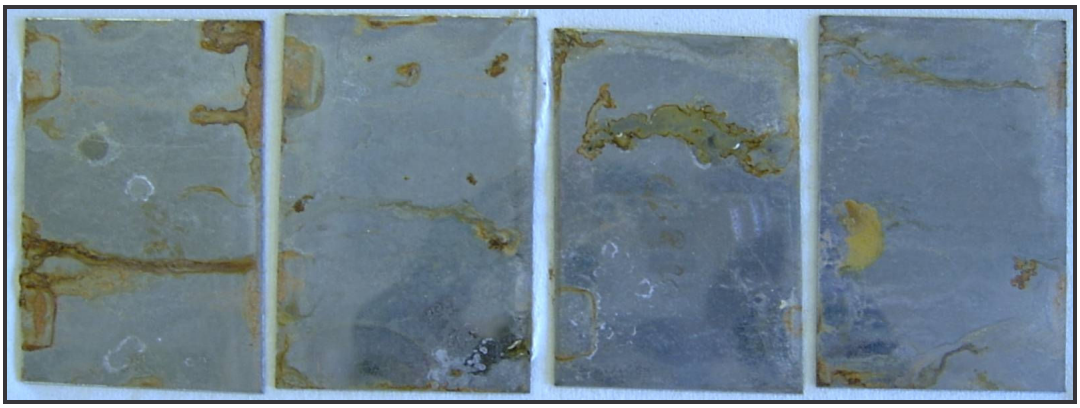


Figure A.3: *Photographs of 434 after exposure to the salt spray (before removing the corrosion products), showing rusted surfaces*

Appendix B

B.1 Electrochemical polarisation results of the synthetic condensates

Petrol condensate

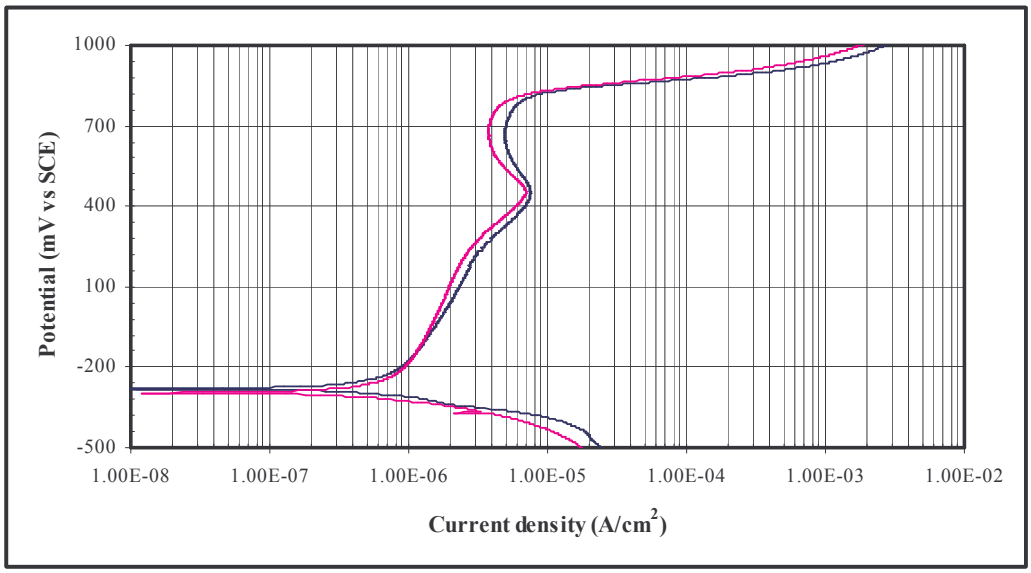


Figure B1: *Anodic polarisation scans of 304 in the petrol condensate*

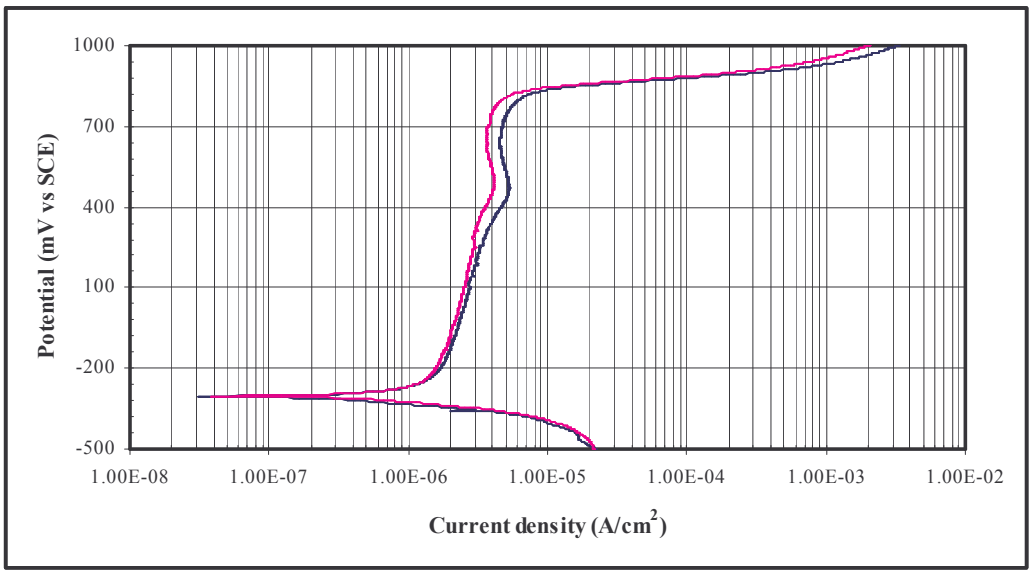


Figure B2: *Anodic polarisation scans of 409 in the petrol condensate*

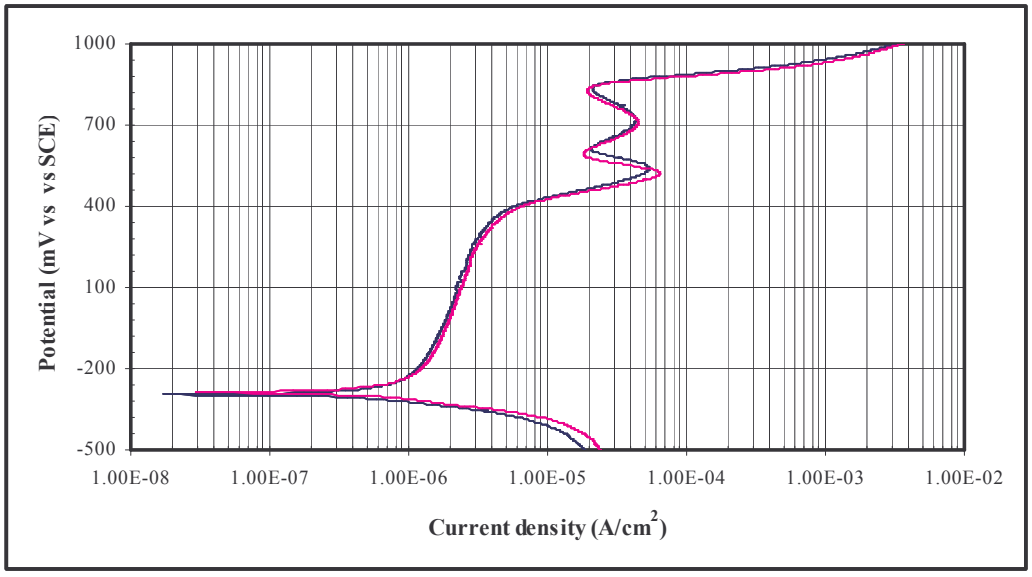


Figure B3: *Anodic polarisation scans of 434 in the petrol condensate*

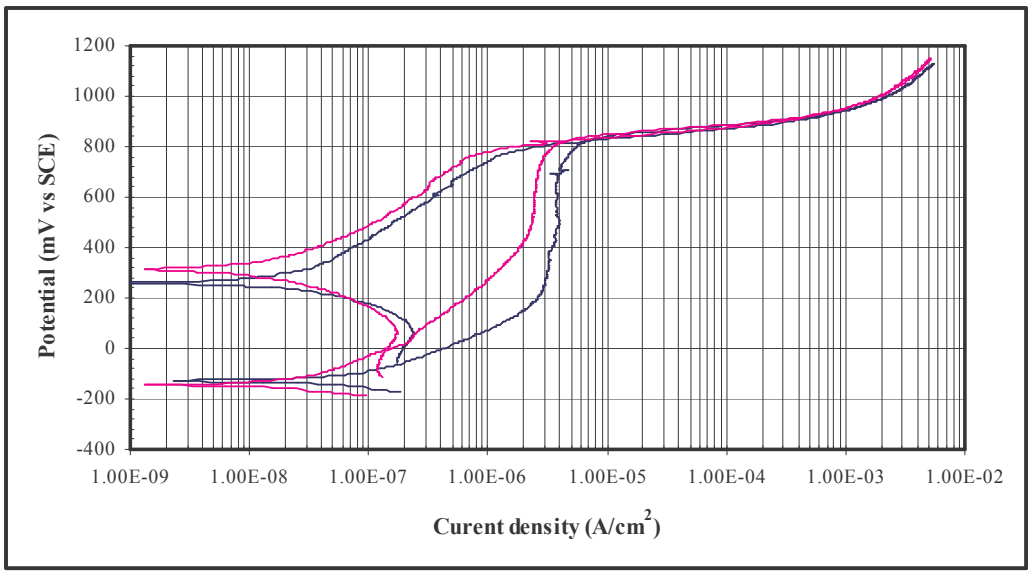


Figure B4: *Cyclic polarisation scans of 304 in the petrol condensate*

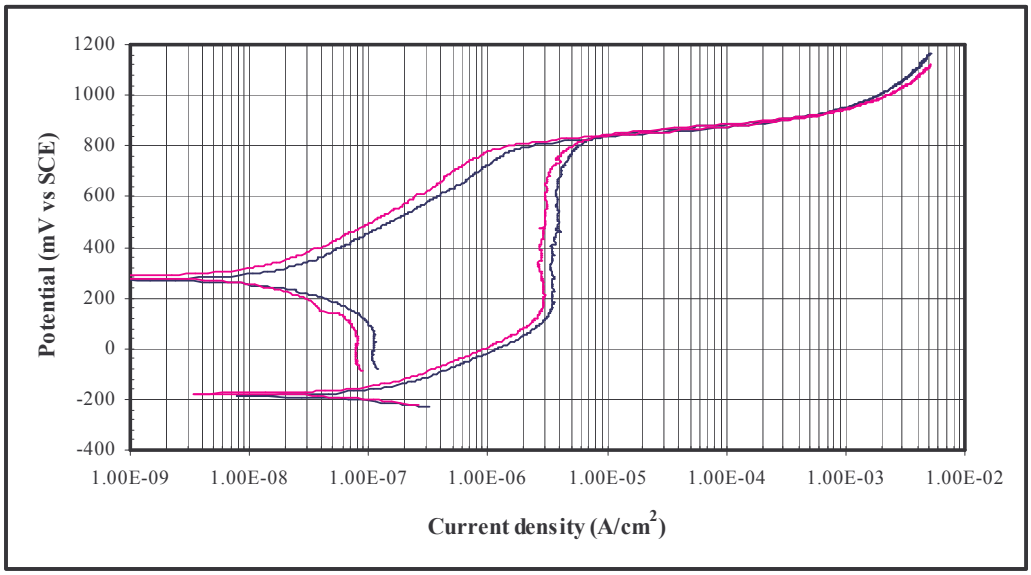


Figure B5: *Cyclic polarisation scans 409 in the petrol condensate*

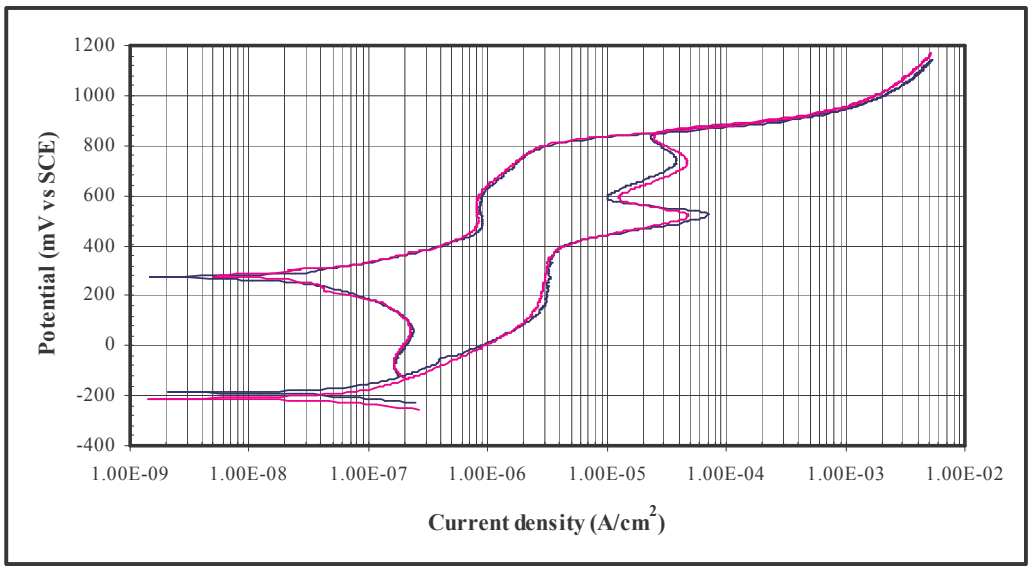


Figure B6: *Cyclic polarisation scans 434 in the petrol condensate*

Diesel condensate

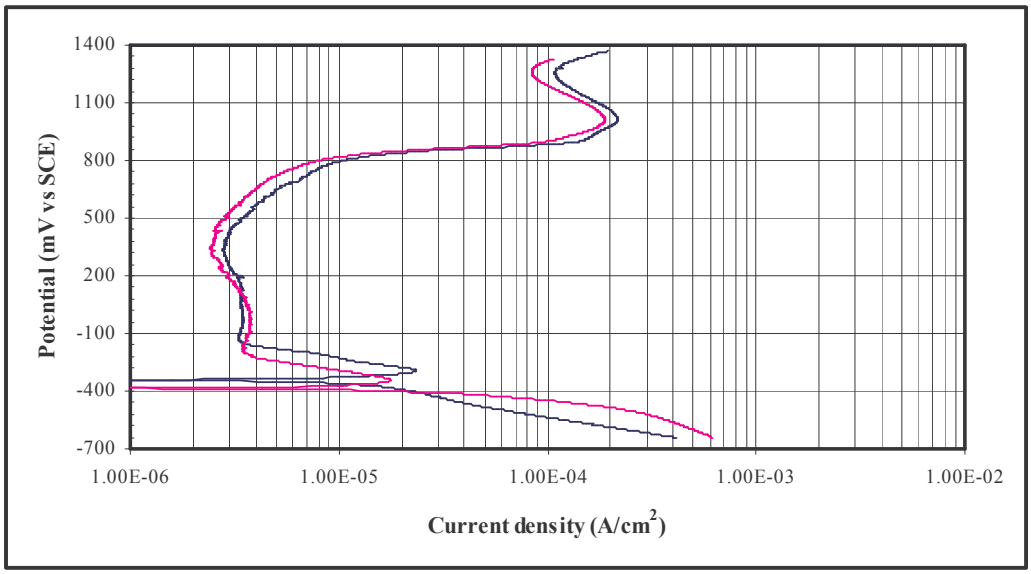


Figure B7: *Anodic polarisation scans of 304 in the diesel condensate*

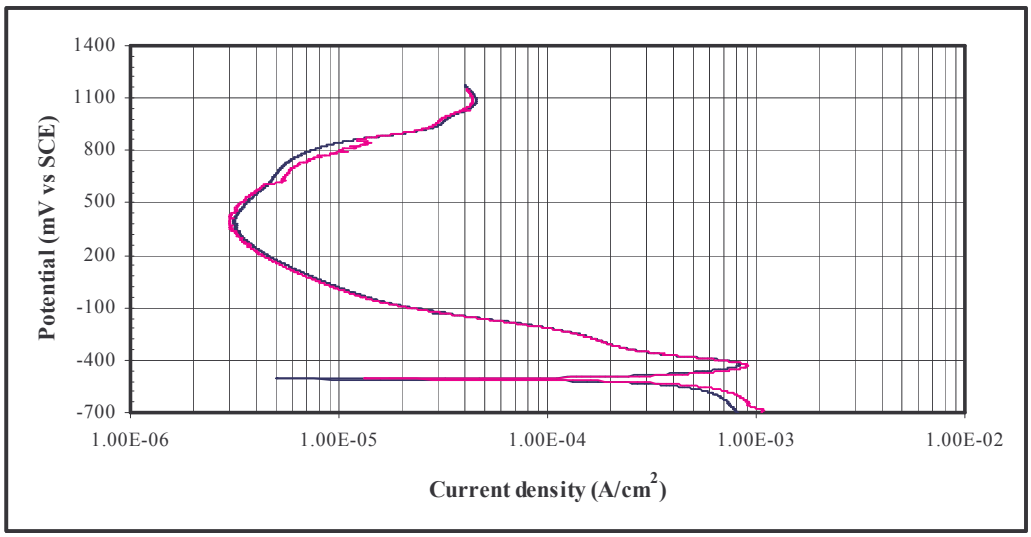


Figure B8: *Anodic polarisation scans of 409 in the diesel condensate*

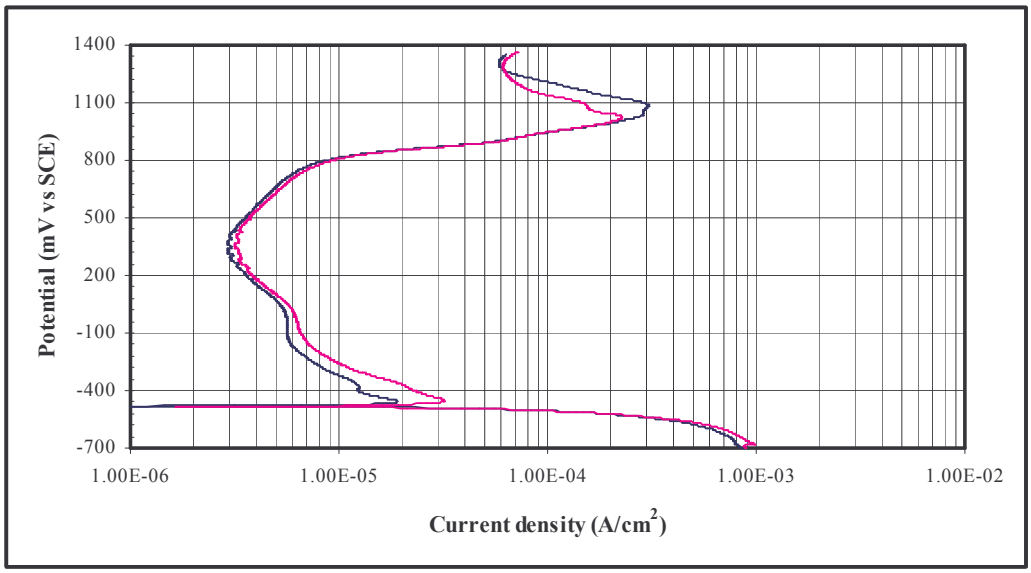


Figure B9: *Anodic polarisation scans of 434 in the diesel condensate*

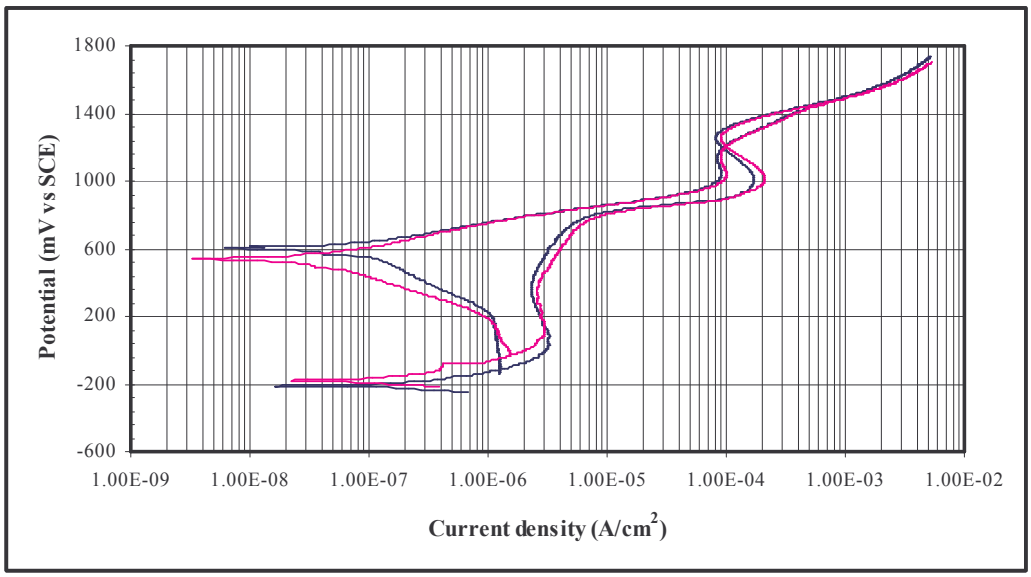


Figure B10: *Cyclic polarisation scans 304 in the diesel condensate*

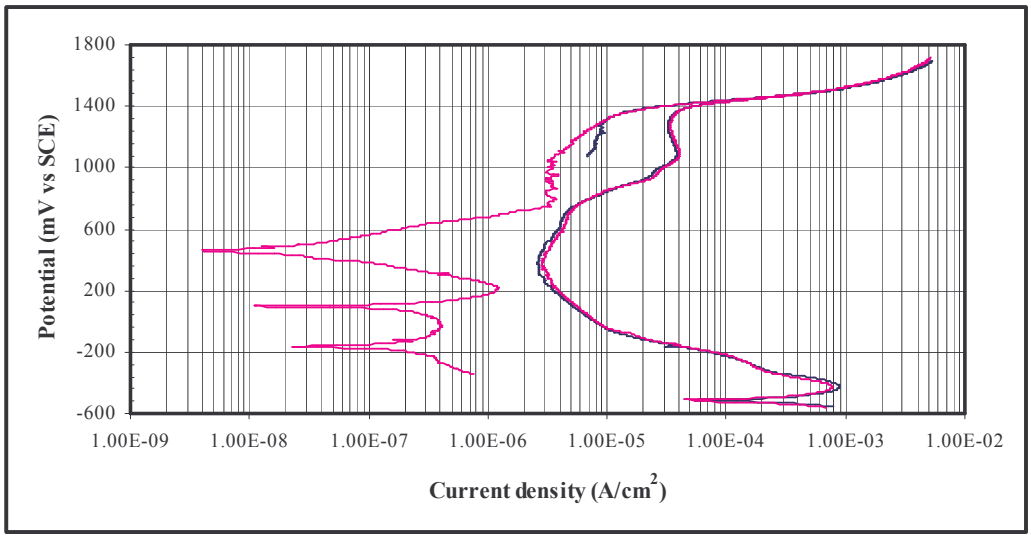


Figure B11: *Cyclic polarisation scans 409 in the diesel condensate*

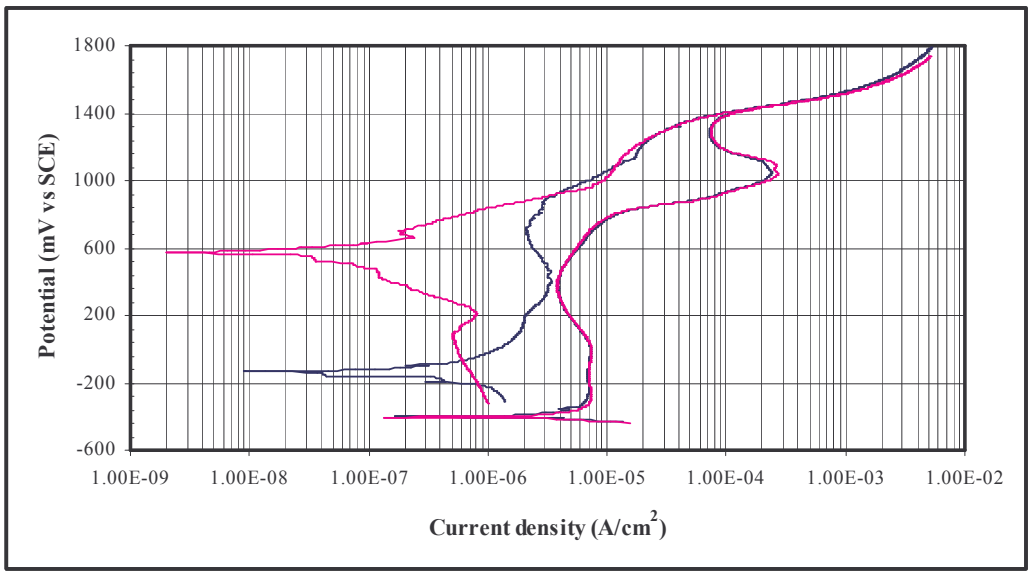


Figure B12: *Cyclic polarisation scans 434 in the diesel condensate*

B.2 Electrochemical parameters from the electrochemical test

Petrol condensate

Table B.1, which shows an average values of the runs performed per condition summarises the parameter obtained from the anodic polarisation scans, and the actual Figures showing the entire scans are shown Figures B3 to B5. Table B.2, which also shows average values from the runs performed per condition, summarises all the parameter obtained from the cyclic polarisation scans, and their actual scans are showed in Figures B6 to B8.

Table B.1: *Electrochemical parameters from anodic polarisation scans in the petrol condensate*

	AISI 304	**AISI 409**	**AISI 434**
E_{corr} (mV vs SCE)	-287	-304	-291
I_{corr} (uA/cm^2)	0.602	0.79	0.685
I_{pass} (uA/cm^2)	4.341	4.062	2.511
CR (mm/y)	0.006434	0.009093	0.007645
Rp (K.ohm.cm^2)	41.44	27.89	31.79

Table B.2: *Electrochemical parameters from cyclic polarisation scans in the petrol condensate*

	AISI 304	**AISI 409**	**AISI 434**
E_{corr} (mV vs SCE)	-135	-182	-199
E_{pit} (mV vs SCE)	820	830	848
E_{prot} (mV vs SCE)	820	830	848
Δ (mV)	0	0	0
R_{pass} (mV)	955	1012	1047

Diesel condensate

Table B.3, which shows an averages of the runs performed per condition summarises all the electrochemical parameters obtained from the anodic polarisation scans, and the actual Figures showing the entire scans are shown in Figures B7 to B9. Table B.4, which also shows average values from the runs performed per condition, summarises all the parameter obtained from the cyclic polarisation scans, and their actual scans are showed in Figures B10 to B12.

Table B.3: *Electrochemical parameters from anodic polarisation scans in the diesel condensate*

	AISI 304	**AISI 409**	**AISI 434**
E_{corr} (mV vs SCE)	-363	-509	-480
I_{corr} (uA/cm^2)	16.883	297.37	58.623
I_{pass} (uA/cm^2)	2.66	3.0629	3.111
CR (mm/y)	0.1801	3.4293	1.4886
Rp (K.ohm.cm^2)	1.336	0.061	0.3758

Table B.4: *Electrochemical parameters from cyclic polarisation scans in the diesel condensate*

	AISI 304	AISI 409	AISI 434
E_{corr} (mV vs SCE)	-196	-514	-401
E_{pit} (mV vs SCE)	1314	1380	1385
E_{prot} (mV vs SCE)	1202	1400	1400
Δ (mV)	112	-20	-15
R_{pass} (mV)	1510	1894	1786

Appendix C

C.1 Electrochemical polarisation results of the effect of NH_4^+ ion in the condensate

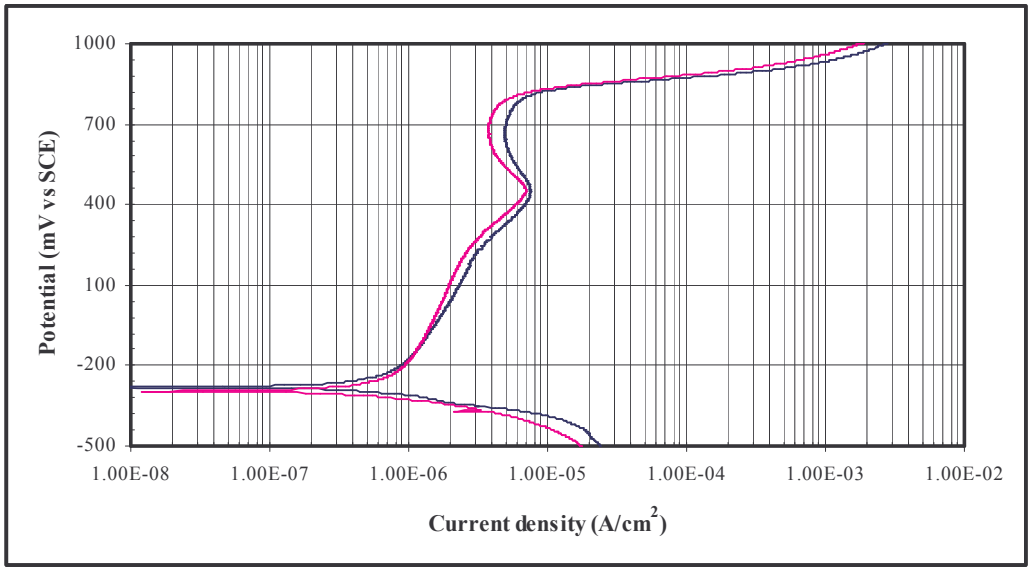


Figure C1: *Anodic polarisation scans of 304 in the petrol condensate with 3740 ppm of NH_4^+*

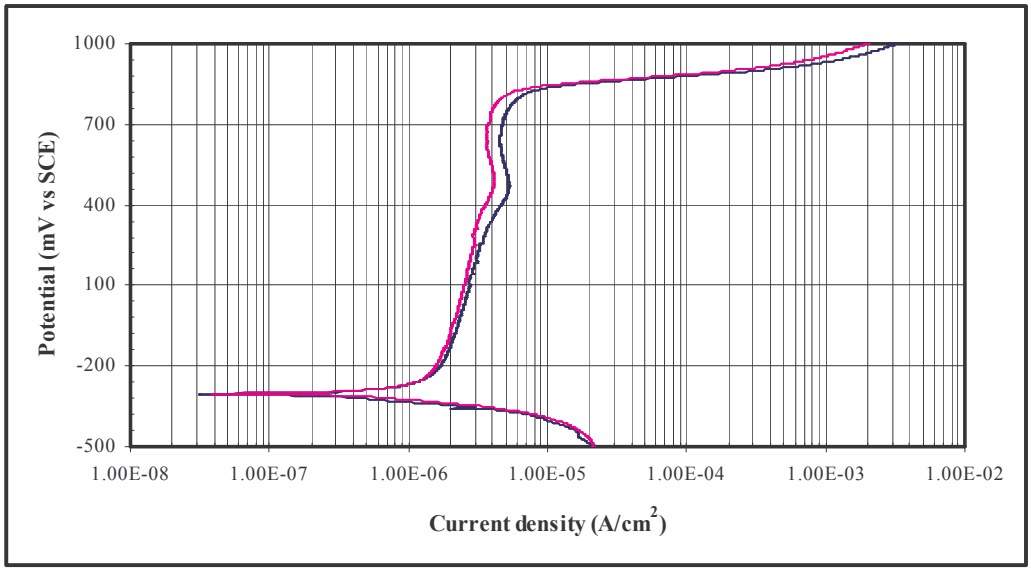


Figure C2: *Anodic polarisation scans of 409 in the petrol condensate with 3740 ppm of NH_4^+*

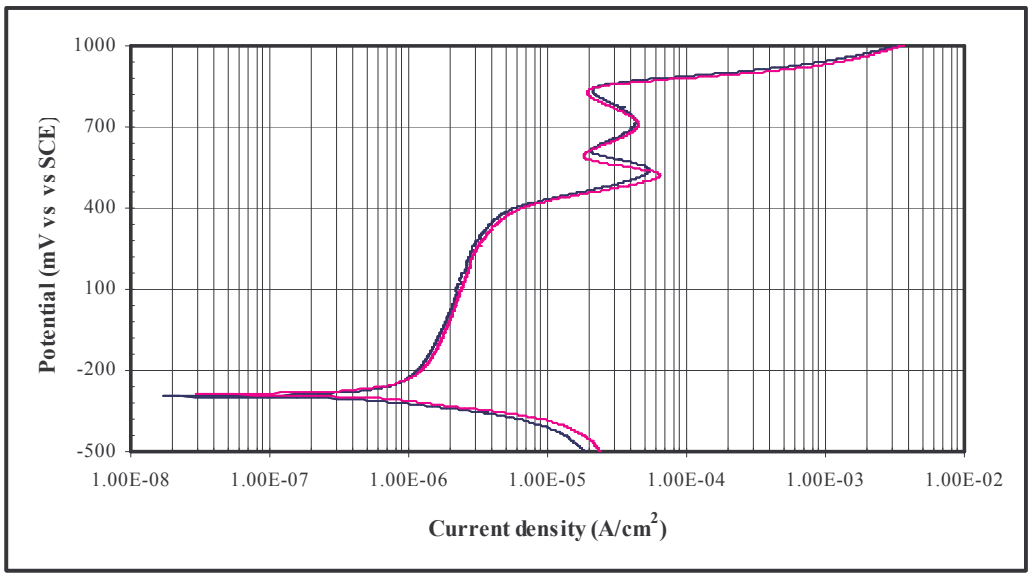


Figure C3: *Anodic polarisation scans of 434 in the petrol condensate with 3740 ppm of NH_4^+*

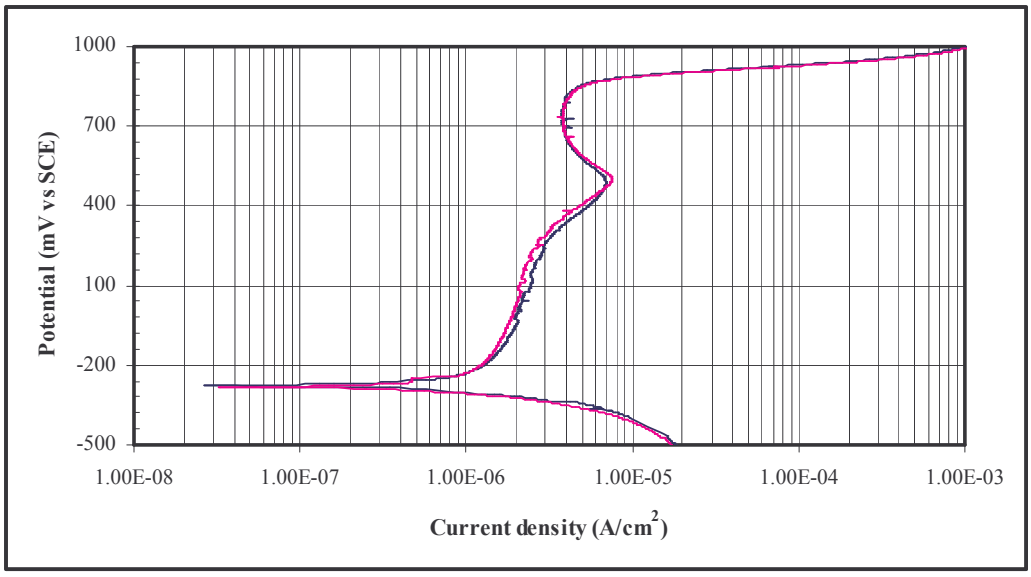


Figure C4: *Anodic polarisation scans of 304 in the petrol condensate with 1800 ppm of NH_4^+*

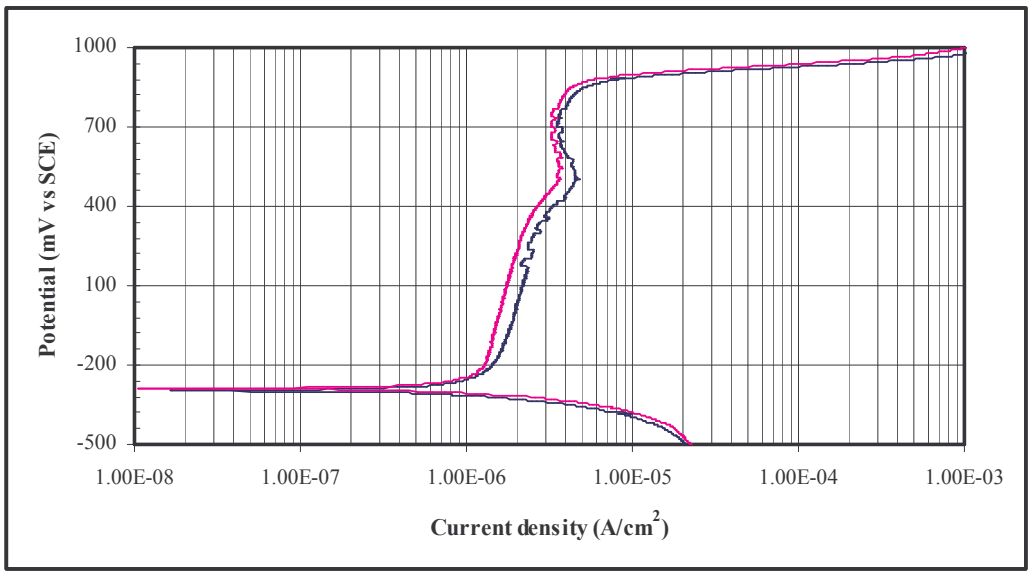


Figure C5: *Anodic polarisation scans of 409 in the petrol condensate with 1800 ppm of NH_4^+*

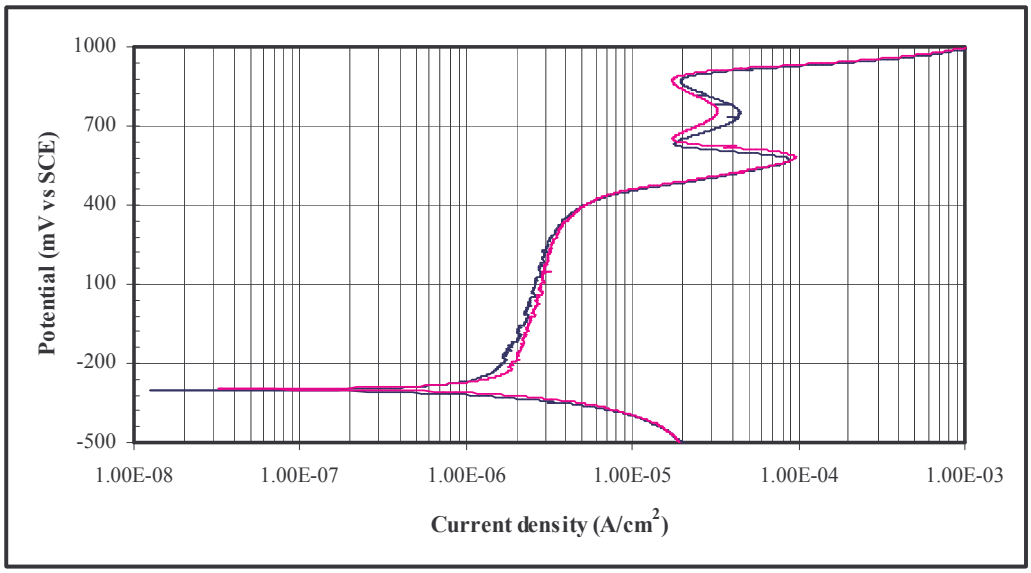


Figure C6: *Anodic polarisation scans of 434 in the petrol condensate with 1800 ppm of NH_4^+*

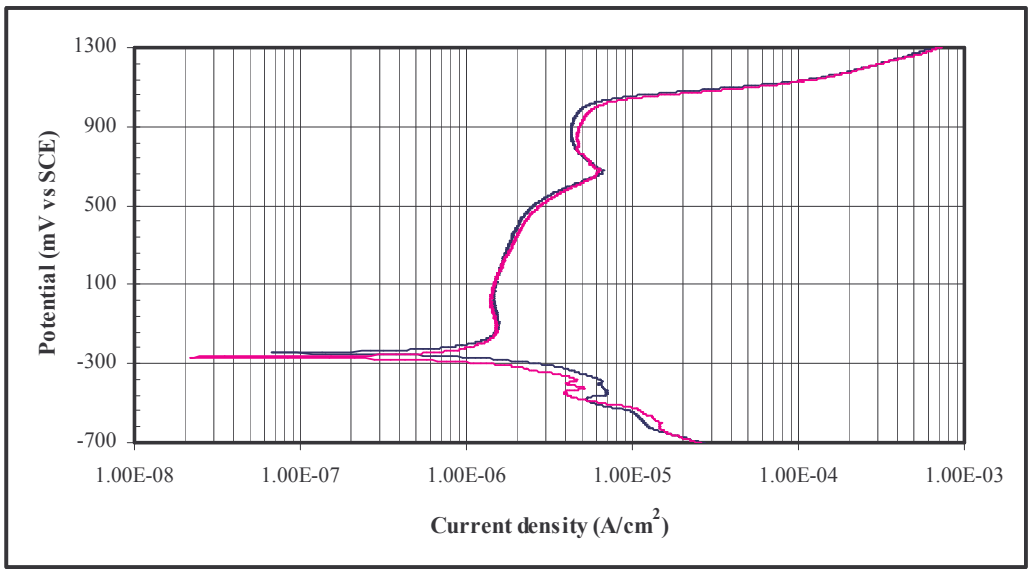


Figure C7: *Anodic polarisation scans of 304 in the petrol condensate with 1000 ppm of NH_4^+*

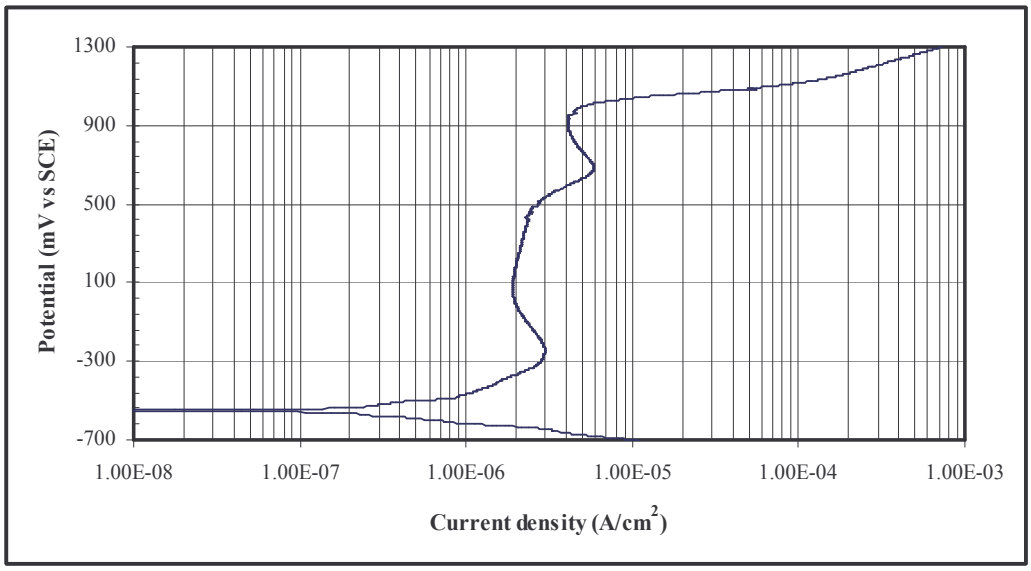


Figure C8: *Anodic polarisation scan of 409 in the petrol condensate with 1000 ppm of NH_4^+*

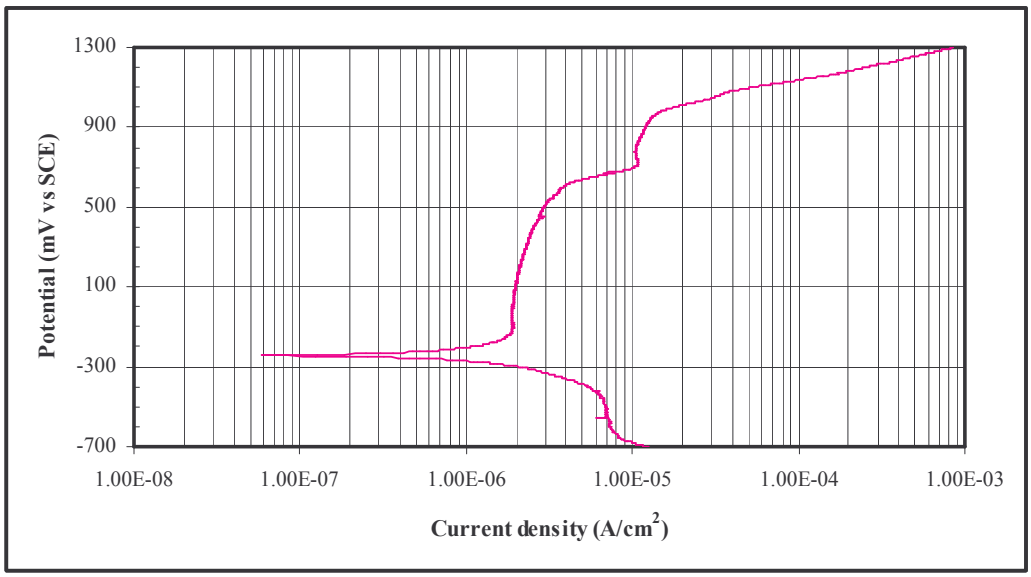


Figure C9: *Anodic polarisation scan of 434 in the petrol condensate with 1000 ppm of NH_4^+*

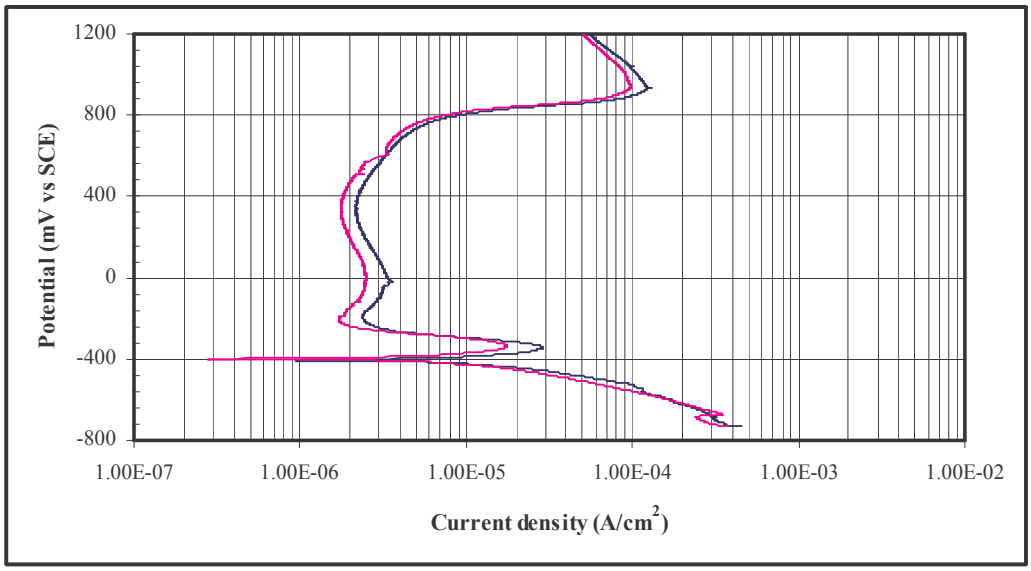


Figure C10: *Anodic polarisation scans of 304 in the petrol condensate with 600 ppm of NH_4^+*

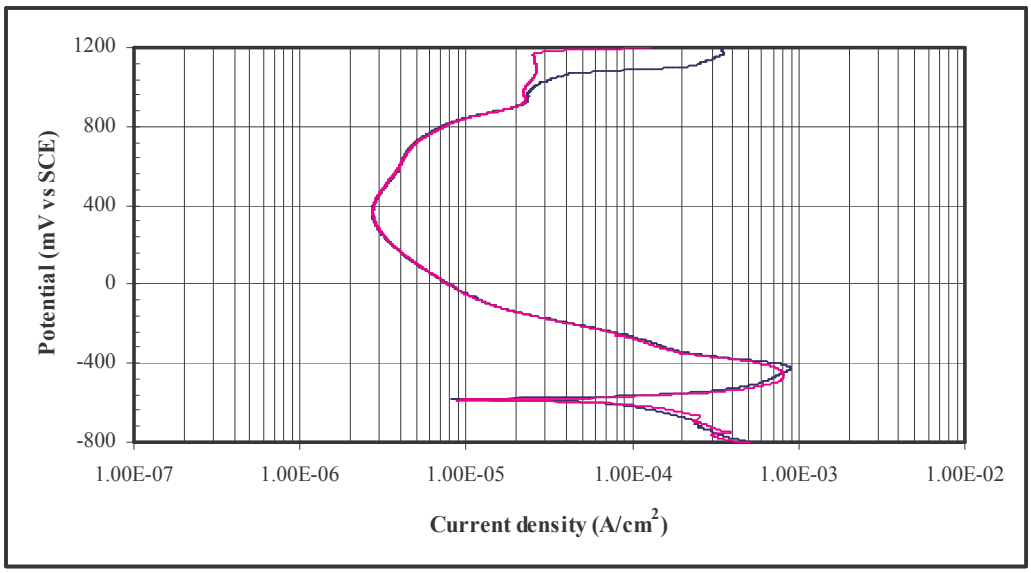


Figure C11: *Anodic polarisation scans of 409 in the petrol condensate with 600 ppm of NH_4^+*

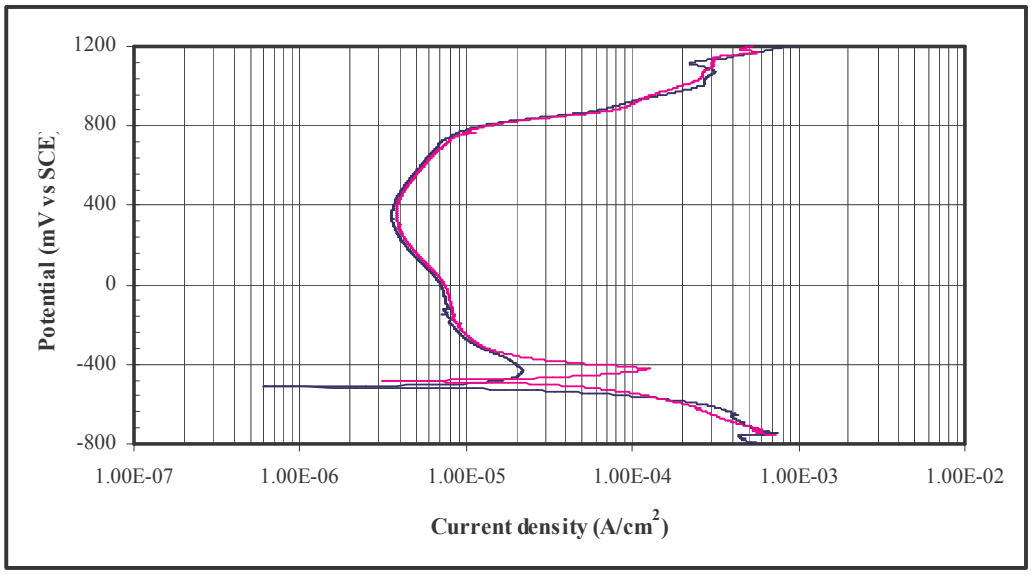


Figure C12: *Anodic polarisation scans of 434 in the petrol condensate with 600 ppm of NH_4^+*

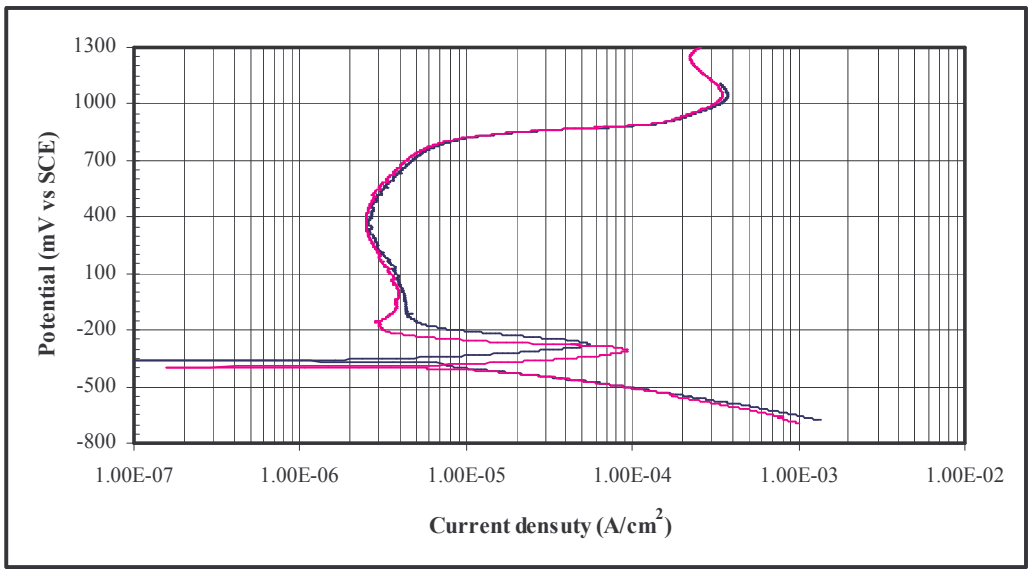


Figure C13: *Anodic polarisation scans of 304 in the petrol condensate with 340 ppm of NH_4^+*

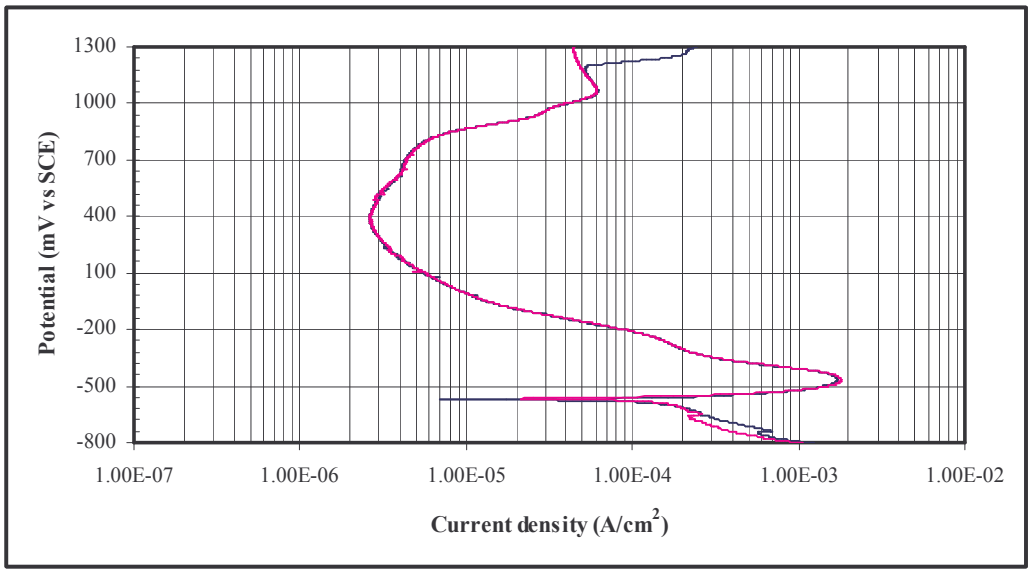


Figure C14: Anodic polarisation scans of 409 *in the petrol condensate with 340 ppm of NH_4^+*

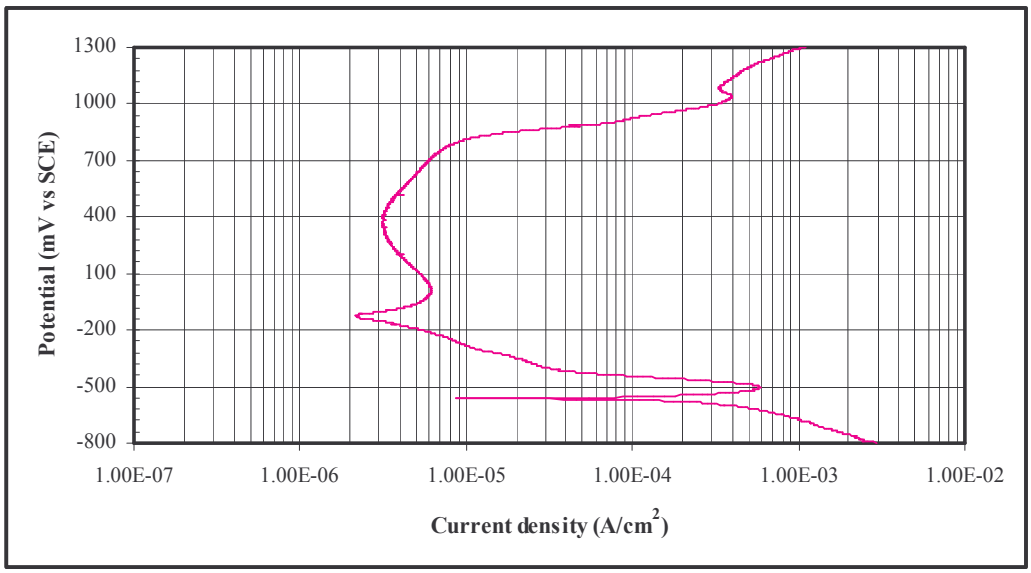


Figure C15: *Anodic polarisation scan of 434 in the petrol condensate with 340 ppm of NH_4^+*

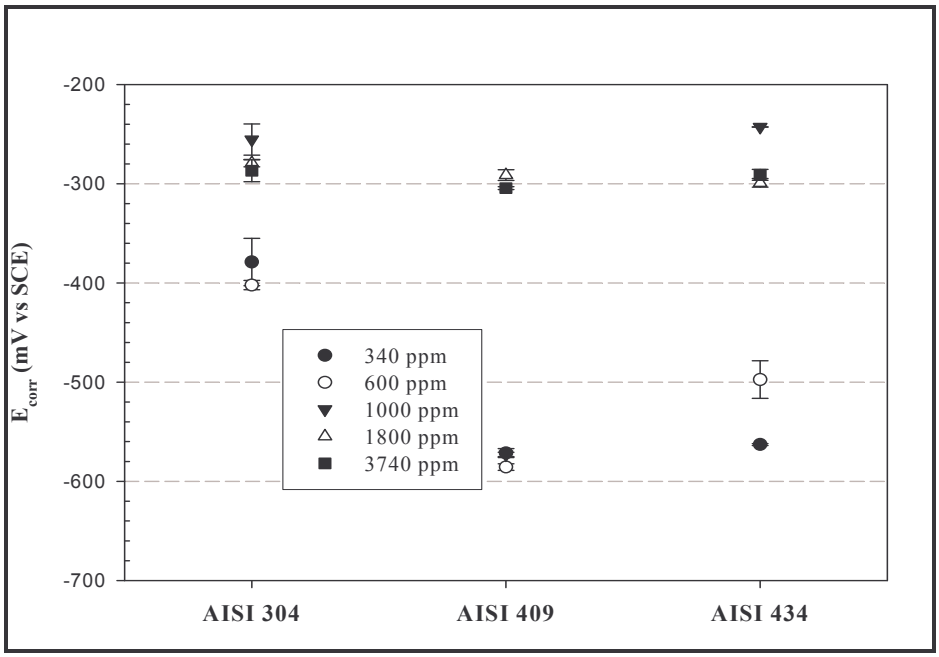


Figure C16: *Comparison of corrosion potentials (E_{corr}) in the petrol condensate with varying NH_4^+ concentrations from anodic polarisation scans*

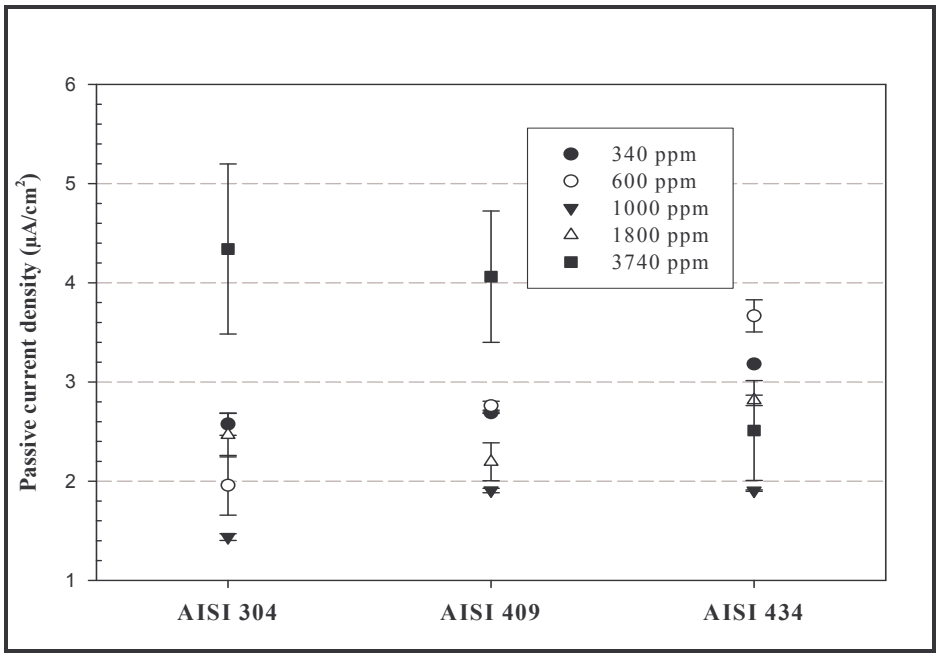


Figure C17: *Comparison of passive current densities in the petrol condensate with varying NH_4^+ concentrations from anodic polarisation scans*

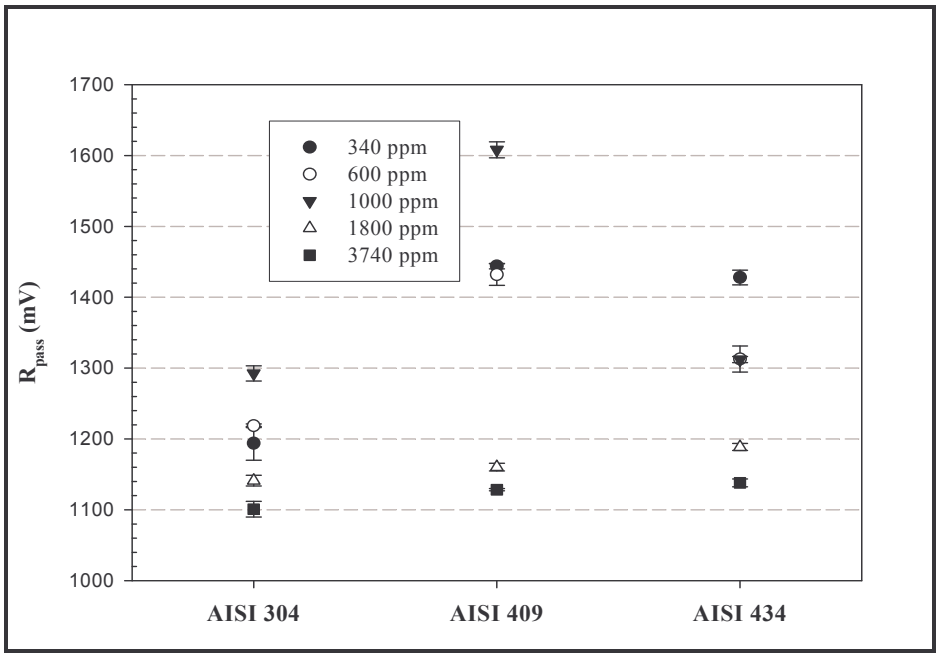


Figure C18: *Comparison of passive range ($R_{pass} = E_{pit} - E_{corr}$) in the petrol condensate with varying NH_4^+ concentrations from anodic polarisation scans*

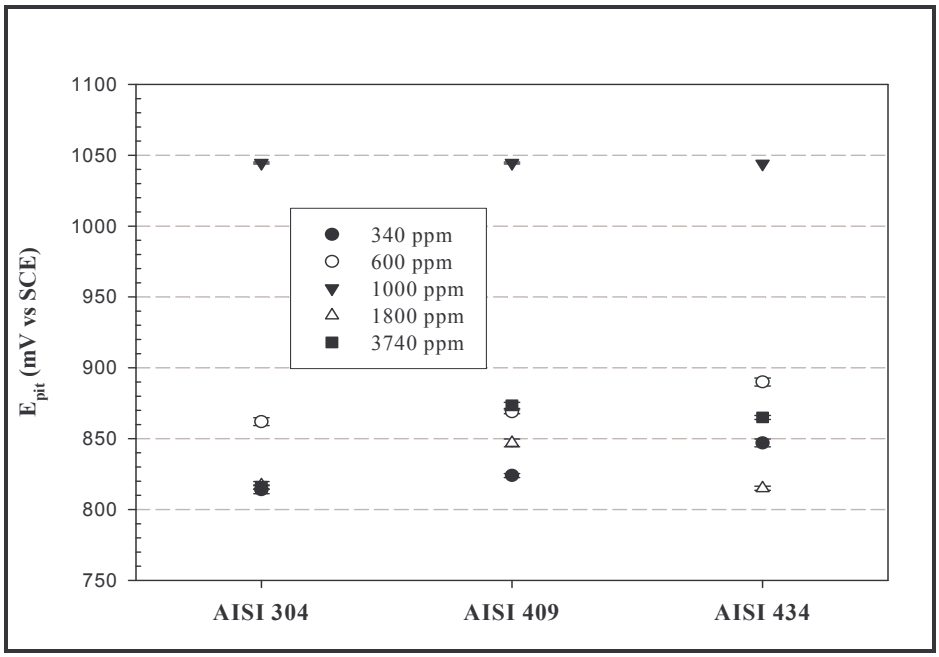


Figure C19: *Comparison of pitting potentials in the petrol condensate with varying NH_4^+ concentrations from anodic polarisation scans*

C.2 Electrochemical parameters from the effect of NH_4^+ ions in the condensate

Table C.1 shows the eelectrochemical parameters obtained from anodic polarization scans using synthetic petrol solution with various NH_4^+ ions solutions. The actual polarization scans are shown in Figures C1 to C15.

Table C.1: *Electrochemical parameters from anodic polarisation scans in the petrol condensate with various NH_4^+ ions*

Solutions	**1 (3740 ppm NH_4^+)**			**2 (1800 ppm NH_4^+)**			**3 (1000 ppm NH_4^+)**			**4 (600 ppm NH_4^+)**			**5 (340 ppm NH_4^+)**		
AISI	**304**	**409**	**434**	**304**	**409**	**434**	**304**	**409**	**434**	**304**	**409**	**434**	**304**	**409**	**434**
E_{corr} (mV vs SCE)	-287	-304	-291	-279	-291	-299	-255	-571	-271	-402	-586	-497	-379	-572	-563
E_{pit} (mV vs SCE)	814	824	847	862	869	890	1045	1045	1044	817	847	816	816	873	865
R_{pass} (mV vs SCE)	1101	1128	1138	1141	1160	1189	1300	1616	1315	1219	1432	1313	1195	1445	1428
I_{corr} (uA/cm^2)	0.602	0.79	0.685	0.69	0.928	1.138	0.725	5.43	0.87	9.76	103.36	29.48	11.884	199.51	248.3
I_{pass} (uA/cm^2)	4.341	4.062	2.511	2.465	2.195	2.815	1.436	1.906	1.905	1.959	2.761	3.666	2.576	2.69	9.106
CR (mm/y)	0.00643	0.00909	0.00764	0.00739	0.0107	0.0122	0.0077	0.062	0.0123	0.105	1.192	0.328	0.128	2.88	2.77
Rp (K.ohm.cm^2)	41.44	27.89	31.79	31.733	23.415	19.328	30.345	3.834	25.105	2.338	0.235	0.818	1.895	0.0871	0.0879

Appendix D

D.1 Electrochemical polarisation scans of the modified electrochemical test

Petrol condensate

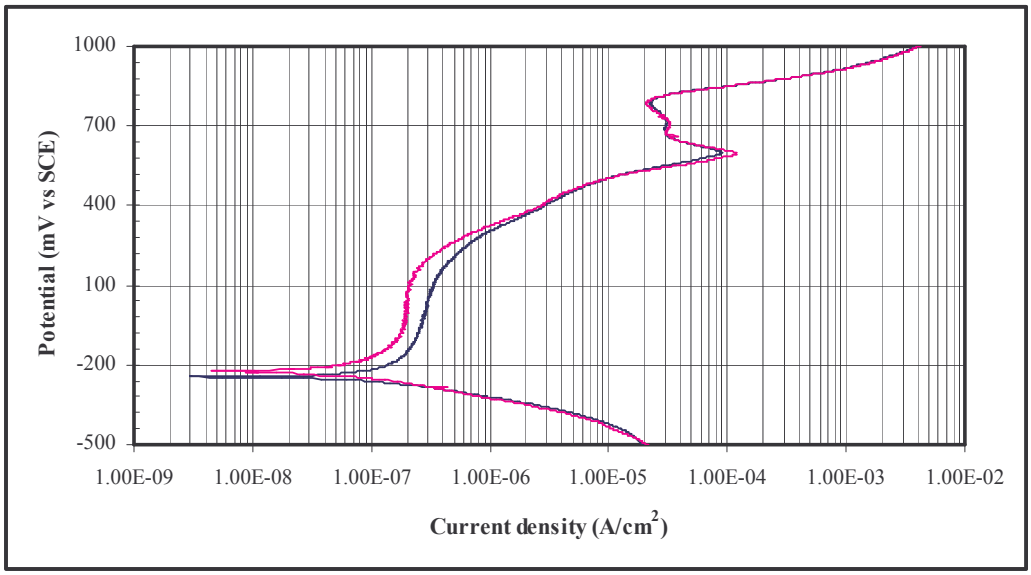


Figure D1: *Anodic polarisation scans of a heat treated 304 in the petrol condensate*

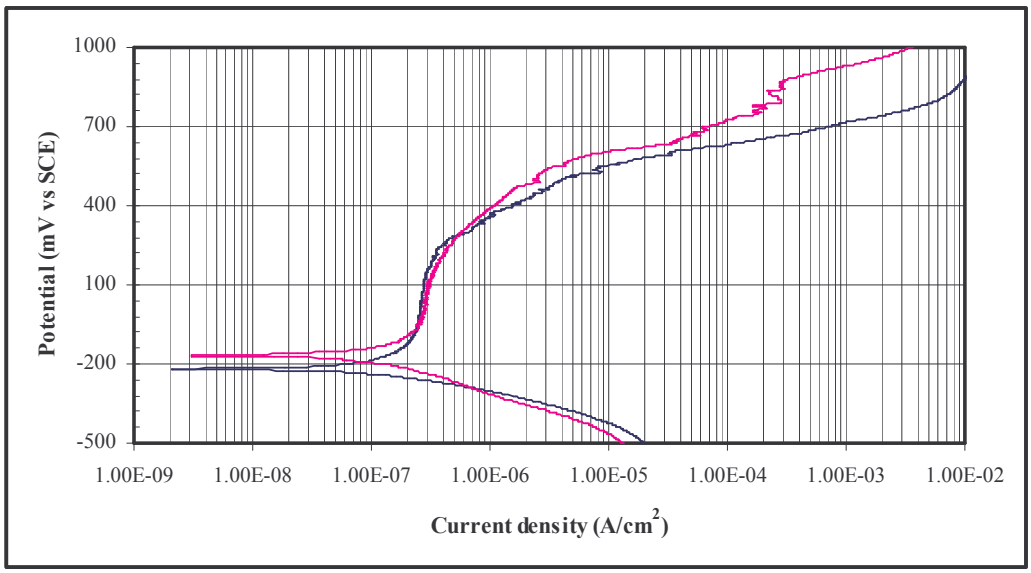


Figure D2: *Anodic polarisation scans of a heat treated 409 in the petrol condensate*

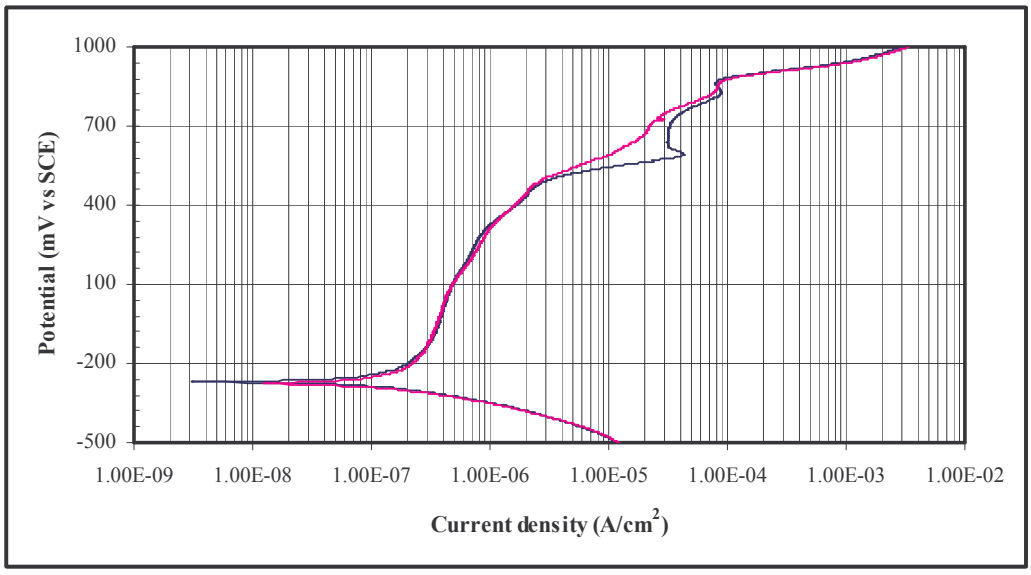


Figure D3: *Anodic polarisation scans of a heat treated 434 in the petrol condensate*

Diesel condensate

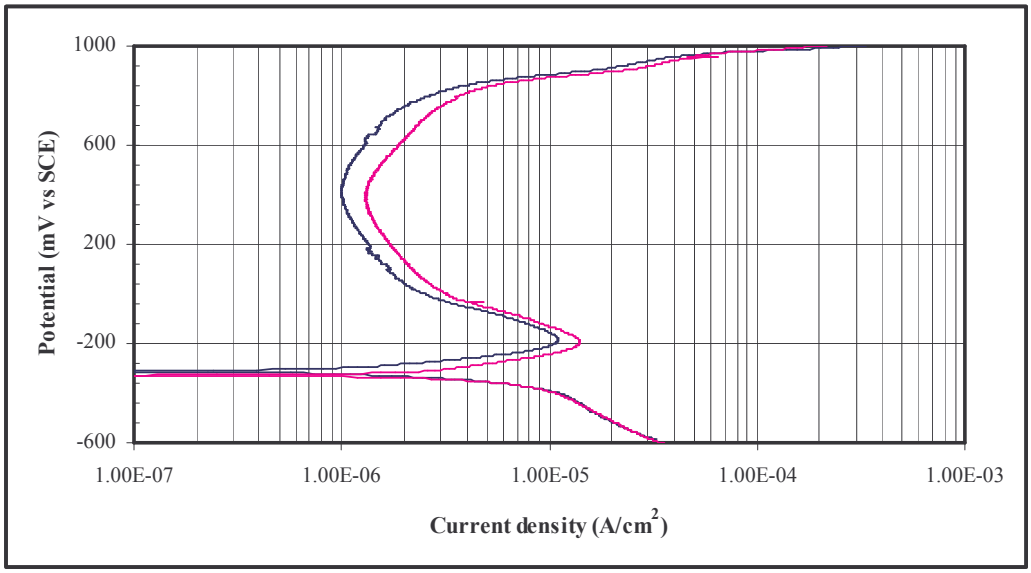


Figure D4: *Anodic polarisation scans of a heat treated 304 in the diesel condensate*

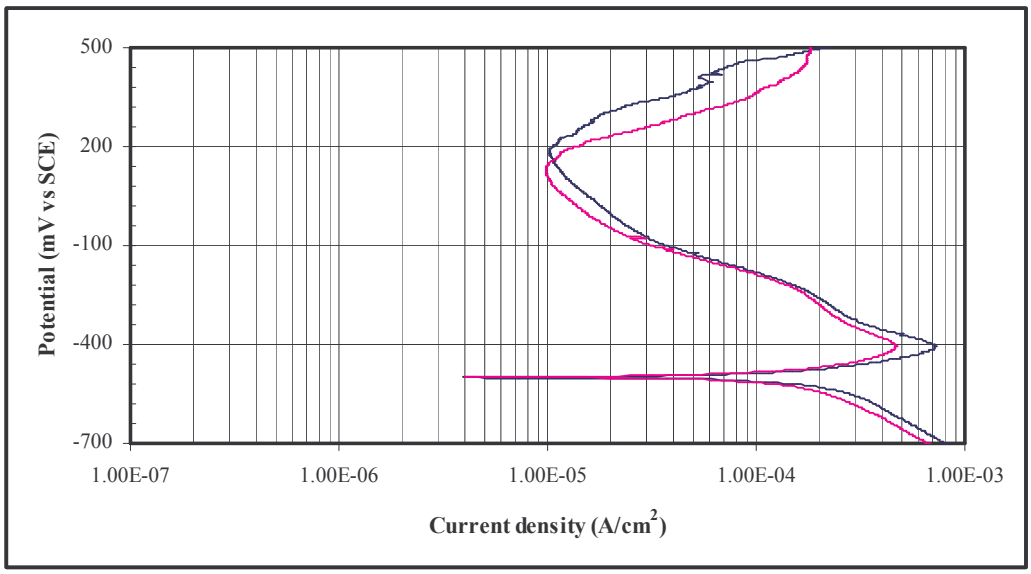


Figure D5: *Anodic polarisation scans of a heat treated 409 in the diesel condensate (note the scale change of the potential)*

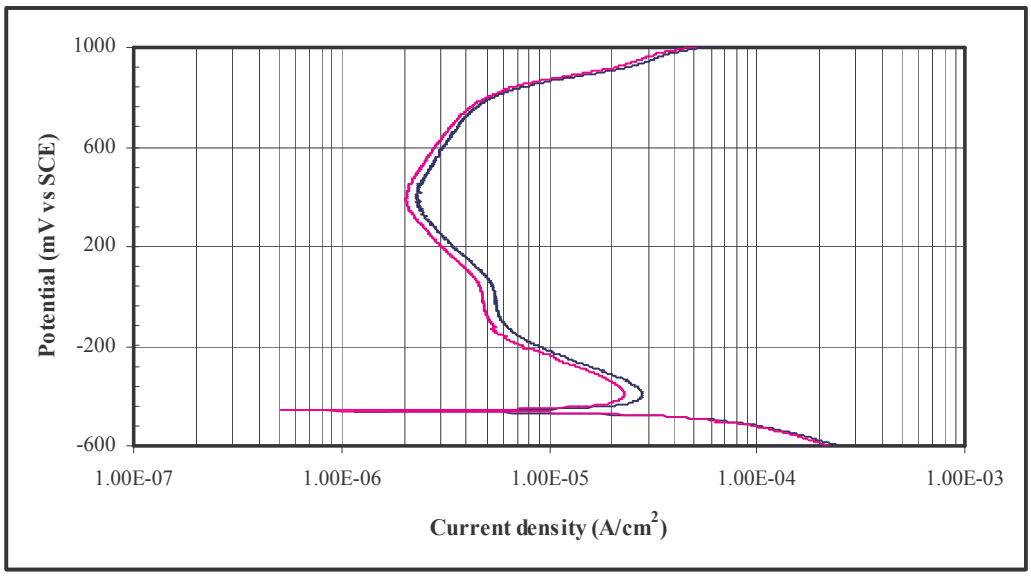


Figure D6: *Anodic polarisation scans of a heat treated 434 in the diesel condensate*

D.2 Electrochemical parameters from the modified electrochemical test

Petrol condensate

Table D.1 shows an average values of the runs performed per condition, which summarises all the parameter obtained from the anodic polarisation scans, and the actual Figures showing the entire scans are shown in Figures D1 to D3.

Table D.1: *Electrochemical parameters of the heat treated materials in the petrol condensate*

	AISI 304	**AISI 409**	**AISI 434**
E_{corr} (mV vs SCE)	-235	-193	-272
E_{pit} (mV vs SCE)	811	654	847
R_{pass} (mV vs SCE)	1046	847	1119
I_{corr} (uA/cm^2)	0.085	0.085	0.1125
I_{pass} (uA/cm^2)	0.2324	0.2759	0.7223
CR (mm/y)	0.000937	0.00098	0.001273
Rp (K.ohm.cm^2)	269.95	257.93	192.03

Diesel condensate

Table D.2 shows average values of the runs performed per condition and it summarises all the electrochemical parameters obtained from the anodic polarisation scans, and the actual Figures showing the entire scans are shown in Figures D4 to D6.

Table D.2: *Electrochemical parameters of the heat treated materials in the diesel condensate*

	AISI 304	**AISI 409**	**AISI 434**
E_{corr} (mV vs SCE)	-320	-499	-459
E_{pit} (mV vs SCE)	860	277	847
R_{pass} (mV vs SCE)	1180	776	1306
I_{corr} (uA/cm^2)	2.718	155.68	29.16
I_{pass} (uA/cm^2)	1.175	10.265	2.193
CR (mm/y)	1.156	70.69	13.258
Rp (K.ohm.cm^2)	9.125	0.141	0.746

Appendix E

E.1 Electrochemical polarisation scans of the electrochemical test in 5% NaCl solution

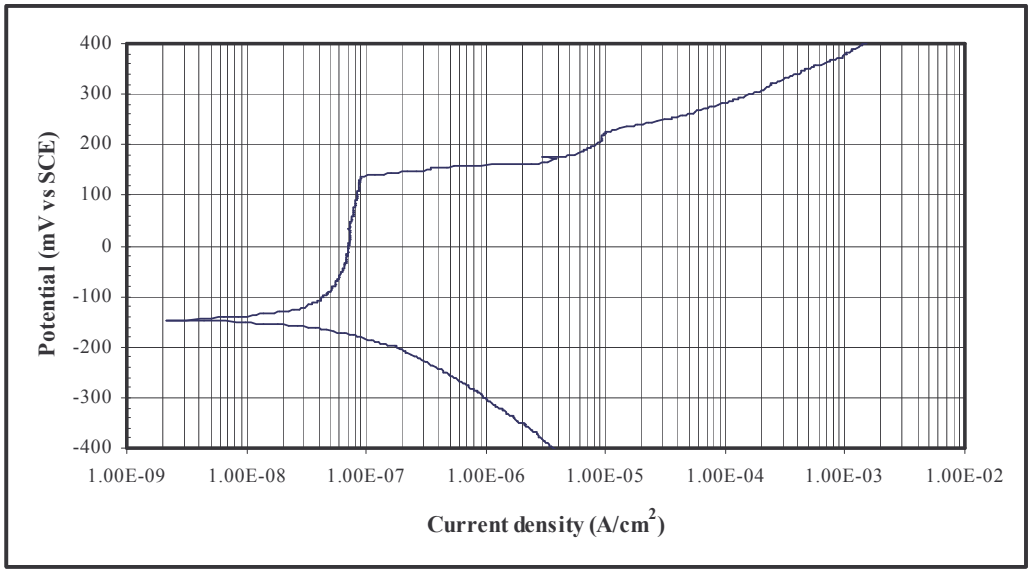


Figure E1: *Anodic polarisation scan of 304 in 5% NaCl solution*

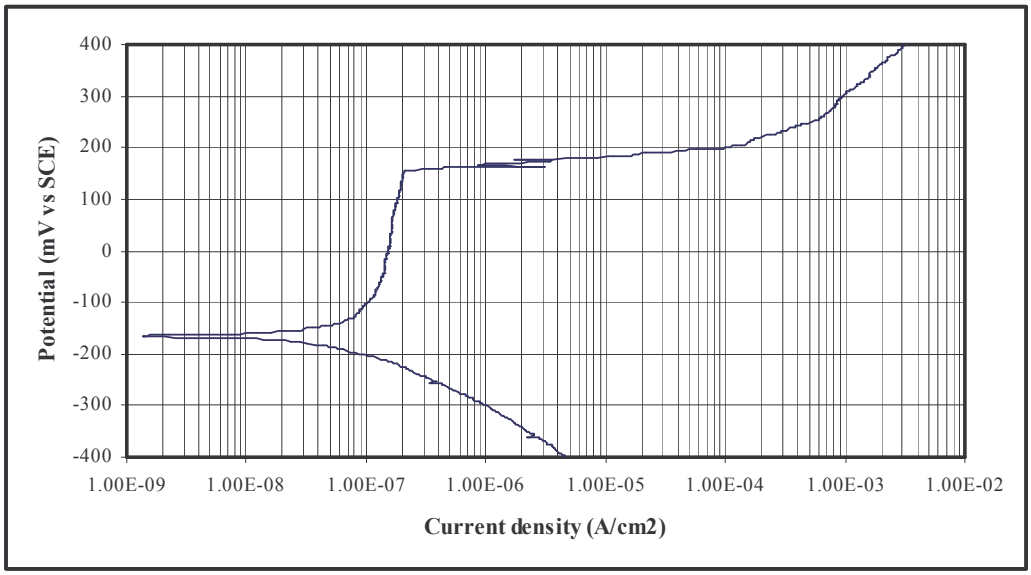


Figure E2: *Anodic polarisation scan of 409 in 5% NaCl solution*

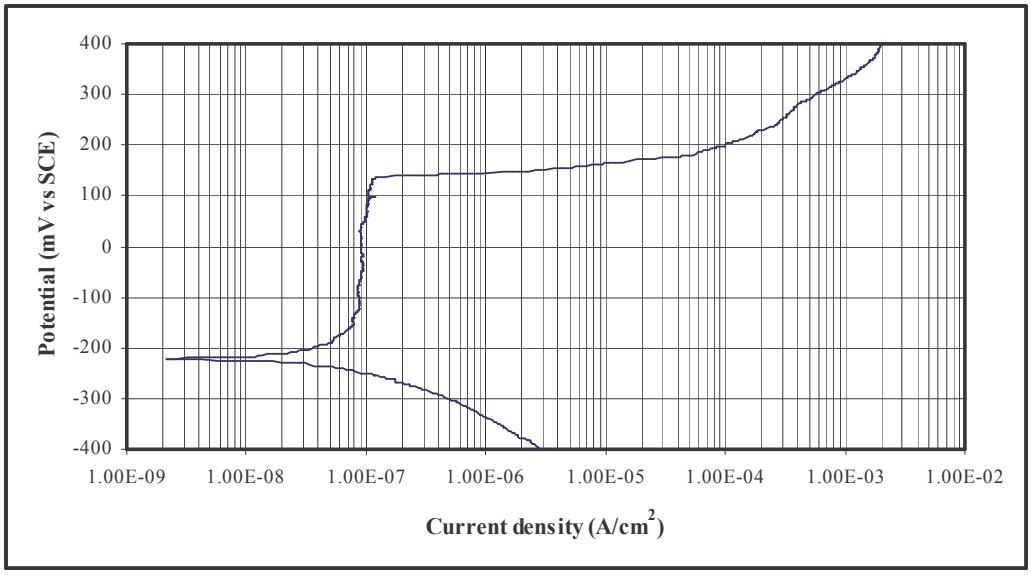


Figure E3: *Anodic polarisation scan of 434 in 5% NaCl solution*

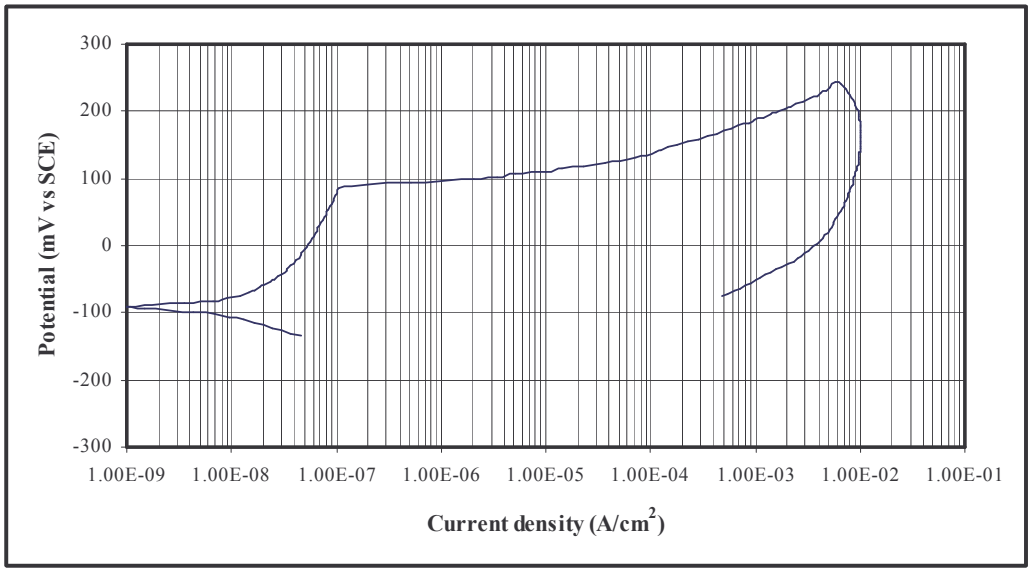


Figure E4: *Cyclic polarisation scan 304 in 5%NaCl solution*

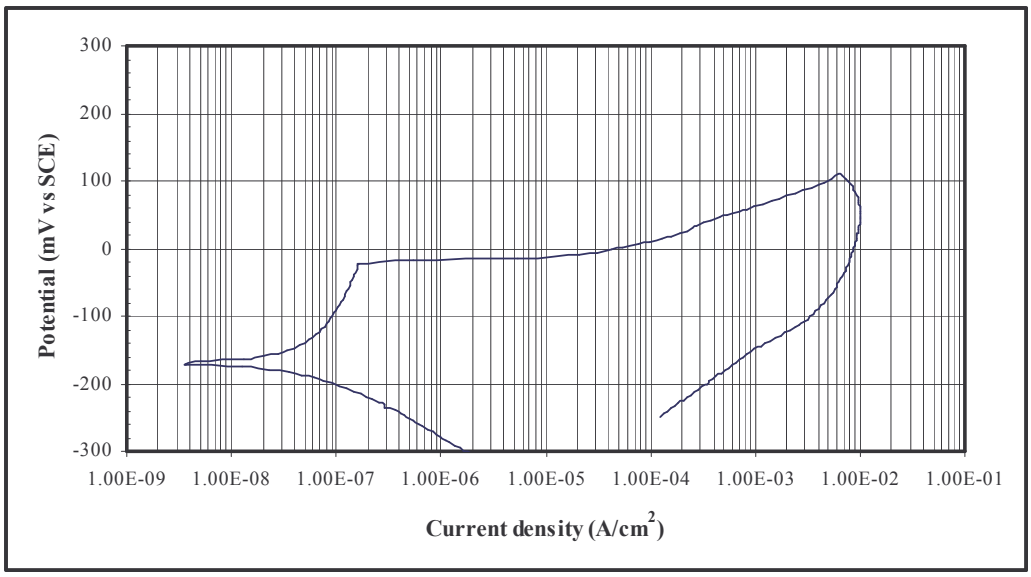


Figure E5: *Cyclic polarisation scan 409 in 5%NaCl solution*

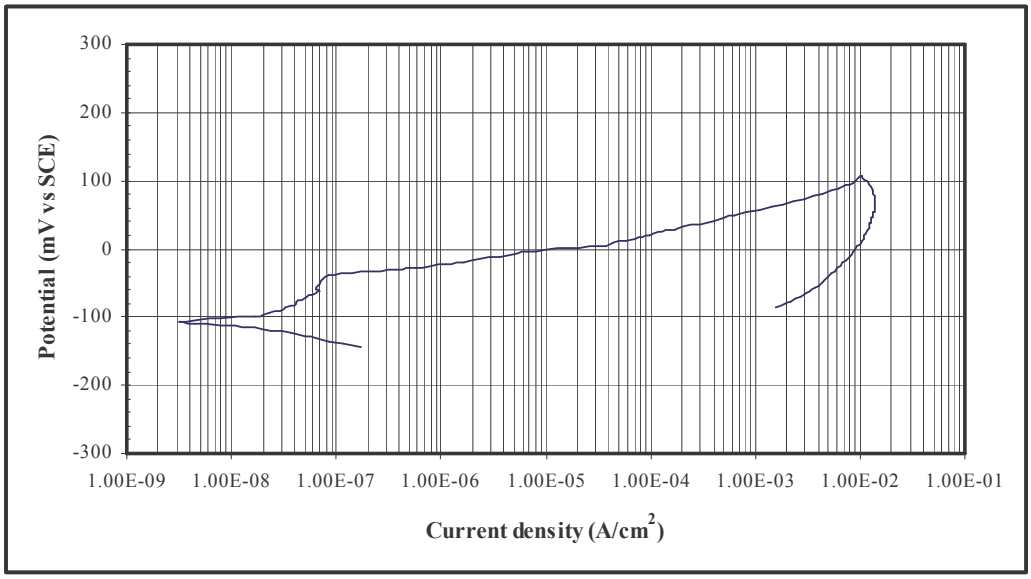


Figure E6: *Cyclic polarisation scan 434 in 5%NaCl solution*

E.2 Electrochemical parameters from the electrochemical test in 5% NaCl solution

Table E.1 shows an average of the runs performed per condition. This Table summarises all the parameter obtained from the anodic polarisation scans, and the actual Figures showing the entire scans are shown in Figures E1 to B3. Table E.2 shows average values of the runs performed per condition from the cyclic polarisation scans, and their actual scans are showed in Figures E4 to E6.

Table E.1: *Electrochemical parameters from anodic polarisation scans in the 5% NaCl solution*

	AISI 304	**AISI 409**	**AISI 434**
E_{corr} (mV vs SCE)	-105	-165	-220
I_{corr} (uA/cm^2)	0.045	0.05	0.053
I_{pass} (uA/cm^2)	0.0942	0.157	0.0921
CR (mm/y)	0.000498	0.000564	0.000627
Rp (K.ohm.cm^2)	469.66	443.93	386.13

Table E.2: *Electrochemical parameters from cyclic polarisation scans in the 5% NaCl solution*

	AISI 304	**AISI 409**	**AISI 434**
E_{corr} (mV vs SCE)	-91	-168	-107
E_{pit} (mV vs SCE)	86	-22	-39
E_{prot} (mV vs SCE)	-	-	-
R_{pass} (mV)	177	146	68

Appendix F

F.1 Calculations of the corrosion rates of exposure in immersion tests

Table F.1: *Calculations of the corrosion rates of internal corrosion tests*

Test	SS	Weight loss (g)	CR (mm/y)
Petrol condensate	**AISI 304**	0.01475	0.00511
	AISI 409	0.03100	0.01074
	AISI 434	0.01225	0.00424
Diesel condensate	**AISI 304**	0.42700	0.14788
	AISI 409	2.19025	0.75854
	AISI 434	0.50050	0.17334

Table F.2: *Calculations of the corrosion rates of external corrosion tests*

Test	SS	Weight loss (g)	CR (mm/y)
Salt damage	**AISI 304**	0.07075	0.02450
	AISI 409	0.05450	0.01887
	AISI 434	0.02150	0.00745
Modified salt spray	**AISI 304**	0.00400	0.00317
	AISI 409	0.02575	0.02038
	AISI 434	0.00350	0.00277
Hot salt	**AISI 304**	13.460	4.662
	AISI 321	4.898	4.523
	AISI 434	9.492	3.287
	DIN 1.4509	19.721	6.830